AGH

TECCO® Slope Stabilization System
and RUVOLUM® Dimensioning Method

Cała Flum Roduner Rüegger Wartmann

New Edition 2020

AGH UNIVERSITY OF SCIENCE AND TECHNOLOGY AGH UNIVERSITY OF SCIENCE AND TECHNOLOGY

THE AUTHORS GROUP

Marek Cała is a professor of Geoengineering at the AGH University of Science & Technology, Cracow, Poland. He is an author of more than 170 papers and books dealing with problems of civil, mining and geotechnical engineering. His main research area covers application of numerical methods and computational techniques for solving practical geoengineering problems.

Since studying for Master of Science at the Department of Civil Engineering at the ETH Zurich until 1999, **Daniel Flum** gained a long standing experience in the area of stabilizing and protecting soil and rock slopes with flexible facings in combination with nailing and anchoring from all around the world. Since 2017, he is the director of the consultant company FlumGeo AG, Solutions in Geotechnical Engineering, St. Gallen, Switzerland.

Armin Roduner got his Master of Science in Civil Engineering at Universities in Switzerland and USA. Afterwards he worked in engineering offices in Switzerland in the field of slope stability, foundations, tunnel construction and water power projects. Since 2009 Armin Roduner is the head of geotechnical engineering at Geobrugg AG in Romanshorn, Switzerland responsible for all the slope stabilization projects worldwide.

Rudolf Rüegger is working in the area of geotechnical engineering since 1973, had been a lectureship at the ETH Zurich about „design and construction in the geotechnics“ and had been director of the consultant company Rüegger+Flum AG, Solutions in Geotechnical Engineering, St. Gallen, Switzerland. He was considerably involved in different federal as well as company based research projects mainly in the area of geosynthetics and slope stabilization. He has published dozens of papers and a couple of books.

As MSc. Civil Engineer from the ETH University of Zurich, **Dr. Stephan Wartmann** worked as project manager in the USA and as general manager in Japan, before he took over the technical department at Geobrugg in Switzerland. During 2003 – 2013, he was CEO of the Geobrugg Group, from 2014 - 2018 he was CEO of the Brugg Rope Technology Holding and since 2019, he is the CEO of the Brugg Group with worldwide activities in more than 60 different countries.

AGH UNIVERSITY OF SCIENCE AND TECHNOLOGY
Faculty of Mining & Geoengineering

TECCO® Slope Stabilization System
and RUVOLUM® Dimensioning Method

Cała Flum Roduner Rüegger Wartmann

Romanshorn, Switzerland 2020 - New Edition

ISBN 978-3-033-03296-5
Electronic version available.

Pictures on the front-page present realized flexible slope stabilization systems designed with high-tensile steel wire meshes:

Top left: Samsung site Dongcheon, South Korea
Top right: Anzenwil, Switzerland
Bottom left: Túnel do Morro Agudo, Brasil [76]
Bottom right: Tokaj Hokurikudo, Gifu Prefecture, Japan

Acknowledgment

The geotechnical, industrial and economical development of the TECCO® slope stabilization system, the RUVOLUM® dimensioning method as well as its corresponding elements and products was supported, co-developed, pushed and driven by various people and consequently, our very big thanks go to Bernhard Eicher (inventor of TECCO® mesh), Xaver Popp, Kaspar Haltiner, Bruno Haller, Andrea Roth, Dr. Roberto Luis Fonseca, Dr. Corinna Wendeler, Hannes Salzmann, Patrick Schwizer, Piotr Baraniak, Carles Raïmat, Otegui Gabriel Polit, Julio Prieto Fernández, Eberhard Gröner, Aron Vogel, Max Bickel, Roland Bucher, Kazuhito Shimojo, Guido Guasti, Gabriele Guglielmini, Marcel Sennhauser, Erik Rorem, John Kalejta, Steve Mumma, Joseph Bigger, Frank Amend, Maria Soares, Dr. Felipe Gobbi, Javier Temiño, German Fischer, Roland Klein, Jürg Atz, Stefan Haas, Manuel Hungerbühler, Max Bühler and Jörg Bär, as well as many others; thank you all very much for everything!

Special support for this publication was given by the AGH University of Science and Technology in Krakow (Poland). We would like to thank the Rector of the University, Prof. Dr. T. Słomka and the group of the processors from the Faculty of Mining and Geo-engineering: Prof. Dr. A. Tajduś, Prof. Dr. Czaja, Prof. Dr. Waldemar Korzeniowski and Prof. Dr. Roman Magda.

Further special thanks go to Prof. Dr.-Ing. L. Wichter from the University of Cottbus (Germany), Faculty for Rock and Soil Mechanics for his support and valuable inputs.

Various additional laboratory and field tests, static and dynamic analysis, investigations, supervisions and reports with and around the high-tensile steel wire mesh technologies were executed, conducted and/or coordinated in Germany, Australia, USA, Japan, Spain and Switzerland, where we would like to thank very much all the involved people at the TÜV Rheinland and LGA Nürnberg (Germany), Rüegger + Flum AG (Switzerland), University of Cottbus (Germany), Bergische University of Wuppertal (Germany), Curtin University and Kalgoorlie School of Mines (Australia), Washington States University (USA), Swiss Federal Institute for Forest, Snow, Landscape WSL (Switzerland), BAREMO GmbH (Switzerland), University of Cantabria (Santander), Institute of Civil and Environmental Engineering at the HSR Hochschule (Rapperswil, Switzerland), TOA GROUT Kogyo Co. LTD (Tokyo, Japan), Luchs und Partner AG (Switzerland), Fatzer AG (Switzerland), Geobrugg AG (Switzerland) and other Geobrugg subsidiaries as well as many others.

Prof. Dr. Marek Cala, AGH University of Science and Technology, Cracow
Daniel Flum, MSc. (civil) Eng. ETH/SIA
Rudolf Rüegger, MSc. (civil) Eng. ETH/SIA
Armin Roduner, MSc. (civil) Eng. Colorado University, USA
Dr. Stephan Wartmann, MSc. (civil) Eng. ETH/SIA; EMBA HSG

Table of Content

1 Preface

Flexible slope stabilization systems made from conventional wire meshes in combination with nails or nailing are widely used in practice to stabilize soil and rock slopes. They are traditional solutions and provide an alternative to measures based on rigid concrete liner walls, shotcrete applications or massive supporting structures.

Slope protection by means of common wire mesh and wire rope nets is known accordingly, but the transfer of forces by mesh as pure surface protection devices is limited on account of their tensile strength and above all also by the possible force transmission to the anchoring points (nails, anchors).

Strong wire rope nets offer certain possibilities for slope stabilizations with greater distances between nails and anchors. However, they are comparatively expensive in relation to the protected surface and the size of the individual nets is relatively small, resulting in higher installation cost and less flexibility to local terrain conditions.

Today, apart from solutions using conventional steel wire, new meshes from high-tensile steel wire are now also available on the market. The latter can absorb substantially higher forces and transfer them onto the nailing.

A new special method has been developed for the designing of flexible slope stabilization systems with high-tensile steel wire meshes for the use on steep slopes in more or less homogeneous soil or heavily weathered loosened rock.

The interaction of mesh and fastening to nails has been investigated in comprehensive laboratory tests. This enabled also to find a suitable fastening spike plate which allows an optimal utilization of the strength of the mesh in tangential (slope-parallel) as well as in vertical direction (perpendicular to the slope).

The trials also confirmed that the high-tensile wire meshes, in combination with suitable plates, enable substantial pretensioning of the system. Such pretensioning increases the efficiency of the protection system. This restricts deformations in the surface section of critical slopes which might otherwise cause slides and movements as a result of dilatation. Suitable dimensioning models permit to correctly dimension such systems.

Various implemented stabilizations in soil and rock, with and without vegetated face, confirm that these measures are suitable for practical application and provide useful information for the optimized handling and installation process.

Both, the new high-tensile steel wire mesh and the new dimensioning method for flexible slope stabilization systems allow simple and safe concepts including cost saving installation processes. This provides new interesting solutions for traditional geotechnical problems which, in the meantime, are executed and applied globally on all continents.

2 Introduction

Application of wire rope nets and the use of wire mesh as a flexible measure to protect surfaces has proved worthwhile in many cases and is often an alternative to stiff and massive constructions of concrete. Hereby the open structure of the mesh also permits full-surface greening and vegetation. Wire mesh from wires of a tensile strength[1] of approx. 400 – 650 N/mm^2 are traditionally used for these kind of protection measures. If an economical spacing of the nails is aimed for, these conventional meshes are often unable to absorb the occurring forces and to transmit them onto the nails. Ropes threaded into the mesh can be used as certain reinforcements. If the distances between nails are kept at an economical level, these simple meshes are often unable to absorb the occurring forces and to selectively transmit them onto the nails.

In the past, high-tensile wires were mostly used only in combination with strand and rope products or combinations of those. Typical for such uses are ringnets and wire rope nets. They are installed for a various number of applications for natural hazard protection, such as rockfall protection barriers[2] (picture 2.1), drapping systems[3], debris flow (picture 2.2) and mudflow barriers[4], avalanche prevention systems[5] (picture 2.3) as well as driftwood protection systems[6] (picture 2.4).

Picture 2.1 Example of rockfall barrier with ringnets made from high-tensile wires

---

[1] For the tensile strength of steel wires, the unit [N/mm^2] is still used as an international industrial standard, however, from a technical point of view, the correct unit would be [MPa]; [44, 45, 48].

[2] References [46, 58, 59, 89, 124, 133, 134, 138, 139] describe various applications and technical background of rockfall barriers with high-tensile steel wire ring nets.

[3] The papers of reference [83, 88] show corresponding drapping and attenuator applications.

[4] References [66, 73, 90, 103, 136, 137, 143] report about design and installation methods for debris flow and mudflow protection systems based on high-tensile steel wire ring nets.

[5] For avalanche prevention systems, the guideline of SLF/WSL Davos (Switzerland) is internationally seen as one of the leading design and installation methods [16, 17, 66].

[6] Driftwood protection measures based on high-tensile wire ringnet technology are explained in references [82, 104, 105, 132, 135].

Picture 2.2 Example of debris flow barrier with ringnets made from high-tensile wires

Picture 2.3 Example of avalanche prevention system made from rope wire nets

Compared to conventional steel wire meshes, wire rope nets [83] allow bigger distances between the individual nails. However, those rope nets are only available for small panel size which means higher installation and connection efforts. Due to the small wires in the ropes, only a limited amount of zinc coating can be applied on the nets. This results in a limited lifetime. Usually, cross clips are connecting the overlapping rope net units, but they are often additional weak points in corrosive environments, because of limited galvanization thickness (picture 2.5).

Picture 2.4 Example of driftwood protection barrier with ringnets made from high-tensile wires

Picture 2.5 Corrosion problem of wire rope nets (cross clips and rope wires do often have no sufficient zinc coating and may rust rather soon)

Today, new special manufacturing processes enable the production of diamond structured mesh from high-tensile steel wires. Based on these new product opportunities, new technical applications are possible. In the fields of natural hazard protection and for security, safety and architectural purposes, various application methods were found, developed and applied more or less worldwide with these new kinds of high-tensile steel wire meshes.

In particular for geotechnical slope stabilization solutions, the development of this new wire mesh with a wire tensile strength of min. 1′770 N/mm^2 offers new possibilities for efficient and especially also economical protection of slopes.

Obviously, a new mesh with such interesting properties alone is not sufficient for serious geotechnical solutions and engineered applications.

Consequently, an adapted new dimensioning method for these kind of flexible slope stabilization systems with high-tensile steel wire mesh had to be found, analyzed and tested in order to finally develop an entire new system.

The authors of this publication would like to point out clearly that most parts of the book were already published in previous years. Several main parts of this book are based on the doctoral thesis of Stephan Wartmann (April 2011; [142]). The publication is summarizing the entire concept and method in a global way and overall view, reflecting on all aspects including environmental, carbon footprint and installation issues. The corresponding publications and technical papers can be found in the list of references.

In that sense, the first chapters of this book are providing an overview of the traditional techniques and conventional dimensioning concepts. Afterwards, the new high-tensile steel wire mesh as well as the corresponding connection components are presented including the necessary laboratory material and force transmission tests.

Based on those parameters and results, the following chapters are illustrating the new dimensioning method as well as dimensioning examples.

Finally, the last chapters provide additional important findings regarding technical project management, installation steps and procedures and report about practical examples of executed projects.

3 Traditional methods using mesh and wire rope nets

In the past, the slope of soil or solid rock to be protected was traditionally cut as suitable and levelled as possible to the profile and then covered with a wire mesh whose individual wires provided a tensile strength of approx. 400 - 650 N/mm^2. The mesh was fastened to short soil or rock nails [74, 83]. If the mesh itself was inadequate, either the distance between nails had to be reduced or the mesh had to be reinforced by threaded-in steel ropes secured to the nail heads. If long nails (generally more than approx. 4 m) are required for protection to a certain depth, the costs of nailing increase comparatively rapidly and systems become of interest which can absorb and transmit substantially higher forces and thereby allow increasing the distance between nails. Wire rope nets could be used in these instances.

3.1 Wire mesh as a flexible measure to protect surfaces

Slopes of soil or rock to be protected were covered by a wire mesh which is fastened to the soil or rock nails by means of spike plates. A boundary rope (tensioning rope) is additionally provided at the top, if necessary retained by rope anchors as shown on the figure 3.1.

Local, superficial instabilities are to be prevented by the mesh as a securing system. The forces occurring from a local instability are to be transmitted over the mesh and the spike plates onto the nails. Hereby the forces which can be transmitted are limited and depend on the strength of the mesh as well as on the size and type of spike plate.

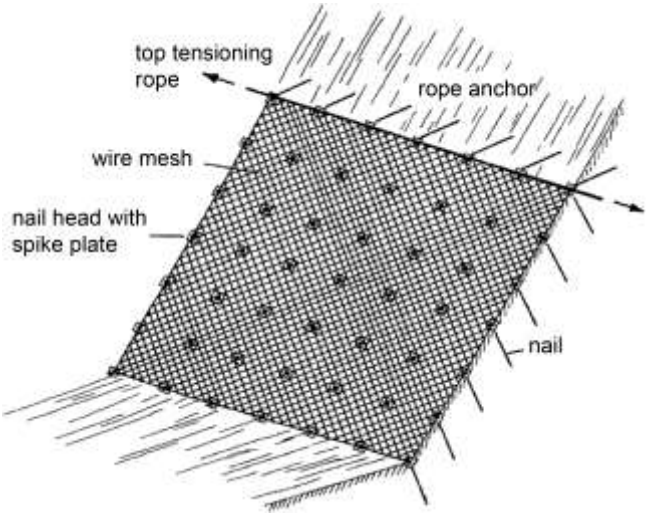

Figure 3.1 Conventional wire mesh in combination with nailing

3.2 Wire rope nets as a flexible measure to protect surfaces

The slope of soil or rock to be protected against erosion or rockfalls is usually first covered with a durable geosynthetic fabric of plastic or if appropriate also with standard steel wire mesh. This is followed by a cover of special rope nets which are sewn together and whose corners are fastened by steel ropes to the soil or rock nails. The mesh size of 150 –300 mm x 150 – 300 mm permits greening and combined with it also planting of higher growing shrubs and small trees suitable for the location [83, 88, 140].

To prevent local superficial instabilities, the retaining forces resulting from the equilibrium consideration can be absorbed by the rope net and passed on directly to the corresponding nails.

The principle of comradeship dominates in the wire rope protection system: if one nail head wants to move downwards due to a high local force, the "surplus forces" are diagonally guided upwards over the upper rope net covers and distributed over several nails (figure 3.2). Important, therefore, is that the uppermost fastening points are always perfectly anchored. Additional rope anchors may be required at the top to transmit and carry these forces into the solid subsoil.

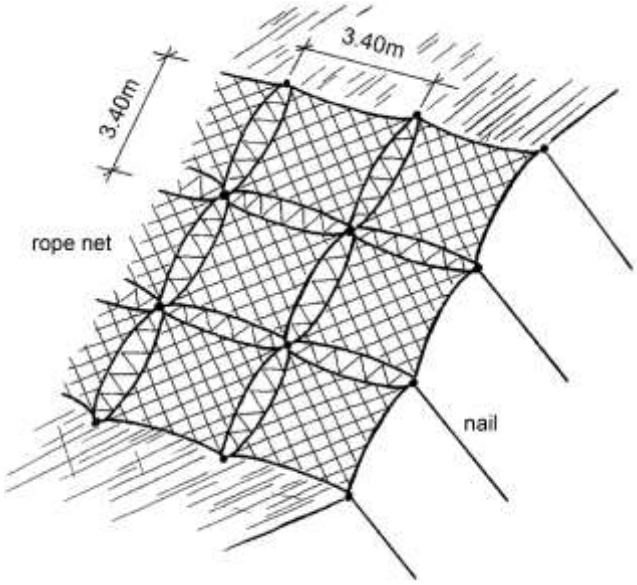

Figure 3.2 Principle of system with rope nets from steel wires (e.g. Pentifix system)

Compared to simple mesh covers, this protection system can absorb very considerable forces. However, the wire rope system is restricted by a fixed nail pattern of 3.3 –3.5 m x 3.3 –3.5 m; in very rare cases even a little bit larger. Extra nails can be placed in the centres of the fields if necessary.

The use of flexible protection systems is basically limited to the prevention of more or less slope parallel instabilities close to the surface, such as they can occur in e.g. weathered, loose cover layers. If a danger prevails from deeper sliding surfaces, the nails alone have to absorb the forces resulting from the overall stability and transmit them to the firm subsoil outside the existing or potential rupture mechanisms.

3.3 Active and passive systems

This publication focuses on “active systems” for slope stabilizations, where a mesh is fixed with nails in relatively short grid distances to the ground, providing pressure to the soil and therefore allowing an active slope protection. One must be clearly distinguish such active systems from so called “passive systems”.

Passive slope safety systems are also often called drape systems since a wire mesh is fixed at the top of a slope and hung down a slope (figure 3.3).

Sometimes additional horizontal or vertical intermediate or bottom ropes and nails are applied, mostly due to local geometries and slope conditions. But in general, such mesh is applied for controlled rockfall trajectories and not for the active fixation of soil and ground. Consequently, they are called “passive systems”. Such passive protection systems are often combined with a ditch at the bottom of the slope and require corresponding maintenance and service efforts.

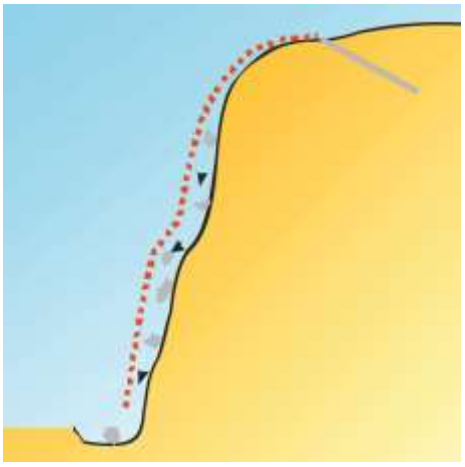

Figure 3.3 Principle drawing of a passive system

3.4 Hard, flexible and soft facing

There are different kind of slope stabilization systems. The draft of European Standard "Soil Nailing" distinguishes between:

- hard – facing
- flexible – facing
- soft – facing

Hard facing is mostly known and applied as concrete or shotcrete slope stabilization systems (picture 3.1). If drainage is solved satisfactory and if applied with sufficient concrete coverage as well as steel reinforcement, such systems are known as reliable stabilization systems.

Picture 3.1 Hard facing (sample for shotcrete slope stabilization system)

Flexible facing is commonly known as active slope stabilization systems where a steel wire mesh is combined with soil nailing (picture 3.2). Depending on the mesh type, nail and anchor grid must be adapted accordingly.

Picture 3.2 Flexible facing (slope stabilization system with high-tensile steel wire mesh)

Flexible facings are often combined with hydro-seeding solutions. Picture 3.3 illustrates a typical combination of high-tensile steel wire mesh slope stabilization system with greening.

Picture 3.3 Flexible facing combined with hydroseeding

Soft facings consist of different kind of geogrids or geomembranes. They are mostly applied for temporary slope coverage. They are inexpensive solutions and often applied for limited time frame, e.g. on construction sites. Nevertheless, special care must be taken in case of sharp surface elements (e.g. weathered rocks, etc.).

Due to limited ultraviolet resistance of such plastic products, aging is a serious problem for a lot of products. Consequently, such soft facings are mostly not recommended for durable and long-term slope stabilization solutions.

Picture 3.4 Soft facing (sample for high-tensile geogrid)

The TECCO® slope stabilization system is a kind of special flexible facing and therefore, the RUVOLUM® dimensioning method as well as this publication focus on flexible facings with high-tensile steel wire meshes.

4 Traditional dimensioning methods

In the past, various geotechnical calculations and dimensioning concepts were developed and because state of the art for general slope protection engineering[7].

For the purpose of dimensioning the surface protection systems of mesh and/or wire rope nets in their interaction with nailing, it is necessary to investigate possible failure mechanisms.

On the one hand, the installation of the protective devices must ensure that a layer of soil or also a layer of weathered and unconsolidated rock of thickness *t* can be retained with a certain safety against sliding off parallel to the slope on a stable layer as illustrated on figure 4.1.

Figure 4.2 on the other hand shows that local wedge-shaped bodies must be stopped from breaking out.

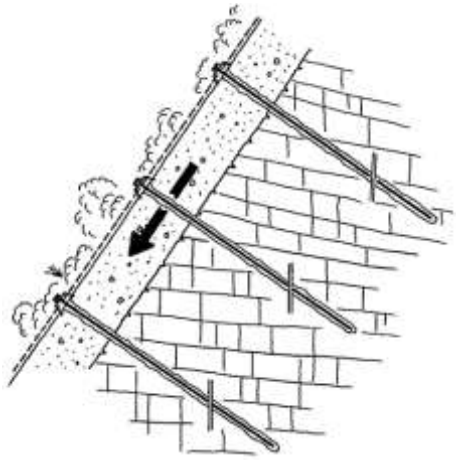

Figure 4.1 Sliding off parallel to the slope

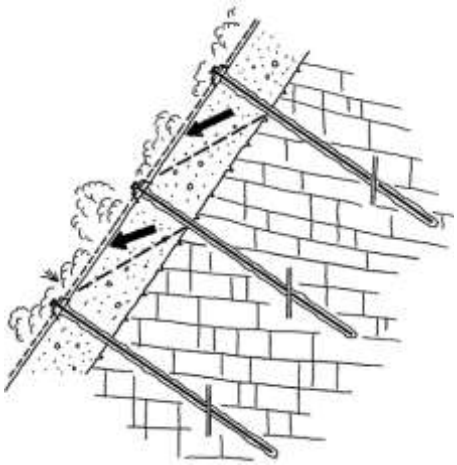

Figure 4.2 Local wedge-shaped rupture bodies

[7] Corresponding (geotechnical) dimensioning concepts are e.g. presented in various publications [47, 75, 109,114].

4.1 Sliding off parallel to the slope

From considerations of equilibrium concerning a body of width *a*, length *b* and thickness *t*, and taking into account the failure condition of Mohr – Coulomb, the following shear force *S* with a stabilizing effect results as far as sliding off parallel to the slope is concerned.

Since the nail heads are fixed against each other, proof of the admissible inner shear resistance of the nail $S_{zul\ (adm)}$ being greater than the shear resistance *S* per individual nail required for a certain safety, is generally sufficient.

Figure 4.3 presents an overview of all forces that are active on the body with a width *a*, a length *b* and a thickness of *t* in order to determine the shear force *S* that is required for a certain safety level [110].

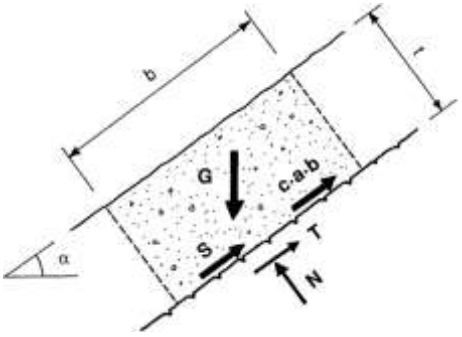

G Dead weight of the cubic body ($G = a \cdot b \cdot t \cdot \gamma$)

γ Unit weight of the soil material

S Resisting shear force required to be absorbed by the nail

t Thickness of the surface layer to be stabilized

c* · *a* · *b Cohesion of the cover layer × ground surface of the body liable to break out

T*, *N Reaction forces from the subsoil

α Inclination of the slope front

Figure 4.3 All forces active on the body of width *a*, length *b* and thickness *t* to determine the shear force *S* required for a certain safety

Based on the overview of all active forces on the body with a width *a*, a length *b* and a thickness *t*, the following equation 4.1 explains the calculation of the corresponding shear force *S*.

$$S\,[\mathrm{kN}] = \frac{a \cdot b \cdot t \cdot \gamma \cdot (F \cdot \sin\alpha - \cos\alpha \cdot \tan\varphi)}{F} - \frac{c \cdot a \cdot b}{F}$$

Equation 4.1 Equation of all active forces on the body of width *a*, length *b* and thickness *t* to determine the shear force *S* required for a certain safety, *F* being the safety factor

4.2 Local wedge-shaped bodies liable to break out

As a result of the investigation of “sliding off parallel to the slope”, the nails are now dimensioned so that the cover layer as a whole can be retained with a certain safety. Further investigation is then required in the area between the individual nails.

Depending on the slope’s geometry it is possible that wedge-shaped rupture bodies come loose unless they are covered by mesh or wire rope nets. Such bodies are to be retained and secured by the use of mesh or wire rope nets as surface protection measures.

The body liable to break out wants to move downwards on a slant. The mesh is held at the top by nails and if appropriate by boundary ropes, is thus subjected to tension. This is applied on the one hand via friction and on the other over the outward movement of the body in question [111].

These interactions are illustrated on the following figure 4.4:

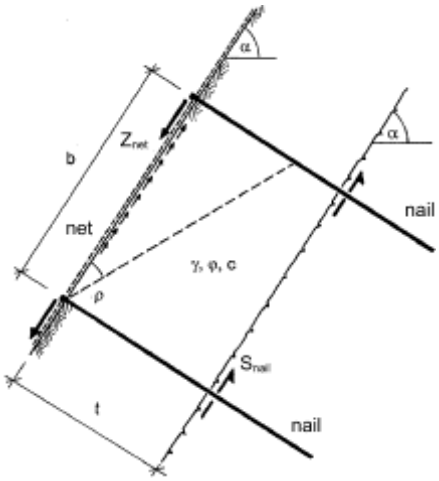

Figure 4.4 Surface stabilization system in combination with soil nailing, local wedge-shaped bodies

The force *Z* parallel to the slope and with a stabilizing effect is called the net or fastening force *Z* (see also figures 4.5 and 4.6).

It is theoretically the force which is transmitted over the mesh or net in the line of slope onto the nail, assuming that the entire force exerted by the mesh or net onto the soil or rock wedge is transmitted onto the nail.

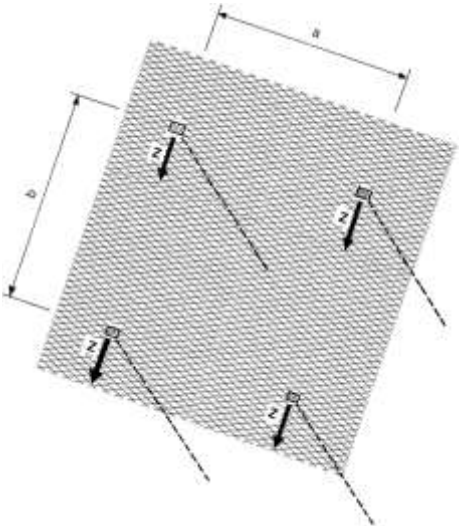

Figure 4.5 Wire mesh with the net force *Z* active on the nail

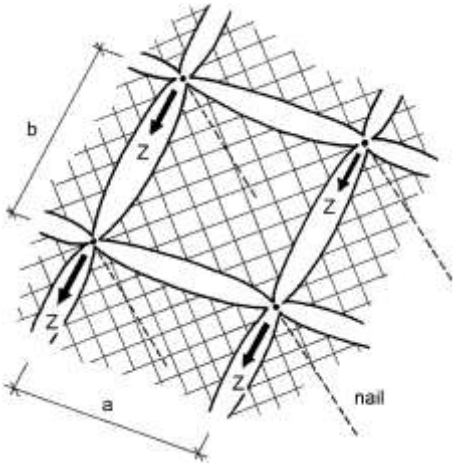

Figure 4.6 Rope net with the net force *Z* active on the nail

The equilibrium conditions are formulated on the basis of the wedge-shaped body in figure 4.7 to determine the net force *Z*. The failure condition of Mohr – Coulomb is again taken into account.

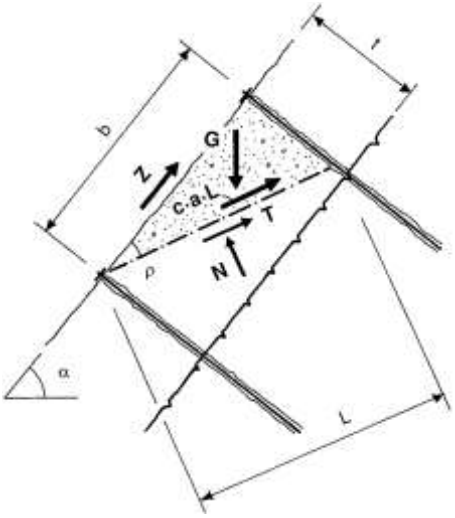

Figure 4.7 All forces active on the wedge-shaped body of width *a*, whereby *N* and *T* represent the reaction forces from the subsoil

The following equation 4.2 results for the net force *Z* per fastening point by solving the equation system and after the corresponding algebraic conversions.

Hereby the angle ρ is varied to such an extent that *Z* is the maximum, whereby $\rho \leq arc\ tan\ (t/b)$ is to be the case.

$$Z\ [\mathrm{kN}] = \frac{a \cdot b \cdot b \cdot \tan\rho \cdot \gamma \cdot (F \cdot \sin(\alpha - \rho) - \cos(\alpha - \rho) \cdot \tan\varphi)}{2 \cdot (F \cdot \cos\rho - \sin\rho \cdot \tan\varphi)} - \frac{c \cdot a \cdot b}{\cos\rho \cdot (F \cdot \cos\rho - \sin\rho \cdot \tan\varphi)}$$

Equation 4.2 All forces active on the wedge-shaped body of width *a*, whereby *N* and *T* represent the reaction forces from the subsoil

Taking into account a certain safety level *F*, the wire mesh plus possibly installed bracing ropes or the wire rope net, respectively, must be able to transmit the force *Z* into the nail.

If this is not possible with the selected distance between nails due to the system, the distances between nails must be adapted accordingly.

4.3 Required input quantities

In order to dimension the surface protection system consisting of wire mesh or wire rope net and nailing, it is necessary, on the one hand to determine the geotechnical characteristic values of the surface layer to be protected.

On the other hand, various geometrical figures such as the inclination of the slope, the horizontal distance between nails and that in the line of slope, or the layer thickness must be stated [75, 112, 115].

The overview below shows the parameters required for dimensioning:

Geotechnical parameters

Friction angle	φ	[°]
Cohesion	c	[kN/m^2]
Unit weight	γ	[kN/m^3]

Geometrical input quantities

Inclination of the slope	α	[°]
Distance between nails, horizontal	a	[m]
Distance between nails, line of slope	b	[m]
Layer thickness	t	[m]
Safety level	F_{mod}	[–]

4.4 Proof of the terrain's resistance against sliding (deep sliding surfaces)

This investigation concerns the proofs of safety against failure of the terrain, for which the nails are included in the stability calculations with the topographically and geologically adapted sliding surfaces, usually as tension elements with a stabilizing effect and in rarer cases as shear elements.

These proofs must be established separately and are not directly related to the proofs for the protection of the surface, except that the nail pattern should correspond as far as possible to the system related, usual nail distances [1, 56, 71].

Typical failure cases are e.g. curved sliding surfaces (figure 4.8) and straight-lined sliding surfaces (figure 4.9).

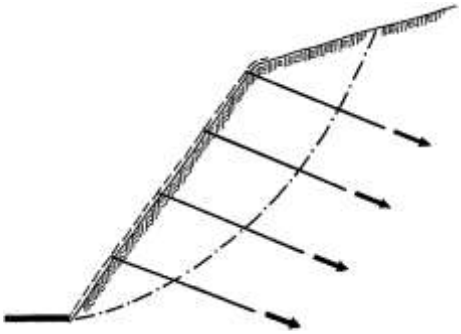

Figure 4.8 Curved sliding surfaces

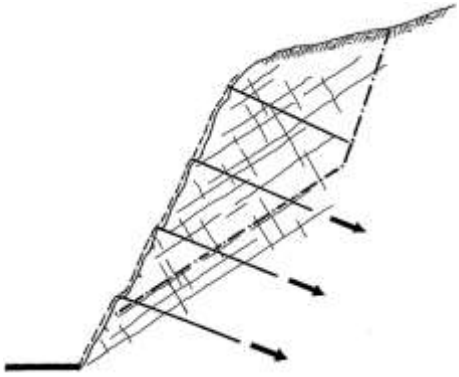

Figure 4.9 Straight-lined sliding surfaces

For further and more detailed information regarding investigations of the global stability, please see chapter 8.8.

5 High-tensile steel wire mesh

High-tensile steel wire meshes were developed by the end of the last century for the very first time and they are commercially available since the early stage of the new millennium. These meshes are produced with different types of high carbon steel wires, using different wire diameters and mesh geometries [44, 45, 48].

Today, these high-tensile steel wire meshes are widely used for different applications such as natural hazard protection systems (pictures 5.1 and 5.2) [138], architecture (picture 5.3), intrusion, escape and blast protection, security fences as well as for certain defence applications and against biological hazard threats.

Picture 5.1 Rockfall barrier with high-tensile steel wire mesh

Picture 5.2 Avalanche prevention system with high-tensile steel wire mesh

Picture 5.3 Architecture safety application with high-tensile steel wire mesh

Picture 5.4 illustrates the high-performance load capacity of high-tensile steel wires, where a car is lifted by a single 3.0 mm wire.

Picture 5.4 A high-tensile steel wire (1'770 N/mm^2) with a diameter of only 3.0 mm is lifting a car[8]

[8] Lifting test with the 3.0 mm high-tensile steel wire was conducted by the Swiss Federal Research institute WSL at the Walenstadt rockfall barrier test site in Switzerland on the occasion of the International Geobrugg Annual Meeting dated June 23rd 2006.

On the following picture 5.5, a heavy concrete block with the weight of 16′000 kg is lifted by a small mesh panel made from high-tensile steel wires with a diameter of 3.0 mm.

Picture 5.5 A concrete block with the weight of 16 metric tons (16′000 kg) is lifted up by a small stripe of a high-tensile steel wire mesh with wire diameter of 3.0 mm[9]

5.1 High-tensile wire mesh as a slope stabilization system

If high-tensile wire mesh is used as a surface stabilization system, the slope of soil or rock to be protected is cut as suitable and levelled as possible to the profile (analogous to the application of simple conventional mesh as protection systems) and then covered with a high-tensile steel wire mesh which is secured to soil or rock nails (figure 5.1). Normally,

[9] Mesh lifting test with the TECCO® G65/3 mm high-tensile steel wire mesh was conducted by the Swiss Federal Research institute WSL at the Walenstadt rockfall barrier test site in Switzerland on the occasion of the International Geobrugg Annual Meeting dated June 23rd 2006.

boundary ropes are threaded into the top, sides and bottom edges, and fixed to rope anchors in the corners. In special cases the top boundary rope and thereby also the mesh can be deep anchored by means of additional rope anchors and intermediate nails [51, 106, 107].

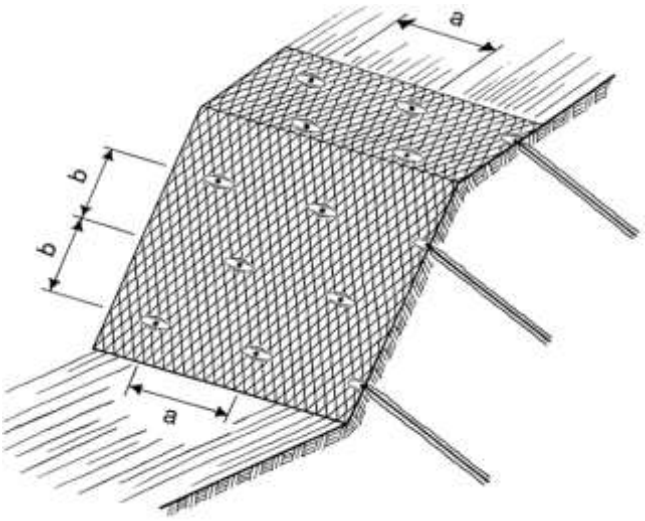

Figure 5.1 General profile and nail arrangement

In comparison with traditional protection systems, the use of high-tensile wire mesh of steel wire for the surface protection of slopes of soil and rock is economical and, thanks to more freedom in the selection of the distances between nails, very flexible. Developments in the material technology enable high-grade and durable products which are ideally matched to the application area.

As it will be explained in chapter 8, the refined dimensioning concept adapted to the new system can be applied to high-performance mesh as well as the traditionally used simple mesh. Hereby the material specific characteristics must be selected to suit the protection system concerned.

Before explaining in detail the new method of designing of flexible slope stabilization systems with high-tensile steel wire meshes, two important novelties compared to the traditional dimensioning of slope protection systems need to be explained. They concern the arrangement and the pretensioning of the nails.

5.2 Nail arrangement

So far, the system often dictated a matrix-type arrangement of the nails – horizontal in rows and below each other in the line of slope[10]. This means that theoretical bodies liable

[10] This is especially the case with wire rope net systems, due to geometrical reasons [83].

to break out can be formed between the nails. They extend over the full height of the slope and are in the maximum as wide as the horizontal distance a between nails. In future, a nail pattern is to be selected on purpose in which the nails in the rows are offset by half a horizontal distance between nails (figures 5.1 and 5.2). This means that the maximum possible bodies liable to break out are limited to a width a and a length of $2 \cdot b$ [52, 108].

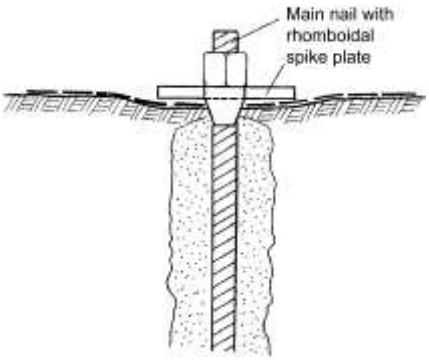

Figure 5.2 Nail head section with spike plate

This nail pattern represents a basic pattern. In the choice of nail positions, the structure of the mesh now enables to deviate from this basic pattern within reasonable limits (figures 5.1 and 5.3). Local discontinuities in the slope can be counteracted in optimum manner. If low points exist, it is recommended to position the nails in those spots so that the mesh is optimally tensioned by the tightening of the nail [53].

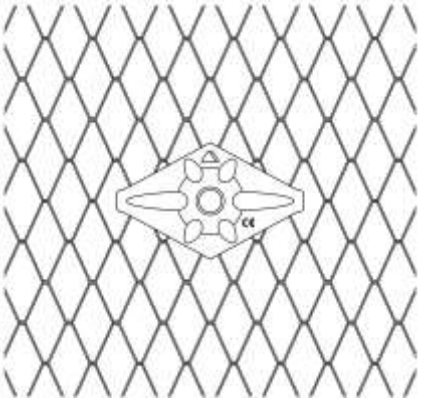

Figure 5.3 Top view of nail head section and spike plate (principle drawing)

5.3 Pretensioning of the nails

The method of designing a flexible slope stabilization system with high-tensile steel wire meshes is providing a new concept of load transfer around the nail head area. This allows substantial increased and optimized force transfer from the mesh to the spike plates and finally into the main nails.

The nail head area is designed so that it can be pretensioned with the force V (see also picture 5.6). This improves the static effectiveness of the system and limits the deformations in the area of the slope.

Pretensioning is enabled by special head plates and the high static effectiveness of the high-tensile mesh itself. Depending on static requirements, the pretensioning forces to be applied by controlled tightening of the nut in the nail's head section amount up to maximum 50 kN (e.g. for the high-tensile mesh with the so called TECCO® system).

Picture 5.6 Spike plate with high-tensile steel wire mesh

Important remark

Only meshes made from high-tensile steel wire can be used as above mentioned. Normal steel wire meshes tend to deform plastically, and those nets are unable to distribute the pretensioning forces and will therefore not be able to transfer the necessary loads[11].

5.4 High-tensile steel wire mesh

As presented at the beginning of chapter 5, there is a wide use for meshes made from high-tensile steel wire. The most well-known ones are the so called ROMBO[12], DELTAX®[13] and TECCO® meshes.

---

[11] For general geotechnical slope protection applications, it is strongly recommended that such conventional steel wire meshes should only be used with smaller nail grids of max. 1.5 m nail distances [108].

[12] ROMBO high-tensile steel wire meshes are normally made from 4.0 mm wire. They are especially used for architectural, security and industrial safety applications.

[13] DELTAX® meshes are made from high-tensile wires with smaller diameters. The mesh DELTAX® G80/2 is a light weight alternative to standard hexagonal steel wire meshes with a diameter of 2.7 –3.0 mm [4]. Due to the very low weight of only 0.65 kg/m^2, they are preferred for many applications, especially also in steep terrain with complicated access.

TECCO® is by far the most common used mesh for geotechnical and geological engineered solutions. It is typically installed for rockfall protection kits, attenuator and drape systems, avalanche prevention systems as well for debris flow, mud flow and landslide protection applications.

For flexible slope stabilization systems, the so called TECCO® G65/3[14] is the most common used high-tensile steel wire mesh. Consequently, this publication will refer often to this type of steel wire mesh.

The high-tensile wire mesh type TECCO® G65/3 has a considerable tensile strength of approximately 150 kN/m in longitudinal direction. Substantially higher forces can be absorbed by this mesh in comparison with the wire mesh traditionally available on the market, offering a tensile strength in longitudinal direction of approximately 50 kN/m at comparable mesh size and similar wire diameter.

Compared to wire rope nets, the high-tensile wire mesh with their special properties provide a statically virtually equivalent surface protection system which is, however, substantially more economical. Figure 5.4 shows the high-tensile mesh of type TECCO® in a three-dimensional, schematic presentation.

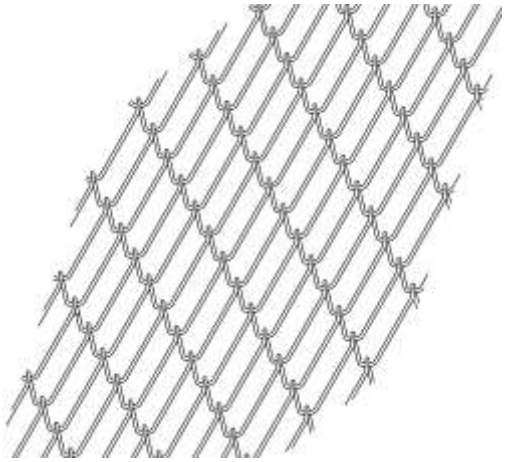

Figure 5.4 Schematic, three-dimensional presentation of high-tensile mesh type TECCO®

5.5 Material properties of high-tensile wire mesh

The new mesh type TECCO® G65/3 of high-tensile wire features a diamond-shaped individual mesh measuring 83 mm × 143 mm[15]. They are produced by single twisting of the wire like for a diagonal mesh. This results in a calibre diameter of 65 mm, which is normally

[14] The technical data sheet of TECCO® G65/3 is shown on appendix B. (Wire diameter is 3.0 mm, mesh unit opening is 65 mm.)

[15] Detailed geometry is shown on the technical data sheet of TECCO® G65/3 in appendix B.

small enough so that no additional mesh of yet smaller mesh size is required. The wire used for the production of the mesh has a diameter of 3 mm. The gentle deflection of the wire to form the individual mesh results in a three-dimensionality of the mesh which improves the connection to the subsoil and possibly applied hydro-seeding to a massive extent.

Thanks to the high carbon steel wires of the mesh, the weight is rather small. One square meter of TECCO® G65/3 mm[16] weighs only 1.65 kg/m^2. The mesh is delivered in rolls of 3.9 m width and 30 m length; consequently, one mesh roll weights 193 kg.

High-tensile wires of a rated wire strength of 1370 N/mm^2 and higher are used for industrial applications such as springs and fastening elements, but in particular also for pretensioning strands and wire ropes. The new mesh can be produced from rope wire according to EN 10264-2 [44, 45] with rated wire strength of up to 2160 N/mm^2.

The production of rope wire is a complicated and expensive process. The hot-rolled rod of diameter 5.5 mm and thicker is first pickled, redrawn and salt bath-patented. This heat treatment provides the steel wire with a structure, referred to as sorbite, which lends itself well to cold forming. The wire's strength is determined by its chemical composition and the reduction of its overall cross-section on cold drawing. Of importance here is the high residual deformability which is reflected by high torsional and rotating bending fatigue strength, a particularly important aspect in ropes for aerial cable cars.

The strength characteristics of the rope wire according to EN 10264-2 vary substantially from the international standards applicable to soft wire qualities[17]. On tensioning over sharp rock edges, for example, the extremely hard wire material EN 10264-2 cannot be pinched off and is easily pulled down into hollows of the terrain.

Apart from this, the extraordinary high stiffness of the wire also helps to prevent so called runners [130].

Chapter 5.5 is providing several sample test series that were conducted with some high-tensile steel wire meshes and other components. This is meant to explain the test methods and to provide an overview about the corresponding results. It is not showing an entire summary of all conducted tests, since on very regular bases those tests are made (internally and externally) by the production companies in order to guarantee quality and performance of these products.

5.5.1 Tensile tests and results on single wire

The tensile tests were performed in compliance with DIN EN 10002 part 1 addendum B [40].

Picture 5.7 shows the corresponding wire test equipment for the determination of the tensile strength.

[16] Because of abbreviations reasons, the TECCO® G65/3mm is normally also called “TECCO® G65/3”.
[17] For instance material commercially available according to DIN 1548, BSS 1052/80–BSS 443/82.

Picture 5.7 Equipment for tests on single wires

The test on a single wire produced the following results[18]:

Parameters of the wires

Nominal diameter of wire: 3.0 mm
Nominal strength: 1′770 N/mm^2
Measured length: 100 mm
Surface treatment: Al-Zn-Coating

The following table 5.1 provides an overview of the tested single wires:

Tensile strength test on single wires			
Sample type	Sample no.	Breaking load, F_m (N)	Tensile strength R_m (N/mm^2)
Single wire with diameter = 3.0 mm, length = 100 mm	1	13′150	1′814
	2	12′920	1′770
Average values		13′035	1′792

Table 5.1 Results of tests on single wires

The elongation value A_{100mm} was between 2.0 and 2.5%.

[18] Test were coordinated and supervised by TÜV Rheinland, LGA Nuremberg, Germany [13, 78, 81].

It is obvious that the above mentioned two wire tests would make it difficult for detailed statistical analysis. However, most high-tensile steel wire manufacturing sites are checking, testing and reporting all main technical data of supplied wires, (e.g. including tensile, bending, torsion and coating tests). In that sense, all wires used for high-tensile steel wire meshes are carefully tested prior to production in order to ensure quality and technical performance.

A wider range of selected TECCO® 3.0 mm high-tensile wire tests is shown on appendix G in order to illustrate the steel wire quality control.

5.5.2 Machinery for the mesh tests in longitudinal and transverse directions

In these test series a new testing installation was used, designed and able to simulate a plane bi-directional tensile load condition of any kind of mesh.

Picture 5.8 shows the overview of the new mesh test equipment.

This new testing installation[19] allows testing a wide variety of nets and meshes, because it has freedom in the number of bracing points of the mesh along the borders and the possibility to adjust the size of the sample.

Picture 5.8 Overview picture of mesh test equipment

[19] Test method was developed by Geobrugg AG (Romanshorn, Switzerland) in coordination with Rüegger+Flum AG (St. Gallen, Switzerland), University of Cantabria (Santander, Spain) and supervised by TÜV Rheinland (Nuremberg, Germany) [13, 78, 81, 128, 129, 131].

The testing installation consists of a modified main frame with increased width and two new anvil blocks mounted within. One of them (in blue colour) is fixed to the main frame and the other one sliding (in red colour) is connected to the pulling cables. The mesh is braced to sliding beams through a set of elements provided with two ring and ball bearings. Six screw bolts that allow the adjustment of the sample width and connect the sliding beam to the lateral fixation support. The bolts on one side were instrumented to register the transversal load transferred to the fixation (pictures 5.9 and 5.10).

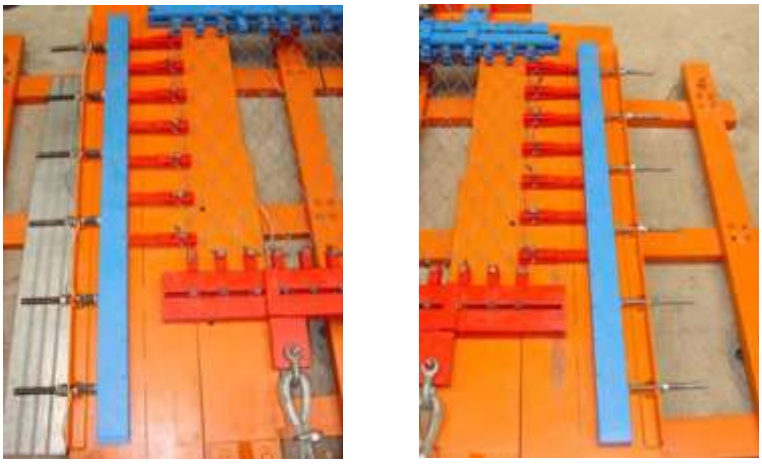

Pictures 5.9 Lateral fixation system of sliding beams to adjust the width of the test sample. In the left the connecting screw bolts that serves as transversal load measurement devices.

In the secondary frame, is installed the hydraulic cylinder with a load measurement cell in the head of the piston. The secondary frame also serves as a guide of the sliding car, which transfers the load applied by the hydraulic cylinder by means of cables to the test sample.

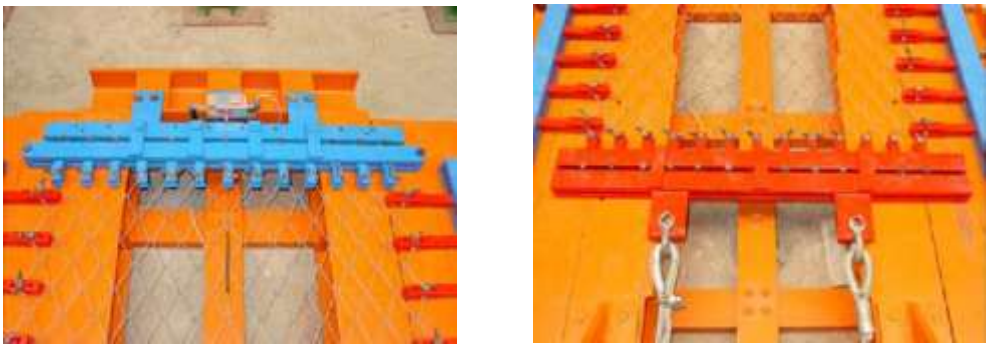

Pictures 5.10 View of the fixed anvil blocks (in blue colour) and the sliding anvil (in red colour) with the points of connection of the sample ends

Details of the device for the measurement of the longitudinal deformation can be seen on the picture 5.11.

Picture 5.11 Detail of the device for the measurement of the longitudinal deformation

Picture 5.12 provides an overview of the secondary frame with the hydraulic cylinder and the connections with the sliding car.

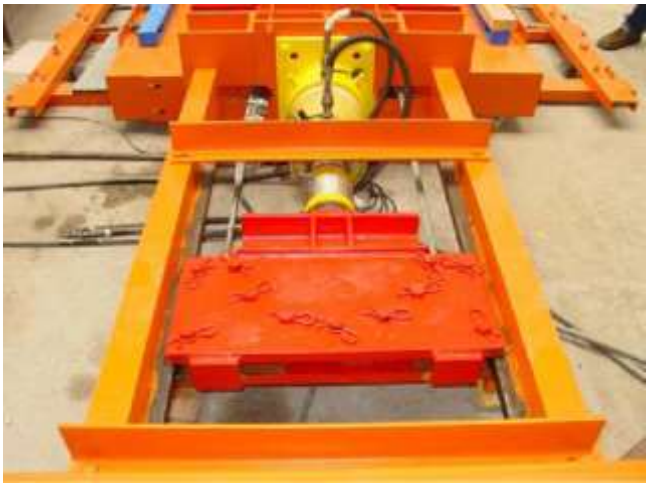

Picture 5.12 View of the secondary frame with the hydraulic cylinder and the sliding car

5.5.3 Test setup and results for tensile test in the longitudinal direction

The main parameters of the tested mesh can be summarized as follows:

Parameter of mesh:

Mesh type: TECCO® G65/3 (opening 65 mm; 3.0 mm wires)

Width: 1′079 mm (13 rhombuses × 83 mm = 1′079 mm)

Length: 1′001 mm (7 rhombuses × 143 mm = 1′001 mm)

No. of meshes in the direction of tension: 7

No. of meshes transverse to the direction of tension: 13

The following picture 5.13 shows the experimental setup for the tensile test in the longitudinal direction.

Picture 5.13 Experimental setup for tensile tests in the longitudinal direction

Table 5.2 presents the results of the longitudinal tensile tests:

Longitudinal tensile strength tests			
Sample type (1079 × 1001 mm)	Sample no.	Unitary elongation (mm/m)	Breaking load (kN/m)
High-tensile steel wire mesh, type TECCO® G65/3	1	58.9	167.5
	2	60.8	165.7
	3	61.8	167.9
Average values		60.5	167.1

Table 5.2 Results of longitudinal tensile strength tests[20]

[20] All tests are coordinated, supervised, documented and reported by TÜV Rheinland, Germany [13, 78, 81, 127].

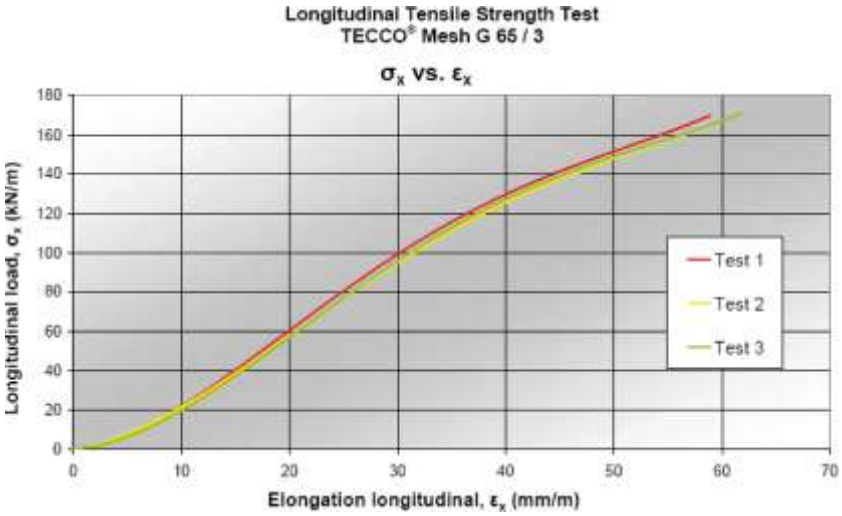

Figure 5.5 Results of the tensile tests in longitudinal direction (TECCO® G65/3)

Summary of the results of the longitudinal direction tests

- The meshes were loaded until failure.
- They broke at loads between 165.7 kN/m and 168.0 kN/m.
- Rupture deformation was between 58.9 mm/m and 61.8 mm/m.
- The load-deformation curve shows an almost unique, smooth and repeatable behaviour of all test meshes.

5.5.4 Test setup and results for tensile test in the transverse direction

For set up of the tensile test in the transverse direction, the parameters of the mesh were as follows:

Parameters of mesh:

Mesh type:	TECCO® G65/3 (opening 65 mm; 3.0 mm wires)
Width:	1′001 mm (7 rhombuses × 143 mm = 1′001 mm)
Length:	581 mm (7 rhombuses × 83 mm = 581 mm)
No. of meshes in the direction of tension:	7
No. of meshes transverse to the direction of tension:	7

Picture 5.14 shows the overview of the experimental setup for the tensile tests in the transverse direction.

Picture 5.14 Experimental setup for tensile tests in the transverse direction

The table 5.3 summarizes the test results of the transverse tensile tests and figure 5.6 illustrates the corresponding results graphically.

Transverse tensile strength tests			
Sample type (1079 x 1001 mm)	Sample no.	Unitary elongation (mm/m)	Breaking load (kN/m)
High-tensile steel wire mesh, type TECCO® G65/3 mm	1	204.6	57.0
	2	211.4	59.6
	3	198.5	56.5
Average values		204.8	57.7

Table 5.3 Results of tests of transverse tensile strength test[21]

[21] All tests are coordinated, supervised, documented and reported by TÜV Rheinland, Germany [13, 78, 81, 127].

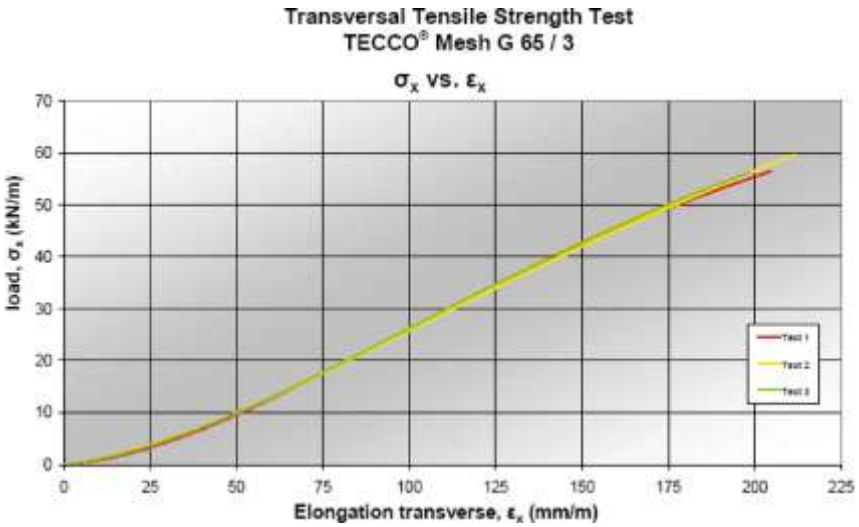

Figure 5.6 Results of the tensile tests in transverse direction (TECCO® G65/3)

Summary of results of the transverse direction test

- The meshes were loaded until failure.
- The meshes broke at loads between 56.5 kN/m and 59.6 kN/m.
- Rupture deformation of the meshes was between 198.5 mm/m and 211.4 mm/m.
- The load-deformation curve shows an almost unique, smooth and repeatable behaviour of all test meshes.

5.5 Corrosion protection

To meet the high demands in respect of durability, the known anti-corrosion process of aluminium-zinc alloying is used to protect the wire surface. The protective layer forms a kind of eutectic alloy. The zinc acts as the cathode towards the steel wire. The admixed aluminium slows down the decomposition process of the zinc layer by a factor[22] of at least 3. The effect of the cathode protection is that local injuries of the protective layer cause no corrosion in the particular spot.

This contrary to plastic-coated wires, where local damage to the plastic layer leads to concentrated corrosion attacks, sometimes additionally combined with underrusting effects which results in even accelerated corrosion activities.

[22] Reference to several publications of Prof. Dr. Rolf Nünninghoff and others [2, 91, 92, 93, 94, 95, 96].

The aluminium-zinc process for wires has been practised for some time and is used on both soft wires for common mesh and fence wires along motorways, but also on high-tensile wires especially in the fishing industry or for vineyards.

The maximum possible deposit of zinc or Al/Zn alloys depends on the wire diameter. The layer thicknesses or the mass per square meter are also laid down by European Standard EN 10244-2 [44]. Although it is known that the decomposition of zinc layers depends in general heavily on the locally prevailing conditions, a sufficient life span is achieved with the advanced technology of Al/Zn protective layer also in a highly corrosive environment.

Important remarks regarding corrosion protection and thickness of coatings:

- The actual thickness of the corrosion protective layer (e.g. zinc coating or zinc aluminium coatings) is important for the life span and for the level of corrosion protection.
- However, the quality and especially the purity degree of such coatings may even be more important since pollution particles and/or impurities can have a negative influence to the processes of corrosion protection. Such impurities may cause accelerated electro-chemical processes and will influence the appropriate functioning of the sacrificial anode corrosion protection of the coatings.
- Consequently, the corrosion protection level can not only be measured by the thickness and the type of the coating. Its quality and purity are often even more important. Therefore, accelerated weathering tests are an important tool to measure and compare corrosion protection of different wire and coating types.

5.6.1 Accelerated weathering tests

In order to ensure the sustainability of the high-tensile steel wire meshes, various accelerated weathering tests were conducted as follows:

SO_2 Test (SO_2 spray test, Kesternich test)

The tests were carried out in accordance with DIN 50018 KFW 2.0 S [10, 42, 63]. The required amount of SO_2 (2 litre) was made with addition of 11.35 g natrium sulphide (NA_2SO_3) in 800 ml, with distilled water, concentrated sulphuric acid. 5 test samples were taken out after 5 and 10 spray cycles for the determination of the corresponding remaining coating thickness.

Salt spray tests (NaCl spray test)

The tests were made according to DIN 50021 SS[23] [3, 10, 43, 63]. 5 test samples were taken out after 100 and 200 hours of spray operation for the determination of the corresponding remaining coating thickness.

Test material

The test material was a high-tensile strength steel wire (same as TECCO® G65/3 wire) with a wire diameter of 3.0 mm. The initial coating thickness (zinc and aluminium zinc coating[24]) was for both types of wire 300 g/m^2. The length of the test samples was 30 cm.

---

[23] DIN 50021 SS is almost equal to ASTM-B117 (USA).

[24] The used Zn–Al-coating was according to GEOBRUGG Supercoating standard.

Results of corrosion laboratory tests

The results are shown on the following figures 5.7. It can be summarized that many similar tests were carried out on various test institutes worldwide and that all test investigations showed that the life time of Zn–Al-coating (supercoating) is at least three times (3×) better than standard Zn-coating.

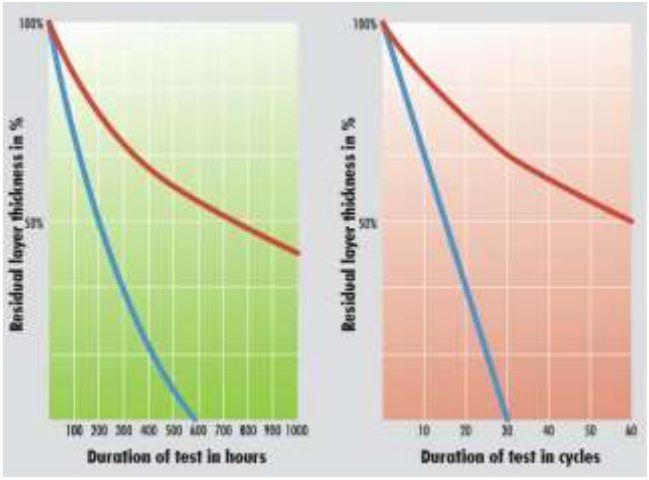

Figure 5.7 Overview of average value results of saltspray test and Kesternich test
Comparison between Zn-coated and Zn–Al-coated wires; red curve = Zn–Al-coating; blue curve = Zn-coating
Left: NaCl – spray test (salt spray test)
Right: SO_2 – spray test (Kesternich test)

5.6.2 Longterm field test for comparison between Zn coated and Zn-Al coated wires

The cross sections illustrated on pictures 5.15 show a comparison of wires treated with Zn–Al-coating[25] and hot-dip galvanization.

The pictures were taken by an electron microscope[26] after the wires had been exposed to environmental influences for 14 years.

The top pictures show the surface of the zinc-aluminium coating whereas the bottom pictures show the surface of a standard zinc coating (hot-dip galvanized).

[25] Geobrugg Supercoating type of Zn–Al coated steel wires were used.
[26] Tests and research done by Bergische Universität Wuppertal (University of Wuppertal), Germany [10, 97, 98] in co-ordination with the Technical Department of Geobrugg AG.

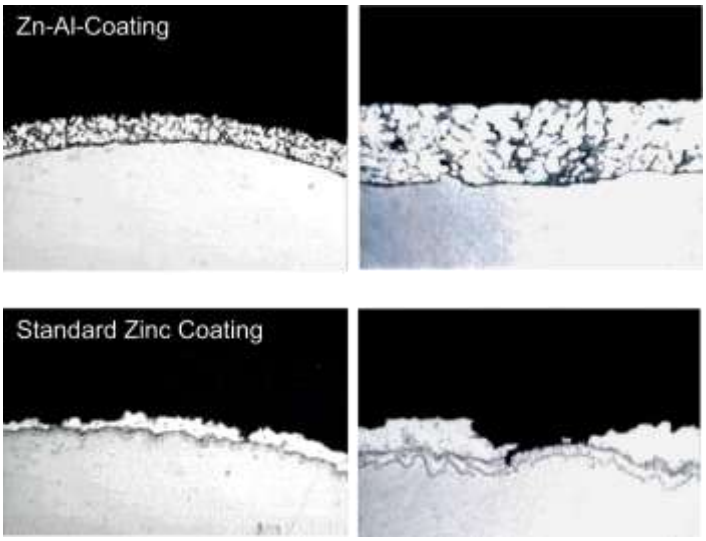

Pictures 5.15 Comparison between Zn–Al coated wires (top pictures) and standard zinc coated wires (bottom pictures) after 14 years

The picture 5.16 provides a more detailed view of the zinc coating surface. The top level (1) shows a heterogeneous surface with partial complete disintegration and with heavy rust components. Below, there is the second layer (2) which is an intermediate hard zinc layer consisting of iron and zinc. And at the bottom, there is the actual steel wire (3).

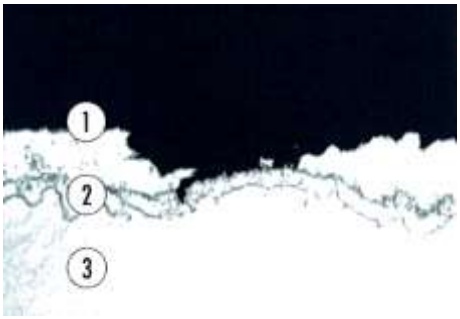

Picture 5.16 Surface of a standard zinc coating (hot-dip galvanized)
1) Heterogeneous surface (zinc), partially complete disintegration and/or already with rust formation
2) Hard zinc layer (iron/zinc)
3) Steel wire (Fe)

The following picture 5.17 shows the details of the zinc aluminium coated wire surface. On the top (1), there is a smooth surface with aluminium oxide layer. The main coating (2) illustrates the darker parts of the structure with the aluminium lamellas of the typical eutectic structure as a homogeneous coating level with zinc and aluminium. And at the bottom (3), there is again the core with the steel part of the wire.

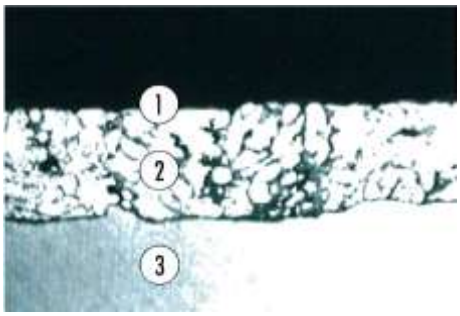

Picture 5.17 Surface of a zinc aluminium coated steel wire
1) Smooth surface (aluminium oxide layer)
2) Homogeneous zinc-aluminium layer
3) Steel wire (Fe)

5.6.3 Long-term field study of Zn–Al-coated wires in alkaline environment

During the installation process it cannot fully be avoided that the high-tensile steel wire meshes are getting in contact with anchor grout, fresh concrete or part of shotcrete. Therefore, the influence of such interactions was investigated during a long-term field test study [9].

The long-term field study that has been carried out that examined for the first time the corrosion resistance of Zn-Al coated wire mesh in an alkaline environment, i.e. in contact with anchor grout.

Unlike non-coated steel wires that do not corrode in fresh concrete with a pH value between 12 and 13, corrosion affects galvanized and Zn-Al coated wires in this medium. However, the CO_2 entering the concrete induces a fast reduction of the pH value. The affection of the Zn and Zn/Al alloys is reduced and protective layers are built up around the wires. Once the protective layer is fully established, the behaviour regarding corrosion can hardly be distinguished from atmospheric conditions.

Experiment set-up

Material used:	TECCO® mesh	G65/3
	Wire diameter	3.0 mm
	Tensile strength	1′770 N/mm²
	Zn/Al-Layer (Coating)	200 g/m²

Different Zn–Al coated high-tensile steel wire meshes where installed on a test site in Romanshorn, Switzerland (see following picture 5.18).

Besides the reference samples, some samples where covered fully or partially with grout. Another sample was splattered with grout but cleaned with a towel after 30 minutes. This procedure aimed to simulate different kinds of contact between mesh and grout that may occur during the installation of such a protection system.

In the detail, the following samples were installed (picture 5.18):

A: Reference surface TECCO® mesh "without grout" (fully covered during grout application)

B: TECCO® mesh, grout and galvanized anchor

C: TECCO® mesh, splattered with grout

D: TECCO® mesh, splattered with grout and cleaned with a towel after 30 minutes

E: Reference area for lab tests and reference values (cut and stored)

F: TECCO® mesh covered with anchor/nail grout

Picture 5.18 Test site in Romanshorn (Switzerland)

Removal of the samples

The removal of the samples took place after 2½ years and was documented with pictures (partially shown on pictures 5.19).

Pictures 5.19 Test site after 2.5 years (left) and detail of sample (right)

Determination of the thickness of zinc aluminium layers

Volumetric method

The thickness of the Al–Zn layers was determined by the volumetric method according to DIN EN 10244-2. The coating is peeled off chemically by HCl and the volume of the hydrogen produced by the reaction is determined. The gravimetric method was discarded, because the result has been falsified by the adhesion of grout parts on the wire.

Metallographic analyses

Metallographic analyses have been carried out for the further assessment of the coatings in the transition area grout/air. The thickness of the layers is given in µm. The conversion into g/m^2 (comparative values to the volumetric analysis) was carried out using the formula 10 µm = 71 g/m^2[27]. The values are only conditionally comparable with those of the volumetric analysis, because grout and mud falsify the results. This is why grindings were only analysed for the transition area grout/air.

Test of adhesion and embrittlement

The adhesion of the coatings on the steel core was carried out by a torsion test according to DIN EN 10244-2, where the wire is revolved around its own diameter.

Summary of the test results

The pictures of the grindings from the transition area air/grout do not show any differences (see following pictures 5.20).

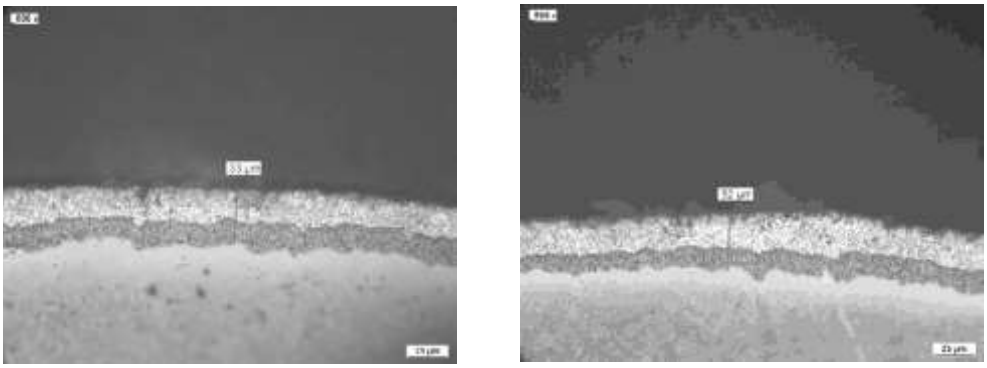

Pictures 5.20 Sample pictures for comparison
Left: Sample that was outside the grout
Right: Sample that was inside the grout

Even under the most extreme conditions (1 ×d), the winding test does not cause any cracks in the Zn-Al layer (pictures 5.21).

[27] 1 µm = 7.14 g/m^2

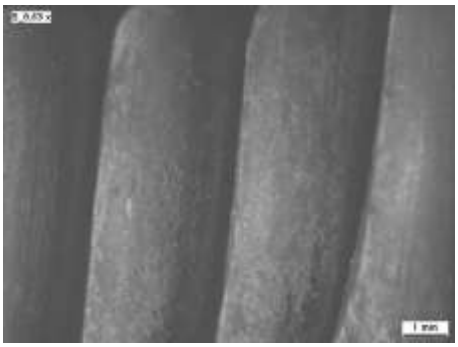

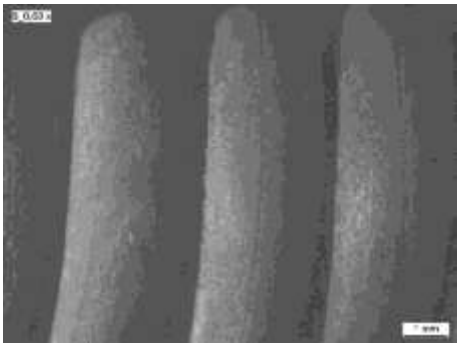

Pictures 5.21 Sample pictures of surface of test materials (after winding tests)
Left: Sample that was outside the grout
Right: Sample that was inside the grout

Conclusions of field study in alkaline environment

It may be stated that after 2½ years of outdoor weathering, no differences between grout free or grout covered parts of the TECCO® mesh can be observed.

According to the present results, it may be concluded that Al–Zn coated wire mesh may be in contact with grout and can be used as shotcrete reinforcement without any impairment concerning their life span.

5.7 Connection of mesh panels

5.7.1 Importance of connection elements

One single mesh roll or mesh panel does not really help to stabilize an entire slope. Therefore it is of great importance that the individual mesh panels can be combined together by simple means in order to ensure the functioning of a uniform membrane structure of the entire mesh area. It is technically very important that this connection is transferring 100% of the load, can be done safe and from an installation point of view, can be applied quick and little time consuming, whenever possible without the need of additional tools and/or hand machines.

5.7.2 Connection clip

The developed connection clip T3[28] is made from high-tensile steel wire with a minimum tensile strength of 1′770 N/mm^2 just like the high-tensile steel wire mesh itself.

For the connection clip T3, a wire diameter of 4.0 mm is used. The clip (figure 5.8) is only 60 × 21 mm and has two reversed end hooks on the one side of the clamp [54].

[28] Drawings are shown on appendix D.

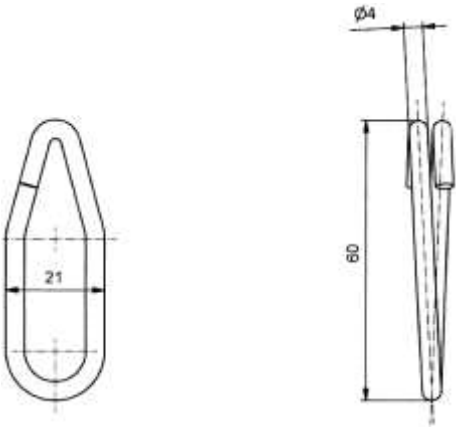

Figure 5.8 Clip for connection of individual mesh panels

This new connection clip can be fixed without any tool which provides an important advantage, especially in steep terrain, where additional tools may cause extra efforts and time-consuming working steps during the mesh connection processes.

On picture 5.22, the hand installation of the connection clip is illustrated.

Picture 5.22 Hand application process for installation of connection clip

The load tests (shown in the following chapter 5.7.2) proof that these connection clips can transfer 100% of the necessary load between the individual mesh panels. And this is of great importance if a uniform membrane structure made from different meshes shall be designed and applied.

5.7.3 Setup and results of connection element tests

In the development of the connection clip T3 on the calibrated tension test bench of Geobrugg AG, tension tests at interconnected TECCO® G65/3 meshes were executed in the transversal direction [54, 125].

Furthermore, tension tests were also executed by Baremo GmbH on their calibrated tension test device in the longitudinal direction.

The following pictures 5.23 show the test arrangement and the conditions before and after loading.

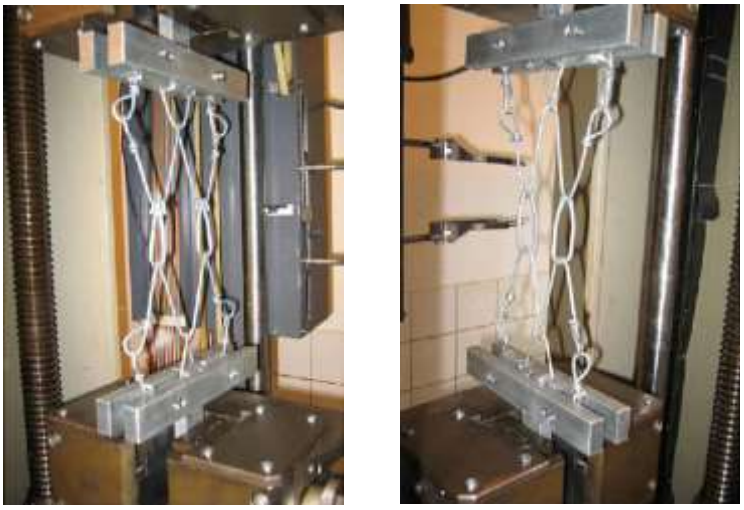

Picture 5.23 Test arrangement for basic clip tests (BAREMO GmbH, Romanshorn, Switzerland)

Picture 5.24 shows an overview of the test arrangement for the mesh connection element tests and picture 5.25 provides a detailed view of the mesh connection for the clip test.

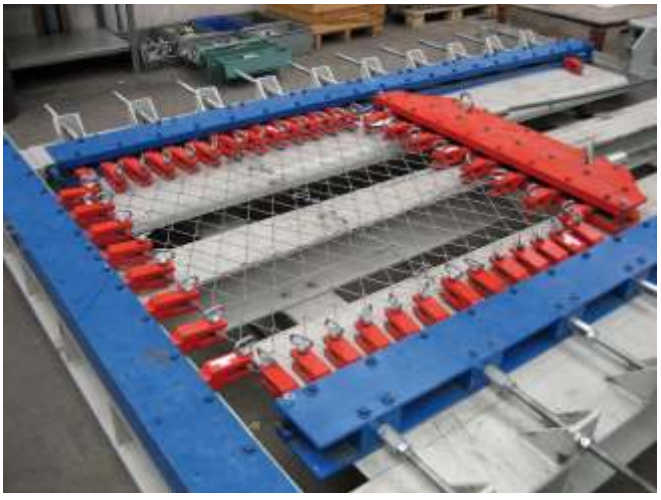

Picture 5.24 Overview of test arrangement for clip tests (Geobrugg AG, Romanshorn, Switzerland)

Picture 5.25 Detail of test arrangement for clip tests

The following pictures 5.26 and 5.27 demonstrate the functioning of the clip connection during and after the load tests.

Picture 5.26 Condition right before the collapse of the high-tensile steel wire mesh

Conclusion of the tensile and load transfer tests

All the tests have shown that the new connection clip T3, used in every diamond mesh, is able to transfer more load than the TECCO® G65/3 for both lateral and longitudinal connection of the mesh.

Correct installation and fixation of the clips and the neighbouring mesh panels are of great importance. Chapters 10.7.3 and chapter 10.7.4 explain the appropriate layout of the different connection options.

Picture 5.27 Condition right after the collapse of the high-tensile steel wire mesh

5.8 System spike plate

Beside the high-tensile steel wire mesh, the TECCO® spike plate is one of the most important system elements. This special plate has been carefully designed in order to meet the best possible load and force transmission between soil, mesh, plate and nail.

It is important that the spike plate is installed horizontally (figure 5.9). This allows the coverage of 16 individual wires of the mesh. If the plate is installed vertically, only 8 individual wires of the mesh are contacted and significant less force transmission can take place. For further information accordingly, please see also chapter 10.7.

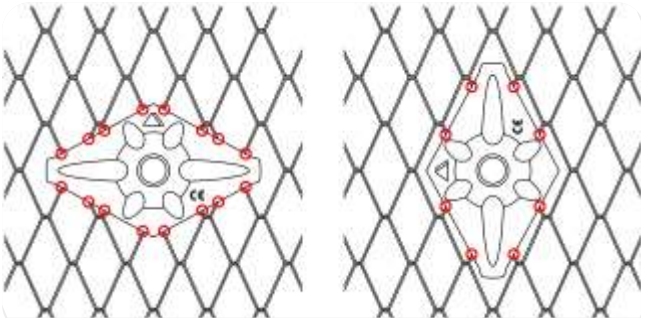

Figure 5.9 Spike plates need to be oriented horizontally; long side must be horizontal. (horizontal installation covers 16 steel wires, vertical installation covers only 8 steel wires)

As a result of various evaluation, material and design tests, the final shape and form of the TECCO® system spike plate was found. The following pictures 5.28 and 5.29 show part of the corresponding material component tests.

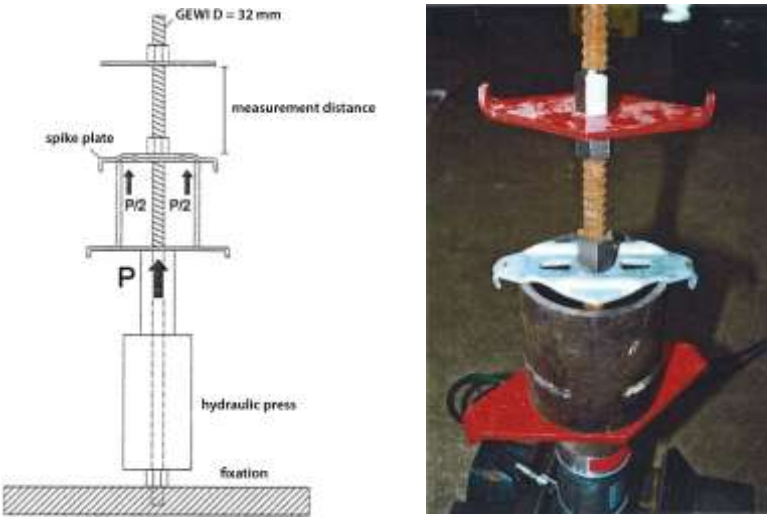

Picture 5.28 Material tests of system spike plate

Picture 5.29 Material tests of system spike plate

It is very decisive that the bending resistance of the system spike plate is high enough in accordance with the TECCO® wire mesh (figure 5.10).

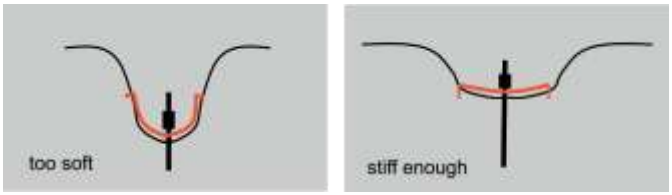

Figure 5.10 Importance of correct stiffness of system spike plate

Important conclusion

The TECCO® slope stabilization system must consist of the official system spike plate. Otherwise, load transmission and system performance will not be possible in accordance with the system's design.

The usage of other plates (even if they look similar) may have serious consequences regarding safety and security of the entire slope stabilization system. Consequently, only the original system spike plate shall be used for the TECCO® system.

5.9 Comparison with traditional steel wire meshes

The previous chapters described the parameters and characteristics of the high-tensile steel wire meshes. In order to demonstrate the significant differences to traditional steel meshes, several comparison tests were conducted. Some of the strongest commercially available wire meshes were chosen in order to provide a fair comparison and show the unique performance and load transformation capacities of high-tensile steel wire meshes.

5.9.1 Comparison test with heavy chain-link mesh made from traditional steel wire

Table 5.4 shows the material parameters regarding the comparison test between a high-tensile steel wire mesh and a heavy chain link mesh made from traditional steel wire.

The following pictures 5.28 and 5.29 show the test setup for the comparison test[29]. The test equipment as well as the test conduction was made in accordance to the test methods described before (chapter 5.5.2). Reference width of test panels was 1.0 m.

[29] Tests were coordinated, supervised, documented and reported by TÜV Rheinland, Germany [80, 126].

Wire types	Mesh with high-tensile steel wire mesh	Mesh with traditional tensile steel wire mesh
Wire diameter	3.0 mm	4.6 mm
Tensile strength	Min. 1′770 N/mm^2	550 - 650 N/mm^2 (according to manufacturer)
Mesh types	TECCO® G65/3 mm	Chain link mesh 50 × 50 mm
Weight	1.65 kg/m^2	5.60 kg/m^2
Mesh unit width	83 mm	80.5 mm
Mesh unit length	143 mm	73.5 mm
Picture of mesh samples	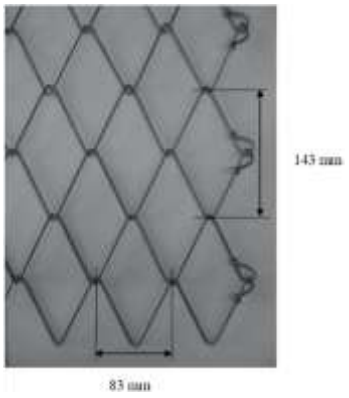	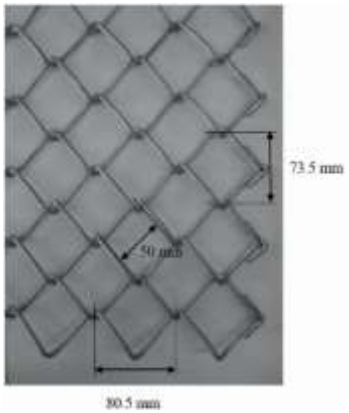

Table 5.4 Parameter and geometries of different mesh types

Picture 5.30 Test setup for the comparison tests with mesh made from high-tensile wires (1′770 N/mm^2)

Picture 5.31 Test setup for the comparison tests with made from normal steel wires (550 – 650 N/mm²)

The tensile tests on the meshes TECCO® G65/3 mm and chain link mesh 50 × 50/4.6 mm showed the TECCO® mesh has a distinctively higher breaking load than the chain link mesh.

Additionally noticeable differences in the failure and deformation behaviour were shown. The TECCO® mesh fails in more or less kind of a sudden bursts showing low deformation and a steep gradient of the tensile force at more than 150 kN/m′.

In contrast the chain link mesh shows two failure behaviours with a deformation clearly bigger than TECCO® starting at approx. 74 kN/m up to maximal 79 kN/m.

At first, the folded wire ends (on the lateral sides of the mesh panel), that are bended around the outer rim of the net, start to loosen. After this movement, a progressive deformation as a zipper like failure occurs.

The load-deformation curves of the different tests of the heavy chain link mesh do not show a smooth behaviour and the different test samples provide different and not repeatable results. This is an important difference between the compared meshes.

This is also visualized on the following diagram (figure 5.9) by the series of peaks of tests Quad: Test 1–3.

The very large deformation of the chain link mesh is a fact of the cross-section geometry due to the mesh production process that is different from the mesh manufacturing of the high-tensile steel wire mesh. The corresponding cross sections are shown on the following figure 5.10.

In terms of the weight per square meter, there is a large difference of the two compared mesh types. The high-tensile mesh has a weight of 1.65 kg/m² whereas the traditional steel wire mesh with 4.6 mm wire has a weight of 5.60 kg/m².

This equals a weight difference of factor 3.4 and of course, this results also in significantly higher transportation and higher installation costs.

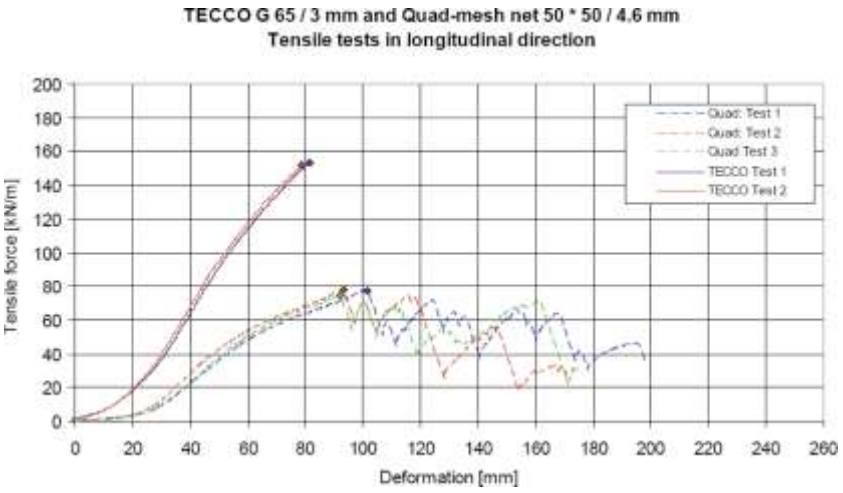

Figure 5.11 Comparison of results of the tensile tests in longitudinal direction of the steel wire mesh TECCO® G65/3 mm and the chain link mesh net 50 × 50/4.6 mm

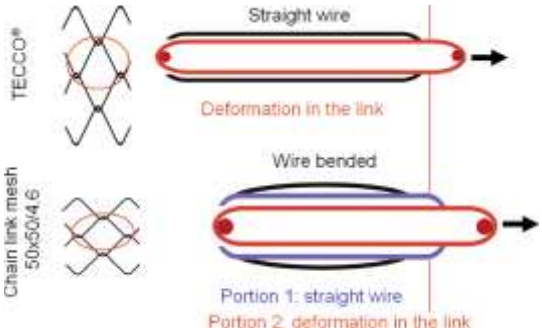

Figure 5.12 Different cross sections of high-tensile steel wire mesh (TECCO®, on top) and traditional steel wire mesh (chain link, at bottom)

These large deformations of traditional steel wire mesh can result in serious deformation and load transfer problems when applied for slope stabilization purposes.

The following picture 5.30 illustrates such deformation problems with steel wire meshes made from normal tensile wires (e.g. below 1′000 N/mm^2).

Because of the weight difference, the available mesh panel sizes are different:

– High-tensile steel wire mesh panel: 3.9 m × 30 m = 117 m^2 per roll

– Traditional steel wire mesh panels: 2.75 m × 6 m = 16.5 m^2 per panel

Consequently, the traditional mesh type panel is around seven times smaller and requires around eight times more panel overlapping than the new mesh made from high-tensile strength steel wire.

Picture 5.32 Slope stabilization system made with traditional steel wire meshes (chain-link, 50 × 50 mm, 4.6 mm wire diameter). Nail distance was chosen too large and consequently, large deformations of the wire mesh occurred in short time.

These facts are also illustrated on figure 5.13 where the horizontal and vertical lines indicate the borders of the individual mesh panels (traditional steel wire meshes) and the yellow section indicates the size of one single panel of high-tensile steel wire mesh (TECCO® G65/3). For comparison reasons, the TECCO® mesh (yellow) is illustrated in a horizontal way.

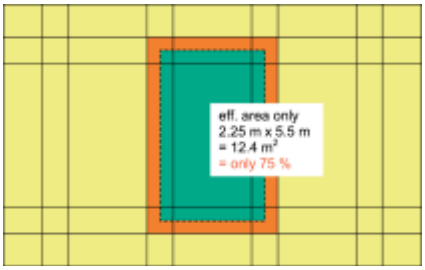

Figure 5.13 Yellow section = area of one roll of high-tensile steel wire mesh
Orange section = area of one roll of traditional steel wire mesh (low tensile wire mesh)
Green section = orange area reduced due to required overlapping of mesh panels

As a conclusion of this comparison, TECCO® G65/3 mesh requires much less mesh overlapping of individual panels. This means that less mesh area is totally needed and that the installation time (and costs) can be significantly reduced due to the fact that much less mesh connections have to be made.

5.9.2 Comparison test with reinforced hexagonal mesh made from traditional steel wire

Table 5.5 shows the material parameters regarding the comparison test between a high-tensile steel wire mesh and a reinforced hexagonal wire mesh.

Wire types	Mesh with high-tensile steel wire mesh	Mesh with reinforced hexagonal mesh
Wire diameter	3.0 mm	3.0 mm
Tensile strength	Min. 1'770 N/mm^2	350 - 550 N/mm^2 (according to manufacturer)
Mesh types	TECCO® G65/3 mm	Hexagonal mesh with reinforcement of 8 mm steel wire ropes
Breaking load of wire rope	–	40.3 kN (according to manufacturer)
Mesh unit width	83 mm	80 mm (measured)
Mesh unit length	143 mm	100 mm (measured)
Picture of mesh samples	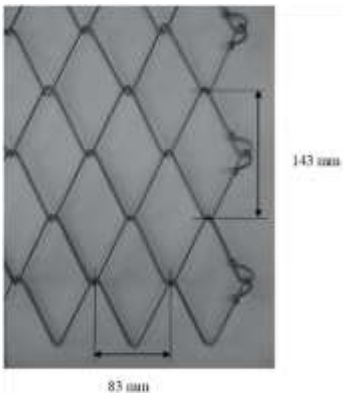	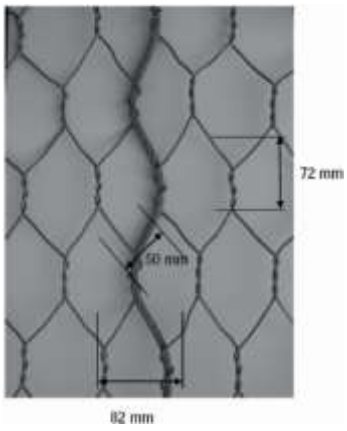

Table 5.5 Parameter and geometries of different mesh types

The following pictures 5.33 and 5.34 show the test setup for the comparison test[30].

The corresponding test equipment as well as the test conduction was made in accordance to the test methods described before (chapter 5.5.2). Reference width of test panels was 1.0 m.

[30] Tests were coordinated, supervised, documented and reported by TÜV Rheinland, Germany [79].

Picture 5.33 Test setup for the comparison tests with mesh made from high-tensile wires (1'770 N/mm^2)

Picture 5.34 Test setup for the comparison tests with the reinforced hexagonal made from normal steel wires (approx. 350 - 550 N/mm^2); reinforcement by 8.0 mm steel wire rope (centrally arranged)

The tensile tests on the meshes TECCO® G65/3 mm and hexagonal wire mesh 80 × 100/3 mm with wire rope 8 mm longitudinal showed that the TECCO® mesh has a distinctively higher breaking load than the hexagonal mesh together with the rope.

Additionally noticeable differences in the failure and deformation behaviour were shown. The TECCO® mesh fails more or less in a kind of sudden bursts showing low deformation and a steep gradient of the tensile force at more than 160 kN.

During the first tensile tests using the hexagonal wire mesh with a wire rope longitudinally arranged, the lateral drillings of the hexagonal wire mesh open after each other. Thereby, the maximum transmissible load amounts to 36.0 kN with a deformation of 119.3 mm.

To avoid any opening of lateral drillings during the tests 2 and 3, the drillings are fixed with wire rope clips. The behaviour is thus improved compared with the real application.

The corresponding breaking loads amount to 44.8 – 51.2 kN with a deformation of 77.7 – 83.1 mm as shown on the load-deformation diagram shown on figure 5.14.

The wire rope transfers noteworthy loads up to approx. 47 kN after nearly all wire meshes failed (after a deformation of about 140 mm). The elements hexagonal wire mesh and wire rope do not act at the same time but after each other.

The load-deformation curves of the different tests of the reinforced hexagonal steel wire mesh do not show a smooth behaviour and the different test samples provide different and not repeatable results. This is an important difference between the compared meshes.

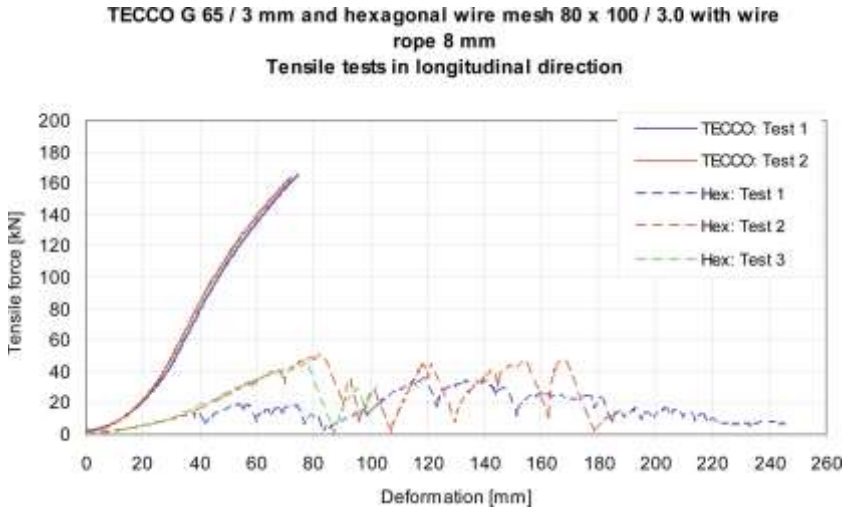

Figure 5.14 Comparison of results of the tensile tests in longitudinal direction of the steel wire mesh TECCO® G65/3 mm and the hexagonal wire mesh 80 × 100/3 mm with reinforcement of the wire rope 8 mm

Picture 5.35 shows the rupture of the hexagonal wire mesh before the rupture of the steel wire rope. This particular status demonstrates the fact that the two different materials, rope and hexagonal mesh, have different material properties and do not really function together.

Picture 5.35 The steel wire rope does not significantly support the hexagonal wire mesh because the wire rope can only transfer load if it is fully straight. As long as the steel wire rope is curved (e.g. “S-form”), it is unable to transmit tensile forces in order to support the loads that are applied to the hexagonal steel wire mesh

6 Tangential force transmission, mesh to nail

Several types of rupture mechanisms are considered in the investigation of local instabilities. Hereby it is assumed that the investigated failure bodies want to move downwards relative to the mesh. By this relative movement and due to the fact that the mesh is held locally by means of spike plates, upwards directed, slope-parallel forces are initiated in the mesh itself. If these forces are integrated over a surface of a_{red} *x* $2b$, the force Z results[31]. The mesh must be able to selectively transmit this force Z with a certain safety onto the nail located immediately above the failure mechanism under investigation.

The test setup was developed with the supervision of TÜV Rheinland, LGA Nürnberg, Germany and in coordination with the company Rüegger+Flum AG, St. Gallen, Switzerland [13, 78, 127]. This collaboration was of great importance since concept, tests and analysis of the results must be fully independent and shall be conducted completely externally. Consequently, it could be ensured that all test results are fully externally and third party approved and certified.

With the aid of this setup it has been possible to investigate the force deformation behaviour of various mesh types and to formulate the corresponding maximum admissible forces in the mesh. Hereby the mesh was locally held by spike plates and subjected to a load in tangential direction by means of a rope tensioning arrangement.

6.1 Test setup for tangential force transmission, mesh to nail

The test setup consists in the main of a metal container which is rigidly secured to two stationary U-profiles, and of a square metal frame into which the mesh to be investigated is clamped.

The metal container is filled with soil to the extent that the surface of the layer of soil is flush with the top edge of the metal container. A nail is arranged in the centre of the metal container. The mesh to be investigated is held by a spike plate which is pressed onto the substrate by means of a nut.

The rope tensioning arrangement pulls at two brackets fastened to the frame. The mesh clamped into the frame is centrally held by means of a spike plate. The forces imparted over the brackets into the frame and thereby into the mesh are locally transmitted onto the nail.

Figure 6.1 provides the principle overview of the setup for the tangential force transmission test. The force Z indicates location and direction of pulling ropes of the hydraulic tension test machinery.

---

[31] Determination of a_{red} is explained in chapter 8.3.

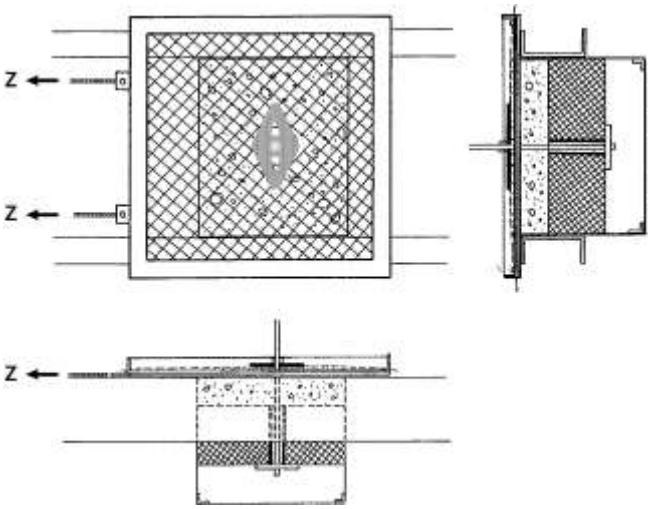

Figure 6.1 Schematic presentation of tangential force transmission test (principle drawing). Force *Z* shows location and direction of pulling ropes of tension test unit.

On picture 6.1, the test unit for the determination of the tangential force transmission test is shown.

Picture 6.1 Test unit for determination of tangential force transmission test

6.2 Test results for tangential force transmission, mesh to nail

The figure 6.2 shows the force deformation behaviour in respect of tangential tensile tests for

(I): a high-tensile mesh with a tensile strength of the individual wires of min. 1′770 N/mm^2 (or a tensile strength of the mesh in longitudinal direction of approx. 150 kN/m),

(II): a traditional wire mesh with a tensile strength of the individual wires of approx. 500 N/mm^2 (or a tensile strength of the mesh in longitudinal direction of approx. 50 kN/m) and

(III): for a geogrid of PET with a tensile strength in longitudinal direction of approx. 40 kN/m, in the form of three families of curves.

The applied spike plate was round and of a diameter of D = 220 mm. The test setup in question is explained in the following paragraph.

Figure 6.2 demonstrates also that by using high-tensile mesh compared to the common wire mesh with a mesh tensile strength in longitudinal direction of approx. 50 kN/m, the tangentially directed force which can be transmitted selectively onto the nail is significantly higher. Various tests with geogrids of PET (polyester) revealed that these products can transmit forces onto a nail only to a very limited degree.

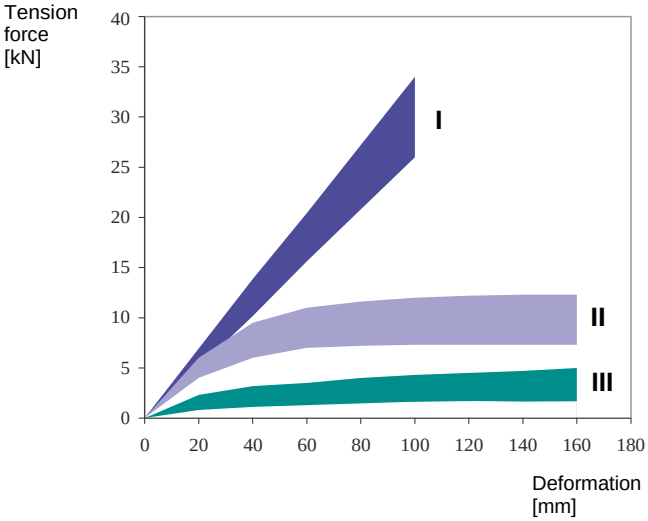

Figure 6.2 Force-deformation behaviour in the tangential tension test
I High-tensile wire mesh with tensile strength of the mesh in longitudinal direction of approx. 150 kN/m
II Common wire mesh with tensile strength of the mesh in longitudinal direction of approx. 50 kN/m
III Geogrid of PET with tensile strength of the mesh in longitudinal direction of approx. 40 kN/m

The selected bearing resistance of a high-tensile wire mesh of a tensile strength in longitudinal direction of approx. 150 kN/m against selective, slope-parallel tensile force amounts to approx. 25 kN when a round spike plate of a diameter of D = 220 mm (figure 6.2) is used.

Tests with a wire mesh of a tensile strength in longitudinal direction of approx. 50 kN/m have shown a load at rupture of approx. 8 - 12 kN. The corresponding, prudently selected bearing resistance against selective, slope-parallel tensile force amounts in this case to Z_R = 6 - 8 kN when a round spike plate of D= 220 mm is used.

For a grid fabric of polyester (PET) of a tensile strength in longitudinal direction of approx. 40 kN/m in combination with a round spike plate of D= 220 mm, loads at rupture of approx. 2 - 4 kN were measured. A prudently selected bearing resistance of Z_R = 1 - 2 kN results from this.

The force-deformation behaviour depends on the shape and size of the applied spike plate.

Average test results with the TECCO® spike plate in accordance to the test setup shown on picture 6.1 are showing a bearing resistance of 48.3 kN[32].

These material characteristics of the TECCO® G65/3 mesh is very important for flexible facings with static function regarding flexible slope stabilization systems.

[32] LGA Nürnberg Test Report BGT 0230101 and BPI 0400046/1, Nuremberg, Germany [13, 78].

7 Force transmission nail to mesh in nail direction

Apart from the bearing resistance of the mesh to be concentrated, slope-parallel tensile strains Z_R, the bearing resistance of the mesh to pressure strains in nail direction D_R must be determined.

Supervised by TÜV Rheinland and in coordination with the company Rüegger+Flum AG, this test arrangement was developed [13, 78, 127] what ensured that concept, tests and analysis could be conducted completely externally, approved by third party and certified accordingly.

The corresponding test setup is presented in figure 7.1 and on picture 7.1.

The objective of this test series was to obtain a force-deformation relation for vertical strains for the different types of mesh, on the basis of which the system-dependent force D_R is to be defined.

Apart from the determination of V, it was possible to investigate the deformation behaviour in the immediate area of the spike plate under certain strains.

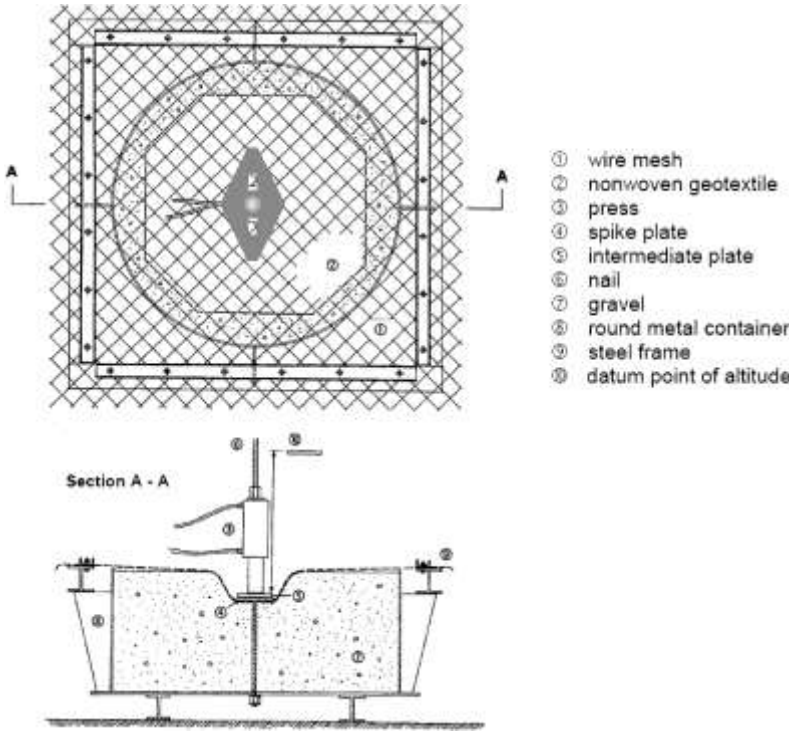

Figure 7.1 Schematic overview of test setup

Picture 7.1 Test setup for puncturing test with TECCO® spike plate

7.1 Test setup for force transmission nail to mesh in nail direction

The test setup consists of a round steel container which is completely filled with soil material. This filled steel container is framed by four squarely arranged HEA profiles which serve to fasten the mesh to be tested.

A GEWI nail is located in the centre. By means of a hydraulic press the spike plate and also the mesh are pressed onto and into the soil. The shape of the resulting compressed body is schematically outlined in section A-A.

7.2 Test results for force transmission nail to mesh in nail direction

Figure 7.2 shows the families of curves resulting from different pressure tests for a high-tensile wire mesh of a tensile strength of the individual wires of approx. 1′770 N/mm^2, for a traditionally common wire mesh of a tensile strength of the individual wires of approx. 500 N/mm^2 and for a geogrid of PET.

For comparison purposes, the behaviour of the test ground without the involvement of a mesh is shown in curve (4). A round spike plate of steel of D = 220 mm was used.

If the hydraulic press presses the spike plate directly onto the ground without involvement of a wire mesh, a corresponding hollow results at a certain force V_{oG} (figure 7.3).

The force V_{oG} is transmitted directly into the substrate over the spike plate. If an analogous test is carried out, but with the involvement of a wire mesh, the vertical force can be further increased by a certain dimension ΔV to V_{mG} until the same deformations

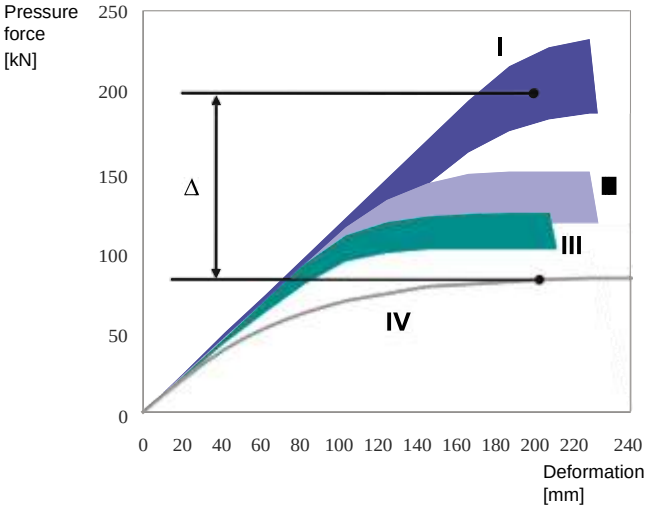

Figure 7.2 Pressure force – deformation relations of three different products as a result of puncture tests in nail direction using a round spike plate of diameter D = 220mm;
I High-tensile wire mesh with tensile strength of the mesh in longitudinal direction of approx. 150 kN/m
II Common wire mesh with tensile strength of the mesh in longitudinal direction of approx. 50 kN/m
III Geogrid of PET with tensile strength of the mesh in longitudinal direction of approx. 40 kN/m
IV Subsoil without contribution from a mesh cover

occur. The difference $\Delta V = V_{mG} - V_{oG}$ is laterally transmitted over the mesh via pressure and friction forces into the solid ground. Hereby the amount of V_{oG} approximately, flows again directly over the spike plate into the substrate.

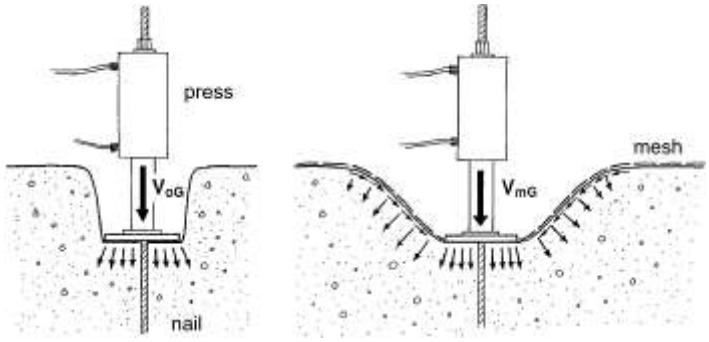

Figure 7.3 Pressing into the ground of the spike plate, without/with mesh

To determine the bearing resistance of the mesh against pressure strains in nail direction D_R, the corresponding differential forces are taken into account. The force D_R therefore, depends more or less on the wire mesh itself only, and no longer on the ground.

Accordingly, the following applies:

$$V_{mG} = V_{oG} + \Delta V$$
$$D_R = \Delta V$$

Equations 7.1

When comparing the three different force-deformation behaviours of the individual mesh types in figure 7.2 it becomes evident that a clearly higher pretensioning force is possible if high-tensile mesh is used (the round spike plate of D = 220 mm was used in those cases).

The families of curves in figure 7.2 apply to a certain test ground (in the case on hand: natural gravel 0– 32 mm). Differences may occur in the force-deformation behaviour of the individual mesh if other test grounds are used.

The bearing resistance of the mesh against shearing-off in nail direction at the upslope edge of the spike plate can be assumed to be half of the bearing resistance of the mesh against pressure strains in nail direction.

Additional tests series were conducted with TÜV Rheinland in order to test and certify the puncture values for the combination of TECCO® spike plate and the high-tensile steel wire mesh[33].

Soil used

For this test purpose a natural coarse aggregate (gravel) with grain size 0/16 mm was used. The tank was filled with the prepared material in three layers of gravel and compacted with a portable vibrant compactor up to a dry density of 22 kN/m^3.

Tests without high-tensile steel wire mesh

The test series initially served to determine the pure bearing effect of the spike plate system compared to the substrate used. The test substrate was loaded until significant deformation (shear failure) occurred.

Test substrate failed at loads between 208.78 kN and 228.52 kN. The deformation measured was between 154.1 mm and 187.8 mm.

Picture 7.2 shows the setup of the puncture test with the spike plate only, whereas picture 7.3 provides an overview of the arrangement for the puncture test with the spike plate including the high-tensile steel wire mesh. The results of these tests are shown on figure 7.4.

[33] TÜV Rheinland Test Report BPI 0400046/1 (Dr. Peter Brändlein), LGA Nürnberg, Germany [78].

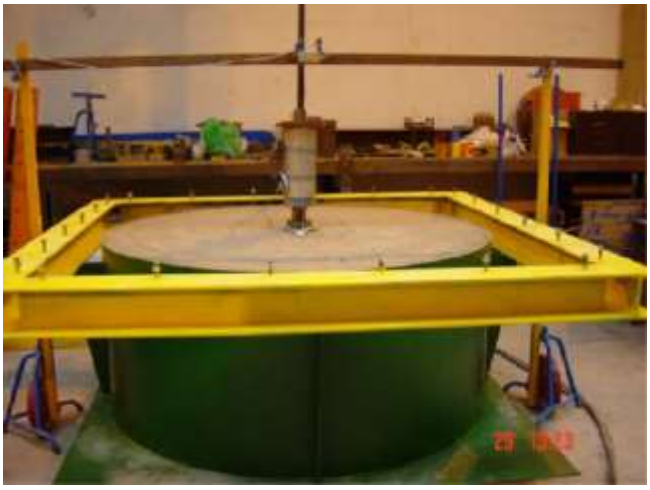

Picture 7.2 Puncture test with spike plate only (without any mesh)

Tests with high-tensile steel wire mesh

The high-tensile steel wire mesh type TECCO® G65/3 mm was used for these tests including the system spike plate.

The length and width of the test frame were 2′000 mm.

The first part of the curves corresponds to the compression of the high-tensile steel wire mesh. The second steep section corresponds to the elastic deformation of the soil foundation and then

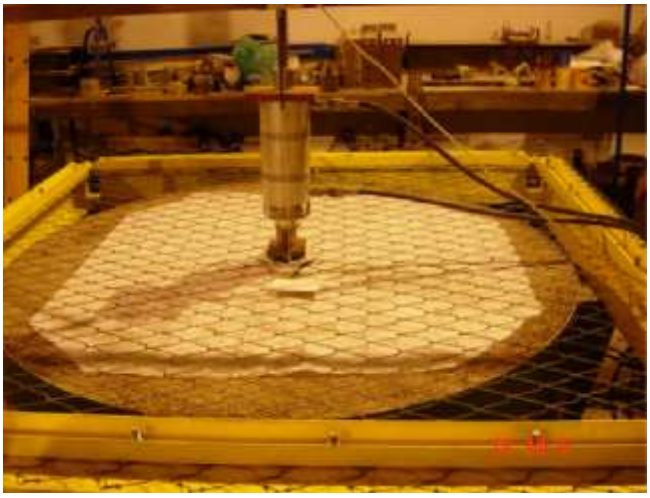

Picture 7.3 Puncture test with spike plate (including high-tensile steel wire mesh)

the rest of the curves corresponds to the movement of the soil along the failure surfaces up to the breaking of the high-tensile steel wire mesh.

The failure occurred at loads between 516 kN and 533 kN with deformations between 164.6 mm and 164.7 mm (see also figure 7.4).

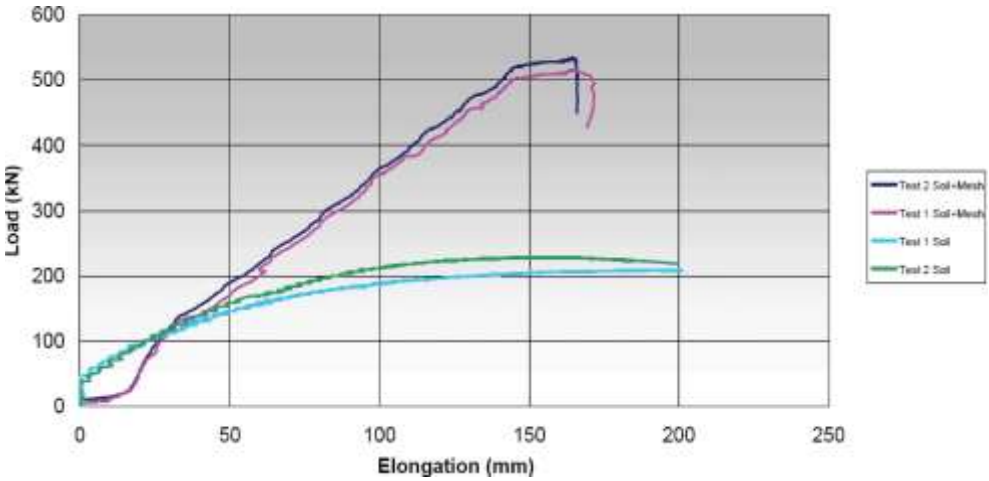

Figure 7.4 Punching test compacted gravel and TECCO® mesh including system spike plate.

Figure 7.4 and the corresponding puncturing test can be summarized as follows:

The puncturing test without the high-tensile steel wire mesh yielded bearing capacities between 208 kN and 228 kN. In the experiments including the TECCO® meshes, the failure was reached at loads between 516 kN and 533 kN.

The difference of the results in a compressive load capacity of the meshes in the direction of the nail (without the influence of the test substrate) was between 287.6 kN and 324.9 kN with an average value of 306 kN.

8 New designing method for flexible slope stabilization systems

The new designing method for flexible slope stabilization system RUVOLUM® is based on the concepts used so far. In principle, it is applicable to all common surface protection systems on the market, which provide for nailing in combination with a mesh or a wire rope net (or a mixture of the two), as a surface protection system which permits any distance between nails in both horizontal and vertical direction. It is pointed out especially that new dimensioning method RUVOLUM® is not restricted to the dimensioning of protection systems using high-tensile steel wire mesh exclusively.

Contrary to the traditional concept and as a major novelty, not only wedge-shaped one-body sliding mechanisms but also two-body sliding mechanisms are investigated when considering local instabilities. Hereby the geometry is selected with simplifications so that a more or less shell-shaped failure body is simulated as far as the sliding mass is concerned.

Moreover, it is assumed for simplification's sake that, as a reaction, a tensile force parallel to the slope is active on the nail immediately above the local failure mechanism to be investigated, and a tensile force in nail direction is active on the nail underneath this mechanism.

The axial tensile forces in the nails can be activated by pretensioning. The application of the pretensioning forces leads to the following advantages:

- The active application of the pretensioning forces onto the nails means that the spike plates and thereby the mesh are pressed onto the subsoil. These outer pressure forces acting on the surface of the steep terrain permit to mobilize additional friction forces along the sliding surfaces under examination. This has a positive effect above all on the stability.
- If no active pretensioning force is applied to the nail and if a local failure body wants to break out, the mesh must first be deformed to be able to mobilize the forces required to retain the shape liable to break out. Slight pressing-in of the spike plate applies the pretensioning forces to the mesh, i.e. the forces necessary to prevent local instabilities are already mobilized. As a result, failure bodies can hardly come loose any more from the layer to be protected.

The new dimensioning method comprises two investigations:

Investigation of superficial instabilities parallel to the slope

The cover layer which is liable to slide off a more stable substrate must be retained as a whole by the nailing. Each nail must be able to hold a body of width *a*, length *b* and thickness *t* with a certain safety. Figure 8.1 illustrates the corresponding superficial instabilities parallel to the slope.

[34] The dimensioning method for flexible slope stabilization system with high-tensile steel wire mesh is often also called "RUVOLUM® concept" or "RUVOLUM® method" [108, 109, 144].

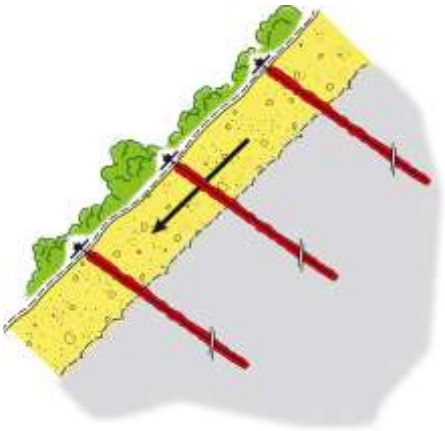

Figure 8.1 Superficial instabilities parallel to the slope

Investigation of local instabilities

If the nailing is dimensioned and laid out so that sliding-off of the cover layer as a whole can be prevented, further investigation is required to clarify whether or not instabilities may occur locally, i.e. between the individual nails (figure 8.2). These possible local failure bodies are to be retained with a certain safety by the application of the surface protection system consisting of nailing and mesh cover.

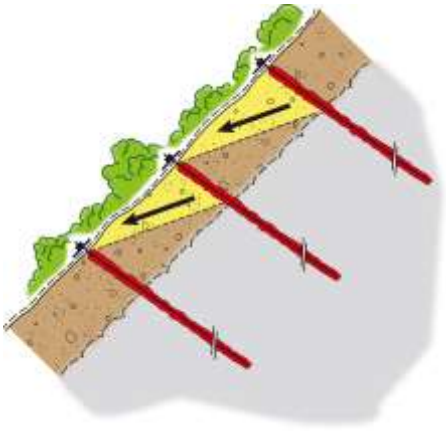

Figure 8.2 Local instabilities between individual nails

8.1 Investigation of superficial instabilities parallel to the slope

The investigation of superficial instabilities parallel to a slope examines a cubic body of width *a*, length *b* and layer thickness *t* which threatens to slide off the firm subsoil. All forces considered and acting on the sliding body are marked in Fig. 8.3.

Hereby it is assumed that no hydrostatic excess pressure and no flow pressure is effective on the sliding body. The force *G* represents the dead weight of the cubic body. The term $c \cdot A$ describes the retaining influence of the cohesion along the investigated sliding surface, inclined at the angle α to the horizontal plane. By means of $c \cdot A$ it is also possible to consider a.o. an existing denticulation (interlocking) effect between the layer of soil to be protected and the stable substrate, or within the layer of loose rock itself. Force *V* is a force with a stabilizing effect in the direction of the nail which prestresses the mesh against the nail head. By tightening the nut, the spike plate and thereby the mesh is firmly pressed onto or slightly into the ground, respectively. *V* is inclined in relation to the horizontal plane by the angle Ψ. Variable *S* represents the shear force which is to be absorbed by the nail and transferred into the stable subsoil. Marked for completeness' sake are the reaction forces *N* and *T* from the subsoil which act in vertical and tangential direction to the sliding surface.

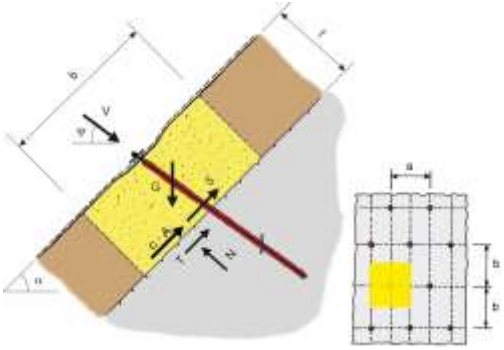

G = dead weight of sliding body

S = resisting shear force required to be absorbed by the nail

V = pretensioning force

c * A = cohesion of the cover layer * ground surface of the body liable to break out, whereby A = a * b

T, N reaction forces from the subsoil

α = inclination of the slope front and sliding surface, respectively, from horizontal

Ψ = inclination of the nail relative to the horizontal plane

φ = effective friction angle of the cover layer

γ_{mod} = model uncertainty correction value

Figure 8.3 All forces acting on the cubic body

From considerations of equilibrium concerning the cubic body shown in figure 8.3 and taking into account the failure condition of Mohr-Coulomb, the general equation 8.1 can be formulated for the stabilizing shear force *S* in function of the geometrical and geotechnical parameters as well as of the pretensioning force *V* and the model uncertainty correction factor γ_{mod} as follows:

$$S\,[\mathrm{kN}] = 1/\gamma_{mod} \cdot \{\gamma_{mod} \cdot G \cdot \sin\alpha - V \cdot \gamma_{mod} \cdot \cos(\Psi + \alpha) - c \cdot A - [G \cdot \cos\alpha + V \cdot \sin(\Psi + \alpha)] \cdot \tan\varphi\}$$

Equation 8.1

The RUVOLUM® dimensioning method is based on the concept with partial safeties proclaimed in EUROCODE 7 [47].

The characteristic values of friction angle φ_k, cohesion c_k and volume weight γ_k are to be reduced or multiplied, respectively, by/with the corresponding partial safety correction values γ_φ, γ_c and γ_γ (whereby the friction angle φ_k is reduced via the tangent).

Resulting from this are the dimensioning values of the geotechnical parameters φ_d, c_d and γ_d. Additionally, the stabilizing force V as an external influence must be multiplied by a so-called load factor. From these results the dimensioning value of the force $V_{dI/II}$. The model uncertainty correction factor γ_{mod} takes geometrical and model uncertainties into account.

8.2 Stability proofs in the investigation of superficial failures parallel to the slope

The following three proofs of stability must be established in the investigation of superficial failures parallel to the slope:

- Proof of the nail against sliding-off a superficial layer parallel to the slope
- Proof of the mesh against puncturing
- Proof of the nail to combined forces

8.2.1 Proof of the nail against sliding-off a superficial layer parallel to the slope

In the proof of the nail against sliding-off of a superficial layer parallel to the slope it must be guaranteed that the cubic body of width a, length b and thickness t does not slide off the investigated sliding surface which is inclined by the angle α in relation to the horizontal plane.

The mathematically required shear force S_d at dimensioning level, determined according to equation 8.2, must be compared with the bearing resistance S_R of the nail in respect of pure shear strain, whereby the resistance correction value γ_{SR} for shearing off of the nail must be considered.

Proof of bearing safety is to be established as follows:

$$S_d \leq S_R / \gamma_{SR}$$

Equation 8.2

The following table 8.1 shows a compilation of the quantities for the proof against sliding-off parallel to the slope:

S_d	[kN]	Dimensioning value of the shear strain under consideration of the dimensioning values of the geotechnical parameters and of the external, stabilizing force V_{dI} at dimensioning level, whereby the following applies: $V_{dI} = V \cdot \gamma_{dI}$ (V_{dI} acts favourably on force S_d, consequently γ_{d1} = 0.80 is generally put).
S_R	[kN]	Bearing resistance of the nail to shear strain, whereby the following applies: $S_R = \tau_y \cdot A$ with $\tau_y = f_y / \sqrt{3}$ = yielding point under shear strain f_y = yielding point under tensile strain A = statically effective cross-section of the nail.
γ_{SR}	[–]	Resistance correction value. Based on EUROCODE 7, γ_{SR} = 1.50 is generally put.

Table 8.1 Proof of the nail against sliding-off parallel to the slope

8.2.2 Proof of the mesh against puncturing

In the proof of the mesh against puncturing it must be investigated whether or not the mesh is able to absorb the force V applied in nail direction and transfer it into the stable subsoil.

Hereby the dimensioning value of the externally applied force V is compared with the bearing resistance of the mesh to pressure strain in nail direction, whereby the resistance correction value for puncturing is taken into account.

Proof of bearing safety must be established as follows:

$$V_{dII} \leq D_R / \gamma_{DR}$$

Equation 8.3

The following table 8.2 shows a compilation of the quantities for the proof against puncturing of the mesh due to pretensioning force:

V_{dII}	[kN]	Dimensioning value of the external force V with which the surface stabilization system is prestressed against the nails. The following applies: $V_{dII} = V \cdot \gamma_{VII}$ with γ_{VII} = 1.50 (as leading influence).
D_R	[kN]	Bearing resistance of the mesh against pressure strain in nail direction; to be determined by tests developed specifically for the purpose.
γ_{DR}	[–]	Resistance correction value, (generally γ_{DR} = 1.50 is put)

Table 8.2 Proof against puncture of the mesh due to pretensioning force

8.2.3 Proof of the nail to combined strain

The nail is subjected to tensile strains by the effectively applied pretensioning force. Additionally, it must prevent a global sliding-off, parallel to the slope, of the layer to be protected.

With the proof of the nail's bearing safety it must be investigated whether or not the applied nail can withstand these combined strains.

The following proof of bearing safety is established[35] as follows:

$$([V_{dII}/(T_R/\gamma_{VR})]^2 + [S_d/(S_R/\gamma_{SR})]^2)^{0.5} \leq 1.0$$

Equation 8.4

The before mentioned variables are explained in table 8.3 as follows:

V_{dII}	[kN]	Dimensioning value of the external force V with which the surface stabilization system is prestressed against the nails. The following applies: $V_{dII} = V \cdot \gamma_{VII}$ $\gamma_{VII} = 1.50$.
T_R	[kN]	Bearing resistance of the nail to pure tensile strain, whereby the following applies: $T_R = f_y \cdot A$ f_y = yielding point under tensile strain A = statically effective nail cross-section.
γ_{VR}	[–]	Resistance correction value. Based on EUROCODE 7, is generally put on $\gamma_{VR} = 1.50$.
S_d	[kN]	Dimensioning value of the shear strain under consideration of the dimensioning values of the geotechnical parameters and of the external, stabilizing force V_{d1} at dimensioning level. The following applies: $V_{d1} = V \cdot \gamma_{d1}$ (V_{d1} acts favourable on force S_d, consequently $\gamma_{d1} = 0.80$ is generally put).
S_R	[kN]	Bearing resistance of nail to shear strain, whereby the following applies: $S_R = \tau_y \cdot A$ $\tau_y = f_y/\sqrt{3}$ τ_y = yielding point under shear strain, f_y = yielding point under tensile strain A = statically effective cross-section of nail.
γ_{SR}	[–]	Resistance correction value. Based on EUROCODE 7, $\gamma_{SR} = 1.50$ is generally put.

Table 8.3 Proof of the bearing safety of the nail (combined strains)

[35] Based on the Swiss SIA 261 Standard [119].

8.3 Investigation of local instabilities between the individual nails

The second investigation looks at bodies liable to break out locally, between the individual nails. The surface stabilization system (nailing in combination with a mesh cover) is to be dimensioned in such a manner that all possible local bodies liable to break are retained, the maximum occurring forces absorbed and transmitted into the stable subsoil (figure 8.4).

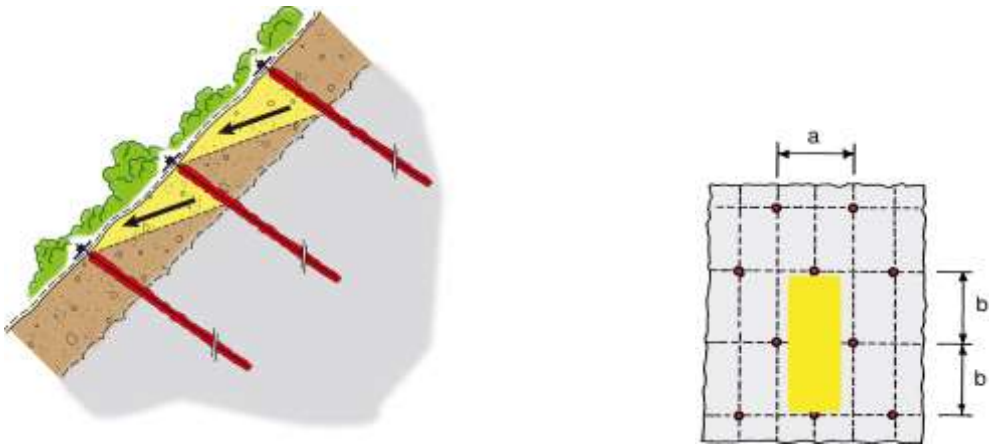

Figure 8.4 Local instabilities between the individual nails (left)
Overview of the general nail arrangement (right)

In the investigation of local bodies liable to break out between the nails, one must reflect which bodies become possible, taking into account the chosen nail arrangement.

Above each nail is a field of width a and length $2 \cdot b$ which must be secured against local instabilities. Starting from this field, bodies liable to break out of a maximum length of $2 \cdot b$ can arise. The cross-section of the maximum possible wedge liable to break out is substantially influenced by the actual protection concept. The mesh is prestressed against the nail head with the force V in that tightening of the nut causes the spike plate to be pressed firmly onto or even slightly into the ground.

Starting from the nail head, a truncated pressure cone arises in the cover layer below the spike plate and the adjoining mesh. This cone can be described by the geometrical parameters ζ, ξ and t. The angle δ represents the inclination of the truncated cone relative to the horizontal plane (figures 8.5 and 8.6).

The variable ζ depends a.o. on the applied spike plate, the mesh and the ground, and must be determined by means of tests. As a simplifying assumption, $\zeta_{min} = 0.5 \cdot D_{Plate}$ can be put.

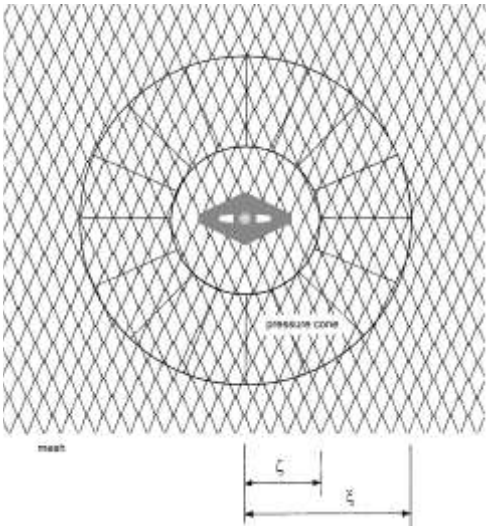

Figure 8.5 Truncated pressure cone: ground plan

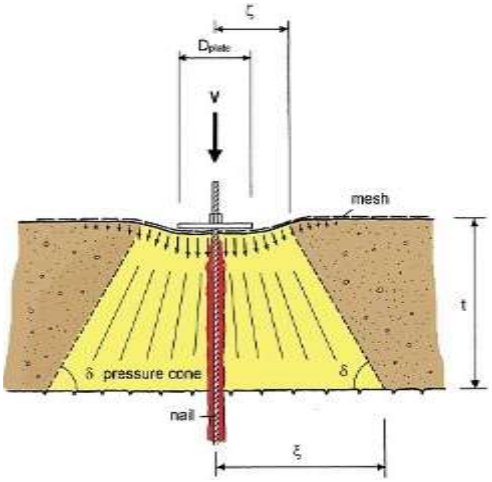

Figure 8.6 Truncated pressure cone: general section

The dimensioning model assumes that the pressure cones are completely outside the body to be investigated. This means that the cross-section of the maximum possible body liable to break out is trapezoidal and features at the top a width of $a - 2 \cdot \zeta$ and at the bottom a width of $a - 2 \cdot \xi = \eta$. For simplification, the trapezoidal cross-section can be transformed to a rectangle of equal area of the width $a_{red} = a - t/tan\ \delta - 2 \cdot \zeta$ and thickness t (figure 8.7).

The body liable to break out and subject of the investigation features a width of a_{red} and a maximum length of $2 \cdot b$. The thickness of the body in figure 8.7 amounts to t.

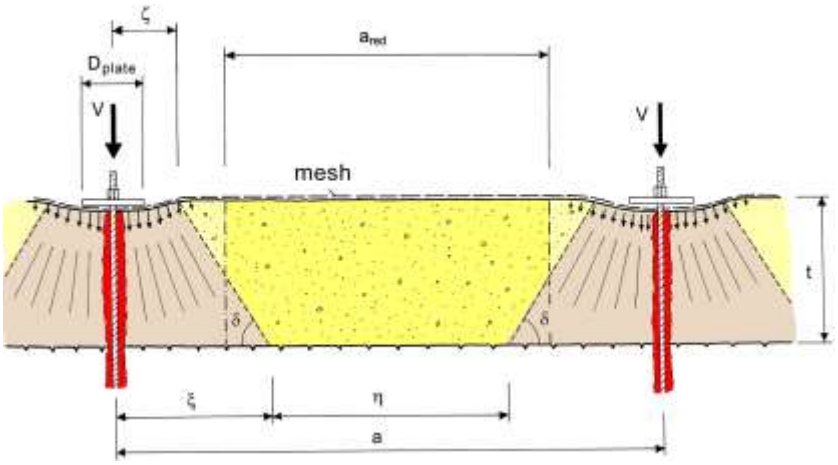

Figure 8.7 Horizontal cross-section of the maximum possible body (liable to break out) of the thickness t

For the proofs of bearing safety in the investigation of local instabilities according to the dimensioning method described in this chapter, it is mandatory to vary the thickness of the bodies to be investigated over the entire interval [0; t] and in this manner to determine the decisive fault mechanism.

Hereby it must be noted that the variable a_{red} depends directly on the thickness of the investigated body liable to break out and accordingly also varies on variation of the layer thickness from 0 to t. If the layer thickness is not varied between 0 and t, this can lead to a substantial underestimation of the effectively occurring forces, particularly if t is selected greater than $^1/_2 \ldots {}^1/_3$ of the distance between nails in the line of slope. In the interest of simplification, only the case thickness of the layer equals t is dealt with in the explanations hereafter.

It must be pointed out that the geometry of the bodies to be investigated and selected in the model should approximately simulate the saucer-shaped fault contours which occur in reality. By the trapezoidal cross-section the actually curved cross-section is described as an approximation.

For the proofs of bearing safety in the investigation of local instabilities, one must differentiate between two failure mechanisms A and B: mechanism A represents a single-body sliding mechanism whose sliding surface, starting from the bottom nail, runs in a straight line to the top nail under the angle β in relation to the horizontal plane. Failure mechanism B is a two-body sliding mechanism. Hereby the top body I of trapezoidal cross-section presses on the wedge-shaped bottom body II.

Figures 8.8 and 8.9 illustrate these two possible failure mechanisms with the accordingly acting forces.

8.3.1 Failure mechanism A

In the investigation of local instabilities with the aid of failure mechanism A, we look at a wedge-shaped body of width a_{red} which threatens to slide off a plane which is inclined in relation to the horizontal plane by the angle β. All considered forces which are active on the sliding body are marked in figure 8.8. Hereby it is assumed, in analogy to the investigation of superficial slope-parallel instabilities, that no excess hydrostatic pressure and no flow pressure acts on the sliding body (this applies also to fault mechanism B). Force G represents the dead weight of the body breaking out. The cohesion along the sliding surface is taken into account with the term $c \cdot A$, whereby $A = L \cdot a_{red}$ applies. With $c \cdot A$ it is in turn possible to describe an existing interlocking effect.

Also active on the body liable to break out, furthermore, are the external forces P and Z with a stabilizing effect. It is assumed that the investigated body liable to break out and wanting to move relatively downwards, is partly retained via friction by the mesh pressed onto the surface. If these friction forces are integrated over the surface $2b \cdot a_{red}$, the resulting reaction is the slope-parallel upwards-directed force Z in the mesh, which is to be selectively transmitted by the mesh to the upper nail. The force P is assumed to be inclined in relation to the horizontal plane by the angle Ψ and is introduced as a general force required from the equilibrium considerations and having a stabilizing effect. For completeness' sake, the reaction forces N and T from the subsoil, acting in vertical or tangential direction in relation to the sliding surface, are marked also.

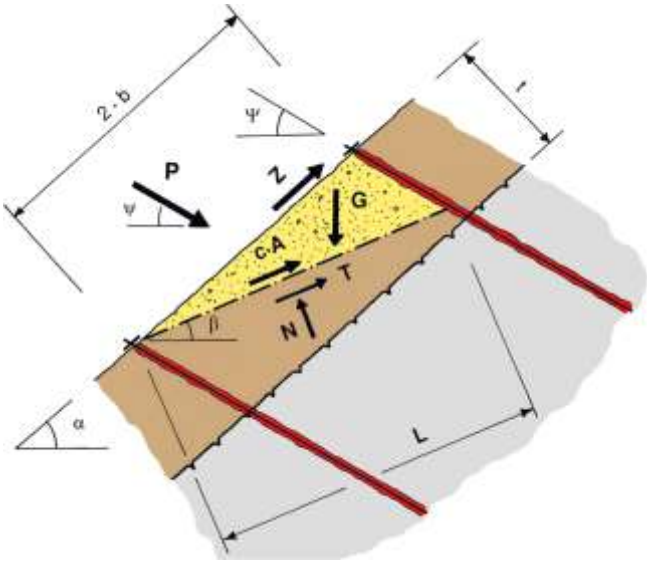

Figure 8.8 Failure mechanism A= one-body sliding mechanism

The relation presented in equation 8.5 results from equilibrium considerations and taking into account the failure condition of Mohr-Coulomb as well as the model uncertainty correction factor γ_{mod}.

The maximum force P is to be determined by variation of the inclination of sliding surface β.

$$P\,[\mathrm{kN}] = \frac{G \cdot [\gamma_{\mathrm{mod}} \cdot \sin\beta - \cos\beta \cdot \tan\varphi] - Z \cdot [\gamma_{\mathrm{mod}} \cdot \cos(\alpha-\beta) - \sin(\alpha-\beta) \cdot \tan\varphi] - c \cdot A}{\gamma_{\mathrm{mod}} \cdot \cos(\beta+\psi) + \sin(\beta+\psi) \cdot \tan\varphi}$$

Equation 8.5

8.3.2 Failure mechanism B

Failure mechanism B is characterized by two bodies liable to break out: The upper, trapezoidal body I presses over the contact force X onto the lower, wedge-shaped body II.

The width of the two bodies amounts to a_{red}. The forces G_{I} and G_{II} represent the weights of the individual sliding bodies and $c \cdot A_{\mathrm{I}}$ and $c \cdot A_{\mathrm{II}}$, respectively, the forces due to cohesion along the investigated sliding surfaces of the individual sliding bodies, whereby $A_{\mathrm{I}} = L_I \cdot a_{\mathrm{red}}$ and $A_{\mathrm{II}} = L_{\mathrm{II}} \cdot a_{\mathrm{red}}$ apply. N_{I} and T_{I}, and N_{II} and T_{II}, respectively, in turn stand for the reaction forces from the subsoil.

Analogously to the preceding paragraph, variable Z denotes the slope-parallel force in the mesh, to be selectively transmitted on the upper nail. The force P is assumed to be inclined in relation to the horizontal plane by the angle Ψ and is again introduced as a general retaining force required from the equilibrium considerations.

For the equilibrium equations, the forces Z and P act on the lower wedge-shaped body II.

On overview of this failure mechanism is shown on the following figure 8.9.

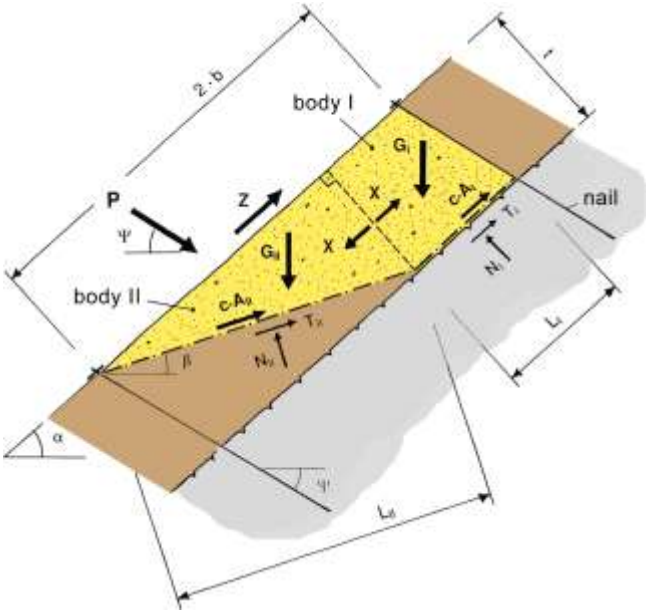

Figure 8.9 Failure mechanism B= two-body sliding mechanism (possible friction forces along the contact surface of the two bodies I and II are neglected.)

The contact force *X* results from the equilibrium equations at the upper body I, whereby the condition of Mohr-Coulomb and the model uncertainty correction factor γ_{mod} are taken into account. To determine the force *P*, the equilibrium conditions are formulated on body II. Hereby the contact force *X* from equation 8.6 and the slope-parallel force Z are entered.

$$X\,[\mathrm{kN}] = 1/\gamma_{mod} \cdot \{G_I \cdot (\gamma_{mod} \cdot \sin\alpha - \cos\alpha \cdot \tan\varphi) - c \cdot A_I\}$$

Equation 8.6

$$P\,[\mathrm{kN}] = \frac{G_{II} \cdot [\gamma_{mod} \cdot \sin\beta - \cos\beta \cdot \tan\varphi] + (X - Z) \cdot [\gamma_{mod} \cdot \cos(\alpha - \beta) - \sin(\alpha - \beta) \cdot \tan\varphi] - c \cdot A_{II}}{\gamma_{mod} \cdot \cos(\beta + \psi) + \sin(\beta + \psi) \cdot \tan\varphi}$$

Equation 8.7

The decisive case is to be found by comparing the maximum force *P* from failure mechanism A with that from mechanism B.

8.4 Proofs of bearing safety in the investigation of local failure mechanisms

The following proofs of bearing safety must be established in the investigation of local instabilities:

- Shearing-off of the mesh at the upslope edge of the spike plate at the lower nail
- Selective passing-on of the slope-parallel force *Z* from the mesh onto the upper nail

8.4.1 Shearing-off of the mesh at the upslope edge of the spike plate at lower nail

In the investigation of local instabilities, it must be ensured that a local body of a maximum length of $2 \cdot b$ cannot break out from the securing superficial layer. For this purpose, the necessary retaining force P_d from the equilibrium conditions has been determined in paragraph 8.3. If a body is about to slide off, it must be possible for this force P_d to be taken up in the area of the bottom nail by the mesh and accordingly also by the spike plate and the nail (see also figure 8.10 accordingly).

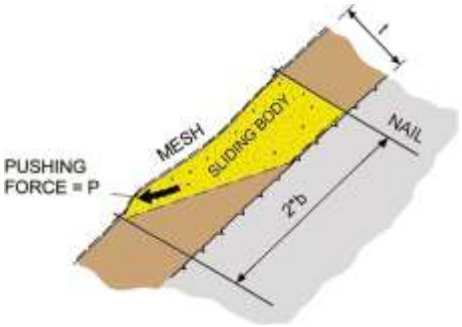

Figure 8.10 Shear stress on the mesh at the upslope edge of the spike plate at the lower nail

In the proof concerning shearing of the mesh at the upslope edge of the spike plate at the lower nail, it must be investigated whether the applied mesh is able to take up the outwards acting force component P_d or is sheared off at the upslope edge of the spike plate. Proof of bearing safety is to be established as follows:

$$P_d \leq P_R/\gamma_{PR}$$

Equation 8.8

The following table 8.4 shows a compilation of the quantities for the proof against shearing-off of the mesh at the upslope edge of the spike plate at the lower nail:

P_d	[kN]	Dimensioning value of the maximum shear stress on the mesh at the upslope edge of the spike plate on the lower nail
P_R	[kN]	Bearing resistance of the mesh against shearing off in nail direction, to be determined by means of the test developed specifically for the purpose
γ_{PR}	[–]	Resistance correction value (γ_{PR} = 1.50 is generally put)

Table 8.4 Quantities for proof against shearing-off of the mesh at the upslope edge of the spike plate at the lower nail

8.4.2 Selective transmitting of the slope-parallel force *Z* from the mesh to upper nail

The slope-parallel force Z has been introduced for the equilibrium considerations in paragraph 8.3. This force Z in the mesh must be transmitted selectively over the spike plate onto the upper nail (figure 8.11).

Proof of the bearing safety concerning selective transmitting of the slope-parallel force *Z* from the mesh onto the upper nail must be established as follows:

$$Z_d \leq Z_R / \gamma_{ZR}$$

Equation 8.9

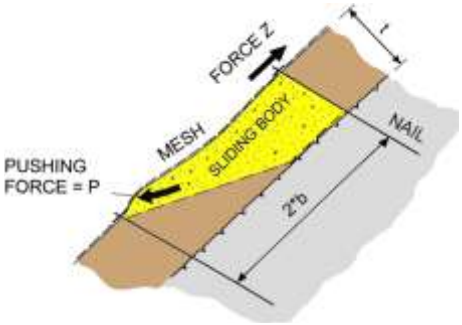

Figure 8.11 Slope-parallel force taken into account in the equilibrium consideration

The following table 8.5 shows a compilation of the quantities for the proof of the selective transmission of the slope-parallel force *Z* from the mesh onto the upper nail:

Z_d	[kN]	Slope-parallel force taken into account in the equilibrium equations= dimensioning value of the stress in slope-parallel direction
Z_R	[kN]	Bearing resistance of the mesh against selective, slope-parallel tensile stress; to be determined by tests developed specifically for the purpose
γ_{ZR}	[–]	Resistance correction value. γ_{ZR} = 1.50 is generally put.

Table 8.5 Quantities for proof of selective transmission of the slope-parallel force *Z* from the mesh onto the upper nail

8.5 Parameters to be determined empirically

In the equilibrium considerations in paragraphs 8.1 and 8.3, the pretensioning force *V*, the retaining force *P* and the net force *Z* have been introduced as external forces.

The question now arises how high these forces may be selected in the maximum so that they can still be absorbed by the used mesh, the applied spike plate and the nails, taking into account appropriate safeties.

The bearing resistance of mesh to pressure strain in nail direction and the bearing resistance of mesh against selective, slope-parallel tensile strains have been determined with the aid of various test series.

The corresponding test setup as well as the results and analysis were discussed in the chapters 6 and 7.

For general assumptions, V = 30 kN for soil and V = 50 kN for weathered rock faces as standard values based on experiences are recommended.

8.6 Load case “earthquake”

Depending on the importance of the structure and the seismological situation, possible additional effects from earthquakes must be investigated when dimensioning slope stabilization systems. Generally, this takes place using the substitute force procedure.

Here, accelerations acting on a fracture body are converted through the factor[36] ε_h and factor[37] ε_v to additional forces in the horizontal and vertical direction. These additional forces must be appropriately taken into account in the equilibrium considerations. With steeper slopes, in general in solid rock, special investigations are necessary, e.g. tilting and sliding individual blocks.

Shown on figure 8.12 are the additions in the formulas resulting from the earthquake load case. The corresponding individual proofs remain the same as previously described.

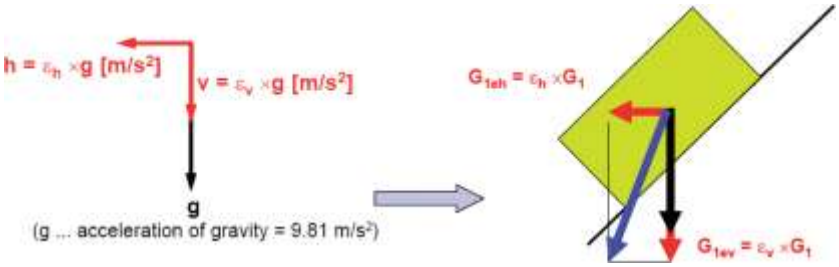

Figure 8.12 Components of acceleration due to earthquake

8.6.1 Investigation of instabilities close to the surface and parallel to the slope

The formula for the variable *S* previously described in equation 8.1 is extended in equation 8.10 with the additional forces as a result of the parameters ε_h und ε_v, factors of the horizontal and vertical acceleration as the result of an earthquake. Here the variable *S* represents the shear force to be taken up by the nail and transferred to the firm bedrock (figure 8.13).

---

[36] ε_h is the horizontal acceleration due to earthquake activities and forces. The unit is [m/s²].
[37] ε_v is the vertical acceleration due to earthquake activities and forces. The unit is [m/s²].

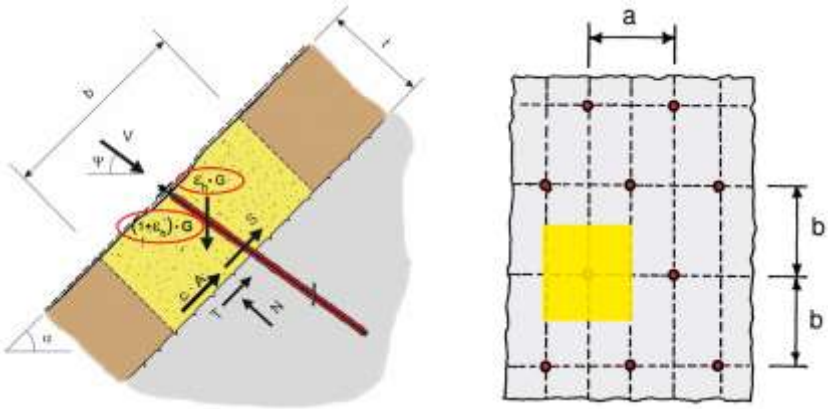

Figure 8.13 Forces applied to a cubic body with the earthquake load case

$$S\,[\mathrm{kN}] = (1+\varepsilon_v)\cdot G\cdot \sin\alpha + \varepsilon_h \cdot G\cdot \cos\alpha - V\cdot\cos(\psi+\alpha) \\ - \frac{[V\cdot \sin(\psi+\alpha) + (1+\varepsilon_v)\,G\cdot\cos\alpha - \varepsilon_h\cdot G\cdot\sin\alpha]\cdot\tan\varphi + c\cdot A}{\gamma_{\mathrm{mod}}}$$

Equation 8.10

8.6.2 Investigation of local instability between the nails

Again, for the proofs of bearing safety in the context of the investigation of local instabilities one must differentiate between two failure mechanisms A and B:

- Failure mechanism A represents a one-body sliding mechanism in which the sliding surface, starting from the bottom nail and extending in a straight line to the upper nail, runs under the angle β to the horizontal plane.
- Failure mechanism B is a two-body sliding mechanism. Hereby the upper body I of trapezoidal cross-section presses onto the wedge-shaped lower body II. Figures 8.8 and 8.9 show these two possible failure mechanisms with the correspondingly active general forces.

Failure mechanism A

The additional force components as a result of earthquake are introduced in the equilibrium consideration previously described with equation 8.5 (see equation 8.11). Here the variables *P* and *Z* represent the external stabilizing forces.

The inclination β of the slip surface must in turn be varied in order to determine the maximum force *P* (figures 8.14).

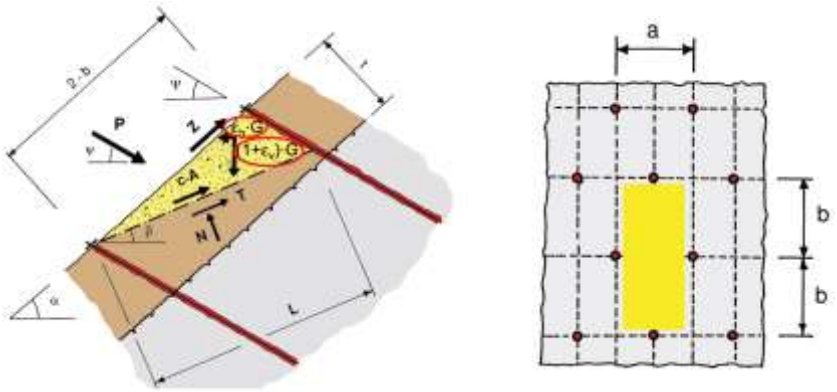

Figures 8.14 Forces applied with failure mechanism A including the earthquake load case

$$P\,[\mathrm{kN}] = \frac{(1+\varepsilon_v)\cdot G\cdot \sin\beta + \varepsilon_h \cdot G\cdot \cos\beta - Z\cdot \cos(\alpha-\beta) - \dfrac{[(1+\varepsilon_v)\cdot G\cdot \cos\beta - \varepsilon_h \cdot G\cdot \sin\beta - Z\cdot \sin(\alpha-\beta)]\cdot \tan\varphi + c\cdot A_c}{\gamma_{\mathrm{mod}}}}{\cos(\psi+\beta) + \sin(\psi+\beta)\cdot \dfrac{\tan\varphi}{\gamma_{\mathrm{mod}}}}$$

Equation 8.11

Failure mechanism B

The additional force components as a result of earthquakes are likewise introduced with fracture mechanism B. For this the contact force *X* of equation 8.6 resulting from the equilibrium considerations at the upper body it must be adjusted as represented in equation 8.12.

The extended calculation of the necessary restraining force *P* is shown in equation 8.13.

Figure 8.15 provides an overview about the forces that are applied with failure mechanism B including the earthquake load case.

By analogy with before, the decisive case must also be determined with the maximum force *P* from mechanism A and B:

$$X\,[\mathrm{kN}] = (1+\varepsilon_v)\cdot G_{\mathrm{I}}\cdot \sin\alpha + \varepsilon_h \cdot G_{\mathrm{I}}\cdot \cos\alpha - \frac{[(1+\varepsilon_v)\cdot G_{\mathrm{I}}\cdot \cos\alpha - \varepsilon_h \cdot G_{\mathrm{I}}\cdot \sin\alpha]\cdot \tan\varphi + c\cdot A_{c,\mathrm{I}}}{\gamma_{\mathrm{mod}}}$$

Equation 8.12 Contact force *X*

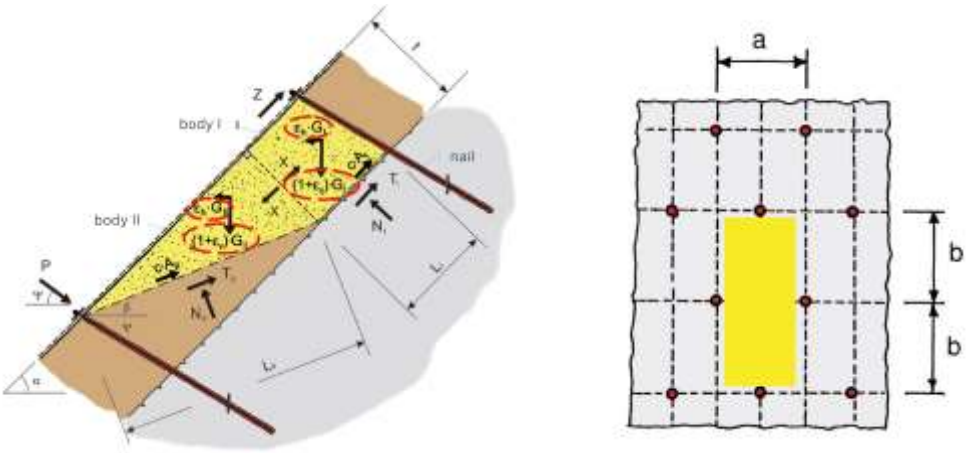

Figure 8.15 Forces applied with failure mechanism B including the earthquake load case

$$P[kN] = \frac{(1+\varepsilon_v)\cdot G_{II}\cdot\sin\beta + \varepsilon h\cdot G_{II}\cdot\cos\beta + X\cdot\cos(\alpha-\beta) - Z\cdot\cos(\alpha-\beta) - \frac{[(1+\varepsilon v)\cdot G_{II}\cdot\cos\beta - \varepsilon h\cdot G_{II}\cdot\sin\beta - Z\cdot\sin(\alpha-\beta) + X\cdot\sin(\alpha-\beta)]\cdot\tan\varphi + c\cdot A_{c,II}}{\gamma_{mod}}}{\cos(\Psi+\beta) + \sin(\Psi+\beta)\cdot\frac{\tan\varphi}{\gamma_{mod}}}$$

Equation 8.13 Retaining force *P*

8.7 Load case “streaming parallel to the slope”

Described below is the influence of streaming pressure as a result of precipitation water, respectively inflowing ground or slope water in loose rock slopes in the equilibrium considerations.

In principle the two types of inflow with precipitation water (from the outside on to the slope) and slope water (from the inside) can be differentiated as shown in figure 8.16:

– Streaming parallel to the slope in case of intensive rain

– Streaming parallel to the slope due to slope water (e.g. waterbearing interbeds, clefts, etc.)

With both cases it is assumed that a streaming parallel to the slope occurs after the saturation of the material.

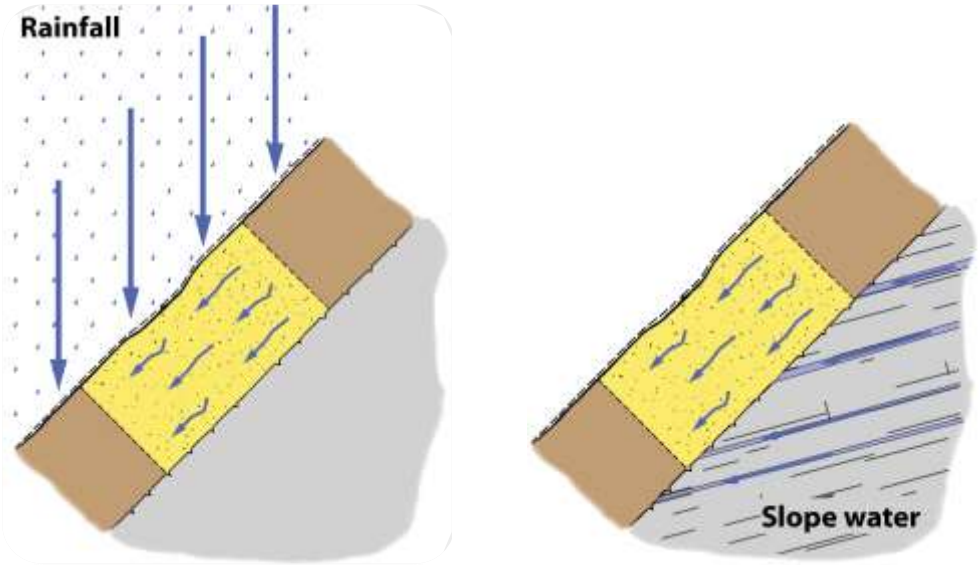

Figure 8.16 Streaming parallel to the slope in case of intensive rain (left) and slope water, e.g. water-bearing interbeds, clefts, etc. (right)

8.7.1 Investigation of instabilities close to the surface and parallel to the slope

The additional force F_s represents the resulting streaming force parallel to the slope and is calculated from the sum of the unit weight of the water γ_w, the hydraulic gradient $i = sin\ \alpha$ and the volume of the fracture body. Force G represents the dead weight of the cubic body. The term $c \cdot A$ describes the remaining influence of the cohesion along the investigated sliding surface which is inclined by the angle α in relation to the horizontal plane. With $c \cdot A$ it is basically also possible to take into account an existing interlocking effect between the superficial layer itself. Force V is the force with a stabilizing effect in the direction of the nail which pretensions the mesh against the slope surface; by tightening the nut, the spike plate and thereby the mesh is firmly pressed onto the ground. The force V is inclined in relation to the horizontal plane by the angle ψ. When calculating according to equation 8.14, buoyancy is taken into account with the own weight G of the cubic body. Figure 8.17 provides a corresponding overview of the applied forces to a cubic body including the streaming load case. The individual proofs remain the same as stated in previous chapters.

The general shear force S formula, previously represented in equation 8.2, is extended by the force F_s.

$$S\,[\mathrm{kN}] = G \cdot \sin\alpha - V \cdot \cos(\psi + \alpha) + F_s - \frac{[V \cdot \sin(\psi + \alpha) + G \cdot \cos\alpha] \cdot \tan\varphi + c \cdot A}{\gamma_{\mathrm{mod}}}$$

Equation 8.14 Shear force S

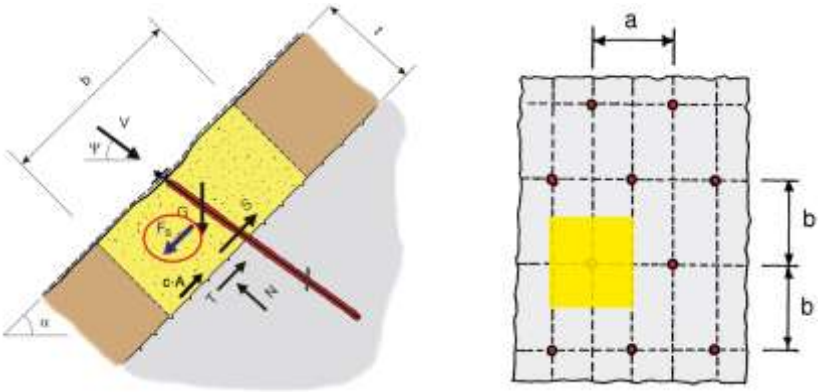

Figure 8.17 Forces applied to a cubic body including the streaming load case
$F_s = \gamma_w \cdot i \cdot a \cdot b \cdot t = \gamma_w \cdot \sin \alpha \cdot a \cdot b \cdot t$

8.7.2 Investigation of local instability between the nails

Equal to the chapter 8.6.2, the two relevant failure mechanisms A and B must be analysed for the investigation of local instabilities between the nails.

Failure mechanism A

Figure 8.18 presents the applied forces with the failure mechanism A including the streaming load case.

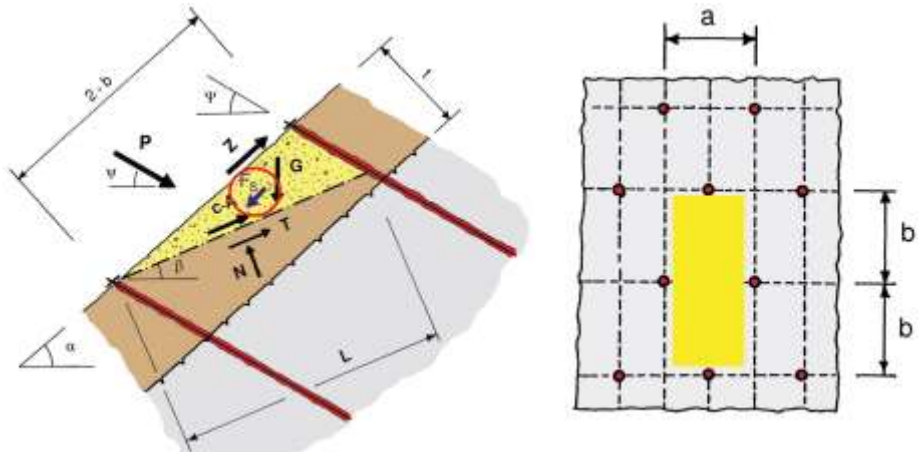

Figure 8.18 Forces applied with the failure mechanism including the streaming load case

The equation for calculating stabilizing force P is enlarged by the force components F_s. The maximum force P is determined by varying the gradient β of the slip face. The uplift is taken into account with the calculation of the own weight G.

$$P\,[\mathrm{kN}] = \frac{F_s \cdot \cos(\alpha-\beta) + G \cdot \sin\beta - Z \cdot \cos(a-\beta) - \dfrac{[G \cdot \cos\beta - Z \cdot \sin(\alpha-\beta)] + F_s \cdot \sin(\alpha-\beta)] \cdot \tan\varphi + c \cdot A_c}{\gamma_{\mathrm{mod}}}}{\cos(\psi+\beta) + \sin(\psi+\beta) \cdot \dfrac{\tan\varphi}{\gamma_{\mathrm{mod}}}}$$

Equation 8.15 Restraining force P

Failure mechanism B

According to the equilibrium consideration, at the upper body 1 the contact force X of equation 8.6 is extended by the force $F_{S,I}$. Represented in equation 8.17 is the extended calculation of the restraining force P. The own weight G is thereby reduced by the uplift components (figure 8.19).

The maximum force P from the two fracture mechanisms A and B is determining for the proofs.

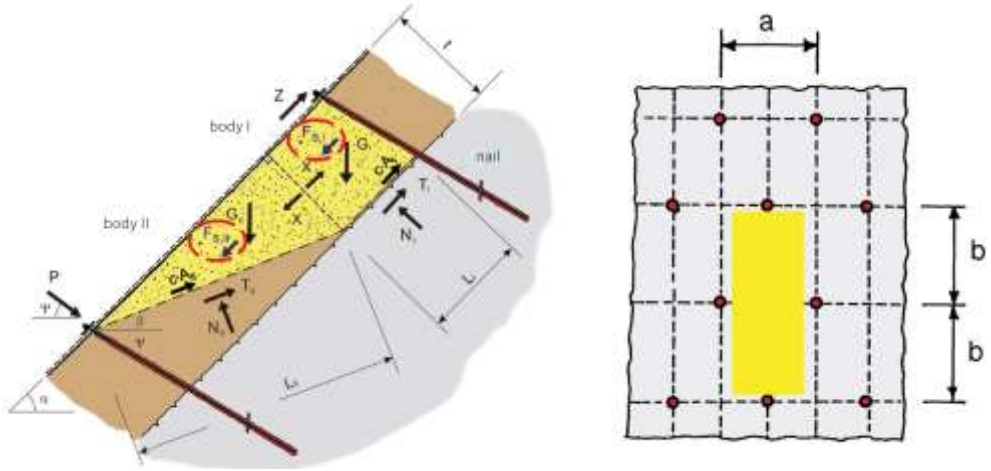

Figure 8.19 Forces applied with the break mechanism including the streaming load case

$$X\,[\mathrm{kN}] = F_{s,\mathrm{I}} + G_{\mathrm{I}} \cdot \sin\alpha - \frac{G_{\mathrm{I}} \cdot \cos\alpha \cdot \tan\varphi + c \cdot A_{c,\mathrm{I}}}{\gamma_{\mathrm{mod}}}$$

Equation 8.16 Contact force X

$$P\,[\mathrm{kN}] = \frac{G_{\mathrm{II}} \cdot \sin\beta + X \cdot \cos(\alpha-\beta) + F_{s,\mathrm{II}} \cdot \cos(\alpha-\beta) - Z \cdot \cos(\alpha-\beta) - \frac{[G_{\mathrm{II}} \cdot \cos\beta - Z \cdot \sin(\alpha-\beta) + X \cdot \sin(\alpha-\beta) + F_{s,II} \cdot \sin(\alpha-\beta)] \cdot \tan\varphi + c \cdot A_{c,\mathrm{II}}}{\gamma_{\mathrm{mod}}}}{\cos(\psi+\beta) + \sin(\psi+\beta) \cdot \frac{\tan}{\gamma_{\mathrm{mod}}}}$$

Equation 8.17 Restraining force *P*

8.8 Investigation of the global slope stability

Slopes in both soil and solid rock sometimes feature deep-seated sliding surfaces reaching deep below the slope surface to be protected, which means that a global stability problem exists as well (figure 8.20) [56, 75].

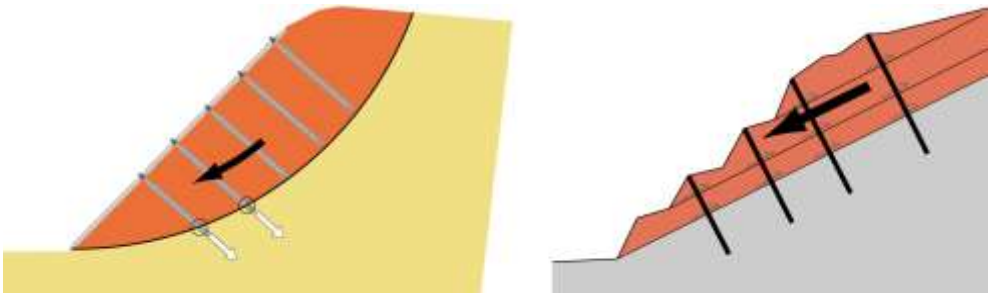

Figure 8.20 Left: Slope of soil
Right: Slope of solid rock

The method of flexible slope stabilization system with high-tensile steel wire mesh (e.g. the TECCO® mesh) is in principle a solution for the stabilization of surface layers. Dimensioning on the basis of the RUVOLUM® method is primarily for layer thicknesses of 1.0 to maximum 2.0 m.

Therefore, the following important questions must be asked:

- What measures should be taken if deeper sliding surfaces exist as well and need to be stabilized?
- Can the high-tensile steel wire mesh slope protection system be applied with reasonable chances of success?
- Can the high-tensile steel wire mesh slope protection system be combined with a subsurface stabilization?

Answer:

This is possible in principle if the nailing and anchoring are matched to the deep-seated sliding surfaces.

The nails and/or slack anchors (without active pretension) stabilized in mortar over their full length must be suitably dimensioned as far as their size/thickness (outer and inner absorption of forces) and length are concerned in order to meet the static requirements of the subsurface stabilization.

Dimensioning of the nailing and proofs of bearing safety are normally based on classical stability calculations with circular (BISHOP, FELLENIUS [1, 71]) or combined, i.e. arbitrarily curved sliding surfaces (JANBU, MORGENSTERN-PRICE, SARMA-HOEK, NONVEILER [1, 71]) which must be adapted to the prevailing geological circumstances. These methods are also used for dimensioning purposes in normal ground or rock nailing operations. The stabilization must provide a specified minimum safety $F_{\min}$ in each case (figure 8.21).

The stability of slopes is traditionally estimated using 2D limit equilibrium methods. However these methods have several disadvantages and may neglect some important factors. Due to the rapid development of computing efficiency, several numerical methods are gaining increasing popularity in slope stability engineering.

Finite Element Method and Finite Difference Method are very often used for that purpose [18, 19, 21]. The factor of safety for slope may be computed by reducing shear strength of rock or soil in stages until the slope fails. This method is called shear strength reduction technique. However, the majority of engineers still prefer using limit equilibrium methods mainly due to its simplicity, tradition of application and relatively low price of available codes.

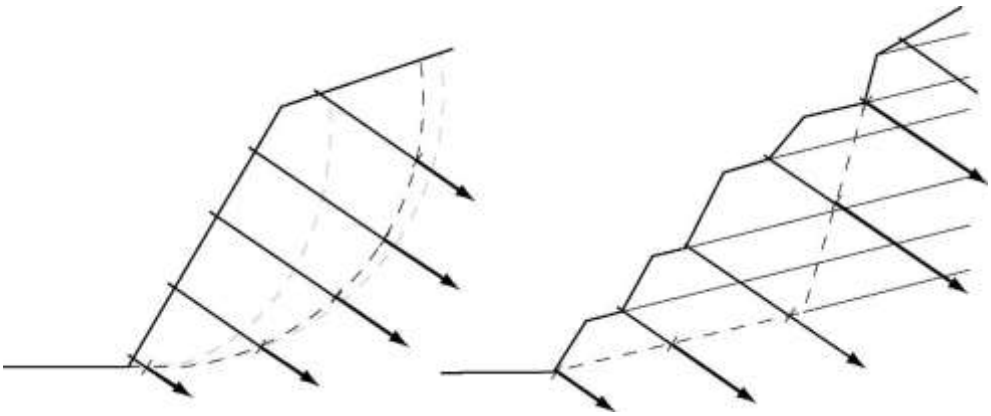

Figure 8.21 Failure mechanism and stabilization method for deep sliding problems

The method of dimensioning via proofs of the global stability eventually provides the minimum required nailing:

- Nail type (thickness, properties, etc.)
- Distance between nails
- Nail length

Hereby it must be possible to dissipate the nail forces to the substrate on both sides of the sliding surface (external bearing safety). Here outwards support is also provided by the pretensioning of the TECCO® system applied in the particular case to the slope surface (table 8.6).

Figure 8.22 illustrates the load distribution over the entire nail length.

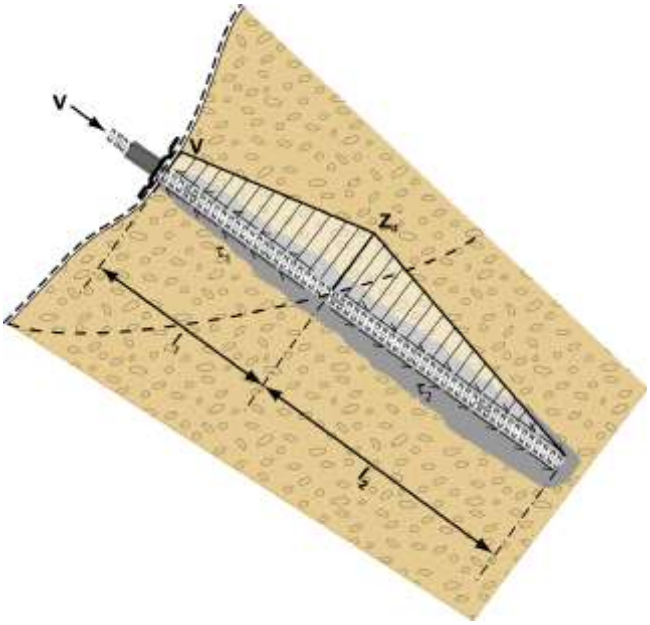

Figure 8.22 Load distribution over the nail length

Investigation for global stability
For the investigation of the overall stability, the nails are generally introduced as tension elements. By checking the internal bearing resistances (steel cross-sections and yield point under tensile load of the nails) and the external bearing resistances (friction forces or maximum head force D_{max} that can be mobilized), the terrain's resistance against sliding η and the utilization factor $1/f$ of the existing shear and system resistances are determined.
The tensile resistance available at the intersection between sliding surface and nail is limited by: 1. the internal bearing resistance of the nail Z_i 2. the external bearing resistance behind the sliding surface: $Z_{AH} = \tau_2 \cdot l_2$ 3. the external bearing resistance ahead of the sliding surface plus the system or the maximum head force that can be mobilized in case of a failure of the system against puncturing D_{max}: $Z_{AVmax} = \tau_1 \cdot l_1 + D_{max}$ whereby the smallest of the values Z_i, Z_{AH} and Z_{AVmax} is decisive.

Table 8.6 Investigation for global stability

It remains to be investigated, then, whether or not this nailing is compatible with the stabilization of the surface layer by means of the TECCO® slope stabilization system and whether or not all proofs can be established for it according to the RUVOLUM® method (figure 8.23).

By this it is guaranteed that the surface layer of delimited thickness is also adequately protected.

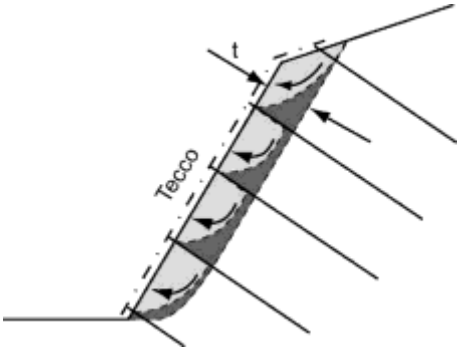

Figure 8.23 Analysis of surface layer slope stabilization investigation

Hereby one often considers only reduced shear strength parameters in the proofs for this surface layer in order to cover the long-term influences of weathering, loosening, etc. In particular, the cohesion c =0 kN/m^2 is put as a rule.

Once the proofs according to the RUVOLUM® concept are established with the nailing to meet the global requirements, nothing needs to be altered any more. If the proofs are not met (distance between nails for the high-tensile steel wire mesh excessive) or if the nails are too weak to oppose any sliding parallel to the surface, an adaptation must be made, e.g:

- Reduction of the distance between nails (nail grid)
- Strengthening of the nails (bigger diameter)
- Additional (shorter) nails

Conclusion

The flexible high-tensile steel wire mesh slope stabilization system (e.g. TECCO® system) designed according to the RUVOLUM® method can be combined with a subsurface stabilization required for the stabilization of the deeper-seated sliding surfaces.

Apart from the proof as per the RUVOLUM® method, classical stability calculations are made with curved sliding surfaces as proofs of bearing safety. The nailing is optimized based on both proofs.

The application of the high-tensile steel wire mesh slope stabilization system depends primarily on the properties of the soil, structure and geometry of ground layers, the slope gradient and the prevailing hillside water situation.

8.9 Greening and revegetation

In steep slopes featuring fine-grained, non-cohesive loose rock or severely weathered rock there is a danger of erosion. Such fine material can be washed through the high-tensile steel wire mesh and flushed away underneath it. Hereby channels and hollows may be formed under the mesh.

Emerging hillside, layer or fissure water must generally be captured and drained. Permanent water outflows will always lead to problems and must be coped with before the slope stabilization measure is started, since corrective action is hardly possible afterwards. Particular care must also be taken that no larger quantities of surface water from above flow over the slopes. If appropriate, drain channels must be provided above the edge of the slope so that the water is drained to the side in a controlled manner.

What remains is the rainwater falling directly onto the protected slope. In case of a high-intensity and long duration of the rain, this can also lead to erosion problems. The impact of the rain drops and the draining water may lead to soil movements, flushing-away and general erosion. The problem can be coped with by means of a full-surface vegetation face. The roots stabilize the surface layer and a substantial quantity of water is stored in the vegetation layer before it starts to flow off.

However, it takes time for an effective vegetation to form and for stable subsoil circumstances to result also in the small sphere. No vegetation can develop in a slope subject to movements and erosion. Immediate spraying of erosion-resistant vegetation material and seeding are not always possible directly after laying of the meshes (vegetation period). It is often necessary, therefore, to provide an erosion protection together with the mesh so that erosion and washing-out are prevented for the time being and optimal prerequisites achieved for successful greening later on.

Regrettably it is usually not possible to achieve the goal with the known erosion protection mats of natural fibres (e.g. jute, choir) because the often irregular surfaces prevent an uninterrupted ground contact of the mats. The mats in question are normally too tight for spraying-through of vegetation material and seeds. The results are undesirable and in the long run critical bare patches which expose the free surfaces to erosion again as soon as the mats have rotted away.

What was sought, therefore, was a flexible mat of a three-dimensional open structure which provides a comparatively good protection against erosion despite relatively large openings. The mat must also be suitable as an adhesion and stabilization layer for the vegetation for as long as the latter is unable to perform this function. Of importance is also that the mat is optically inconspicuous, i.e. adapted in its colour to the substrate.

After various suitability tests with different products, with dry and wet greening also in extreme locations exposed to the south, a 3-dimensional mat of a loop structure, a so-called random-laid nonwoven fabric of polypropylene was eventually found, which meets the partly opposing requirements of erosion protection and vegetation face in optimum manner. The technical data compiled on the following page apply to this erosion protection mat, developed especially for use in combination with the TECCO® stabilization system and available under the trade name of TECMAT (picture 8.1).

Picture 8.1 TECMAT Erosion control mat installed underneath the TECCO® mesh

Technical data of TECMAT

Raw material:	polypropylene
Type of mat:	irregular, three-dimensional loop structure with punctiform bondings
Thickness:	approx. 18 mm
Areal weight:	600 g/m^2
Opening width:	approx. 5–15 mm
Colour:	curry-green

Picture 8.2 right shows a typical application of the erosion control mat TECMAT in combination with a high-tensile steel wire mesh.

Revegetation with integrated erosion protection mat

Alternatively to the TECMAT erosion control mat the TECCO® G65/3 GREEN can be used where the erosion control mat is already integrated in the mesh.

Picture 8.2 Erosion control mat integrated with high-tensile steel wire mesh

8.10 External examination and inspection of the new designing method

The new method of the designing of flexible slope stabilization systems with high-tensile steel wire meshes, (also called the "RUVOLUM®" dimensioning method), was developed in coordination with the company Rüegger+Flum AG, St. Gallen, Switzerland in the context of the development of high-tensile steel wire mesh.

The entire concept of the RUVOLUM® dimensioning method for flexible slope stabilization systems for wire meshes and nails was also inspected by Prof. Dr.-Ing. L. Wichter, University of Cottbus, Faculty for Rock and Soil Mechanics, Germany [145].

The RUVOLUM® method was checked by Prof. Dr.-Ing. Wichter to the plausibility of the assumptions. He was also asked to comment on the geotechnical and safety-theoretical aspects of the dimensioning concept. The resulting basic conclusions are thereby:

- The assumptions via the kinematics of the slides are traceable.
- The assumptions on which the concept is based are plausible and in accordance with the observations made in reality.
- The simplifications and idealizations are comprehensible.
- The bearing resistances of the system elements and the system itself have been determined in many tests under the supervision of the LGA Nürnberg and it is allowed to take them into account.

As a conclusion of this external inspection, the entire dimensioning method and concept, the relevant test setups, all mechanical formulas and equations, etc. were checked and approved in detail.

Another detailed external system investigation was made by the German Federal Office for Railroad (EBA, Deutsches Eisenbahn Bundesamt). As an official certification by this Federal Office, the entire TECCO® slope stabilization system and its elements were approved.

8.11 General remarks about natural hazard protection

Slope instabilities, rockfall, landslides, debris flows or avalanches are sporadic and unpredictable. Causes can be e.g. human (construction, etc.) or environmental (weather, earthquakes, etc.). Due to the multiplicity of factors affecting such events it is not and cannot be an exact science that guarantees the safety of individuals and property.

However, by the application of sound engineering principles to a predictable range of parameters and by the implementation of correctly designed protection measures in identified risk areas, the risks of injury and loss of property can be reduced substantially.

Inspection and maintenance of such systems are an absolute requirement to ensure the desired protection level. The system safety can also be impaired by events such as natural disasters, inadequate dimensioning parameters or failure to use the prescribed standard component, systems and original parts; and/or corrosion (caused by pollution of the environment or other man-made factors as well as other external influences).

9 Dimensioning examples

9.1 Base for example hand calculation

To present the way of dimensioning of flexible slope stabilization systems against superficial instabilities in a detailed way, an example hand calculation has been carried out. Thereby, the following summarized data has been assumed:

Slope inclination	α	=	60 degrees
Layer thickness	t	=	1.00 m
Radius of the pressure cone on top	ζ	=	0.15 m
Inclination of the pressure cone to horizontal	δ	=	45 degrees
Friction angle of soil (characteristic value)	φ_k	=	36 degrees
Cohesion of soil (characteristic value)	c_k	=	0 kN
Unit weight of soil (characteristic value)	γ_k	=	20 kN/m^3
Slope-parallel force	Z_d	=	15 kN
Pretensioning force of the system	V	=	30 kN
Inclination of the nail to horizontal	Ψ	=	25 degrees

Based on the partial safety concept proclaimed in EUROCODE 7, the following partial safety correction values have been considered:

Partial safety correction value for friction angle	γ_φ	=	1.25
Partial safety correction value for cohesion	γ_c	=	1.25
Partial safety correction value for unit weight	γ_γ	=	1.00
Model uncertainty correction value	γ_{mod}	=	1.10

The resulting dimensioning values of the geotechnical parameters are thereby:

Friction angle of soil (dimensioning value)	φ_d	=	arctan (tan φ_k/γ_φ)	= 30.17 degrees
Cohesion of soil (dimensioning value)	c_d	=	c_k/γ_c	= 0 kN
Unit weight of soil (dimensioning value)	γ_d	=	$\gamma_k \cdot \gamma_\gamma$	= 20 kN/m^3

The following system elements have been considered:

- High-tensile steel wire mesh TECCO® G65/3
- System spike plate P33 adapted to the steel wire mesh TECCO®
- Nailing

For the nailing, the following nail type has been proposed. Rusting away is thereby generally taken into account by reducing the nail diameter by 4 mm:

- Nail type GEWI
- Nail diameter 32 mm
- Yield point by tensile strain 500 N/mm^2
- Cross-section surface of the nail 616 mm^2
- Bearing resistance of the nail to tensile force 308 kN
- Bearing resistance of the nail to shear force 178 kN

The following bearing resistances have been taken into account. Those of the TECCO® mesh are determined in tests carried out under the supervision of the independent technical institute LGA (Landesgewerbe Anstalt) in Nürnberg, Germany (see also pictures 9.1 and 9.2 accordingly).

- Bearing resistance of the TECCO® mesh to selective, slope parallel tensile strain Z_R = 30 kN
- Bearing resistance of the TECCO® mesh to pressure strain in nail direction D_R = 180 kN
- Bearing resistance of the TECCO® mesh against shearing-off at the spike plate in nail direction P_R = 90 kN

For the proposed nail type, the following bearing resistances have been considered whereby rusting away is generally taken into account by reducing the nail diameter by 4 mm:

- Bearing resistance of the nail of type GEWID= 32mm to tensile force T_R = 308 kN
- Bearing resistance of the nail of type GEWID= 32mm to shear force S_R = 178 kN

Picture 9.1 Test setup to determine Z_R

Picture 9.2 Test setup to investigate the puncturing resistance

9.2 Investigation of slope-parallel, superficial instabilities

9.2.1 Consideration of equilibrium

The way of determining the maximum shear strain as well as all corresponding proofs of bearing safety are presented in the following in a detailed way. Figure 9.1 illustrates the cubic body that needs to be investigated.

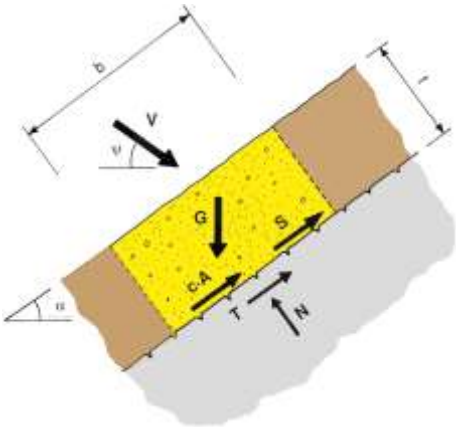

Figure 9.1 Cubic body to be investigated

Thickness of the superficial layer to be investigated	$t = 1.00\,\text{m}$
Inclination of the slope to horizontal	$\alpha = 60$ degrees
Inclination of the nailing to horizontal	$\Psi = 25$ degrees
Nail distance horizontal	$a = 3.0\,\text{m}$
Nail distance in line of slope	$b = 3.0\,\text{m}$

G = dead weight of the sliding body to be investigated

A = sliding surface of the body to be investigated

$$G = a \cdot b \cdot t \cdot \gamma_d = 3.0 \cdot 3.0 \cdot 1.00 \cdot 20.0 = 180\,\text{kN}$$

$$A = a \cdot b = 3.0 \cdot 3.0 = 9.0\,\text{m}^2$$

Pretensioning force effectively applied on nail	$V = 30.0\,\text{kN}$
Load factor for positive influence of pretension	$\gamma_{VI} = 0.80$
Dimensioning value of the applied pretensioning force by positive influence of V	$V_{dI} = 24.0\,\text{kN}$

$$S_d = 1/\gamma_{mod} \cdot \{\gamma_{mod} \cdot G \cdot \sin \alpha - V_{dI} \cdot \gamma_{mod} \cdot \cos(\Psi + \alpha) - c_d \cdot A - [G \cdot \cos \alpha + V_{dI} \cdot \sin(\Psi + \alpha)] \cdot \tan \varphi_d\}$$

$$S_d = 1/1.10 \cdot \{1.10 \cdot 180 \cdot \sin 60 - 24.0 \cdot 1.10 \cdot \cos(25 + 60) - 0 \cdot 9.0 - [180 \cdot \cos 60 + 24.0 \cdot \sin(25 + 60)] \cdot \tan 30.17\} = \mathbf{93.6\ kN}$$

9.2.2 Proofs of bearing safety

Proof of the nail against sliding-off of a superficial layer parallel to the slope

$S_d \le S_R/\gamma_{SR}$
$S_d = 93.6$ kN
$S_R = 178$ kN
$\gamma_{SR} = 1.50$

$S_R/\gamma_{SR} = 178/1.50 = 118.7$ kN > 93.6 kN → Proof of bearing safety fulfilled!

Proof of the mesh against puncturing

$V_{dII} \le D_R/\gamma_{DR}$

Pretensioning force effectively applied on nail	$V = 30.0$ kN
Load factor for negative influence of pretension	$\gamma_{VII} = 1.50$
Dimensioning value of the applied pretensioning force by negative influence of V	$V_{dII} = 45.0$ kN

$D_R = 180$ kN
$\gamma_{DR} = 1.50$

$D_R/\gamma_{DR} = 180/1.50 = 120$ kN > 45 kN → Proof of bearing safety fulfilled!

Proof of the nail to combined strain

$([V_{dII}/(T_R/\gamma_{VR})]^2 + [S_d/(S_R/\gamma_{SR})]^2)^{0.5} \le 1.0$

$V_{dII} = 45.0$ kN
$T_R = 308$ kN
$\gamma_{VR} = 1.50$
$S_d = 93.6$ kN
$S_R = 178$ kN
$\gamma_{SR} = 1.50$

$([V_{dII}/(T_R/\gamma_{VR})]^2 + [S_d/(S_R/\gamma_{SR})]^2)^{0.5} = ([45.0/(308/1.50)]^2 + [93.6/(178/1.59)]^2)^{0.5} \le 1.0$

→ Proof of bearing safety fulfilled!

$([P_d/(T_R/\gamma_{VR})]^2 + [S_d/(S_R/\gamma_{SR})]^2)^{0.5} \leq 1.0$

P_d = 58.5 kN (cf. Chapter 9.3.2)
T_R = 308 kN
γ_{VR} = 1.50
S_d = 93.6 kN
S_R = 178 kN
γ_{SR} = 1.50

$([P_d/(T_R/\gamma_{VR})]^2 + [S_d/(S_R/\gamma_{SR})]^2)^{0.5} = ([58.5/(308/1.50)]^2 + [93.6/(178/1.59)]^2)^{0.5} \leq 1.0$

→ Proof of bearing safety fulfilled!

9.3 Investigation of local instabilities between single nails

9.3.1 Failure mechanism A

In the following, an example hand calculation is carried out in a very detailed way investigating 1-body sliding mechanism:

Thickness of the investigated sliding mechanism	t_i = 0.85 m
Thickness of the superficial layer to be investigated	t = 1.00 m
Inclination of the slope to horizontal	α = 60 degrees
Inclination of the nailing to horizontal	Ψ = 25 degrees
Nail distance horizontal	a = 3.0 m
Nail distance in line of slope	b = 3.0 m

$\beta = \alpha - \arctan\{t_i/[2b + t_i/\tan(\alpha + \Psi)]\}$	= 52.03 degrees
$\beta_2 = \alpha - \arctan\{t/[2b + t/\tan(\alpha + \Psi)]\}$	= 50.7 degrees
$\rho = \alpha - \beta$	= 7.97 degrees
$h = 2b \cdot \sin\rho$	= 0.84 m
$L_1 = h/\tan(\Psi + \beta) = (2b \cdot \sin\rho)/\tan(\Psi + \beta)$	= 0.19 m
$L_2 = 2b \cdot \cos\rho$	= 5.94 m
$F_1 = h \cdot L_1/2$	= 0.08 m^2
$F_2 = h \cdot L_2/2$	= 2.49 m^2
$F = F_1 + F_2$	= 2.57 m^2
$a_{red} = a - t_i/\tan\delta - 2 \cdot \zeta = 3.0 - 0.85/\tan 45 - 2 \cdot 0.15$	= 1.85 m

G = dead weight of the investigated sliding mechanism
A = sliding surface of the mechanism to be investigated

$G = F \cdot a_{red} \cdot \gamma_d = 2.57 \cdot 1.85 \cdot 20.0$	= 95.1 kN
$A = (L_1 + L_2) \cdot a_{red}$	= 11.34 m^2

$$P_d = \{G \cdot [\gamma_{mod} \cdot \sin\beta - \cos\beta \cdot \tan\varphi_d] - Z_d \cdot [\gamma_{mod} \cdot \cos(\alpha - \beta) - \sin(\alpha - \beta) \cdot \tan\varphi_d] - c_d \cdot A\}/\{\gamma_{mod} \cdot \cos(\beta + \Psi) + \sin(\beta + \Psi) \cdot \tan\varphi_d\}$$

P_d = {95.1 · [1.10 · sin 52.03 – cos 52.03 · tan 30.17] – 15
· [1.10 · cos (60 – 52.03) – sin (60 – 52.03) · tan 30.17] – 0 }/
{1.10 · cos (52.03 + 25) + sin (52.03 + 25) · tan 30.17}

P_d = 41.1 kN

9.3.2 Failure mechanism B

In the following, an example hand calculation is carried out in a very detailed way investigating a 2-body sliding mechanism:

In a previous investigation, the inclination of the sliding surface β has been varied between 0 … β_l on the one hand. On the other hand, the thickness t_i has been changed between 0 … t with the aim to find the most critical case.

Thickness of the investigated sliding mechanism	t_i = 0.85 m
Inclination of the slope to horizontal	α = 60 degrees
Inclination of the investigated sliding surface	β = 45 degrees
Inclination of the nailing to horizontal	Ψ = 25 degrees
Nail distance horizontal	a = 3.0 m
Nail distance in line of slope	b = 3.0 m

ρ_1 = arctan (t_i/2b) = 8.06 degrees
$L_1 = 2b - t_i/\tan(\alpha - \beta) + t_i/\tan(\alpha + \Psi)$ = 2.90 m
$L_2 = t_i/\sin(\alpha - \beta)$ = 3.28 m
$F_1 = t_i \cdot [2b - t_i/\tan(\alpha - \beta)] + t_i^2/[2 \cdot \tan(\alpha + \Psi)]$ = 2.43 m²
$F_2 = t_i^2/[2 \cdot \tan(\alpha - \beta)]$ = 1.35 m²
$F = F_1 + F_2$ = 3.78 m²

$a_{red} = a - t_i/\tan\delta - 2 \cdot \zeta = 3.0 - 0.85/\tan 45 - 2 \cdot 0.15$ = 1.85 m

G_1 = dead weight of the investigated body I
G_2 = dead weight of the investigated body II
A_1 = sliding surface of the investigated body I
A_2 = sliding surface of the investigated body II

$G_1 = F_1 \cdot a_{red} \cdot \gamma_k \cdot \gamma_\gamma = 2.43\ m^2 \cdot 1.85\ m \cdot 20\ kN/m^3 \cdot 1.00$ = 89.91 kN
$G_2 = F_2 \cdot a_{red} \cdot \gamma_k \cdot \gamma_\gamma = 1.35\ m^2 \cdot 1.85\ m \cdot 20\ kN/m^3 \cdot 1.00$ = 49.95 kN

$A_1 = L_1 \cdot a_{red} = 2.90\ m \cdot 1.85\ m$ = 5.37 m²
$A_2 = L_2 \cdot a_{red} = 3.28\ m \cdot 1.85\ m$ = 6.07 m²

$X = 1/\gamma_{mod} \cdot \{G_1 \cdot (\gamma_{mod} \cdot \sin\alpha - \cos\alpha \cdot \tan\varphi_d) - c_d \cdot A_1\}$
= 1/1.10 · {89.91 kN · (1.10 · sin 60 – cos 60 · tan 30.17) – 0 kN/m² · 5.37 m}
= **54.1 kN**

$P = \{G_2 \cdot [\gamma_{mod} \cdot \sin\beta - \cos\beta \cdot \tan\varphi_d] + (X - Z_d) \cdot [\gamma_{mod} \cdot \cos(\alpha - \beta) - \sin(\alpha - \beta) \cdot \tan\varphi_d] - c_d \cdot A_2\}/\{\gamma_{mod} \cdot \cos(\beta + \Psi) + \sin(\beta + \Psi) \cdot \tan\varphi_d\}$

$$P = \{49.95\ \text{kN} \cdot [1.10 \cdot \sin 45 - \cos 45 \cdot \tan 30.17] + (54.1\ \text{kN} - 15.0\ \text{kN}) [1.10 \cdot \cos(60 - 45) - \sin(60 - 45) \cdot \tan 30.17] - 0 \cdot 6.07\} / \{1.10 \cdot \cos(45 + 25) + \sin(45 + 25) \cdot \tan 30.17\} = \mathbf{58.5\ kN}$$

9.3.3 Proofs of bearing safety

Comparing the result from on the investigation based on case A with that based on case B, then, the maximum force of $P_d = 58.5$ kN has to be considered.

Proof of the mesh against shearing-off at the upslope edge of the spike plate

P_d = 58.5 kN
P_R = 90.0 kN
γ_{PR} = 1.50

P_R/γ_{PR} = 60 kN

Proof of bearing safety: $P_d \le P_R/\gamma_{PR}$ → fulfilled!

Proof of the mesh to selective transmission of the slope-parallel force Z

Z_d = 15.0 kN
Z_R = 30.0 kN
γ_{ZR} = 1.50

Z_R/γ_{ZR} = 20 kN

Proof of bearing safety: $Z_d \le Z_R/\gamma_{ZR}$ → fulfilled !

9.4 RUVOLUM® dimensioning example

Another example for the investigation of superficial instabilities is to demonstrate the application of the RUVOLUM® method, for example for dimensioning the flexible slope stabilization system TECCO®. Hereby it is assumed that the stable subsoil (rock) is covered by a soil layer (sandy gravel) of thickness t which must be protected against instabilities. All necessary geometrical and geotechnical input data are compiled in the table 9.1 below.

System elements considered in the dimensioning example

- High-tensile wire mesh TECCO®G65/3
- TECCO® system spike plate
- Nail type GEWI D = 28 mm (rusting away of the nail taken into account: diameter reduced by 4 mm)

Input data for the example to dimension the TECCO® slope stabilization system

Input quantities	Abbreviation	Values
Slope inclination	α [degrees]	60.0
Layer thickness	t [m]	0.50/1.00
Friction angle of soil (characteristic value)	φ' [degrees]	35.0
Cohesion of soil (characteristic value)	c' [kN/m^2]	0.0
Unit weight of soil (characteristic value)	γ [kN/m^3]	22.0
Partial safety correction value friction angle	γ_φ [–]	1.25
Partial safety correction value cohesion	γ_c [–]	1.25
Partial safety correction value unit weight	γ_Y [–]	1.00
Model uncertainty correction value	γ_{mod} [–]	1.10
Slope-parallel force	Z [kN]	15.0
Pretensioning force of the system	V [kN]	30.0
Nail inclination to horizontal	ψ [degrees]	25.0

Table 9.1 Input data for the example to dimension the TECCO® slope stabilization system

Taking into account the above mentioned system elements and the input quantities compiled in table 9.1, the dimensioning calculation results in the maximum possible distance a (horizontally), and b (in the line of slope):

for t = 0.50 m: $a = b$ = 3.00 m.
for t = 1.00 m: $a = b$ = 2.65 m.

If the layer thickness is t = 0.50 m, the mesh becomes decisive. Hereby the proof of the mesh against shearing-off at the upslope edge of the spike plate is the determining proof of bearing safety, as compiled in table 9.2.

Decisive proof of bearing safety of the mesh against shearing off at the edge of the spike plate for a layer thickness t = 0.50 m

Input quantities	Abbreviation	Values
Dimensioning value of the max. force on the mesh for shearing-off at the upslope edge of the spike plate at the lower nail	P_d [kN]	58.8
Bearing resistance of the mesh against shearing-off in nail direction at the up-slope edge of the spike plate (determined in tests)	P_R [kN]	90.0
Resistance correction value for shearing of the mesh	γ_{PR} [–]	1.5
Dimensioning value of the bearing resistance of the mesh against shearing-off	P_R/γ_{PR}	60.0
Proof of bearing safety	$P_d \leq = P_R/\gamma_{PR}$	Fulfilled

Table 9.2 Decisive proof of bearing safety of the mesh against shearing off at the edge of the spike plate for a layer thickness t = 0.50 m

In case of a layer thickness t= 1.00 m it is no longer the mesh which is decisive in the dimensioning example, but the nail, whereby the mesh is utilized in optimal manner. The determining proof of bearing safety in this case is the proof of the nail against a slope-parallel sliding-off of the surface layer. This is compiled in table 9.3.

Proof of the nail to combined stress

Input quantities	Abbreviation	Values
Pretensioning force effectively applied on nail	V [kN]	30.0
Load factor for positive influence of pretension	γV_{I} [–]	0.8
Dimensioning value of the applied pretensioning force by positive influence of V	$V_{d\mathrm{I}}$ [kN]	24.0
Load factor for negative influence of pretension	γV_{II} [–]	1.5
Dimensioning value of the applied pretensioning force by negative influence of V	$V_{d\mathrm{II}}$ [kN]	45.0
Calculation required shear force at dimensioning level in function of V	S_d [kN]	80.2
Max. force on the mesh for shearing-off	P_d [kN]	42.0
Bearing resistance of the nail to tensile force	$T_{R\mathrm{red}}$ [kN]	226.0
Bearing resistance of the nail to shear force	$S_{R\mathrm{red}}$ [kN]	131.0
Resistance correction value for tensile force	γ_{TR} [–]	1.5
Resistance correction value for shear force	γ_{SR} [–]	1.5
Proof of bearing safety: $\{(V_{d\mathrm{II}}/(T_{R\mathrm{red}}/\gamma_{\mathrm{TR}}))^2 + (S_{\mathrm{d}}/(S_{R\mathrm{red}}/\gamma_{SR}))^2\}^{0.5} \leq 1.0$	0.966 ≤ 1.0	fulfilled!
Proof of bearing safety: $\{(P_{\mathrm{d}}/(T_{\mathrm{Rred}}/\gamma_{\mathrm{TR}}))^2 + (S_{\mathrm{d}}/(S_{R\mathrm{red}}/\gamma_{SR}))^2\}^{0.5} \leq 1.0$	0.960 ≤ 1.0	fulfilled!

Table 9.3 Proof of the nail to combined stress for the layer thickness t = 1.00 m

Remark regarding lateral nails

The stabilizing effect of the lateral nails is not taken into account, which means that a hidden safety exists. Due to the high transverse stiffness as compared to the lengthwise stiffness, the effect of this safety shows up in case of major deformations only.

9.5 Dimensioning software

The hand calculation in chapters 9.1 – 9.3 is providing an overview of the calculations that are required for the new dimensioning method for flexible slope stabilization.

For practical use, a corresponding software[38] was programmed in order to make dimensioning easier. Additionally, such software tools avoid to make mathematical calculation mistakes and allow quick studies with material and geometrical variations.

The software offers also the possibility of considering streaming pressure and accelerations due to earthquake in horizontal as well as in vertical direction. The calculations can be done on the basis of international as well as American units in English, German, Polish, French, Italian, Spanish, Portuguese, Chinese, Russian and Romanian. The language versions are important for local knowledge transfer and again in order to avoid mistakes or misunderstandings.

A corresponding software manual provides the most important references and function descriptions to enable users to utilize the program correctly. The aim has been to develop a program which, despite its complexity of structure and application, is as clear and straightforward as possible as far as aspects of graphic presentation and user-friendliness are concerned (figure 9.2 shows overview of conducted calculations variants). Numerous parameters need to be entered for the dimensioning operations. It is the responsibility of the user of this program to select and enter these parameters correctly.

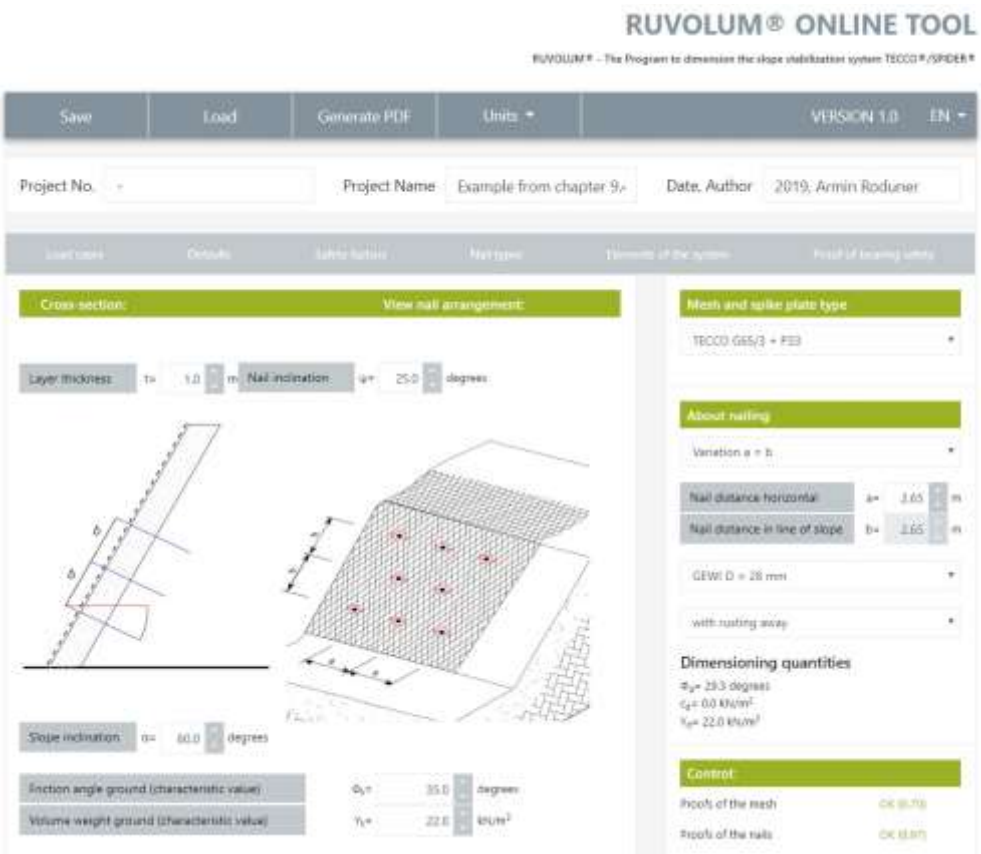

Figure 9.2 Overview of RUVOLUM® software calculation tool

[38] This dimensioning software is named "RUVOLUM® Software" and was developed originally by Ms. Ana María Brisbé York in Spain and by Mr. Daniel Flum in Switzerland [14].

It shall not be the target of this publication to describe the software tool in a more detailed way. Nevertheless, for overview reasons, some selective programming views are provided on figure 9.3 and figure 9.4. Appendix H is showing the output data sheet of the sample calculation from chapter 9.4.

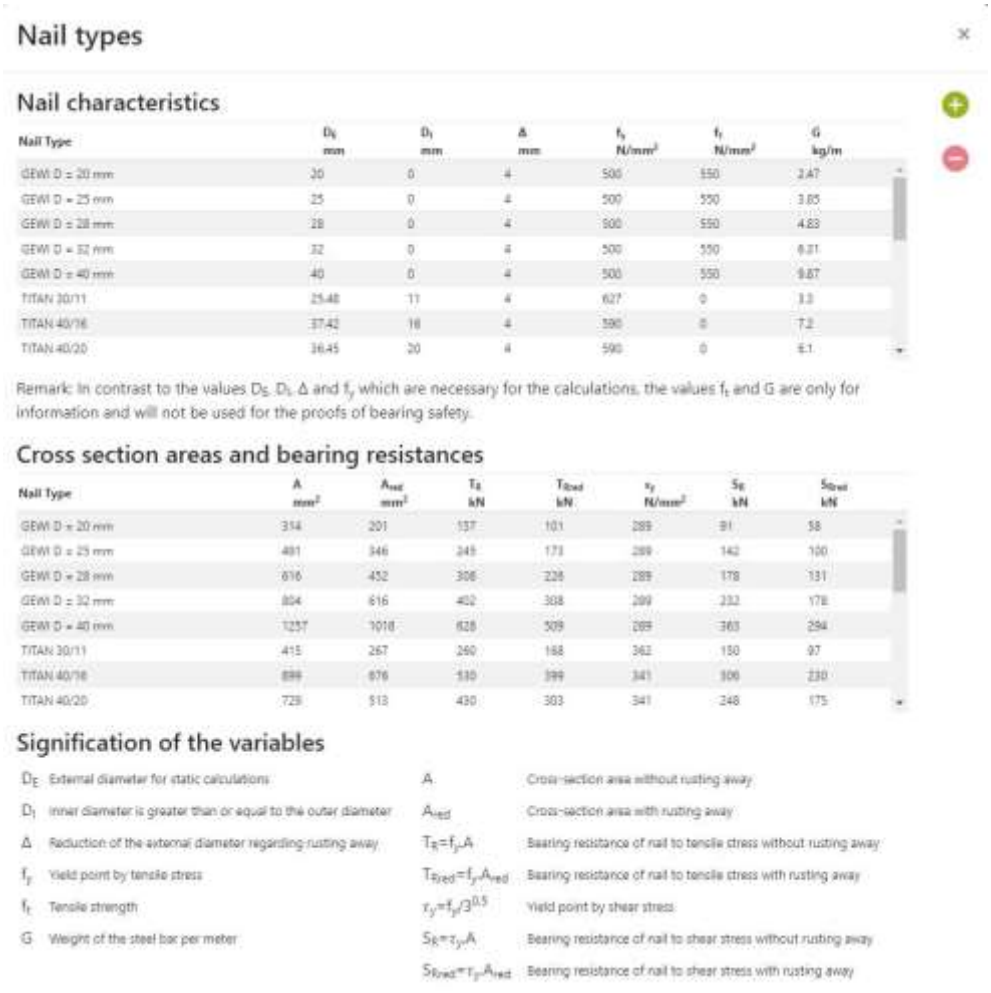

Nail types

Nail characteristics

Nail Type	D_E mm	D_I mm	Δ mm	f_y N/mm²	f_t N/mm²	G kg/m
GEWI D = 20 mm	20	0	4	500	550	2.47
GEWI D = 25 mm	25	0	4	500	550	3.85
GEWI D = 28 mm	28	0	4	500	550	4.83
GEWI D = 32 mm	32	0	4	500	550	6.31
GEWI D = 40 mm	40	0	4	500	550	9.87
TITAN 30/11	25.48	11	4	627	0	3.3
TITAN 40/16	37.42	16	4	590	0	7.2
TITAN 40/20	36.45	20	4	590	0	6.1

Remark: In contrast to the values D_E, D_I, Δ and f_y which are necessary for the calculations, the values f_t and G are only for information and will not be used for the proofs of bearing safety.

Cross section areas and bearing resistances

Nail Type	A mm²	A_{red} mm²	T_E kN	T_{Ered} kN	τ_y N/mm²	S_E kN	S_{Ered} kN
GEWI D = 20 mm	314	201	157	101	289	91	58
GEWI D = 25 mm	491	346	245	173	289	142	100
GEWI D = 28 mm	616	452	308	226	289	178	131
GEWI D = 32 mm	804	616	402	308	289	232	178
GEWI D = 40 mm	1257	1018	628	509	289	363	294
TITAN 30/11	415	267	260	168	362	150	97
TITAN 40/16	899	676	530	399	341	306	230
TITAN 40/20	729	513	430	303	341	248	175

Signification of the variables

D_E	External diameter for static calculations	A	Cross-section area without rusting away
D_I	Inner diameter is greater than or equal to the outer diameter	A_{red}	Cross-section area with rusting away
Δ	Reduction of the external diameter regarding rusting away	$T_E = f_y A$	Bearing resistance of nail to tensile stress without rusting away
f_y	Yield point by tensile stress	$T_{Ered} = f_y A_{red}$	Bearing resistance of nail to tensile stress with rusting away
f_t	Tensile strength	$\tau_y = f_y / 3^{0.5}$	Yield point by shear stress
G	Weight of the steel bar per meter	$S_E = \tau_y A$	Bearing resistance of nail to shear stress without rusting away
		$S_{Ered} = \tau_y A_{red}$	Bearing resistance of nail to shear stress with rusting away

Figure 9.3 Example of nail types in the dimensioning software

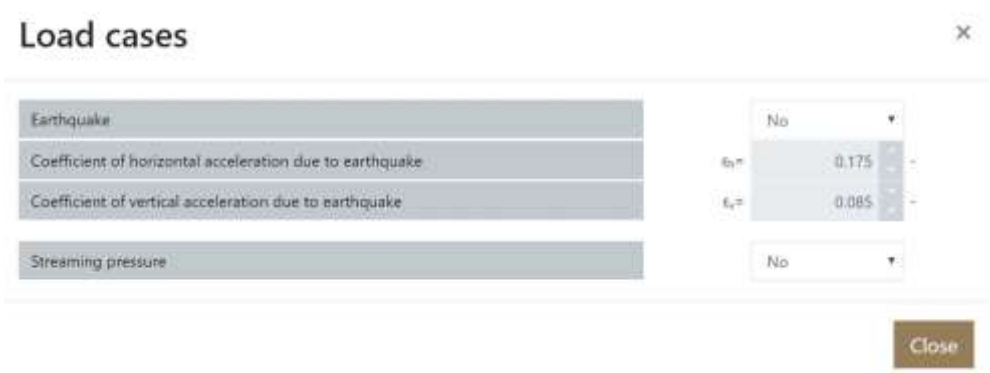

Figure 9.4 Example of load cases in the dimensioning software

10 Project execution and installation

The method of designing flexible slope stabilization systems with high-tensile steel wire meshes was explained in the chapters 5–9 of this book and so far, mainly the theoretical geotechnical aspects, calculations, evaluations and dimensioning were illustrated and discussed.

However, a successful slope stabilization system is only then safe and secure, if it is properly installed and maintained.

Consequently, chapter 10 shall give some important information, advise and practical recommendations for the appropriate application and execution of such slope stabilization systems with high-tensile steel wire meshes [141].

10.1 Project

10.1.1 Planning steps

Professional planning of a slope stabilization system with high-tensile steel wire meshes requires the following planning sequence to be carried out right to the final objective of an execution project [118]. The sequence must include a summary of masses and details of particular measures (e.g. drainage) to guarantee the suitability for the intended purpose:

Planning steps

1. Problem	Formulate the problem in general
2. Slope Stabilization System	General deployment possibilities as per scope of application
3. Function	– Slope stabilization – Protection against breaking out – Rockfall protection – Erosion protection
4. Planning fundamentals as per TECCO® check list	– General project information – Topography – Terrain profiles – General Geology – Subsoil circumstances – Course of layers – Surface layers – Soil and rock characteristic values – Deep sliding surfaces – Water – Special aspects
5. Dimensioning by means of the RUVOLUM® dimensioning concept	– Proofs of bearing capacity and safety – Measures to ensure the suitability for the intended purpose

	From the above follows: – Maximum distances between nails – Nail types and lengths – Pretensioning forces – Object-specific measures
6. Project	– Dimensions of the safety measures – Nails plan – Preparation of the terrain – Scope, material requirement – Ordering of special measures – Erosion protection – Drainage – Greening, planting – Call for tenders

10.1.2 Planning fundamentals

In order to enable expert planning of a slope stabilization system with high-tensile steel wire meshes, the most varied fundamentals need to be available and marginal conditions must be known.

The recommended basis for this is a check list which permits recording of all relevant basic data and marginal conditions required for dimensioning and for project work. Total completion of the check list is a prerequisite before processing of the project can be continued.

Various data and information must be procured from thirds (plans, geology, characteristic values of the soil, etc.). Hereby it is important to state the sources of documents and data so that the responsibilities can be delimited. If, for example, a geologist or geotechnical engineer provides the important information on the subsoil and the decisive characteristic values, this person is also responsible for these details which serve to dimension the system and to establish proof of the bearing safety. The supplier of the system cannot be held liable for damages originating from misjudgements in this respect. Unless also entrusted with the geological-geotechnical clarifications and surveying, the system supplier is only liable for damages which can be traced to faulty materials or dimensioning (provided that dimensioning was in the supplier's care).

10.1.3 Variables of the slope stabilization system with high-tensile steel wire meshes

The following variables exist for slope stabilization systems with high-tensile steel wire meshes:

– Distance between nails a = horizontal distance from nail head to nail head

– Distance between nails b = distance between the rows of nails measured in the line of slope

– Nail type (with specific tensile strength and shear resistance)

– Nail length

– Nail inclination

These variables are determined by the dimensioning of the slope stabilization system.

10.1.4 Marginal conditions and parameters

Various general conditions must be known for each project to permit determination of the variables by proofs of the bearing capacity and stability (see also figure 10.1).

Marginal conditions

1. Terrain profile	– Height of slope (measured vertically)	H
	– Length of slope (measured parallel to slope)	L
	– Width of slope (measured horizontally)	B
	– With adequate bottom boundary section	$R_u > H/2$
	– With adequate top boundary section	$R_o > H$
	– Mean decisive slope gradients	α
2. Layer structure in the subsoil	Description of the subsoil (Classification for uncons. material or rock)	
	Layers from bottom to top marked	A, B, C, ...
3. Surface layer	Thickness of the surface layer to be secured, measured at right angle to the surface, with classification relative to the subsoil layers A, B, C, ...	t_A, t_B, t_C, ...
4. Soil characteristic values	Differentiation between decisive subsoil layers associated surface layer	
	Subsoil layer A, B, C, ...	
	– unit weight	$\gamma_{A,B,C,...}$
	– friction angle	$\varphi_{A,B,C,...}$
	– cohesion	$c_{A,B,C,...}$
	Surface layer pertaining to A, B, C ... of thickness t_A, t_B, t_C, ...	
	– unit weight	$\gamma_{At,Bt,Ct,...}$
	– friction angle	$\varphi_{At,Bt,Ct,...}$
	– cohesion	$c_{At,Bt,Ct,...}$
5. Global stability	Assessment of the need to secure deeper existing or potential sliding surfaces by means of the nailing to achieve an adequate safety against rupture of the terrain.	

Additional special marginal conditions are:

- Hillside or ground water, hillside springs
- Difficulties due to obstacles (trees, buildings, etc.)
- Need for greening, planting (altitude, exposure, climate, natural vegetation)
- Requirements applying to greening, planting
- Additional erosion protection in case of fine-grained subsoil
- Additional rockfall protection in case of special hazards

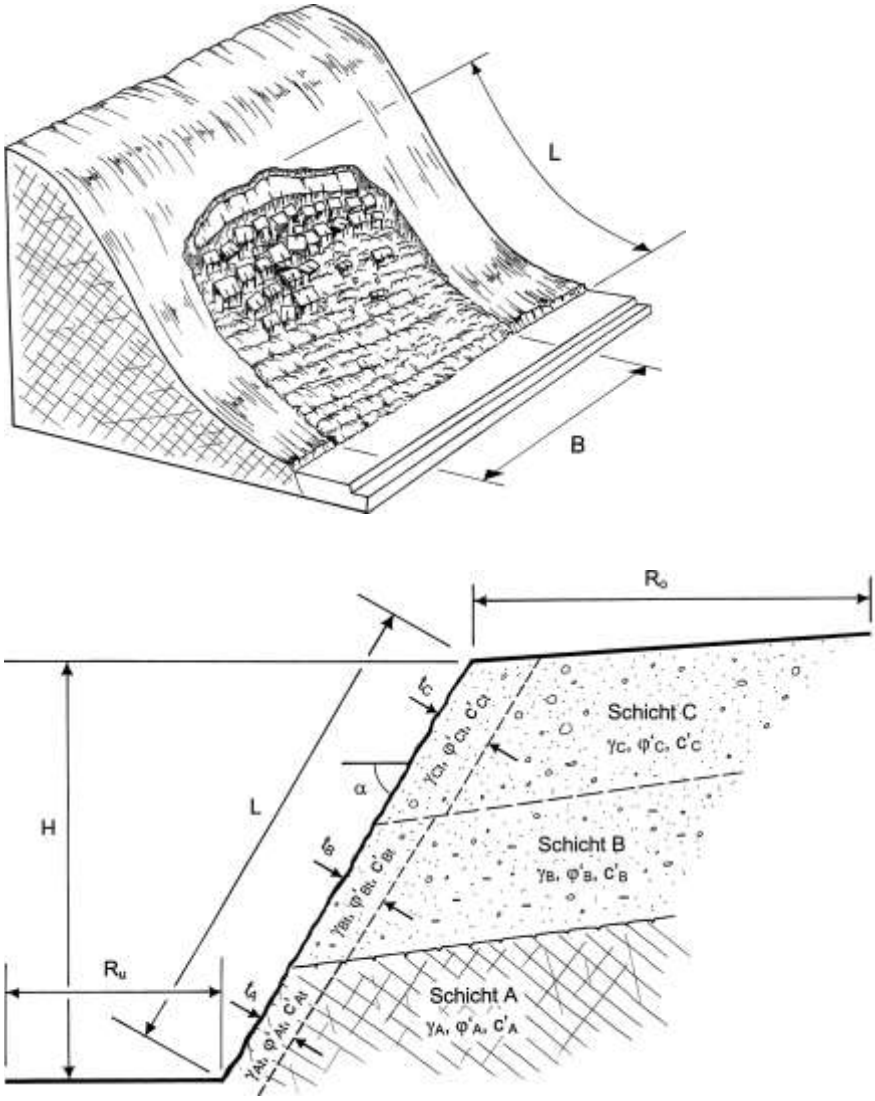

Figure 10.1 General aspects and marginal conditions

Particular main specifications of the stabilization systems are:

- Nail type
- Nail length, e.g. for securing deep sliding surfaces
- Drilling process to suit the subsoil

10.1.5 Surveying of the terrain

For the preliminary project phase, simple but true-to-situation surveying by means of measuring tape and circular protractor is generally sufficient. Current documents such as situation plans or cross-sections may be used if existing.

The final terrain surveys are best carried out after the preparatory tasks (see chapter 10.3), otherwise only inaccurate information will be available for the arrangement of the meshes.

- Trigonometric surveys with the theodolite and electronic distance measurement or also via cross-sections.
- Preparation of a model of the terrain comprising a situation with contour lines and cross-sections. Distinct shapes of the slope (dells, humps, overhangs) must be evident from the planning documents to enable correct detail planning and to avoid surprises during the execution.
- With these planning documents, finally, it should be possible to plan the arrangement of the meshes (mesh sheets) and of the nails. Hereby the position of the nails is determined according to the specifications from the stability proofs (maximum horizontal and vertical distances), with adaptations to the prevailing local circumstances (dells, low points). The later adaptations, however, usually need to be made directly in the terrain.

10.1.6 Dimensioning of slope stabilization system

The dimensioning method was presented in the previous chapters (see chapters 5–8) and shall not be repeated at this point.

10.1.7 General remarks about project development

Required for the project at hand are the mentioned planning fundamentals (topography, geometry of the terrain, profiles, etc.) plus the dimensioning results with the proofs of bearing capacity which define the maximum admissible distances between nails, the nail types and lengths as well as the minimum pretensioning forces.

In determining the area to be protected it is important to extend this sufficiently (generally by at least 2 m) beyond the existing or potential starting zones and terrain edges (figure 10.2).

The boundary terminations (with/without boundary rope) must be specified in the project. If boundary ropes are used, the pertaining rope anchors must be defined.

Levelling and shaping of the terrain must be stated where existing slopes are to be protected.

Where existing slopes with vegetation are concerned, moreover, the clearing, cutting of shrubs and trees to the rootstock, mowing of grass slopes (areas, number, dimensions, etc.) must be shown separately.

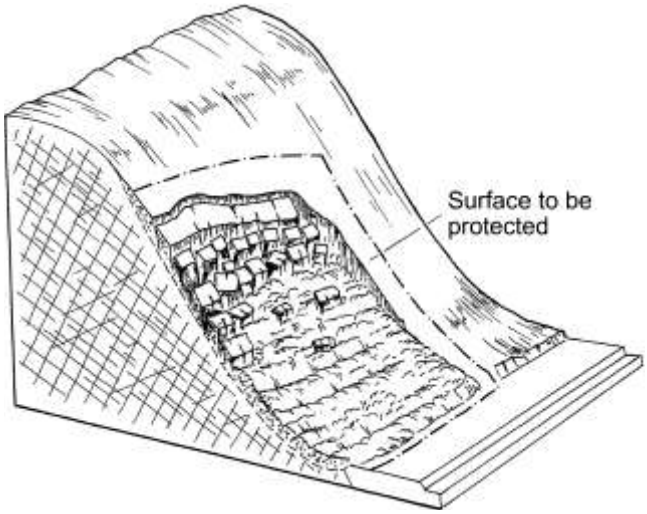

Figure 10.2 General overview of slope to be stabilized

The following circumstances, furthermore, must be dealt with in the project and presented in the plans and / or described specifically to the extent possible (the list below is not complete):

- Large hollows
- Projecting blocks which must be circumvented or specially secured
- Existing trees to be kept alive
- Springs, water pressure areas and corresponding drainage measures
- Special measures such as shotcrete fillings
- Structural parts such as post foundations, etc., to be circumvented
- Need for erosion protection measures
- Greening, planting

10.1.8 Requirements regarding call for tenders

The invitation for tenders for the TECCO® system work must contain all major material supplies and tasks to be carried out. Properties and requirements applying to the TECCO® system materials must be specified so that other systems must provide and meet these also for the sake of equality.

Included for this purpose are:

- Minimum tensile strength
- Maximum mesh size

- Minimum shear force of the nail fastening (see chapter 6)
- Minimum puncture force expressed as increase of the bearing capacity from the difference of the test without/with mesh (see chapter 7)
- Minimum tensile strength of the mesh sheet connections (see chapter 5.7)

To be specified for the nails:

- Nail type
- Minimum internal/external load bearing power
- Corrosion protection measure
- Minimum drilling diameter
- Length of nails
- Drilling method (dry with air flushing/if appropriate mortar flushing in case of self-drilling nails)
- Number and type of test nails (if necessary preliminary tests to determine the external load bearing power)
- Number of nail tests up to dimensioning resistance (random sample testing of the system nails)

10.2 Recommended elements of the system and auxiliary equipment

10.2.1 Elements of the system

A slope stabilization system with high-tensile steel wire meshes consist of the following main elements:

Surface material

- Mesh made from high-tensile steel wires
- Connection clips and/or connection elements

Soil/rock nails

- Main nail (with nut)
- System spike plate

Optional individual parts

- Short nails
- Driven nails
- Boundary ropes
- Rope anchors

The main technical data of the high-tensile steel wire mesh TECCO® are shown on the following table 10.1.

Technical data	**TECCO® G45/2**	**TECCO® G65/3**	**TECCO® G65/4**
Tensile strength wire mesh	min. 85 kN/m	min. 150 kN/m	min. 250 kN/m
Number of meshes transversal	16.1 pcs./m	12 pcs./m	12 pcs./m
Number of meshes longitudinal	10.5 pcs./m	7 pcs./m	7.2 pcs./m
Wire diameter	2.0 mm	3.0 mm	4.0 mm
Steel quality	high-tensile steel wire		
Tensile strength of steel wire	≥ 1'770 N/mm²		
Mesh shape	diamond		
Mesh unit sizes	62 · 95 mm (+/–3%)	83 · 143 mm (+/–3%)	83· 138 mm (+/–3%)
Mesh width	48 mm (+/–3%)	65 mm (+/–3%)	63 mm (+/–3%)
Weight per m²	1.15 kg/m²	1.65 kg/m²	3.3 kg/m²
Corrosion protection	Zn/Al coating of steel wires		
Compound of protection	95% Zn/5% Al		
Coating thickness	≥ 115 g/m²	≥ 150 g/m²	≥ 150 g/m²
Bearing resistances	Spike plate P25 / P33	Spike plate P33 / P66	Spike plate P33 / P66
Bearing resistance of the mesh against puncturing D_R	40 / 55 kN	90 / 120 kN	140 / 185 kN
Bearing resistance of the mesh against shearing-off at the upslope edge of the spike plate P_R	10 / 10 kN	30 / 45 kN	50 / 75 kN
Bearing resistance of the mesh against slope-parallel tensile stress Z_R	40 / 55 kN	90 / 120 kN	140 / 185 kN

Table 10.1 Technical data of the high-tensile steel wire mesh TECCO®

The relevant technical data of the system spike plates are summarized on the table 10.2 as follows:

Technical data	**P25/34 N**	**P33/40 N and P33/50 N**	**P66/50 N**
Size	250 x 155 mm	330 x 205 mm	667 x 300 mm
Thickness	5 mm	7 mm	10 mm
Hole diameter	34 mm	40 and 50 mm	50 mm
Length of the spikes	min. 16 mm	min. 20 mm	min. 30 mm
Weight	0.9 kg	2.2 kg	6.7 kg
Bending resistance	≥ 1.25 kNm	≥ 2.5 kNm	≥ 8.0 kNm
Corrosion protection	hot-dip galvanized based on EN ISO 1461, layer thickness in average 55 µm		
Steel quality	S355J		

Table 10.2 Technical data of system spike plates

Figure 10.3 illustrates three dimensional principle drawings of the system spike plates.

Figure 10.3 System spike plates P25, P33 and P66 (3D principal drawings)

The following table 10.3 gives an overview about the key data of main nails.

Technical data for main nails (soil and rock nails)	
Common nail types	e.g. GEWI D = 25, 28, 32 or 40 mm or self-drilling nails of type TITAN 30/11 or 40/16 as well as IBO R32 S/N or similar. Other nail types may be used if the relevant proofs can be fulfilled.
Common nail pattern	Distances between nails a = 2.0 - 4.0 meters (in horizontal direction) b = 2.0 - 4.0 meters (in line of slope) or to suit local requirements.
Length	as required, generally more than L ≥ 2.0 m
Corrosion protection	Normally the nails are installed raw *). It is customary to take into account either a corrosion of 4 mm based on the diameter or to calculate with reduced steel strains. In exceptional cases (partially)-galvanized nails or even nails with double corrosion protection can be utilized. It is reasonable depending on project requirements to paint the head area of the nail with zinc after setting and cutting to length. * In general, the nail is several times over dimensioned in the head section because its resistance against tension and shear to protect from sliding parallel to the slope is decisive for dimensioning purposes.
Nuts	Generally hexagonal nuts with spherical bearing faces or spherical nuts should be used. If nails with diameter < 28 mm are going to be installed, the installation of corresponding washers is generally recommended.

Table 10.3 Technical data for main nails (soil and rock nails)

10.2.2 Connecting elements

Table 10.4 presents an overview of the main data regarding the connection clips and press claws.

Technical data of connection clips and press claws		
	Connection clips T3	**Press claws type 2**
Application purpose	connection elements to interlink the individual mesh sheets	connection elements to fasten the TECCO® mesh at the boundary rope
Execution	open eyelet for installation on site by hand	open eyelet for compression after installation on site
Material quality	4 mm high-tensile steel wire, tensile strength ≥ 1'770 N/mm²	Steel S235 JRG, material diameter 6 mm
Corrosion protection	Zn/Al coating with a minimum thickness of 150 g/m²	hot-dip galvanized, layer thickness 55 µm

Table 10.4 Technical data of connection clips and press claws

Picture 10.1 shows the system connection clip and the press claws.

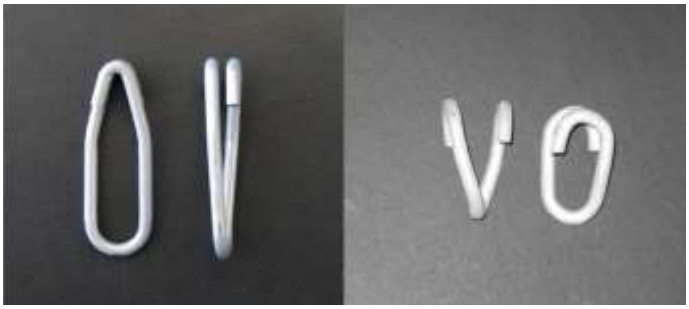

Picture 10.1 Connection clip T3 (left) and press claw type 2 (right)

10.2.3 Optional material and elements

Table 10.5 describes the technical data of additional nails and short nails as optional parts of the systems, depending on local conditions.

Technical data of additional nails, short nails (optional individual parts)	
Standard nail types	e.g., GEWI D = 20 or 25 mm The utilization of other nail types is allowable if they are adapted to the project-specific requirements.
Application area	As auxiliary reinforcement in spots in the border areas, in low points, etc. Diameter according to need, as a rule D = 20, 25 mm
Length	Usually predetermined: L = 1.5 m
Corrosion protection	Normally the nails are installed raw. In exceptional cases (partially)-hot dip galvanized nails are used. It is reasonable depending on project requirement to paint the head area of the nail with zinc after setting and cutting to length.

Table 10.5 Technical data of additional nails, short nails (optional individual parts)

The following table 10.6 explains the technical data of driven and short nails and on picture 10.2, a sample for a driven nail is shown.

Technical data of driven nails, short nails (optional individual parts)	
Application area	for possible required intermediate fastening and boundary fastening of the mesh
Execution	e.g. ribbed TOR-steel D = 16 mm with bracket welded to top, L = 0.6 m or 1.0 m
Corrosion protection	hot-dip galvanized, layer thickness 85 µm

Table 10.6 Technical data of driven nails, short nails (optional individual parts)

Picture 10.2 Sample for driven nail

For top and side support ropes (boundary ropes), galvanized steel wire ropes with diameters of 10 mm or 12 mm are usually recommended. Table 10.7 provides the suggested technical data accordingly.

Technical data for boundary steel wire ropes		
Application area	for fastening and reinforce the edge areas	
Light type	rope, steel wire minimum breaking force	D = 10 mm 63 kN
Heavy type	rope, steel wire minimum breaking force	D = 12 mm 91 kN
Corrosion protection	zinc coating according to DIN EN 10244-2	

Table 10.7 Technical data for boundary steel wire ropes

For the side anchoring of above mentioned boundary ropes, spiral wire rope anchors are recommended. The wire ropes are connected and fixed to the spiral wire rope anchors in accordance with DIN EN 13411-5.

The following table 10.8 is presenting the main technical data of such spiral wire ropes and on the pictures 10.3 and 10.4, two different versions of such spiral anchors are illustrated.

Technical data of spiral wire rope anchors	
Application area	under critical circumstances as tension anchor for fastening of possibly required boundary
Execution	spiral rope, 2-rope exec., with double steel tube in loop section
Corrosion protection rope	Heavy galvanized in accordance with DIN EN 10244-2, minimum coating weight 230 g/m^2 (D 10.5 mm), 255 g/m^2 (D 14.5 mm)
Corrosion protection tubes	Hot dip galvanized in accordance with EN 10240, minimum layer thickness 55 µm
Light type	D = 10.5 mm, admissible service load capacity 100 kN length depending on subsoil: L = 2 - 3 m
Heavy type	D= 14.5 mm, admissible service load capacity 195 kN length depending on subsoil: L = 2 - 4 m
Flex head	Flexhead anchors can also be used instead of the spiral rope anchor. It attaches to the nail by hand-screwing it directly onto the nail. The flexhead has the same technical data as the spiral rope anchor.

Table 10.8 Technical data for boundary steel wire ropes

Picture 10.3 Spiral rope anchor and connection installation of the border ropes

Picture 10.4 Flexhead of spiral rope anchor for application to GEWI or self drilling anchors

10.2.4 Auxiliary equipment and tools

The following list of equipment and tools are often used and required for the installation and execution of slope stabilization systems with flexible meshes.

This list is only a certain selection of possible equipment and tools. Of course, other products, tools, machines, etc. may be useful, too.

- Drilling machine (mounted drilling appliance, portable drilling devices if appropriate), minimum drilling diameter = 1.5 times the nail diameter or depending on project requirements = nail diameter + 2 x 20 mm grout cover
- Injection pump for mortar-stabilization of the nails, e.g. SIG-Jet 2000 (Lumesa SA), MAI-Mungg (GD-Anker AG) or a device of Morath GmbH

- Rope shears with cutting force for minimum ø 12 mm (e.g. type Felco)
- Tool case with set of box spanners, M10–M32
- Torque wrench for pretensioning of the system, range 0.3 – 0.6 kNm depending on the anchor system (chapter 10.7.7)
- Water pump pliers for compressing (closing) of the press claws by the boundary ropes
- Lightweight rope pulling devices (come-along, pully) if needed (e.g. LUGAL, Habegger, etc.)

10.3 Preparation of the terrain

The terrain must be suitably prepared before the flexible slope stabilization system with high-tensile steel wire meshes is put in place:

- Clearing of the slope
- Cleaning of the slope
- Levelling of the slope
- Trimming of the slope (as required and in case of new cuttings)
- Drainage measures (if required)

Fracture zones are often characterized by vertical or even overhanging parts of the terrain. Levelling or evening-out of the terrain is frequently required. This work consists of the cutting of terrain edges, the removal of loose blocks and the filling of dells in the terrain (picture 10.5).

A part of this is also the specific removal of individual trees which are of no particular value. Tree-stalks must be cut off as near to the ground as possible so that the mesh remains tensioned over it after the rotting of the tree stumps. Certain trees may also be left in place, whereby these fixed points must be taken into account determination of the net locations. Shrubs are cut back completely to the rootstock.

Picture 10.5 Left: Slope during preparation measures (clearing, levelling, partial cutting, etc.)
Right: Slope after preparation measures

10.4 Stake out

Good staking out and marking of all points of importance for the operation facilitates the execution and provides a good overview at all times. The stake-out should mark the items listed below with pegs, nails or dots of paint in accordance with project specifications, and local adaptations to terrain shapes, obstacles, etc. (see also figure 10.4 accordingly).

- Boundaries
- Corner points
- Sheets (mesh) delineation
- Nails, numbered for subsequent protocolling
- Rope anchors (optional in combination with boundary ropes)

During stake-out, care must be taken that the distances between nails as stated in the project are adhered to and above all not generally exceeded. The distances between nails are based on the dimensioning and stability proofs for the system, taking into account the prevailing subsoil circumstances and slope gradients.

For the position of the individual nails, a maximum deviation of +/–10% from the nail distance specified by the project, measured in the horizontal and the line of slope, is generally admissible. A reduction of the distances between nails or the arrangement of extra nails for adaptation to local circumstances (e.g. fastening in low spots) is always admissible.

In slopes to be protected, adaptations to the actually prevailing circumstances are often required. The project specifications must not and cannot simply be translated regardless. However, if major adaptations become necessary or if the profiles (gradients) or the subsoil do not correspond with the assumptions on which the project is based, the project management and if appropriate the responsible author of the project must be informed without delay.

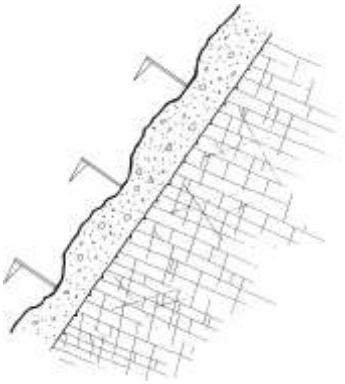

Figure 10.4 Principle drawing of stake out of the drilling points

10.5 Installation options

We differentiate basically between two laying variants:

- Option A: Laying of the meshes after setting of the nails
- Option B: Laying of the meshes before setting of the nails (for TECCO® G65)

The option to be selected depends on e.g. the type of nails, the drilling method and in some cases also on the installation instructions.

10.5.1 Option A: Laying of the meshes after setting of the nails

This installation option is necessary if drilling diameters of more than 65 mm (respectively more than 90 mm using the drilling device) are specified or required. This may be the case if:

- the outer load bearing power of the nails requires an accordingly large drilling diameter (specified by test nail or the author of the project)
- infiltration tubes have to be installed because of a poor stability of the bore holes
- drill bits, in-the-hole hammers of dia. > 65 mm (respectively > 90 mm using the drilling device) can be used
- piped (cased) bore holes are required

Installation option A, therefore, is usually envisaged for:

- protection features in loose, unconsolidated rock of a medium deposition density requiring a borehole diameter of more than 65 mm (respectively more than 90 mm).
- in severely weathered, disintegrated rock with bigger fissures which, under certain circumstances, require the use of fabric hoses to limit the mortar consumption.
- generally unstable bore holes
- a potential requirement to provide piped (cased) bore holes
- situations with major quantities of hillside water possibly requiring drainage bores with filter installation

Installation sequence for installation option A:

- stake-out of the starting points for drilling with nail pattern as by project specification taking into account low spots
- excavation of the dell (for pretensioning), preferably before drilling
- drilling of the nails (nail head should not project over the terrain line) and if appropriate of the rope anchors holes
- setting and mortar-stabilizing of the nails (and if appropriate of the rope anchors)
- laying bare of the nail heads
- laying of the wire meshes

- connecting the mesh sheets to each other
- fitting of the boundary ropes
- installation of the spike plates and active pretensioning with torque wrench or hydraulic press to the specified forces

Advantages of installation option A:

- independence for the drilling process and the borehole diameter
- mortar-stabilizing before laying of the meshes, e.g. no danger of contaminating the mesh with anchor mortar
- subsequent work on the nail heads (removal of mortar) and in the environment of the nail heads (recess for spike plate) is possible
- no obstacles to drilling operations (also especially in case of major hollows, dells, etc.)
- possibilities of intervening for drainage measures, etc. are available right to the last moment

Disadvantages of installation option A:

- excessively projecting nails are a hindrance when laying the meshes; if appropriate they should be shortened beforehand
- optimal nail positions for tensioning of the mesh are not as easily visible as in subsequent drilling according to installation option B
- no rockfall protection (during drilling and setting) by the mesh as in option B, i.e. there might be a need for provisional protective measures

10.5.2 Option B: Laying of the meshes before setting of the nails

This installation option is possible if borehole diameters below 65 mm (respectively below 90 mm using the drilling device) are admissible and if:

- the substrate circumstances allow the use of a small drill diameter and the outer bearing capacity is guaranteed uniform (test nails may be required)
- stability of the bore holes can be expected and no installation of infiltration tubes is required for support
- no locally larger borehole diameter is required for the installation of pipes (casing), drainage pipes and fabric hoses, either

Installation option B can be envisaged for:

- protection features in densely deposited, firm unconsolidated material in which the bore holes are stable without problems right to the specified end depth;
- rock that is weathered and disintegrated to a slight to medium degree only and in the absence of major fissures which would require the use of fabric hoses to limit the mortar consumption;
- sites with little or no hillside water requiring special drainage measures.

Installation sequence for option B:

- stake-out, drilling, setting and mortar-stabilizing of the top boundary nails
- stake-out of the drilling points for the nails taking into account low spots within the tolerance range of the nail pattern according to static requirements
- excavation of the dells in the area of the nails
- securing of the meshes to the boundary nails
- unrolling/laying of the meshes
- connecting the mesh sheets to each other with connection clips
- optimization of the drilling points for the nails considering low spots within the tolerance range of the nail pattern according to static requirements
- drilling of the nails through the mesh using the special drilling device (see chapter 10.5.4).
- setting and mortar-stabilizing of the nails
- installation of the spike plates and active pretensioning with torque wrench or hydraulic press to the specified forces

Advantages of installation option B:

- easier laying of the meshes without obstacles in the form of projecting nail heads
- easier determination of the optimal nail positions for tensioning of the mesh than with prior drilling according to variant A
- protection by the mesh (against rockfall) is already available while work is in progress
- walking (climbing) and belaying in steep terrain can be facilitated (use of crampons with front spikes, carabiners or snap-hooks can be clipped to mesh)

Disadvantages of installation option B:

- drilling diameter is generally limited to 90 mm using the drilling device (see chapter 10.5.4)
- subsequent work on the nail heads (removal of mortar) and in the environment of the nail heads (recess for spike plate) is encumbered by the mesh
- contamination of the mesh with mortar, i.e. need for cleaning
- once the meshes are laid, interventions for drainage measures, etc., are no longer possible

10.5.3 Remark on stability of the slope

Where new slope cuts are concerned, the size of the possible execution stages to be carried out in one step (drilling, setting of the nails, mesh cover) depend on the slope's stability in each smaller area.

The stability is determined primarily by the existing actual or apparent cohesion of the subsoil and the water. Water in the form of emerging hillside, layer or fissure water, but also rainfalls, can influence the stability substantially.

10.5.4 Drilling device for TECCO® G65

The inner circle diameter of the presented main high-tensile steel wire mesh[39] is 65 mm. The special drilling device is designed to allow a drilling diameter of up to maximum 90 mm without damaging the mesh and its corrosion protection. It is placed in the mesh above the drilling position. The safety rim of the drilling funnel is placed completely through the mesh. The fixation bolt is put into a mesh to avoid turning of the drilling device while drilling. The drilling funnel is opened by turning the handle. Use a ratchet wrench to open the drilling device up to 90 mm. Easy drilling through the mesh is now guaranteed without damaging the mesh and its corrosion protection.

Technical information about drilling device:

- Weight: approx. 5 kg
- Material: galvanized steel
- Turning handle: with nut for ratchet wrench
- Size: 480 × 220 mm
- Fixation bolt: length 160 mm
- Drilling funnel with rim for slip safety: opening up to maximum 90 mm

Picture 10.6 Drilling tool to drill through high-tensile steel wire meshes

[39] TECCO® G65/3 mm is the most common high-tensile steel wire mesh for slope stabilization purposes.

The opening and closing process of the drilling tool is shown on the picture 10.7 as follows:

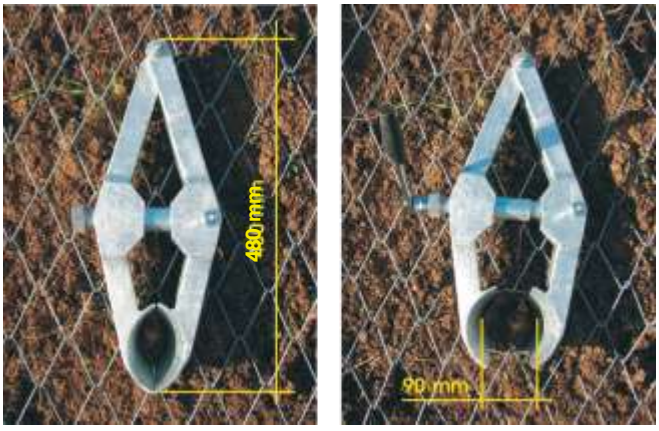

Picture 10.7 Drilling tool closed (left) and open with diameter up to 90 mm (right)

Pictures 10.8 and 10.9 demonstrate the nail drilling process with the drilling tool explained above from a crane basquet (platform).

Picture 10.8 Drilling process from crane basquet using the drilling tool

Picture 10.9 Detail of drilling process using the drilling tool

10.6 Drilling and installation of nails

10.6.1 Drilling work

Drilling and nailing work must be coordinated with slope cutting (job planning, planning for safety at work, etc. [50]).

Stake-out of the drilling points must comply with the project specifications (maximum nail distances a, b).

Hereby mean deviations of +/–10% from the nominal distances *a* and *b* are admissible for adaptation to the local circumstances (low spots, niches in the rock, etc.). It is always admissible for smaller distances or extra nails if the terrain properties require this so that the mesh lies optimally on the slope.

The nails should be installed in deeper locations if possible.

The use of portable drilling equipment is only rarely possible. Mounted drilling devices are used in most cases.

Generally speaking, one starts at the top and works down towards the bottom.

The suitable drilling method is primarily determined by the subsoil (unconsolidated material, rock). Depending on the circumstances it is also possible to apply different drilling methods, in which case the most suitable one is determined by the available devices and their capacity.

The nail inclination has to be chosen in accordance with the slope inclination.

Dry drilling processes operating with air flushing are to be preferred (figure 10.10). Water or direct mortar flushing are the exception and must be agreed up on with site management and client.

Important is, that the required outer load bearing capacity is achieved with the nails and also that proof of this is established with tests.

The outer load bearing capacity is primarily determined by the bond between mortar and subsoil. The effective skin surface is decisive for this in substrates of soft to rigid consistency and deposits of loose to medium density. The load bearing capacity, therefore, can determine the minimum drilling diameter.

Big drilling diameters (more than 65 mm) large result in better embedment in the mortar and thus corrosion protection. In unstable bore holes, large drilling diameters enable the installation of protective tubes, fabric hoses or other measures to avoid loss of mortar in fissured rock or coarse scree.

Generally, the following minimum drilling diameters D_{min} should be observed for main nails:

- in fine-grained unconsolidated material $D_{min} = 90$ mm
- in mixed-grain, unconsolidated material of low stability $D_{min} = 90$ mm
- in mixed-grain, unconsolidated material of good stability $D_{min} = 65$ mm
- in fine-grained rock (clay/siltstone) $D_{min} = 65$ mm
- in rock without major fissures, stable boreholes $D_{min} = 50$ mm

A drilling diameter of $D_{min} = 50$ mm is generally sufficient for secondary nails to hold down the meshes, for boundary stabilizations, drill to a depth of a maximum 1.5 m.

Boreholes in stable material may be made without casing. In unstable material it is necessary to change to a method with casing (requires appropriate drilling equipment) or, depending on dimensioning requirements, self-drilling anchors may also be suitable.

As an option, a perforated protection or stabilization tube can be inserted in the hole (immediately after drilling), so that the borehole cannot collapse until the insertion and mortar-stabilizing of the nail.

Picture 10.10 Drilling work using a crawler-mounted drilling device (dry drilling)

Stabilization tubes must be set to a height of approx. 20 cm below the surface of the terrain, so that subsequent prestressing is possible (see also chapter 10.6.3 in this context).

Depending on local access conditions, special drilling support methods may be applied. Picture 10.11 shows drilling work that is carried out from a lifting platform.

Picture 10.11 Depending on local terrain conditions, drilling work can also be carried out from a small crane platform or lifting platform

10.6.2 Installation and mortar (infiltration) of the nails

For centring purposes, main nails must be provided with spacers in the borehole.

If fissures are to be expected (resulting in loss of mortar), the nails must be lined with a suitable fabric bag.

For mortar-stabilization, use a suitable, tested and frost resistant injection-type mortar without shrinkage measure [11, 12, 16, 122, 147].

The mortar is prepared with a mortar pump with mixing container. To guarantee impeccable filling of the borehole, a plastic tube (lance) is inserted along the nail right to the bottom of the borehole. The mortar is pumped through this tube so that the borehole is filled from the bottom outwards. The lance is steadily withdrawn as the hole is filled.

For main nails: Filling from the bottom of the borehole with infiltration hose

For short nails: Prefilling of the hole is admissible

Mean mortar consumption (assumption for calculation):

Drilling hole diameter	D = 50 mm	approx. 8 kg/m′
	D = 65 mm	approx. 12 kg/m′
	D = 90 mm	approx. 20 kg/m′

The above values are an assumption for calculation purposes. In principle the mortar consumption always depends also on the permeability of the subsoil and the degree to which it is fissured.

10.6.3 Recessing of the nail heads

In the soil, the nail heads must be recessed in a dell (approx. 20–30 cm). The nail's thread must be laid bare and cleaned (see also figure 10.5).

By tightening the nut or by means of a hydraulic press it is possible to press the spike plate and thereby the mesh tightly onto or slightly into the ground. The objective of prestressing the slope stabilization system is to press the mesh as tightly as possible onto the substrate to be stabilized. At the location of the boundary nails the dells does not have to be excavated so that the installation of the boundary ropes is more favourable.

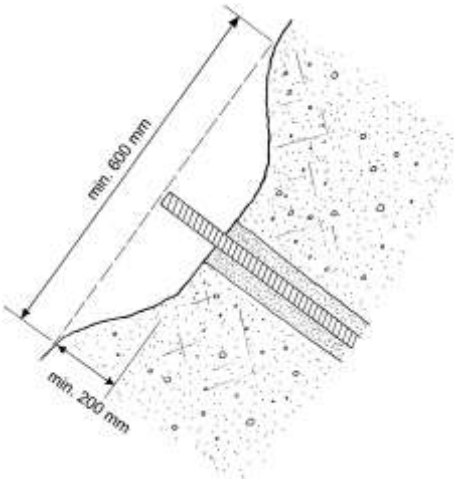

Figure 10.5 Nail head section: Dell for optimal prestressing of the mesh in soil applications

10.6.4 Test nails

On testing of test nails we differentiate between pull-out test (A) and pull test (B) [122]:

Pull-out test A:

- Test nails for preliminary tests to determine the load bearing capacity, the required nail length, drilling diameter, etc.
- The test nails are subjected to strain until rupture.
- General rule: In case of bigger objects and in the absence of reliable experience values, at least 3 test nails per decisive and characteristic soil layer should be arranged in preferably different areas of the slope to be protected.

Pull test B:

- Test nails in the system itself. They are only strained up to a defined testing force.
- The testing force should correspond at least to the force for which the nail is dimensioned.
- Number of test nails per decisive, characteristic ground layer in dependence of the object size and the total number of nails to be installed:
  - 0 – 100 nails: 3 test nails (minimum)
  - 100 – 200 nails: 5 test nails
  - more than 200 nails: 2.5% of the number of nails to be installed = number of test nails

10.6.5 Particular aspects

The nail heads for the flexible slope stabilization system with high-tensile steel wires must be laid out so that, with sufficient free thread length, the mesh can be prestressed with the spike plate to the specified value by applying a controlled force with the torque spanner or a hydraulic press.

Depending on the laying option (see chapter 10.5), the rod nails are set and stabilized with mortar before or after laying of the mesh.

Before installing the high-tensile steel wire mesh, the nails have to be cut back on approximately the level of the slope surface to enable an appropriate and tight installation of the mesh. Thereby, a proper installation of the system spike plates still has to be guaranteed. The nail head needs to be excavated according to chapter 10.6.3 if possible.

In case of a loose installation of the mesh not being sufficiently tensioned against the subsoil to be stabilized according to this product manual, corresponding deformations in the subsoil cannot be excluded. In the worst case, this could cause a certain failure of a part of the system.

10.7 Mounting of the high-tensile steel wire mesh

10.7.1 Cutting of the high-tensile steel wire mesh

High-tensile steel wire meshes are available in different sizes. However, for logistic, handling and installation reasons, the standard length of a roll of high-tensile steel wire meshes is 20 - 30 m. The standard width is 3.5 – 3.9 m. The roll weight varies between 135 - 230 kg.

Cutting the mesh sheets to size is done by the separation of meshes on the two lateral edges (cutting of the wire next to the knot, using a pair of suitable cutting pliers). One wire spiral can then be turned out and the mesh is separated.

It is recommended to cut the mesh sheets to size before assembly, in a suitable area at the installation site. The advantage of this is that there is no need to transport complete rolls to the actual place of installation, since all tasks on the actual slope take up much more time.

10.7.2 Unrolling of the high-tensile steel wire mesh

Laying of the meshes is usually done from top to bottom. Hereby it must be ensured that the mesh is secured to the top edge of the slope before it is unrolled. In principle, however, it is also possible to lay the mesh from the bottom to the top.

Unrolling of the mesh in case of prior setting of the nails (installation option A according to chapter 10.5.1):

It must be taken special care that the mesh sheets are suspended from the nails in such a manner that, after prestressing, they rest on the slope surface as tightly as possible. Hereby the uppermost nails can serve directly for fastening of the rolls for laying. It is not allowed to cut off the high-tensile steel wire mesh, e.g. in the nail head area to enable a correspondingly tight installation of the mesh. In general, with the exception of holes for planting or of bypassing stumps or parts of civil engineering structures, it is not allowed to cut-off the mesh without noteworthy reasons!

Unrolling of the mesh before installing the nails (installation option B according to chapter 10.5.2):

With option B the meshes are laid out first and only afterwards are the nails set. This installation option offers advantages regarding laying and an optimal adaptation of the nail positions.

The mesh sheets (rolls) are first fastened above the edge of the slope to be protected. This can be done either to previously set main nails for protection purposes or to auxiliary nails. In principle, however, it is also possible to lay the mesh from the bottom to the top. Care must be taken that the mesh rests as fully as possible on the slope surface.

Picture 10.12 illustrates the unrolling of the high-tensile steel wire mesh panels before the installation of the nails.

Setting of the nails is done afterwards through the mesh. The procedure in principle is as explained in chapter 10.6 (setting and mortar-stabilizing of the nails). However, the bore-hole diameter is limited to maximum 65 mm (inner circle diameter of one mesh = 65 mm).

Picture 10.12 Unrolling of the mesh before installation of the nails

10.7.3 Vertical mesh connection

The mesh sheets can be laid out without overlap at the side.

The mesh sheets must be connected lengthwise (normally in the line of the slope) by means of connection clips illustrated as follows (figures 10.6 and 10.7).

Hereby each individual edge-mesh must be secured with a single connection clip to the neighbouring mesh. Therefore, there are 7 connection clips per meter needed for the G65/3 and 10.5 clips per meter for the G45/2.

For the stronger mesh, TECCO® G65/4, each individual edge-mesh must be secured with two connection clips to the neighbouring mesh. Therefore, there are 14 clips per meter needed.

By this arrangement it is guaranteed that the lateral connection of the mesh sheets provides the required transverse tensile strength of the mesh and that the deformations under load are limited to an admissible degree.

Figure 10.6 Left: Connection without overlap for TECCO® G45/2 and TECCO® G65/3
Right: Connection with overlap of 2 diamond mesh units for TECCO® G45/2 and TECCO® G65/3

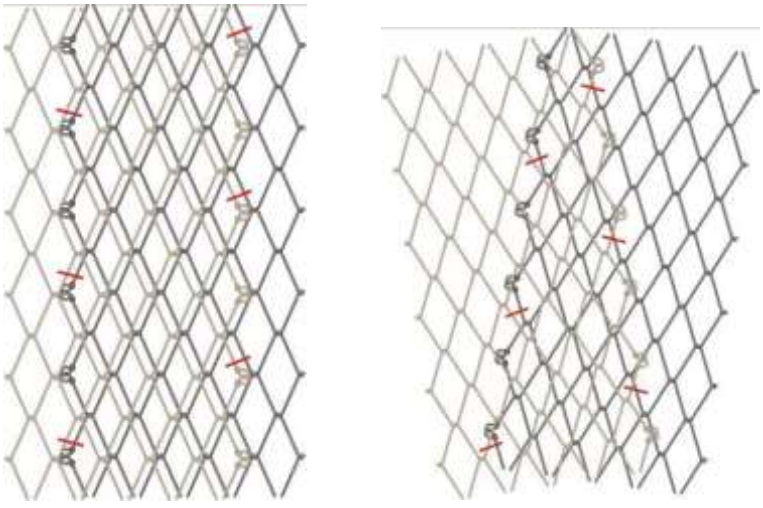

Figure 10.7 Mesh panel connection with overlaps >2 diamond mesh units

10.7.4 Horizontal mesh connection

In principle there are two possibilities:

– Standard case: connection by turning-in of a wire spiral

– Alternative: connection by means of connection clips or shackles

10.7.5 Positioning of the spike plates

On positioning of the spike plates, care must be taken that the spike plates fit well between the individual meshes and that they are firmly pressed into the ground. This ensures that both mesh and plate are optimally pressed to or against the ground to enable a correct transmission of the forces.

Thereby, the mesh panels need to be laterally attached to each other and installed in a tight manner at first before the spike plates are going to be installed and actively pressed against the surface. If necessary, the mortar column in the nail head area needs to be removed accordingly to enable a proper tensioning of the system.

Tightening the nut, individual wires could get stacked in the thread of the nail. In this case, the nut has to be loosened again trying to push the wire further against the subsoil afterwards.

Picture 10.13 demonstrates the appropriate positioning of a spike plate, set into the deep point and tightened correctly.

Picture 10.13 Positioning of spike plates

It is important that the system spike plates are applied correctly. It is important that the plates are positioned horizontally that a maximum of high-tensile steel wires of the mesh can be covered. Figure 10.8 explain the great importance of the correct positioning on the example with the P33.

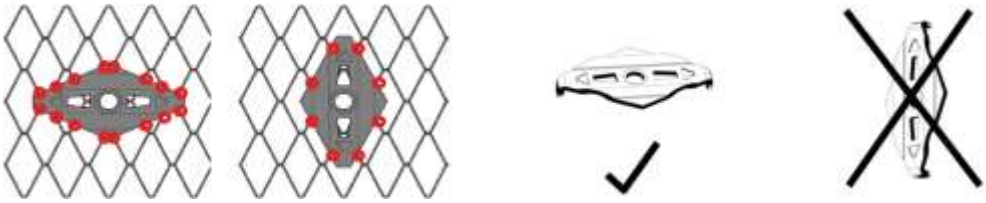

Figure 10.8 Spike plates need to be oriented horizontally; long side must be horizontal (horizontal installation covers 16 steel wires; vertical installation covers only 8 steel wires)

10.7.6 Positioning of the spike plates in areas of hollows in the terrain

If a spike plate is positioned in the area of a hollow in the terrain, care must be taken again that the spikes engage in the individual meshes evenly and in the best possible way (see also picture 10.14 as an example).

If, due to the local topography as e.g. in the picture below, the mesh cannot be pressed firmly onto the ground, the nails should be set as far as possible at a right angle to the mesh surface, so that the spike plates are more or less parallel to the mesh without provoking a one-sided strain on the mesh.

In such cases the prestressing force must be limited to maximum 30 kN.

Picture 10.14 Positioning of principal spike plates in areas of hollows (in the terrain surface)

10.7.7 Pretensioning of the slope stabilization system

By tightening the nut or with the aid of a hydraulic press, the spike plate and thereby the mesh are firmly pressed onto the ground and the mesh is tensioned.

The load table 10.9 below shows a summary of the required torques for three different nails of type GEWI for the application of a pretensioning force of at maximum V = 30 kN in soil and maximum V = 50 kN in rock, respectively. For the TECCO® G45/2 the maximum pretensioning force should be reduced to maximum 20 kN.

Nail type	Pretensioning force V	Required torque	
GEWI D = 25 mm and TITAN 30/11	20 kN	0.20 kNm	148 ft-lbs
	30 kN	0.30 kNm	221 ft-lbs
	50 kN	0.50 kNm	369 ft-lbs
GEWI D = 28 mm	20 kN	0.25 kNm	184 ft-lbs
	30 kN	0.35 kNm	258 ft-lbs
	50 kN	0.55 kNm	406 ft-lbs
GEWI D = 32 mm and TITAN 40/16	20 kN	0.30 kNm	221 ft-lbs
	30 kN	0.40 kNm	295 ft-lbs
	50 kN	0.60 kNm	443 ft-lbs

Table 10.9 Load table for pretensioning of spike plates (1 kNm = 224.81 lbs · 3.281 ft = 737.6 ft-lbs)

Picture 10.15 shows the process of applying the pretension to the spike plate.

Picture 10.15 Pretensioning of spike plates

10.7.8 Fixation of the mesh edges

It is generally recommended to reinforce the edge areas of the mesh with boundary ropes.

The boundary ropes are secured to rope anchors located on the side and tensioned against these.

In case of irregular edges there may be a need under certain circumstances for short or driven nails. These serve to tense the mesh to the soil as tightly as possible everywhere and to secure the edges in the best possible way.

The two schematic drawings (see figure 10.9) show the arrangement of the top, side and bottom boundary ropes and the rope anchor. Hereby the minimum distances of the boundary nails to the edge of the mesh are maintained correctly.

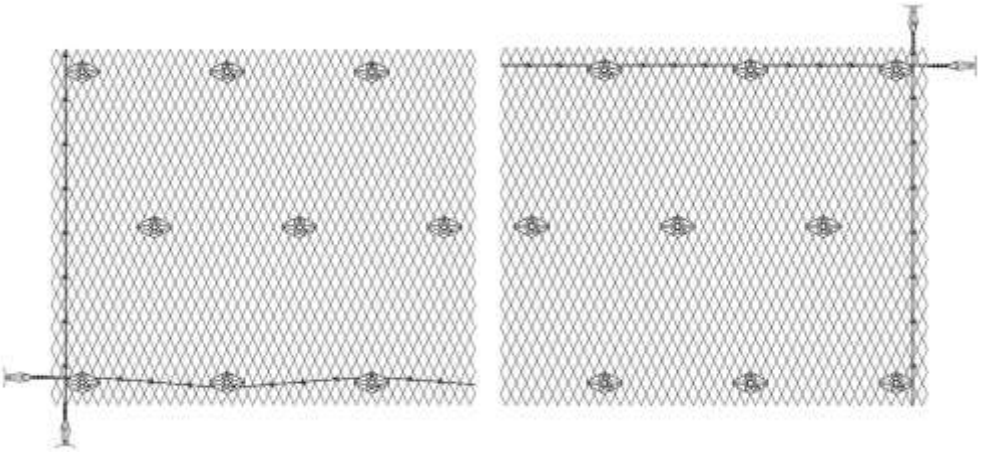

Figure 10.9 Principle drawing of side fixations of mesh edges

Generally, the horizontal boundary wire ropes at the bottom should be installed alternating once above and once below the nails. Thus, a slipping out of the boundary wire rope underneath the spike plate can be avoided. Especially if the boundary nails are not continuing straight on or if the slope geometry is very irregular this is important as well.

Fastening of boundary rope to rope anchors by means of wire rope clips

Instructions below apply to all wire rope clips according FF-C-450 type 1 class 1 (similar EN 13411-5 type 2).

The distance e between the wire rope clips should be at least **1 x t** but not exceed **2 x t** , where t is the width of the clamping jaws. The loose rope end has to be **3 x e** at a minimum. It is recommended looping up the remaining free section and fixing it directly behind the last wire rope clip on the tightened rope.

If you are using a thimble in the loop structure, the first wire rope clip must be attached directly next to the thimble. For loops without a thimble the length **h** between the first wire rope clip and the point of load incidence must minimally be 15-time the nominal diameter of the rope. In unloaded condition the length **h** of the loop should be not less than the double of the loop width **h/2.**

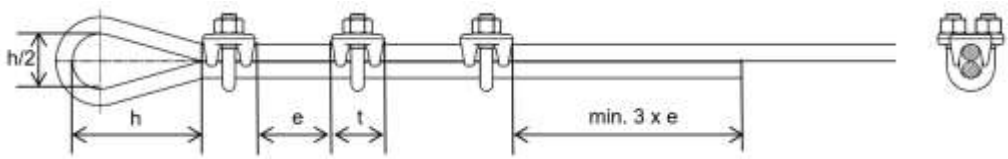

Figure 10.10 Fixation principle of wire rope clips

Table 10.10 provides the required forces and numbers for the wire rope clips

Torques and number of wire rope clips					
Wire rope clip diameter [mm]	Nominal size wire rope clip	Required number of wire rope clips	Required torque **with** greasing [Nm]	Required torque **without** greasing [Nm]	Wrench size [mm]
8	5/16“	3	20	50	18
9 - 10	3/8“	3	30	75	19
11 - 12	7/16“	3	40	110	22

Table 10.10 Torques and number of wire rope clips

The clamping brackets (U-brackets) must always be fitted to the unstressed end of the rope, the clamping jaws (saddle) must always be fitted to the strained rope („never saddle a dead horse“).

The required tightening torques with lubrication apply to wire rope clips whose bearing surfaces and the threads of the nuts have been greased. During tightening the nuts have to be tensioned equally (alternately) until the required tightening torque is reached.

After the first load application the tightening torque has to be checked and if not fulfilled adjusted to the required value. A visible contusion of the wire ropes positively indicates that the wire rope clips have been tightened to the required tightening torque.

10.7.9 Fixation in combination with concrete foundation beam

Below a road or in special local conditions, the top of a TECCO® slope stabilization system can be secured with a reinforced concrete beam. The following figures 10.11 and 10.12 illustrate the corresponding construction and design.

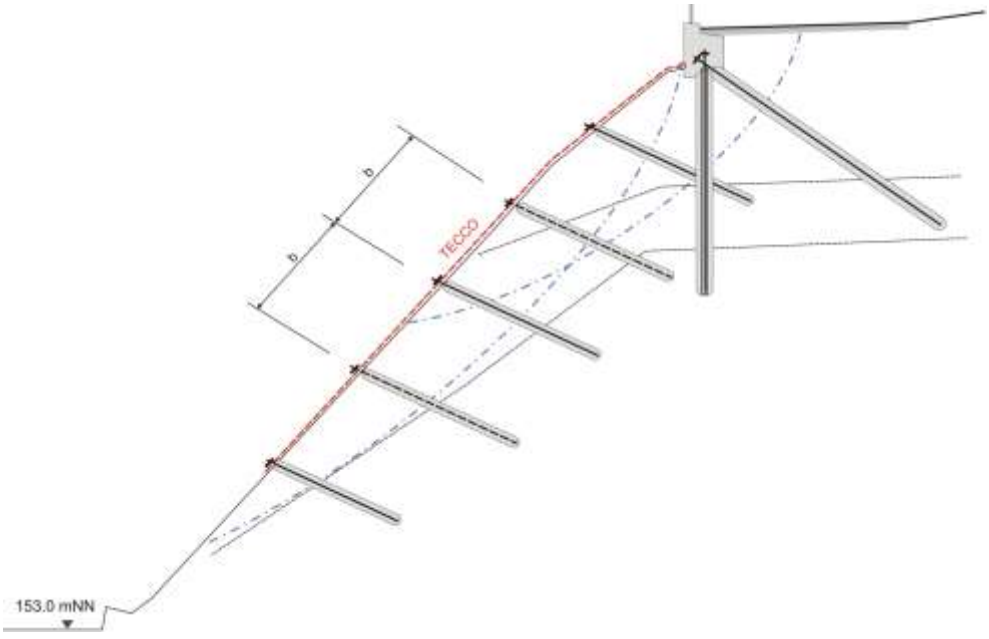

Figure 10.11 Reinforced concrete beam at the top of the TECCO® slope

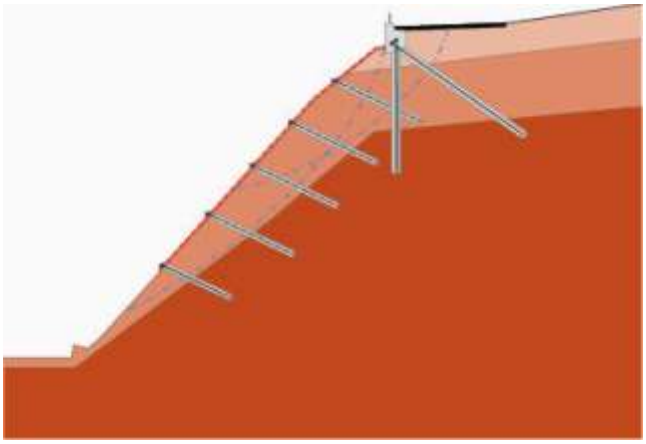

Figure 10.12 Top support rope is fixed with ring connection elements to the concrete beam

10.8 Water and drainages

Outflows of water must be caught and the water must be drained outside or below the slope area to be protected. Depending on the type of water pressure and the quantities, drainage can be accomplished by means of drainage hoses (e.g. slotted, perforated corrugated tubes) or special drainage-geotextiles in combination with hoses (pictures 10.16 and 10.17). Concrete ribs for filtering purposes may also be suitable and provide a supporting function in critical areas at the same time.

For slope stabilizations, where aggressive, sour or otherwise corrosive slope water is to be expected, it is necessary to keep an eye on it, so that the hillside-water is drained away well. At such an environment the application of high-tensile stainless steel wire mesh is possible.

Picture 10.16 Drainage hose to drain arising hillside water

Picture 10.17 Filter drain filled with concrete to drain arising hillside water

10.9 Erosion control

In the case of fine-grained substrates with a strong tendency to erode, it is normally necessary to install a mat protecting against erosion so that protection is already provided from the moment the slope stabilization is installed. Some time usually elapses before greening can be carried out because it is uneconomical to do this work in smaller stages.

Erosion control measures are required if soil material can be flushed away in fine-grained, non or insufficiently cohesive substrates. This erosion control may need to be of a temporary (in case of subsequent greening) or permanent nature (without greening).

General assessment of the need for erosion control measures:

- Mandatory in cases of fine-grained, non-cohesive unconsolidated materials (e.g. silt, sand).
- Normally required in cases of mixed-grain, unconsolidated rolling materials (e.g. sand, gravel).
- Recommended in cases of relatively fine-grained soils if there is a risk of water flowing over the surface from areas above the slope stabilisation with the flexible high-tensile steel wire mesh.
- In general not required in cases of rocky slopes without loose rock or soil cover.

For protection against erosion, finer-meshed geogrids or structural mats must be installed below the mesh. Slopes with a risk of erosion, in general, need to be greened. The mats must be matched to the intended greening process. Weather resistant mats of plastic (preferably UV-stabilized PP, PE or PET) are generally used.

With decomposing mats (jute, sisal, coco fibre) we experienced some revegetation problems. The so called TECMAT Erosion Control Mat, consisting of Polypropylene, is specially designed and tested for the use with the high-tensile steel wire mesh slope stabilization system (see Chapter 10.10.3).

The mats should only be opened in the area where the nails are passing through. Along the edges they should overlap by approx. 0.1–0.2 m. Bigger overlaps should be avoided.

The mats must be placed on the slope before the mesh is laid and can be secured by short nails or with U-shaped pieces of reinforcing steel.

Alternatively high-tensile steel wire mesh where the erosion control mat is already integrated in the mesh can be used as well.

10.10 Greening, revegetation and planting

It can be desirable, recommended or mandatory to green and/or plant a slope where a flexible slope stabilization system is installed.

Greening is always compulsory if the substrate is relatively fine-grained and endangered by erosion, and if flushing away of material (formation of erosion gutters) is expected during rainfalls/snow melting periods. In such cases greening is an integral part of the entire mitigation measure.

10.10.1 General assessment of the need of greening (technical view)

The following important points are recommended to be considered for the general assessment of the need of greening:

- Mandatory in cases of fine-grained, non-cohesive unconsolidated materials (e.g. silt, sand).
- Normally required in cases of all remaining substrates of unconsolidated material and rocky slopes highly prone to weathering, particular in case of marl, siltstone, sandstone.
- Recommended in cases of rocky slopes of medium proneness to weathering, with distinct layers and fissures.
- Not required in general for rocky slopes whose individual components (stones, blocks) are resistant to weathering and which the slope stabilisation system simply has to stop from sliding off and/or breaking out.

In fine-grained soils with a high risk of erosion, an erosion control mat must usually be installed to ensure there is erosion control immediately after the installation of the slope stabilization system. Some time usually elapses before greening can be carried out because it is uneconomical to do this work in smaller stages.

Erosion control mats may not be necessary if the stability can be guaranteed by the planned greening method, the type of vegetation layer and taking into account the point in time when greening becomes effective after the installation of the slope stabilization system.

Greening/planting may also be required for reasons of landscape preservation, for example if major new slope cuts must be recultivated. It is especially in these cases that the high-tensile steel wire mesh slope stabilization system is chosen in combination with nailing as an alternative to larger, permanently visible engineering structures.

In the question of greening/planting, an aesthetic aspect can often take precedence over safety-technical considerations.

Special remark:

Modern greening processes with special vegetation layers allow greening on substrates that are less suitable for vegetation and/or under difficult climatic conditions. Such vegetation layers are accordingly more elaborate and also more expensive. Normally greening is possible until a slope inclination up to approximately 60°. For steeper slopes all the factors as water content, date of seeding etc. are important and specialist should be contacted.

10.10.2 Vegetation face

Greening of steep slopes as enabled by the high-tensile steel wire mesh slope stabilization system is in principle reserved for experienced specialists which already should be contacted in the planning stage. It is important that these experts are aware of the local circumstances (climate, exposition, natural plant population, subsoil, etc.) and that they can match the vegetation face to these circumstances.

A prerequisite for successful greening is often the application of a minimum vegetation layer to permit the plants to begin growing. This layer must be matched to the subsoil, the need for nutrients and possibly other factors. It must be possible to apply this layer with full surface contact to the ground. The layer must be able to resist erosion a few hours after the application so that it cannot be flushed away by sudden heavy rainfalls. If erosion protection mats are used, it is important to match the vegetation layer material to the mat in such a way that penetration and filling of the mat is guaranteed.

10.10.3 Revegetation with erosion control mat

Dense mats of natural fibres, seed mats (with pregreening) are normally not suitable for these purposes unless the slope can be shaped very evenly so that the mats lie tightly on the entire surface and are pressed against the slope by the high-tensile steel wire mesh.

The TECMAT erosion control mat (see also chapter 8.9) is tested in detailed field studies for permeability of hydro and dry seed. Thus, the TECMAT is the ideal solution for irregular slopes.

The erosion control mat will be placed on top of the soil and fixed before installation of the main mesh. For irregular slopes it is required to fix the mat with soil nails to local dells (picture 10.18). This ensures an improved erosion control. The fixation is carried out with soil nails of different length, depending on the thickness of the subsoil layer. Based on experience, it is recommended to install one soil nail every 3–6 m^2. Along the edges the mats should overlap by approximately 0.1–0.2 meter and if required fixed with plastic ties.

For the laying option B (laying of the meshes before setting of the nails) it is required to cut a hole with scissors in the erosion control mat to avoid snarl of the mat while drilling.

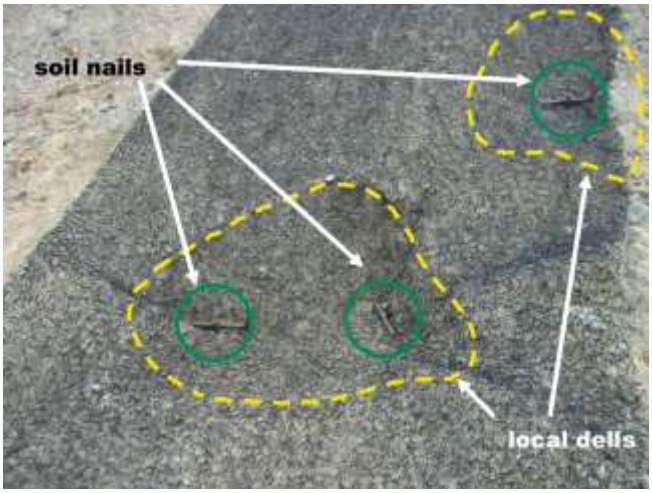

Picture 10.18 Fixation of erosion control mat with soil nails

Auxiliary equipment and tools

- Long scissors for cutting of the mat panels to the appropriate length. Alternatively, it is possible to use a universal scissor with rechargeable battery (e.g. "Bosch", GUS 9.6 V).
- Universal scissors to cut holes in the mat for drilling through.
- Sledge hammer (e.g. 4 kg) to drive in the soil nails

10.10.4 Seeding methods

The TECMAT erosion control mat is specially designed for greening with hydraulic or dry seeding respectively.

The main components of the hydro seeding are:

- seeds adapted to the soil and the climatic conditions
- biodegradable soil covering mulch (max. fibre length 3 mm)
- organic adhesive glue,
- purified, clean water
- if required, an organic-mineral fertilizer.

The materials will be mixed in the tank of a seeding machine to ensure homogeneity of the mixture. After mixing, the material is sprayed in liquid form over the surfaces to be treated. For slopes with bad access or economically small areas, there is the option to do dry seeding with a so called "greening backpack" (picture 10.19). The components are seeds adapted to the soil and the climatic conditions, organic adhesive glue, if required, an organic-mineral fertilizer.

In any case it is strongly recommended to contact a local greening specialist for successful revegetation.

Picture 10.19 Left: Example for hydraulic seeding machine
Right: Greening backpack (hand machine) for dry seeding

10.10.5 Planting

In principle, the additional planting of shrubs (trees in exceptional cases only) is possible. This must be planned carefully and suit the particular location. There are various possibilities, ranging from dendro seeding, cuttings of vegetatively multiplying shrubs and trees (e.g. types of willows), to the planting of grown plants with roots.

Holes for trees

It is possible to integrate trees and equivalent crops in exceptional cases into the slope stabilization system. A cut out of the mat panel is sized accordingly to the crops. The cut out is carried out after laying of the mesh panels. Thus, the panel is open to the side and it is possible to lay it around the crop. The two mesh panels are connected according to chapter 10.7 with connection clips. Approximately two meshes from the cut edge, a boundary rope (diam. 8 mm) is seamed into the mesh. The boundary rope is connected at the end with 3 pcs. 5/16" (NG 8) wire rope clips[40].

The figure 10.13 and the picture 10.20 explain more detailed the recommended setup for holes for trees in a slope stabilization system with high-tensile steel wire meshes.

[40] Wire rope clip connections shall be done in accordance to DIN EN 13411-5 (2003) [41].

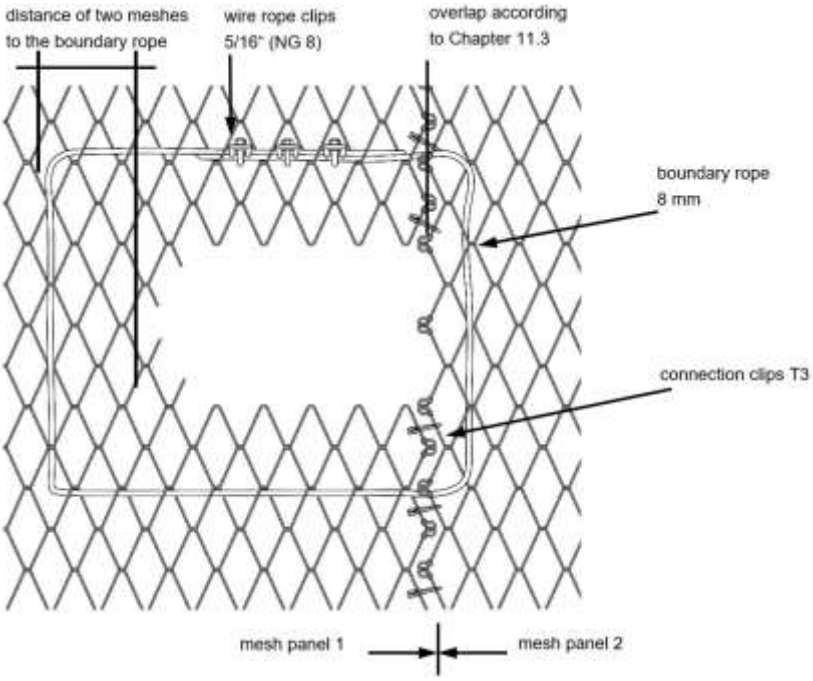

Figure 10.13 Principle drawing for holes for trees or planting holes

Picture 10.20 Example for tree hole installation

Holes for planting

The planting of plants with roots (e.g. so-called container plants) is possible with adaptations to the mesh (after consultation with the mesh manufacturer). It is recommended to obtain the service of an experienced specialist for both planning and execution.

The plant holes will be carried out after laying of the mesh and before the final tensioning of the claw plates. The mesh is cut according to the size of the required opening. Fixation and installation are according to the description of tree holes.

10.10.6 Maintenance

Please note that every "green" solution in the form of greening/planting requires a minimal amount of maintenance. This is usually most intensive in the first two years and then decreases, particularly in the case of planted slopes.

First cut

Indispensable for successful greening is a first nursing cut after the first full growth. This should be done under all circumstances, otherwise there is a danger of the grass and herbs drying and covering the slope in a manner restricting regrowth. The dry material can also result in rot setting in underneath and encouraging moss to grow all over the slope.

This first cut must be made after a growth to a height of approx. 20–30 cm, and a cut level of 10 cm should be maintained. A cut too short can lead to drying up in droughts.

Cutting should generally not be done in hot weather or after long dry periods, as the generally thin grass sod can easily dry out. A good time for cutting is in early autumn, after the end of the vegetation period.

Follow-up maintenance

In the first two years one cut per vegetation period is generally enough, and this preferably also in early autumn.

After two vegetation periods the long-term fertilizer is used up and an extensive vegetation adapted to the locally prevailing conditions forms. There is no strong growth anymore, so that there is generally no need for further maintenance with nursing cuts. Cuts may only be required in parts of the slope from now on if subsequent inspections indicate a need for them.

Slopes with shrubs

Where shrubs are planted on slopes, maintenance in the first two vegetation periods is the same as on slopes with grass.

Depending on the selected types, shrubs require a nursing cut at intervals of approx. 3–5 years or whenever the periodic inspections show that it is necessary.

A nursing cut is also appropriate to guarantee a minimum incidence of light in the slope so that the remaining greening (grass and herbs) does not disappear completely together with the erosion protection and the stabilization by the roots.

If tall trees grow in the course of time, they must be felled since they might be blown over by strong winds. Dead wood must be removed.

General remarks regarding maintenance

More intensive maintenance in the first vegetation period encourages an optimal function of the vegetation and reduces the need for subsequent maintenance.

It makes sense to include maintenance with the 1st nursing cut and follow-up maintenance during two vegetation periods in the project and to have it offered as part of the scope of performance.

In this way it is possible to agree on a formal acceptance of the greening of the construction after expiry of these two vegetation periods and the company doing the work can be held responsible. Thereby one can practically exclude a low-cost offer of an inadequate greening quality, since the supplier is aware of the pending assessment after two vegetation periods. Furthermore, experience shows, that a well-developed vegetation will continue to hold and grow also after the two years.

10.11 Dells, hollows and recesses

Natural slopes can often have various types of dells, hollows and recesses. In this chapter several methods to ensure appropriate solutions for such cases are suggested.

Dells and recesses up to approx. 0.5 m

Whenever possible the nails should be set in low spots, so that the pre-stress pulls the mesh cover into these. Major hollow spaces are thus avoided and in case of greening there is no need to spray on an excessive quantity of vegetation layer material or filler material. If the nail pattern does not permit setting nails in low spots, it may be necessary to set additional short nails (figure 10.14).

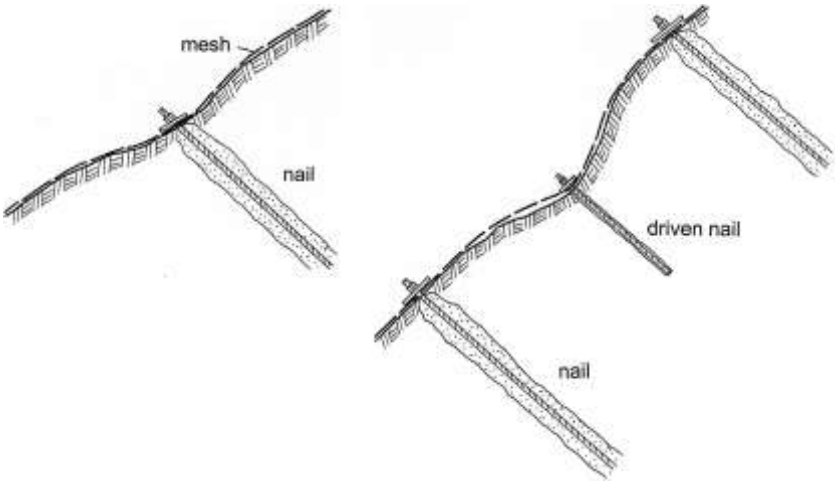

Figure 10.14 Arrangement of the main nails and short nails in low spots

Hollows, dells and recesses deeper than 0.5 m

If the hollow spaces are too deep, prefilling with a special mixture to which concrete may be admixed is possible before a vegetation layer is sprayed on. In this case the mesh does not need to be pressed or pulled right into the low spot.

Hereby care must be taken to ensure that the mesh upslope of the nail is tensioned so that a gradient of no more than 75° results, otherwise correct greening is no longer possible.

Filling of hollows with a static task

If overhangs in rock, projecting blocks, etc. need to be secured statically, this can be achieved with sprayed concrete fillings secured as required with nails and if appropriate reinforced additionally with welded wire fabric (figures 10.15 und 10.16).

If these fillings are to be greened, the sprayed concrete surface should be at a level so that the high-tensile steel wire mesh is tensioned at a distance of at least 10 cm above it. This will allow the subsequent application of a sufficiently thick vegetation layer.

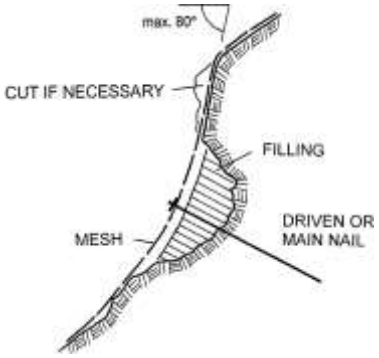

Figure 10.15 Detail arrangement in case of deep hollows with prefilling

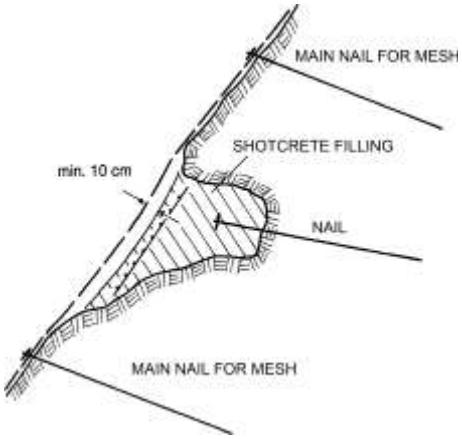

Figure 10.16 Sprayed concrete fillings

10.12 Acceptance of the construction

10.12.1 Acceptance inspection

A general acceptance inspection must be carried out on completion of the work and before the possible application of a vegetation face.

Hereby the following must be checked:

Construction components

- The nails are correctly placed and grouted.
- The positions of the nails are adapted to the local topography in the best possible manner and the maximum admissible distances between nails are complied with the design.
- Nails must be placed in low spots whenever possible.
- Auxiliary nails are placed where necessary, in order to tense the mesh as much as possible onto the surface.
- The nails are allowed to protrude by maximum approx. 20–25 cm.
- The system's spike plates are installed correctly (horizontal alignment).
- The system's spike plates are actively pressed onto the mesh and the substrate without bottoming on the nail itself due to e.g. a thread cut too short.
- The mesh is tensioned onto the surface to the best possible extent.
- The mesh sheets are fully connected without interruptions with the connection clips.
- Openings in the mesh e.g. for trees, adaptations to components, etc. are correctly closed.
- The boundary terminations are of a neat execution and the mesh is correctly fastened to the boundary ropes.
- The boundary ropes are installed tightly and laterally tensioned against rope anchors whenever possible.
- There is no evidence of unconformities (damaged/defective system).

Slope in general

- The system covers the critical area of the slope adequately in principle.
- Any drainage measures immediately above the protected slope and in the slope itself are of correct execution. Any observed outflows of water must be recorded in a protocol. If indicated, suitable supplementary work must be carried out to collect the arising water and to drain it away in a controlled manner.
- If any signs of erosion are already evident, they must be recorded.
- Any more substantial movements in the fields between the nails must be recorded.
- Any fracture lines above the top boundary must be recorded.

If any sort of construction sensitive to deformation (e.g. a road) is located above the flexible slope stabilization, it is recommended as a matter of principle to provide a stiffening measure in the form of e.g. a deep-anchored concrete partition in addition to the mesh cover in combination with nailing. If no such measure has been taken, the current condition must be recorded and the possibility of damage resulting from possibly inadequate protection measures in the boundary area must be pointed out.

10.12.2 Acceptance protocol

Deficiencies detected during acceptance inspection must be eliminated by the executing contractor and a formal final acceptance protocol must be issued and signed by the parties involved (client, project editor, site manager and contractor).

Potential problem areas in the slope must be recorded in this acceptance protocol and documented with photographs, so that any changes can be detected during subsequent inspections.

If required or desired, a vegetation face can be applied by means of a suitable process after acceptance is completed. The acceptance inspection must be made beforehand because constructive deficiencies within the system itself might otherwise be hidden by the sprayed on vegetation or greening layer.

10.13 Maintenance and periodic inspection of the flexible slope stabilization system

10.13.1 Maintenance of the system

No maintenance as such is required if the slope stabilization system was correctly laid out and put in place and if suitable measures were taken against the problems of water outflows and erosion.

The flexible stabilization system elements themselves require generally no maintenance thanks to their high-grade coating against corrosion.

Certain weathering and loosening processes are possible, however, since a protected slope is also exposed to the influences of the environment (e.g. cycles of rains, frost, dew, etc.). Such effects cannot be prevented by the open high-tensile steel wire mesh system, which is why it may become necessary to remove any fine material which has been washed to the foot of the slope or rippled there.

Maintenance is actually only called for if inspections reveal mechanical damage to the mesh or its fastening devices due to external influences. Such defects must be corrected.

If the mesh or a fastening feature has become loose, the problem can normally be solved by further tightening (tensioning). In extreme cases, additional nails may have to be put in place.

If, in the extreme case, weathering, loosening and the influence of water have caused intolerable material washout or movements with resulting hollows behind and pouches in the

meshes, the need for comprehensive maintenance including detaching of the meshes, emptying and reinstalling must be considered. If appropriate, local hollows must be filled and stabilized with shotcrete.

10.13.2 Periodic inspection of the system

The periodic inspections must be specified within the framework of a maintenance schedule.

In the first two years an annual inspection should be carried out, preferably in spring. If two consecutive inspections reveal no major changes with a negative influence on the safety and function of the protective construction, the intervals between the periodic checks can be extended to two years.

Additional inspections may have to be made after special events (e.g. after extreme rainfalls, falling of material over the protected slope and more severe seismic influences) in order to detect damage to the system or major erosion and movements.

The periodic inspections comprise in the main:

- General condition
- Condition of problem spots according to the acceptance protocol
- Damage to the system itself (construction components)
- Damage due to erosion/movements in the context of the substrate
- Condition of the greening/vegetation (general/local)
- Documentation of defective areas/changes in relation to the previous inspections

The findings must be detailed in a protocol and documented by photographs so that changes from the condition at the time of the acceptance inspection and preceding inspections are recorded.

Observing the weathering and erosion processes is important in slopes without greening or vegetation. In cases of local loosening or material erosion it must be checked whether the situation can be improved by retensioning alone or additional measures such as securing of hollows with shotcrete, greening, emptying of material deposits are called for. The critical areas must be documented with photographs.

In slopes with greening or vegetation it must be checked how the plant life develops. Is the surface covered completely, bare spots require regreening. The need for maintenance (mowing, cutting back to the rootstock) must be determined.

10.14 Carbon footprint and environmental aspects

The climate change is increasingly recognized as a major global challenge. It is widely accepted that the greenhouse gas emissions caused by humans are having a negative impact on the environment [64].

By far the most important greenhouse gas, arising from human activity, is carbon dioxide (CO_2). Virtually all human activities cause the CO_2 emissions that lead to climate change. By using electricity generated from fossil fuel power stations, burning gas for heating or driving a petrol or diesel car, every person is responsible for CO_2 emissions.

Furthermore, every system, product or service consumed by humans indirectly creates CO_2 emissions; energy is required for their production, transport and disposal. These products and services may also cause emissions of other greenhouse gases. Understanding and addressing the full range of our impact is crucial for the effects of climate change to be minimised.

The total set of greenhouse gas emissions caused directly and indirectly by an individual, organisation, event or product is commonly called their carbon footprint. Establishing the carbon footprint of an organisation can be the first step in a programme to reduce the emissions it causes. This idea is aimed at helping businesses and organisations establish their carbon impact and introduces some of the key issues faced in the calculation of a carbon footprint.

10.14.1 What is a carbon footprint?

The term "carbon footprint" is commonly used to describe the total amount of CO_2 and other greenhouse gas (GHG) emissions for which an individual or organisation is responsible. Footprints can also be calculated for events, products or systems.

The full footprint of an organisation encompasses a wide range of emissions sources from direct use of resources and fuels to indirect impacts such as employee travel or emissions from other organisations up and down the supply chain. When calculating a system's footprint it is important to try and quantify as full a range of emissions sources as possible in order to provide a complete picture of the organisation's or system's impact.

In order to produce a reliable footprint, it is important to follow a structured process and to classify all the possible sources of emissions thoroughly. A common classification is to group and report on emissions by the level of control which a system or an organisation has over them.

10.14.2 Why calculate a carbon footprint?

There are typically two main reasons for wanting to calculate a carbon footprint:

- To manage the footprint and reduce emissions over time
- To compare and report the footprint accurately to a third party.

Footprinting for management of emissions

Calculating an organisation's carbon footprint can be an effective tool for ongoing energy and environmental management. If this is the main reason that an organisation requires a carbon footprint, it is generally enough to understand and quantify the key emissions sources through a basic process, typically including gas, electricity and transport. This approach is relatively quick and straightforward. Having quantified the emissions, opportunities for reduction can be identified and prioritised, focusing on the areas of greatest savings potential.

Footprinting for comparison and accurate reporting

Organisations increasingly want to calculate their carbon footprint in detail for public disclosure in a variety of contexts:

- For public relation and/or marketing purposes.
- To fulfil requests from tender specifications, business or retail customers, or from investors. This can especially be the case for public investments where the construction work for new installations and maintenance has a big impact regarding the total carbon footprint.
- To ascertain what level of emissions they need to offset in order to become "carbon neutral". This can often be the case for private companies in order to distinguish from competition.

Conclusions for construction and building processes

The importance of carbon footprint calculations and comparisons will increase in the near future. It will become a more and more serious demand for any public organisation and private companies. Consequently, services, products and applied systems will have to be checked, analysed and compared regarding their carbon emissions. It is obvious that especially the building and construction sector for infrastructure and maintenance have a big impact accordingly.

10.14.3 CO_2 footprint comparison between slope stabilizations with shotcrete and with high-tensile steel wire mesh

Two alternative slope stabilisation methods were analysed in terms of their respective contribution towards the greenhouse effect ("climate friendliness"):

- A conventional slope stabilisation method, using shotcrete, anchors and welded wire mesh (see picture 10.21)

Picture 10.21 Slope stabilization using traditional reinforced shotcrete system

– the slope stabilization with high-tensile steel wire mesh (TECCO® system, see also picture 10.22).

Picture 10.22 Slope stabilization using high-tensile steel wire meshes in combination with nailing (TECCO® System)

In order to do this, the emissions which affect climate change and occur during the life cycle of the building materials used as well as during the utilisation of the slope stabilisation structures are to be logged and compared. This method is called the "CO_2 footprint" as mentioned in the previous chapters 10.14.1 and 10.14.2. The "CO_2 footprint" method used here essentially follows the Life Cycle Assessment (LCA) method in accordance with ISO 14040.

The corresponding investigations, calculations and analysis were made by the Institute of Civil and Environmental Engineering of the Technical University of Rapperswil in Switzerland (Hochschule Rapperswil)[41].

The figures 10.17 and 10.18 show two comparable slope stabilisation structures, each realised by using one of the two methods to be compared.

These two structures are comparable in terms of:

– Functionality: the slope stabilisation function; other functions such as e.g. landscape protection will not be taken into consideration.

– Life cycle: both methods have the same service life.

– Maintenance/repairs: it has been assumed that neither of the methods will require any maintenance/repairs to be carried out during their service life.

[41] Details of this analysis are shown in the paper by Prof. Susanne Kytzia and Prof. Paul Hardegger of HSR Hochschule Rapperswil [64].

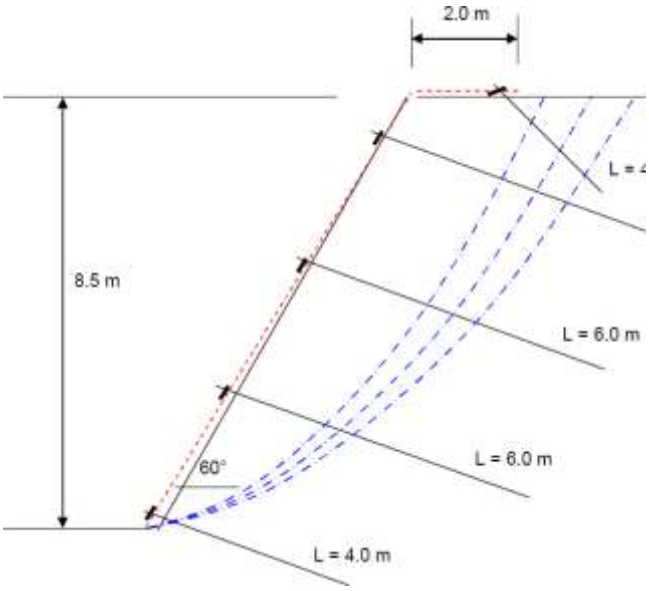

Figure 10.17 Slope stabilisation using flexible slope stabilization system with high-tensile steel wire mesh (TECCO® System)

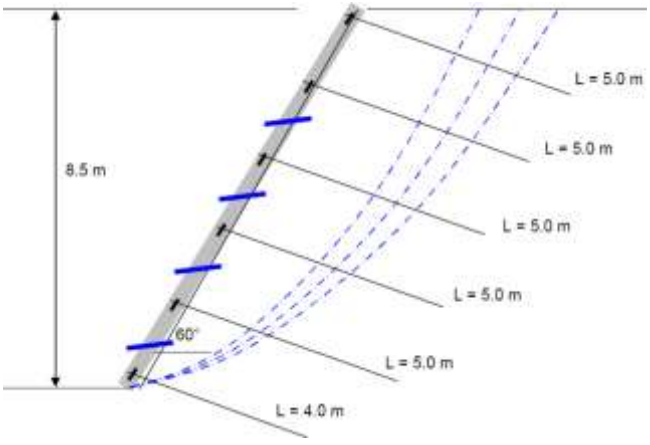

Figure 10.18 Slope stabilisation by means of shotcrete placement

Accordingly, the materials used for these two structures are listed on tables G.1 and G.2 in the appendix G. These quantities correspond to a stabilisation structure consisting of a slope 100 m long in each case as represented in the diagrams shown in figures 10.15 and 10.16.

The service life analysis was limited to the manufacture of the building materials and their transport to the construction site. Construction, operation, maintenance, removal and disposal were not be taken into consideration.

This definition is based on the following considerations:

- Studies published on life cycle assessment of structures are based on the assumption that the creation of the structure will only make a relatively small contribution towards the pollution of the environment. Kasser [67] and Geiger and Fleischer [57] come to the conclusion that in the case of residential buildings, less than 1% of the cumulative energy demand of a building can be attributed to construction. The construction of the structures considered here is not expected to result in (relatively) higher energy expenditure.
- It has been assumed that in general, there will be no expenditure on operation and maintenance.
- When the two structures are removed, it is mainly steel and concrete which will need to be dealt with. If these two waste materials are collected separately, then their processing and disposal will only result in very low energy consumption and thus only to a low level of emissions which might affect climate change.

The emissions from the manufacture of materials which might affect climate change (incl. the recovery of materials, the manufacture of fabricated materials and the supply of energy) as well as from transport processes have been taken from the Ecoinvent database from the domain of the Polytechnical University ETH of Zurich, Switzerland. Within the context of this conservative estimate of emissions (consideration of the "worst case scenario"), in case of doubt, processes which produce the highest level of environmental pollution was chosen in each case.

Emissions which might affect climate change have been selected by the level of carbon dioxide emissions from the burning of fossil fuels (in kg of "CO_2-fossil") on the one hand. On the other hand, all the emissions which contribute towards climate change have been recorded and weighted according to their specific contribution – relating to carbon dioxide as a reference variable – and added together to give an overall index. This overall index is known as the "Global Warming Potential" ("GWP" for short); the unit in which it is measured is kg CO_2 equivalent. This method of assessment has been used as part of the Life Cycle Assessment in many studies and is internationally recognized.

Results of the carbon footprint comparison

The comparison of all the emissions which might affect climate change during the service life of the two structures clearly shows that the TECCO® system contributes to the greenhouse effect far less than the shotcrete placement (see Figure 10.19).

This statement applies to both "CO_2-fossil" and to the "Global Warming Potential (GWP)". **The impact is around 4–5 times less for the TECCO® system for both methods of assessment.**

This difference can be attributed to the differences in the quantities of materials used. In the construction of the shotcrete placement, around 14'700 kg of steel, 40'300 kg of cement and 564'000 kg of concrete are used. With the TECCO® system, the same construction uses 8'100 kg of steel and 23'400 kg of cement.

These differences have a considerable effect on the environmental impact which would be caused: both in respect of the manufacture of the materials and transport. These differences are described in detail in the appendix G on table G.3. This also shows the different contributions made by the different parts of the structure (nailing, mesh and shotcrete) as well as the contribution of the different materials.

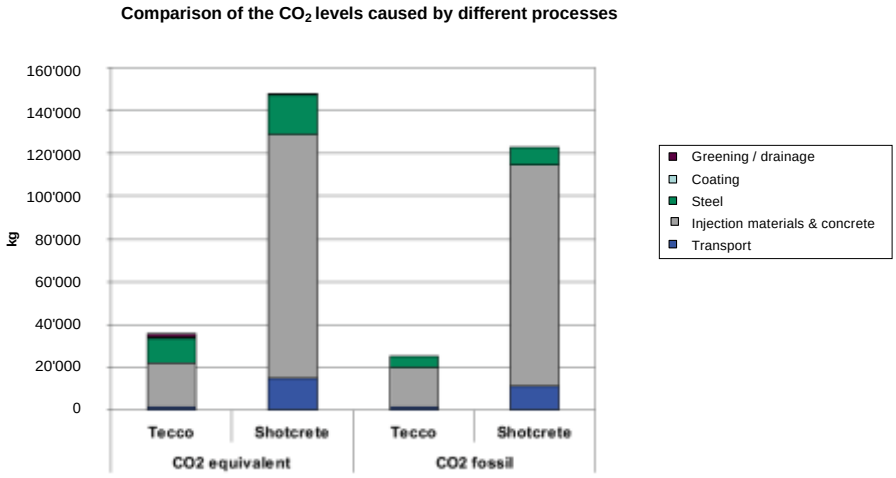

Figure 10.19 Emissions which might affect climate change during the service life of a comparable structure produced using different processes. The impact is around 4–5 times less for the TECCO® system (compared to the shotcrete solution) for both methods of assessment.

This shows the following regarding the TECCO® system:

- that nailing contributes towards the greenhouse effect far more than the mesh and greening;
- the cement used accounts for most of the total level of pollution caused, followed by the steel (in a ratio of 3 to 1);
- the contribution made by transport is relatively small at 5% of the total level of pollution caused.

This shows the following regarding the shotcrete structure:

- that the shotcrete accounts for 70% of the total level of pollution caused and thus contributes towards the greenhouse effect more than the pinning which accounts for 30% of the total level of pollution caused;
- the cement used is responsible for most of the total level of pollution caused, followed by the steel (in a ratio of 12 to 1);
- the contribution made by transport at approximately 9% is more than that made by the steel.

10.14.4 CO_2 footprint comparison between slope stabilizations with concrete and with high-tensile steel wire mesh

The carbon footprint comparison analysis between slope stabilization systems with concrete structure and high-tensile steel wire meshes [117] confirmed the results and conclusions of the previous chapter (10.14.3) in a similar way.

The Kyoto Protocol to the United Nations Framework Convention on Climate Change is an international agreement negotiated on 11 December 1997 at the 3rd Conference of the Parties in Kyoto (Japan). The purpose is to require countries to lower their emissions of six greenhouse gases that cause global warming. Under the protocol, for instance, the country of Japan is required to reduce greenhouse gas emissions by six percent compared to the 1990 level over the period of 2008–2012. To achieve such targets, it is necessary to develop innovative technologies that produce less greenhouse gasses and emissions. The TECCO® system, which offers slope stability with a high-strength mesh and soil nails, is expected as a less CO_2-producing alternative measure than a conventional shotcrete technique, because the system requires less construction materials. Picture 10.23 show the two systems that were compared.

Picture 10.23 Compared systems for carbon footprint comparison in Japan
Left: Slope stabilization system with TECCO® meshes
Right: Concrete slope stabilization system (frame system)

The table G.4 (appendix G) shows the emission ratios of greenhouse gasses in each processes of concrete life cycle. As illustrated in the previous chapter and according to this, the emissions amount in a material manufacture process is extremely large compared with other processes. Moreover, source unit of CO_2 emissions according to used material in each system is shown in table G.5[42].

In addition, although the value of wire and steel bar was assigned directly, grout and shotcrete were comparatively converted based on the standard compounding ratio (w/c = 50%). The emission basic unit of the cement contained into them is 0.75kg-CO_2/kg, sand is 0.0034 kg-CO_2/kg, water is 0.02 kg-CO_2/m^3, and decided emission basic unit of grout and shotcrete from the quantity contained in per 1.0 m^3.

The corresponding CO_2 emissions in the material manufacture stage of the TECCO® system and the concrete frame system are calculated respectively based on the quantity of the used material per 1000 m^2.

The calculation results are shown in the appendix G (table G.6). Material quantity of each system was taken as the specification which can respond to shallow landslide level. For the

[42] The CO_2 emissions source unit of each material in table E.5 was extracted from "Center of Environmental Information Science corporation: Table of CO_2 emissions standard physical unit"(2007) [29, 65].

High-tensile steel wire mesh system, the nail interval is 2.5 m, and the nail length 2.1 m. The concrete frame set the beam interval to 2.0 m and the cross section to 300 × 300 mm. These are standard values for both systems.

Conclusion

According to this calculation result shown in appendix G (tables G.6 and G.7), the CO_2 emissions of the high-tensile steel wire mesh system in the material manufacture stage are approximately 1/9, as compared with those of the shotcrete frame.

In other words, the adoption of the high-tensile mesh system can reduce CO_2 emission 89% (figure 10.20).

Of course, this example may only illustrate a particular and single case. Country and/or area specific values and influences can cause additional variation of results. Nevertheless, the very large difference of carbon footprint between high-tensile steel wire mesh systems and corresponding alternative solutions executed with concrete will always be significant.

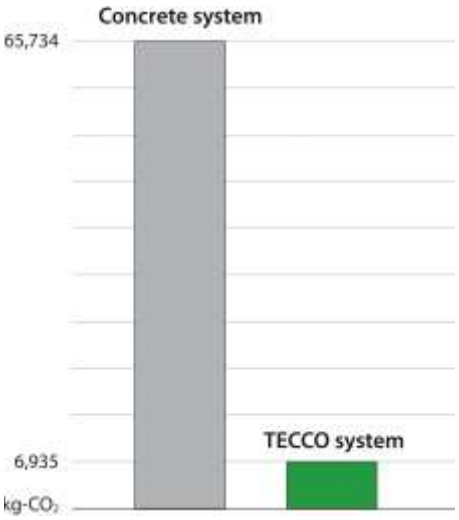

Figure 10.20 Carbon footprint comparison between concrete and high-tensile steel wire mesh slope stabilization systems

11 Practical examples

The following practical examples shall provide additional information about several field applications and installation of projects that were designed according to the new method for the design of slope stabilization systems with high-tensile steel wire meshes. A selection of executed projects is shown in order to illustrate various implementation aspects of the new method; therefore and for overview reasons, not all details of these projects are shown in this chapter.

11.1 Project built at Anzenwil, Switzerland

Because of the new bridge at Anzenwil, the main road at the Neckartalstrasse between Mogelsberg and Ganterswil had to be widened and therefore, the existing slope had to be cut, prepared and secured.

Picture 11.1 provides an overview of the slope during installation of the flexible slope stabilization system. In the front, the old wooden bridge can be seen. The new bridge was installed parallel to the old bridge where first concrete foundation is shown on the left side of the picture.

Picture 11.1 Cut slope at the bridge of Anzenwil during the construction phase

Project and geotechnical data

Superficial friction angle (charact. value)	φ_k	=	34 degrees
Friction angle (characteristic value)	φ_k	=	32 degrees
Cohesion (characteristic value)	c_k	=	0 kN/m^2

Unit weight (characteristic value)	γ_k	=	20 kN/m^3
Stabilized area	A	=	850 m^2
Max. slope height	H	=	16.0 m
Slope length	L	=	50 m
Slope inclination actual state	α_{before}	=	30–25°
Slope inclination final state	α_{after}	=	55°
Altitude		=	700 m.a.s.
Exposition		=	south-west

The surface layers consisted of scree and moraine soil which covered the deeper layers of molasse (Nagelfluh) and marl material (figure 11.1).

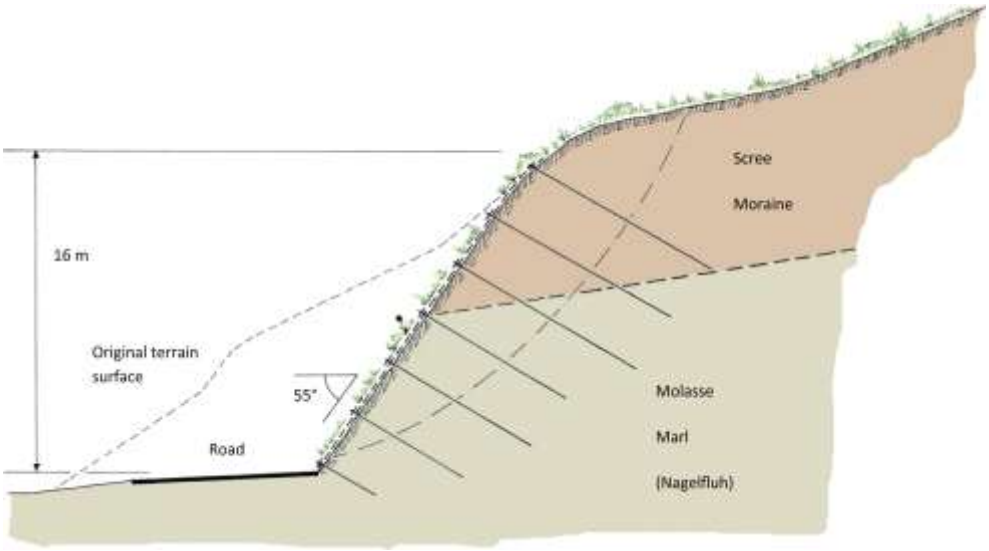

Figure 11.1 General cross-section with nailing and high-tensile mesh as protection system

Special local mountain water conditions with hillside water, water along stratification and joint systems as well as several small slope springs required a careful design of the drainage system including water management. Consequently, additional dimensioning steps had to be included for the design of the final slope stabilization system. The following figure 11.2 provides additional overview information accordingly.

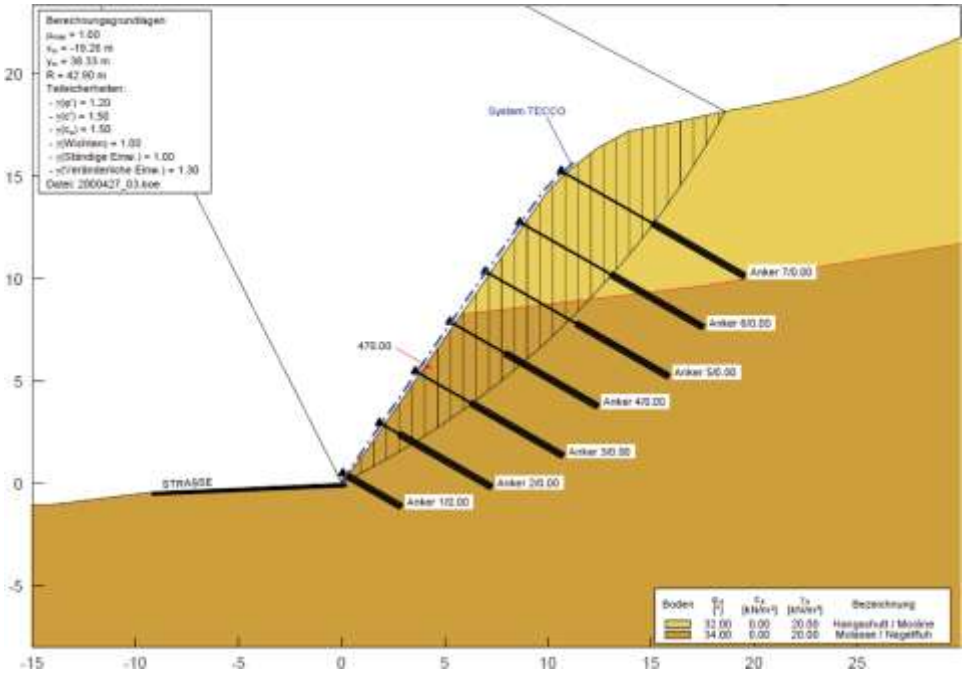

Figure 11.2 General cross-section for stability analysis

Picture 11.2 Drainage measurements before mounting of the TECCO® mesh

Picture 11.3 Completed slope stabilization system including greening (new bridge in front)

11.2 Project built at Mülheim, Germany

Close to the city of Mülheim (Germany), at the location Mendener Strasse, a rocky slope approx. 420 meter long and on average approx. 12 m high is permanently protected against rockfalls and local instabilities by means of nailing in combination with a TECCO® mesh cover.

The inclination of the slope front to the horizontal plane amounts to between 45 and 70°. Locally, above all in the upper areas, the rockface (sandstone, siltstone, mudstone) is covered by slope clay and slope scree (see also figure 11.3).

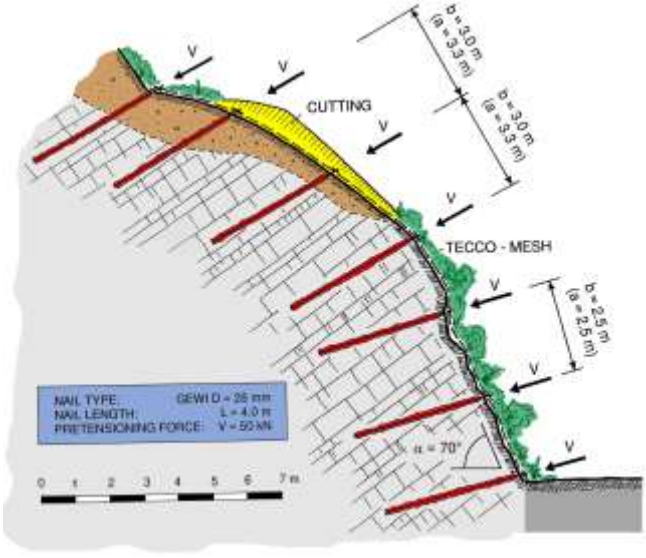

Figure 11.3 General cross-section with nailing and high-tensile mesh as protection system

The rock is very prone to weathering. Based on the geotechnical situation, the overall stability of the slope is not endangered. The protection measures are limited to the section close to the surface.

The surface protection was dimensioned on the basis of the RUVOLUM® method. For the rocky section with a slope inclination of $\alpha = 70°$ and a long-term loosened, weathered layer of thickness $t = 0.50$ meter to be protected, a nail pattern of $a = b = 2.5$ meter resulted.

In the area of the unconsolidated rock covers with a slope inclination of 45–50° and with $t = 0.80$ m, a nail pattern of $a = 3.3$ m and $b = 3.0$ m resulted. The slope was greened with the Fibrater system.

Picture 11.4 presents the situation with the closed road before the slope stabilization work started.

Picture 11.4 View of the slope and sliding areas before installation

The cleaning and natural grading with an excavator is shown on the following picture 11.5.

Picture 11.5 Cleaning and natural grading with excavator

The drilling machinery and drilling process is illustrated on the picture 11.6. Picture 11.7 provides a partial overview of the installed high-tensile steel wire mesh, shortly before the spike plates are finally tensioned.

Picture 11.6 Drilling process

Picture 11.7 Installation of high-tensile steel wire mesh

Pictures 11.8 and 11.9 emphasize the natural and green appearance of a slope stabilization system with high-tensile steel wire mesh. Mesh and spike plates can hardly be seen only several months after installation due to natural greening effects.

Picture 11.8 Completed installation with protected slope

Picture 11.9 Completed installation with protected slope (rocky section)

11.3 Project built at Odernheim, Germany

Between the towns of Odernheim and Duchroth in Germany, a landslip occurred along the regional road L 235. This was followed by falling blocks, so that the road in question had to be closed. Suitable measures to protect the particular slope permanently were called for urgently (see also picture 11.10). Protective measures taken in the area of the slope at an earlier stage had failed because, in the main, the applied nails were too short and consequently pulled out of the terrain together with the blocks. The fence of 2 m height along the foot of the slope was intended as a rockfall barrier for rocks of maximum head size but was clearly not laid out for the events which subsequently occurred.

The rocky subsoil consists of partly-cut rocks of the “Unterrotliegenden” type, arranged in alternating layers of various thicknesses of sandstone, siltstone and claystone. The rocky slope of maximum 45 m height and approx. 100 m length is partly covered by colluvium and scree. The ground characteristic values, compiled on the following page, generally apply to the decompressed subsoil.

The high-tensile system TECCO® was selected to stabilize the slope against instabilities starting from the oversteep rock ledge and against slips near the surface in the area of the scree and colluvium, respectively. This flexible slope stabilization system is ideally suitable for the purpose. Thanks to its flexibility it can be optimally adapted to the irregular surface of the terrain. Apart from the static requirements to be satisfied, the individual nails must be positioned in recessed spots as far as possible so that the mesh can be tensioned to the maximum extent onto the surface.

Picture 11.10 Slide, causing the temporary closing of the regional road

The fence at the foot of the slope was repaired and put into its original condition to protect against rockfall from the forest located above the surface covered by the mesh.

Slips at a deeper level could be excluded in principle. To dimension the high-tensile steel wire mesh slope stabilization system, the investigations on the basis of the RUVOLUM® method concerned slope-parallel instabilities near the surface on the one hand, and local slips between the individual nails to a maximum depth of 1.0 m on the other. Dimensioning indicates that, using nails of type GEWI D = 28 mm and allowing for a rusting-away of 4 mm with reference to the diameter, the maximum distances between nails listed in the following overview are admissible. The nails must be incorporated in the compact rock to a depth of at least 3 m. The overall length of the nails is 4.0 m, i.e. they are twice as long as the originally installed ones which revealed to be too short. Figure 11.4 provides an overview of the cross section of the protection system.

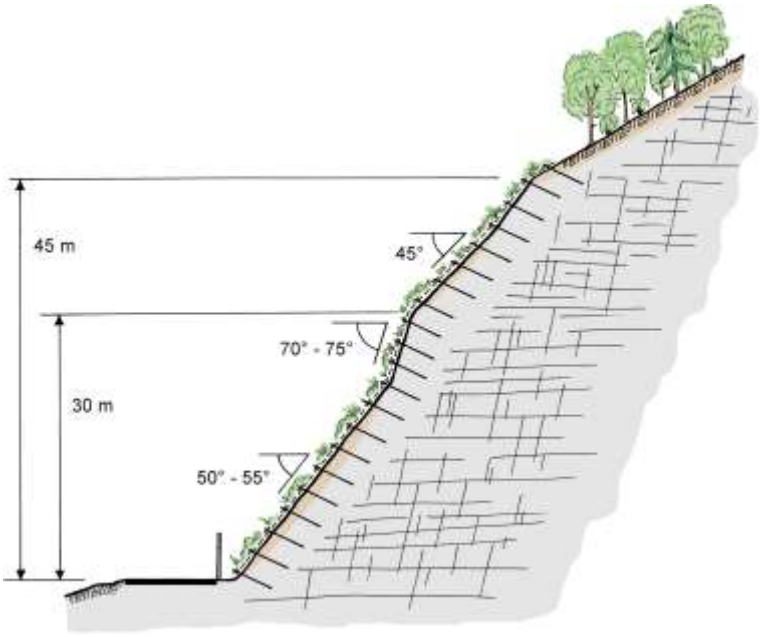

Figure 11.4 General cross-section with nailing and high-tensile steel wire mesh as protection system

Project information

Geotechnical parameters of the superficial area of the subsoil

Friction angle (characteristic value)	φ_k	= 35 degrees
Cohesion (characteristic value)	c_k	= 0 kN/m^2
Unit weight (characteristic value)	γ_k	= 23 kN/m^3

Maximum nail distances using nails of type GEWI *D* = 28 mm

Inclination of slope	α	≤ 55°	> 55°
Max. nail distance horizontal	a	3.00 m	2.50 m
Max. nail distance in line of slope	b	3.00 m	2.50 m

Project data

Stabilized area	3′500 m^2
Number of nails of type GEWI *D* = 28 mm	500 pcs.
Nail length	4.0 m
Total nail length	1,950 m
Time for installation	3.5 months

The picture 11.11 below illustrates an overview of the stabilized slope just by the end of the construction work and picture 11.12 presents the greened slope several months after the completion of the slope stabilization.

Picture 11.11 Overview stabilized area (after completion of installation work)

Picture 11.12 Overview stabilized area (several months after installation)

Picture 11.13 shows a closer view of the middle (steeper) part of the slope where mixed rock and soil sections are stabilized with the high-tensile steel wire mesh system.

Picture 11.13 Detail from the middle steeper part (mixed rock and soil sections)

The location of nails and spike plates at low points in combination with intermediate steel wire ropes can be seen on the following picture 11.14.

Picture 11.14 Location of nail and spike plate in deep point of the slope

11.4 Project built on Island of Helgoland, Germany

In the North Sea, on the Island of Helgoland there is a steep East to South-East-facing rock slope of severely fissured sand and silt stone, the so-called “Falm” edge. The highly loosened rock material close to the surface endangers the properties located below the slope. In some places loose layers of rock have already slipped away and partly backfilled and damaged several dwellings beneath (picture 11.15). The superficially very loose slope was secured by means of the TECCO® system consisting of the high-tensile steel wire mesh and nailing (figure 11.5).

Picture 11.15 Sliding mass at the foot of the slope

Dimensioning was only carried out for the loosened layers of unconsolidated rock near the surface and was based on the RUVOLUM® method. Large area, deep-seated stability problems could be excluded in this case.

For the given example, using a nail of type GEWI 32 mm and taking into account a rusting-away of 4 mm of the diameter, the maximum admissible nail distances result in dependence of the slope inclination and at an assumed layer thickness of 1.0 m. In the area of the top cover layer nail lengths of 6.0 m were selected, and in the rock slope itself generally of 4.0 m. Greening was indicated in view of this fine-grained and loosened subsoil highly liable to weathering.

The proximity to the sea with the salty, aggressive air demanded a mesh displaying a high resistance to corrosion, as it is guaranteed by the TECCO® mesh with its aluminium-zinc coating. A much longer useful life can be expected from this mesh in comparison with one galvanized in the normal manner.

Because of the complicated location above the residential areas with private houses, most of the cleaning work had to be made by hand (figure 11.16).

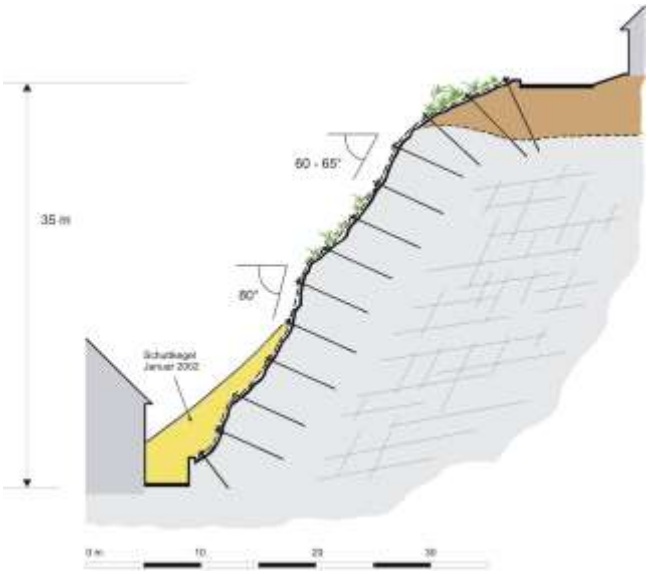

Figure 11.5 General cross-section with nailing and high-tensile steel wire mesh as protection system

Picture 11.16 Cleaning work

Mesh installation and drilling processes had to be executed with special safety measurements in order to reduce impact to the houses and infrastructures below (picture 11.17).

Picture 11.17 Left: Installation of TECMAT and high-tensile steel wire mesh
Right: Drilling processes with light weight equipment

The project information below provide an overview of the relevant design parameters.

Project information

Geotechnical parameters of the superficial area of the subsoil

Friction angle (characteristic value)	φ_k	= 45 degrees
Cohesion (characteristic value)	c_k	= 0 kN/m^2
Unit weight (characteristic value)	γ_k	= 24 kN/m^3

Maximum nail distances using nails of type GEWI D= 28 mm

Inclination of slope	α	55°	65°	80°
Max. nail distance horizontal	a	3.65 m	3.00 m	2.35 m
Max. nail distance in line of slope	b	3.65 m	3.00 m	2.35 m

Project data

Stabilized area	7′300 m^2
Number of nails of type GEWI D = 28 mm	950 pcs.
Nail length	4.0–6.0 m
Total nail length	4’600 m
Time for installation	5 months

Pictures 11.18 and 11.19 show the slope several months after completion of the installation work.

Picture 11.18 Several months after greening

Picture 11.19 Overview of the slope stabilization of the Falm edge of Helgoland (Germany)

11.5 Project Kaiserslautern, Germany

A cutting was made in mottled variegated sandstone prone to weathering along the highway A63 from Kaiserslautern to Mainz, Germany. This cutting is up to 30 m deep on the northern and 15 m on the southern side with a total area to be stabilized of 31′400 m^2 [86]. The inclination of the slope is generally 45° and flattens off slightly towards the top edge of the slope. The altitude amounts to about 220 m a.s.l. Transverse to the slope surface there are several fissures going right across, with a width up to several cm.

Relaxation processes in the form of removal of rock masses at the front led to a tremendous loosening of the rock compound with the result that the tectonic-based fissure systems were

visibly activated (see also pictures 11.20 and 11.21). Approx. two years after the excavation the slopes revealed to be unstable and required subsequent protection measures.

Picture 11.20 Situation before stabilizing

Picture 11.21 Wedge-shaped failure due to relaxation

Figure 11.6 presents the cross section of the problem situation including the protection measure.

The nailing as well as the flexible mesh cover were dimensioned on the one hand against superficial instabilities considering various individual wedge-shaped bodies (figures 11.7 and 11.8) susceptible to break out up to a depth of 4.5 m and of a width of up to 10 m varying distances between fissures as well as based on the RUVOLUM® method.

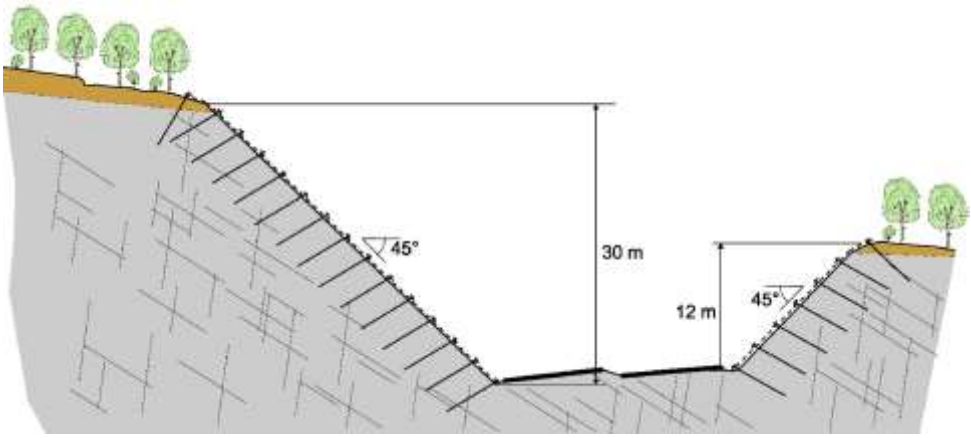

Figure 11.6 Cross section including protection measure

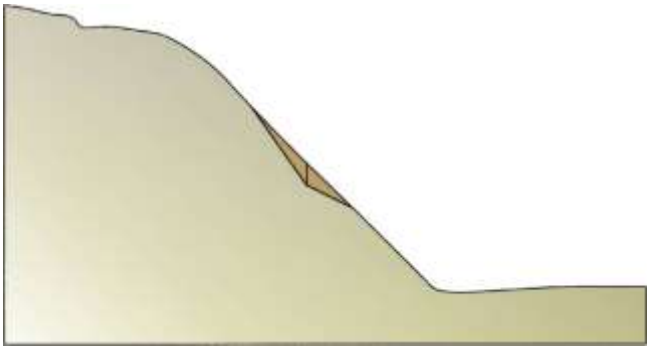

Figure 11.7 Analysis of specific wedge-shaped failures

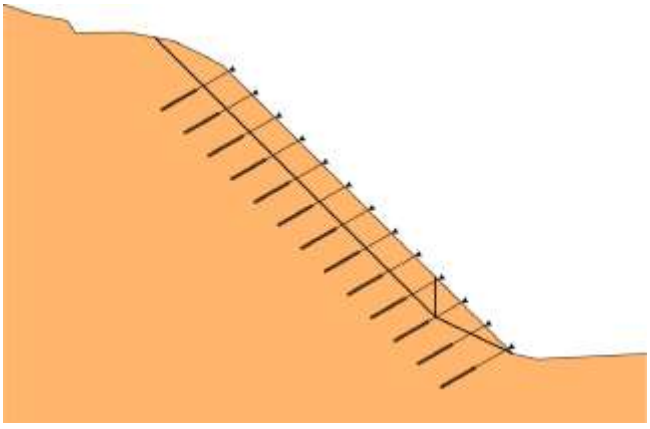

Figure 11.8 Investigation of the overall stability

On the other hand, the global stability was investigated according to the sliding-block method (figure 11.9). As a result of the dimensioning, the maximum admissible nail spacing as well as the nail length minimum required were determined.

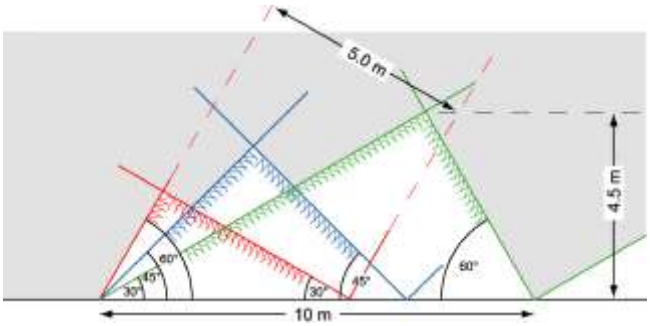

Figure 11.9 Investigation of individual wedge-shaped failures

Project information

Geotechnical parameters of the superficial area of the subsoil

Friction angle (characteristic value)	φ_k = 35 degrees
Cohesion (characteristic value)	c_k = 0 kN/m^2
Unit weight (characteristic value)	γ_k = 23 kN/m^3

Maximum nail distances using nails of type GEWI *D* = 32 mm

Inclination of slope	α	45°
Max. nail distance horizontal	a	3.40 m
Max. nail distance in line of slope	b	3.40 m

Project data

Stabilized area	31′400 m^2
Number of nails of type GEWI *D* = 32 mm	3′300 pcs.
Nail length	6.0–8.0 m
Total nail length	22′950 m

Due to the fact that the newly built highway could be used as a very comfortable access without any restrictions and taking into account that the summer 2003 was extraordinary dry, the installation of both sections of a total area to be stabilized of 31′400 m^2 took only about three and a half months.

As a base for the determination of the required nail length as well as to guarantee the quality of the fully mortared nails, numerous pulling tests were carried out. Pictures 11.22, 11.23 and 11.24 show different views of installation locations and steps.

To guarantee a full force transmission from one steel wire mesh panel to the neighbour one, special compression claws (picture 11.27) were used in accordance to the system instructions.

To avoid any further erosion, a hydroseeding adapted to the local condition needed to be applied as well. Thereby, the consideration of the regional micro climate was a very important factor for the selection of the seed to be applied. A part of the stabilized slope is shown on picture 11.25.

Picture 11.22 South-eastern slope: drilling work

Picture 11.23 Drilling work using mobile cranes

Picture 11.24 North-western slope

Picture 11.25 Stabilized slope

The slope stabilization system with high-tensile steel wire mesh could be adapted to the site specific and static conditions in an optimal manner. It offers the possibility to arrange the nails in an economical way due to the capability of absorbing and transferring of high loads. Unlike stabilization with concrete solutions, with TECCO® stabilized slopes regain a natural green appearance, which is well appreciated and more pleasant to the eye.

Picture 11.26 Pulling tests

Picture 11.27 Connection of mesh panels

Designed to be maintenance free, the slope will further grow into the surrounding landscape and contribute to a safe and economical operation of the highway. Numerous applications have proven that the fully designable TECCO® system can ideally combine slope stabilization with revegetation measures tailored to the actual climatic and environmental conditions.

Based on the analyses of wedge-shaped failure mechanism as well as on the RUVOLUM® method, the high-tensile steel wire mesh system could be properly dimensioned against superficial instabilities.

The following pictures 11.28 and 11.29 show the completed slope stabilization several months after the installation. First results of the hydro-seeding can already be seen on the slopes.

Picture 11.28 State of the stabilized slope several months after installation

Picture 11.29 State of the stabilized north-western slope several months after installation

11.6 Project built at Grodziec Śląski, Poland

Several deep cuts were executed along the expressway S1 from Bielsko-Biała to the Polish border with Czech Republic in Cieszyn. One of those cuts was characterized by flysh and clay soils prone to weathering and environmental exposure. According to the local water and soil conditions, slope stabilization investigations and analysis were carried out and solutions for global and surface stability were engineered.

Due to heavy and continuous rainfalls in autumn 2006, after the excavation and before the beginning of the stabilization work, approximately one third of the slope surface failed and collapsed up to 3–4 meters deep. Moreover, in several locations on the slope surface, shallow slides were observed. After that, new design had to be prepared and submitted. This new concept included removement of down-slided soil material, fill-up of corresponding surface gaps and decreasing of inclination of the slope from 34 to 26 degrees. Finally, for the new slope stabilization, nailing and high-tensile steel wire meshing was determined. Accordingly, self-drilling soil nails (Titan 30/11) and the TECCO® system were applied.

Project information

Name of project	Express Road S-1, Grodziec Śląski/Poland
Slope height (in line of slope):	max. 22 m
Geology:	Flysch, clays
Slope angle:	1:2
Slope exposition:	North and South
Protected area:	approximately 8′600 m^2
Measure type:	Soil nailing together with flexible face cover made out of high-tensile steel wire mesh
Investor:	National Roads Dept., Division Katowice
General Contractor:	SKANSKA S.A.
Nailing contractor:	Soley Spółka z o.o.
Installation:	2007
Measure type:	TECCO® System
Mesh:	TECCO® G65/3 mm
Spike plates:	TECCO® System Spike Plates
Pretensioning force:	V = 30 kN
Nails:	TITAN 30/11
Nails length:	L = 4, 6, 7, 8 m
Nails pattern:	$a \cdot b$ = 2.5 m · 2.5 m

Pictures 11.30 and 11.31 show the self drilling processes on the slope and picture 11.32 presents the installation of the high-tensile steel wire mesh.

Picture 11.30 Drilling process from with access from the top of the slope

Picture 11.31 Slope under nailing works. Partially covered with crushed stones due to local failures of the slope surface

Picture 11.32 Installation of the high-tensile steel wire mesh

On picture 11.33, the nail head area and the spike plates with the corresponding local dells for pretensioning are illustrated.

Picture 11.33 System spike plates allow active pretensioning (system fully installed)

The following pictures 11.34 and 11.35 show the express road with the slope stabilization system. After several weeks, first results of greening can already be seen.

Picture 11.34 Slopes after completion. Slope partially covered with crushed stones, no greening was applied and no erosion mat was used

Picture 11.35 Completed slope after completion of Express Road works

11.7 Project Laliki, Poland

In the south of Poland at the express road S69 near Laliki, approximately 3′500 m^2 of slope is protected with combination of nailing and high-tensile steel wire mesh surface cover. During planning the slope, at the very beginning of this project, the slope was somehow assumed to be a self-stable hard sandstone rockface. However, the following excavation and ground works asserted flysh as main slope material.

The excavation works were partly done using explosives (picture 11.36) and this seems to be the main reason why the face of the slope was partially heavy structured and fractured. Since it is often not simple to conduct geotechnical investigations and determine parameters for flysh, so called Rock Lab analysis (figure 11.10) was conducted in order to obtain the geotechnical parameters demanded for slope stabilization calculations. In a first concept, the entire area of approximately 7′000 m^2 was considered to be stabilized.

Due to costs optimization, the project was changed from one angled plane (34°) to two angled slope (45° in lower part and 26° in upper part of slope). The lower part acts as ground retaining structure secured with nails and mesh. Both upper and lower part are drained and revegetated.

Project information

Project name:	Express Road S69, Laliki, Poland
Slope height:	max. 6.0 m in nailed part, up to 15 m above the berm
Geology:	Flysch, clays, sandstone
Slope angle:	45° (1:1) in nailed face, 26° (1:2) above the berm
Slope exposition:	South
Protected area:	approximately 3′500 m^2
Measure type:	Soil nailing together with flexible face cover made out of TECCO®, cocomat, hydro-seeding
General Designer:	Transprojekt – Krakowskie Biuro Projektów Dróg i Mostów Sp. z o.o
General Contractor:	BOGL& KRYSL Polska Spółka z o.o.
Nailing:	Soley Spółka z o.o./PPI Gerhard Chrobok Sp.j.
Meshing and greening:	AKG Architektura Krajobrazu Sp. o.o.
Installation:	March–May 2009
Mesh:	TECCO® G65/3 mm
Spike plates:	System spike plates (TECCO®)
Pretensioning force:	V = 30 kN
Nails:	TITAN 40/16, L = 3–4.5 m
	TITAN 30/11 L = 3, 6–9 m
Nail pattern:	$a \cdot b$ = 1.5 m · 1.5 m
Cocomat type:	GREENFIX Eromat typ 6S

The following charts show some results of the investigations that was done with Rock Lab in order to obtain the relevant parameters of the flysh soil material.

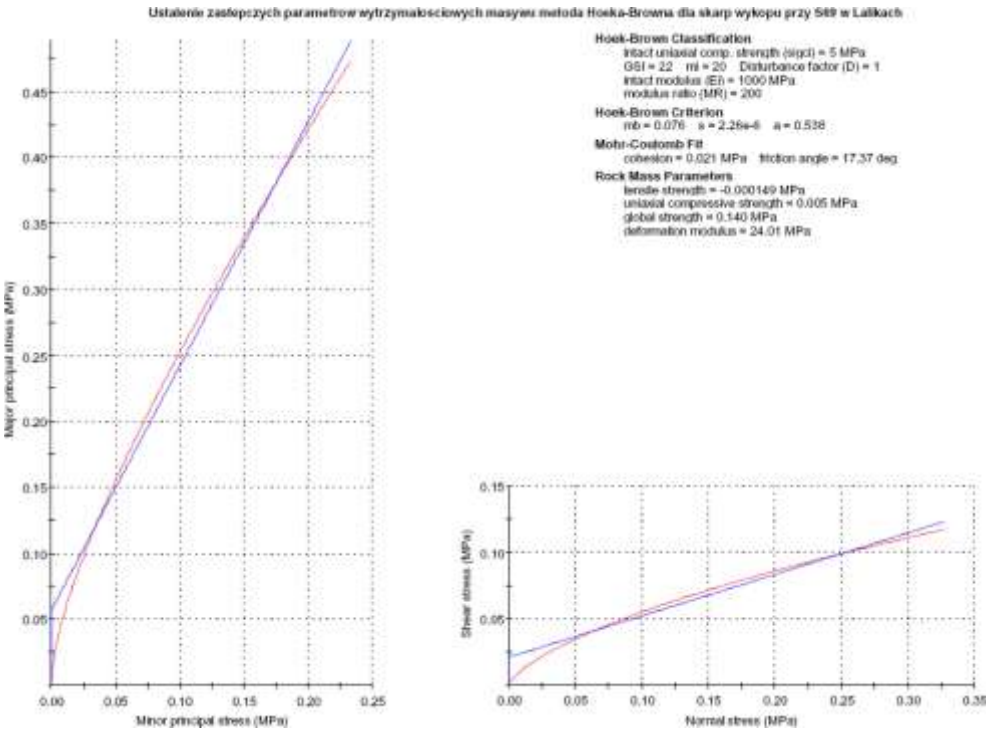

Figure 11.10 Rock Lab investigation for flysh geotechnical parameters

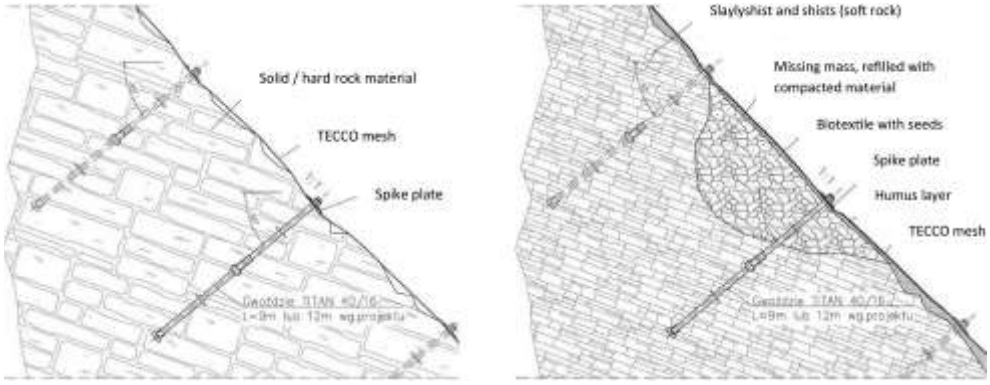

Figure 11.11 Cross section of flysh slope protected with nails and TECCO® system

The following picture 11.37 provides an overview of the reprofile slope surface including the self drilling nail heads (before installation of mat and mesh).

Picture 11.36 Rough slope after cutting; the drainage system is visible at the upper part of the slope over the bench

Picture 11.37 Reprofiled and nailed slope face

Picture 11.38 shows a view of the slope during the installation. Most cocomat cover is already installed whereas the high-tensile steel wire meshes are only partially unrolled on the surface. Picture 11.39 shows a slope three months after completion of installation work.

Picture 11.38 Slope covered with cocomat during high-tensile steel wire mesh installation

Picture 11.39 Picture of the slope three month after completion of installation work

11.8 Selection and samples of further TECCO® projects

The following pictures shall give a wider overview of TECCO® system installation and global application in different slope conditions.

Picture 11.40 TECCO® system installed at Brot-Dessous, Rochefort, Switzerland

Picture 11.41 TECCO® system installed at Brot-Dessous, Rochefort, Switzerland

Picture 11.42 TECCO® system installed at Dodoni, Greece

Picture 11.43 TECCO® system installation at Polymilou, Greece (under construction)

Picture 11.44 TECCO® system installation at Santa Barbara, USA (under construction)

Picture 11.45 TECCO® system installed at La Luz, Santiago de Chile

Picture 11.46 TECCO® system installed at Dandong Highway, China

Picture 11.47 TECCO® system installed at Gifu Prefecture, Japan

Picture 11.48 TECCO® system installed at Railway in Czech Republic

Picture 11.49 TECCO® system installed for railway protection at Kyle, UK

Picture 11.50 TECCO® system installed at Tunnel do Morro Agudo, Brazil

Picture 11.51 TECCO® system installed at Tunnel do Morro Agudo, Brazil

Picture 11.52 TECCO® slope stabilization at Carajas in Brazil (for VALE)

Picture 11.53 TECCO® system installation at Cavalcanti, Rio de Janeiro, Brazil

Picture 11.54 TECCO® system installed at Barbados Wood, Tintern, UK

Picture 11.55 TECCO® installation at open pit mine in Western Australia

Picture 11.56 TECCO® installation at Mount Tambourine, Australia

Picture 11.57 TECCO® installation at Puntilla Hydro Power Plant, Chile

Picture 11.58 TECCO® installation at Xativa, Spain

Picture 11.59 TECCO® installation at Monte Rosa Cali, Colombia

Picture 11.60 TECCO® installed at the Panama Channel, Panama

Picture 11.61 TECCO® installation in Malaysia

Picture 11.62 TECCO® slope stabilizations incl. greening for SAMSUNG in Korea

Picture 11.63 TECCO® slope stabilization at Neilston, UK, Railway cutting near Glasgow (left during installation; right several months after completion of installation)

Picture 11.64 TECCO® slope stabilization USA
(left during installation; right several months after completion of installation)

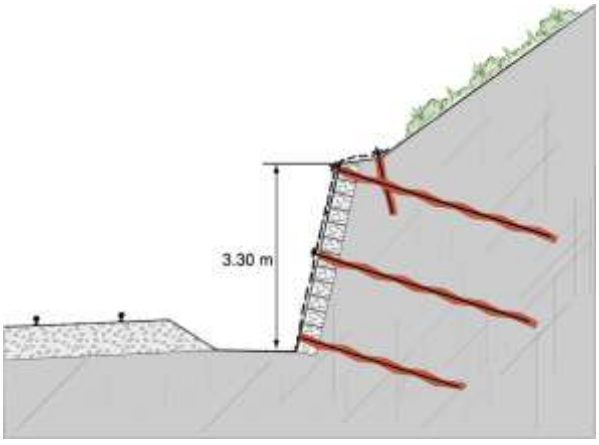

Figure 11.12 Stabilizing of an old unstable stone block wall along a railway line with high frequency, Kreuztal, Germany (see also following pictures 11.65 and 11.66)

Picture 11.65 Old, partly broken brick wall at railway line

Picture 11.66 Stabilized brick wall (covered and nailed with TECCO® mesh)

Picture 11.67 TECCO® stabilization of brick walls at Markgröningen, Germany

Picture 11.68 Special TECCO® application at Alptransit exhibition centre, Bodio, Switzerland

Picture 11.69 Slope stabilizations in Sendai area (close to Fukushima, Japan) after the heavy earthquakes in March 2011. Left pictures show a failed concrete slope stabilization due to earthquake influences. Right pictures show a TECCO® slope stabilization that resisted all earthquake influences perfectly without any damages.

12 Outlook and recommendation for further research – status 2020

By means of the presented dimensioning models it is now possible in principle to dimension so-called “flexible” surface protection systems in combination with nailing. Corresponding proofs of safety can be submitted for such systems provided that the necessary input quantities are known or have been established by suitably adapted tests for a specific system.

It is in the nature of the dimensioning models that they include substantial simplifications which can simulate reality to a limited degree only. Uncertainties are to some extent covered by appropriate safety factors.

A future task is to check these dimensioning models and the forces calculated with their aid in appropriate large field tests and to make adaptations and/or fine tunings where necessary.

Scale 1 : 1 trials are suggested for this purpose on a test slope with the installation of an artificial cover layer to be stabilized. In the large-scale test it will then be possible to measure both deformations and effective forces acting on the system, and to compare these with the calculated values. Additionally, detailed and advanced geotechnical numerical simulations and calculations may support corresponding analysis.

These endeavours to establish the forces and to define adequate proofs of safety are intended to make the presented technique a recognized construction process which satisfies the usual requirements as regards the safety and “fitness-for-use” of a long-term construction with permanent support and stabilization functions.

This will eventually permit to replace many elaborate conventional support and stabilization measures consisting of solid and visible constructions in a manner which is gentle on the landscape and the environment.

Since the TECCO® systems with high-tensile steel wire meshes is containing substantial safety factors, even more economic and cost-effective solutions may be achieved accordingly in the future.

Other than that, further research regarding design and application of the new dimensioning concept for flexible slope stabilization systems should be made concerning application for rock slopes since meshes and nets from high-tensile steel wires will also provide new potential for economical rock slope stabilizations.

Last but not least, new geotechnical numerical modelling in 2D and 3D will certainly support analysis of the interaction between mesh, nails and soil/rock. Consequently, such new numerical simulations will help with the design process of flexible slope stabilization systems and should be studied more detailed in the future.

After 2012 the large-scale field tests have been performed and are described in chapter 13.

In chapter 14 the significance and advantage of EAD and CE marking of geohazards products in general and specific for slope stabilization is explained.

13 Large-scale field tests

Goals

The overarching goal for the execution of large-scale field tests was to analyse and better understand the load bearing capacity of this type of slope stabilization system under different limiting conditions and under conditions which are as real as possible. This was done with view to the optimal application of such systems in practice. Only instabilities close to the surface with a maximum thickness of 1.20 m were examined in this research project. The overall stability and thereby the dimensioning of the nail anchoring system to prevent fracture mechanisms with low-lying sliding surfaces will not be discussed.

Testing equipment

The testing equipment consists of a 13 x 15 m steel frame which can be filled with soil material through a 10 x 12 m surface up to a layer thickness of 1.20 m (picture 13.1). The incline of the frame can vary between 0° and 85° by lifting it with a 500 to crane (pictures 13.2-13.4). The base and side areas of the test area are covered flat with rough wooden planks. To ensure that the sliding surfaces of instabilities close to the surface form within the filling material and do not follow the board floor, wooden slats with a cross sectional area of 30 x 60 mm were applied to increase roughness in the transverse direction. The mesh cover was sewn to upper and lower edge ropes. Depending on the safety system, they exhibit a diameter of 14 - 22 mm and are braced against laterally positioned bollards. To create a cut-out from an infinitely long slope which is as realistic as possible, the mesh cover was screwed to the side of the frame using U-profiles. This created a bedding which was immovable in the lateral direction. GEWI D = 28 mm or D = 32 mm with solidified cladding tubes were used as nails. The connection to the framework construction was made with a base plate welded to the nail which was itself screwed onto another steel plate. The cladding tube was led into a steel tube fastened to the base plate. The nail is considered bend-proof in its connection to the frame. Conventional solidification of the nail was not possible due to reasons concerning the installation and time frame.

Spike plates adjusted to the mesh were used to fasten it. The upper support cable was not held up with nails; instead, it was fastened against bollards using fixing ropes. The lateral distance between the bollards corresponded to the respective horizontal distance between the nails. The mesh webs exhibited widths of 2.0 to 3.5 m and were connected to one another in a force-locking manner via system-specific connectors. To prevent the non-compacted gravel from falling out between the mesh, a mesh with an opening width of 20 x 20 mm with low-tensile strength and no static function was laid out under the mesh cover starting with the 4th test.

Picture 13.1 Test no. 13, TECCO® G65/4 + P33, after dismantling mesh cover and removing material, nail grid 3.5 x 3.5 m

Picture 13.2 Total overview of testing equipment

Measurement equipment

The surface including nail heads and steel frames were scanned flat using laser scans to serve as a reference level (picture 13.5). White cones set on the nails and various mirrors served as orientation aids and reference points. The scan was repeated after changing the incline by 5° each time. Picture 13.3 shows a cross-fade of individual scans. A pendulum and an automatic inclinometer are used to determine the inclination of the steel frame.

The displacements of the top middle nail were measured via a rope potentiometer to verify the scan data and monitor the deformation during the test. In addition, the forces in the upper and lower support wire ropes were determined using load cells specially adapted to the conditions.

Information on developments in selected nails during changing conditions was gathered using strain gauges. Analysing this would go beyond the scope of this book.

Test results

The large-scale field tests also show the positive influence of the installation of the spike plates in previously-created recesses. Creating troughs makes it possible to actively stretch the mesh during installation. This significantly reduces deformations when lifting the steel frame, which makes a significant effect on the load bearing capacity of the entire system (picture 13.4).

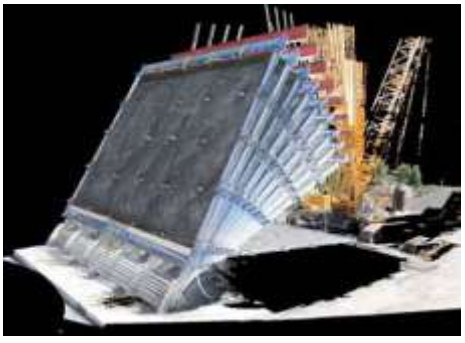

Picture 13.3 Test no. 4, TEECO® G65/3 + P33, cross-fade of individual scans

Picture 13.4 Test no. 5, TECCO® G65/3 + P33 = 85° sandy gravel 0 – 63 mm

Verification of RUVOLUM® dimensioning concept

The RUVOLUM® dimensioning concept was developed on the basis of many years of experience in the area of flexible slope stabilization systems and was verified in 2008 using only model tests. The large-scale field tests performed in the scope of the CTI research project make it possible for the first time to examine the theoretical model approach and the underlying assumptions under realistic conditions and using repeatable tests. The graphic analysis of the laser scan shows good agreement with the model approach in accordance with the RUVOLUM® concept. Comparative calculations were performed. The results of the back-calculation correlate quite well with the situation in which the first instabilities close to the surface were observed. If all partial safety factors are set to 1.00 and if the nail inclination is assumed to be perpendicular to the slope surface as before, the break is calculated to occur and matches very well with the test results.

Conclusions from the large-scale field tests

The large-scale field tests performed create an ideal foundation for a better understanding of the load bearing capacity of flexible slope stabilization systems as well as for further developing them and adapting them to project-specific requirements.

The size of the test frame seems to have been well-selected for simulating instabilities near the surface. In supplementary tests, additional results on impacts to the nails and especially in the nail head area will be gathered. It was possible to verify the RUVOLUM® dimensioning concept.

The results agree well with the test results and the experience gathered over the last 15 years. They are based on a model approach which illustrates the real conditions in a simplified but sufficiently exact manner.

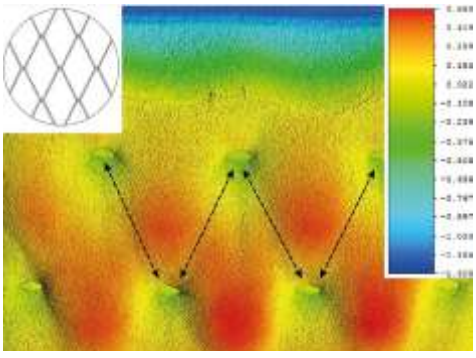

Figure 13.1 Test no. 14, TECCO® G65/3 + P66, nail grid 3.5 x 3.5 m, round gravel 16 – 32 mm, α = 60°

Picture 13.5 Test no.11, TECCO® G65/3 + P33, nail grid 3.5 x 3.5 m, sandy gravel 0 – 63 mm, α = 53°, first slides close to the surface

14 CE Marking

Significance and Advantage of EAD and CE Marking of Geohazard Products

In a globalized world the standardization of products is essential to make sure that they perform as expected. The basis of their performance can either be that the product solves a described problem or performs in a specific way. This article describes how standardisation in the European Union helps to achieve a certain quality standard and what users must be aware of to compare different products.

Why CE marking and what does this mean?

Existing in its present form since 1985, the CE Marking has the symbol CE. The letters "CE" are the abbreviation of French phrase "Conformité Européene" which literally means "European Conformity". CE marking is a certification mark that indicates conformity with health, safety and environmental protection standards for products sold within the **E**uropean **E**conomic **A**rea (**EEA**). The CE marking is the manufacturer's declaration that the product meets the requirements of the applicable EC directives. The added value of CE marking is that all EU countries must allow the selling of construction products bearing the CE mark. This means that public authorities cannot ask for any additional marks or certificates or any additional testing. It is however important to know the basics of a CE marking.

Responsibility for CE marking

The responsibility for the CE marking lies with whoever puts the product on the market in the EU, i.e. an EU-based manufacturer, the importer or distributor of a product made outside the EU, or an EU-based office of a non-EU manufacturer.

CE marking for construction products and how to get it

Under the wing of the EUROPEAN COMISSION the EUROPEAN COMITEE FOR STANDARDI-ZATION takes care of all European Standards and supports the EU Legislation.

The **C**ONSTRUCTION **P**RODUCT **R**EGULATION No. 305/2011 (**CPR**) of the European Parliament and of the European Council is a regulation of 9 March 2011 that lays down harmonized conditions for the marketing of construction products. The EU regulation is designed to simplify and clarify the existing framework for the placing on the market of construction products. The CPR helps authorities and consumers to receive high quality and safe products and to be able to compare different products.

By testing the products either to a HARMONIZED EUROPEAN STANDARD or a EUROPEAN ASSESSMENT DOCUMENT (EAD) it is made sure that the basis for comparing product performance is the same. The test results display all relevant parameters in a detailed manner. Customers can ask the producers to provide them with the details to enable comparison of products and their performance.

If no harmonized standard exists for a specific product, then a **E**uropean **A**ssessment **D**ocument (**EAD**) can be written. This is the documentation of the methods and criteria accepted in the **E**uropean **O**rganisation for **T**echnical **A**ssessment (**EOTA**) as being applicable for the assessment of the performance of a construction product in relation to its essential characteristics.

Based on an EAD the **T**echnical **A**ssessment **B**ody **(TAB)** is performing the tests on the product and issues an **E**uropean **T**echnical **A**ssessment **(ETA)**. As soon as the European Commission approves and lists the ETA the notified Body issues the CE-Marking. Finally, the **D**eclaration **O**f **P**erformance (**DoP)** must be drawn up by the manufacturer, who then assumes responsibility for the conformity of the product with the declared performance. It is a key part of the Construction Products Regulation. It provides information on the performance of a product.

Natural hazard prevention: The new standardisation for rockfall, debris flow, shallow landslides and slope stabilisation

In the field of geohazard products one can find the following three main EAD which cover different special applications:

- EAD 230025-00-0106 “Flexible facing systems for slope stabilization and rock protection”
- EAD-340020-00-0106 “Flexible kits for retaining debris flows and shallow landslides/open hill debris flows”
- EAD-340059-00-0106 “Falling rock protection kits

All available EADs can be found officially on the website of EOTA:
http://eota.eu/en-GB/content/eads/56/

What are the details of an EAD?

Using the EAD "Flexible facing systems for slope stabilization and rock protection" as an example. In this EAD several tests are described for flexible facing which have been used worldwide for decades. They are available in two different qualities, mild steel wire and high-tensile steel wire. For both qualities of steel in combination with soil nailing / rock bolting there exist three key characteristics for the products.

1. Puncturing at the nail head plate (shearing-off resistance at the upslope edge of the spike plate)
2. Slope parallel load transfer into the nail with interaction of the soil (tensile strength)
3. Deformation / elongation of the mesh under load in percent

The tables below show the groups and classes to categorize the performance of the flexible facings.

Table 2 – Informative: groups of meshes/nets regarding tensile strength and shearing-off resistance

Group	Shearing-off resistance P_R at the upper surface of spike plates (kN)	Slope parallel tensile strength Z_R (kN)
1	$P_R > 135$	$Z_R > 50$
2	$80 < P_R \leq 135$	$29 < Z_R \leq 50$
3	$50 < P_R \leq 80$	$19 < Z_R \leq 29$
4	$25 < P_R \leq 50$	$4 < Z_R \leq 19$
5	$0 < P_R \leq 25$	$0 < Z_R \leq 4$

Table 3 – Informative: groups of meshes/nets regarding relative elongation in longitudinal tensile strength test

Class	δ
A	≤ 6
B	6 to 10
C	10 to 14
D	> 14
$\delta = \Delta L_{mesh}/L$ ΔL_{mesh}: see Annex B	

What does this mean for users?

This means that using these tables one could clearly define in the tender documents the bearing resistances for a flexible facing which are needed for a specific project. Different products can be compared easily.

The main advantage is that based on these tables one could clearly define in the tender document the three characteristics for a flexible facing which are needed for a specific project. So different products can be compared on a unique level. Of course, the basis of the tender specifications must be the design in accordance with the expected failure scenario.

It is important to know that it is possible to get a CE-Marking without having performed all tests. For example, often only the tensile strength of a mesh has been tested but all other parameters are missing. But if these parameters are unknown, it is impossible to dimension an economic and safe solution.

To avoid failures in installations and liability risks it is important to make sure that the parameters in the DoP (Declaration of performance) or ETA are in accordance with the corresponding design of the project. So, if investors, designers and contractors want to be sure to get the right product with the expected performance the test results must be checked in detail.

15 Summary and conclusions

The TECCO® slope stabilization system with high-tensile steel wire meshes is introduced in this publication. The first chapters explain the traditional solutions using wire mesh and wire rope nets for slope stabilizations with flexible measure to protect surfaces. Also, the corresponding dimensioning concepts including sliding off parallel to the slope, local wedge-shape bodies liable to break out and required inputs quantities and proofs of the terrain's resistance against sliding (deep sliding surfaces) are presented and discussed.

High-tensile steel wire meshes and their most common uses are then introduced, especially with the focus on flexible surface stabilization systems. Due to the uniform membrane structure of high-tensile steel wire TECCO® meshes, advanced nail patterns can be applied. The structure of the mesh enables to deviate from the basic pattern within reasonable limits; local discontinuities in the slope can be counteracted in optimum manner.

A new concept of load transfer around the nail head area is provided by the method of designing of flexible slope stabilization systems with meshes made from high-tensile steel. Pretensioning is enabled by special spike plates and the high static effectiveness of the high-tensile mesh itself. This allows substantially increased and optimized load transfers from the meshes into the plates and finally into the main nails which improves the static performance of the entire system and limits its deformations. Only meshes with high-tensile steel wires can be used accordingly; normal steel wire meshes tend to deform elastically, cannot distribute such pretensioning forces and will therefore not be able to transfer the necessary loads which was illustrated with corresponding comparison tests.

The relevant material properties of high-tensile steel wire TECCO® meshes were deter-mined, tested and analysed with corresponding test infrastructures, methods and comprehensive laboratory tests. Externally supervised test series proofed the load bearing capacities of the system elements, their functioning and interactions.

Long-term field tests as well as different accelerated weathering tests were carried out in order to ensure sufficient corrosion protection levels.

The dimensioning part of the RUVOLUM® design method with TECCO® mesh consists of different necessary investigations, load cases and stability proofs. This includes investigations of superficial and local instabilities, puncturing and stability proofs as well as bearing capacities of the nails. Additionally, the load cases "earthquake" and "streaming parallel to the slope" were analysed and corresponding design methods developed and explained. Design examples provide an in-depth explanation with hand calculations of the entire dimensioning concept.

A detailed description of typical project executions and installation options explain the recommended system elements, different planning steps problem analysis, preparation, stake-out, drilling, grouting, mounting and connecting the mesh to greening, revegetation and planting aspects. Also, important advice is given for acceptance, maintenance and periodic inspections of the flexible slope stabilization system.

Environmental and carbon footprint aspects are analysed and discussed with comparisons of all the emissions which might affect climate change during the service life of different slope stabilization structures. It was shown that the TECCO® system with high-tensile steel wire mesh contributes to greenhouse effects far less than shotcrete or concrete structures.

In that sense, increased use of such slope stabilization systems would definitely help to reduce and slow down global warming.

A few international examples of executed flexible slope stabilization solutions are presented with various selected aspects of design, execution and installation in order to complete the introduction of the method of designing flexible slope stabilization system with high-tensile steel wire meshes.

Conclusions about the TECCO® system and the RUVOLUM® method of designing of flexible slope stabilizations with high-tensile steel wire meshes:

- The method provides a slope protection and stabilization system which is used to stabilize slopes of any soil and unconsolidated, rocky material on the one hand, and on the other hand to prevent stones and blocks in disintegrated, loose or weathered rockfaces from breaking out.
- This design method serves dimensioning slope stabilization systems which consist of high-tensile steel wire mesh cover in combination with nailing. The dimensioning concept also includes the investigation of superficial slope parallel instabilities as well as the investigations of local instabilities between the individual nails.
- Further, the design method provides a comparatively very low carbon footprint as well as various visual advantages in order to allow respectful, environmentally friendly and forward-looking solutions.
- In the meantime, installations and applications in more than forty different countries and on all continents demonstrate the method's global geotechnical acceptance, approval and economical effectiveness.

List of Appendices

Appendix A General overview drawing of TECCO®G45/2 System (1/3)

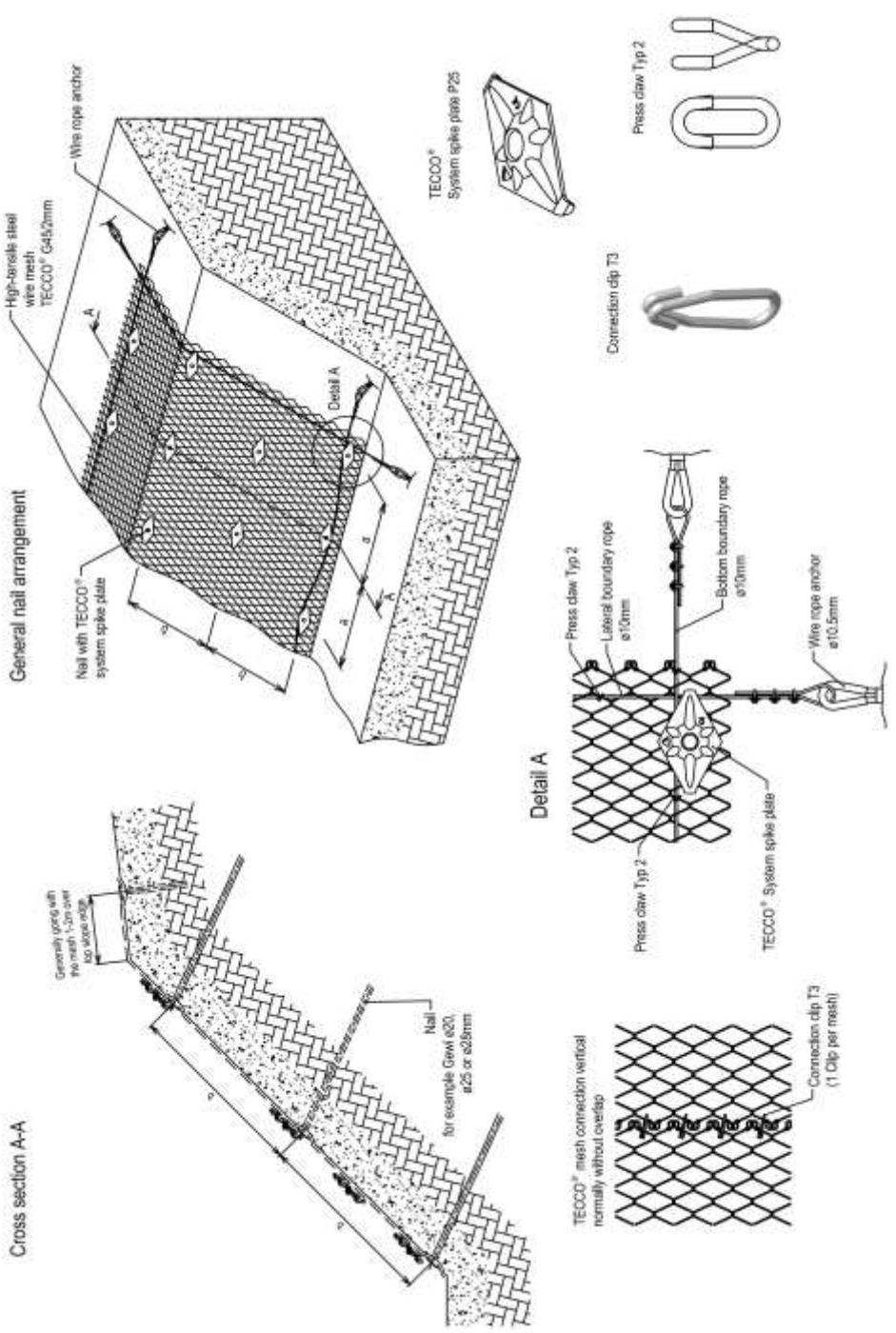

Appendix A General overview drawing of TECCO®G65/3 System (2/3)

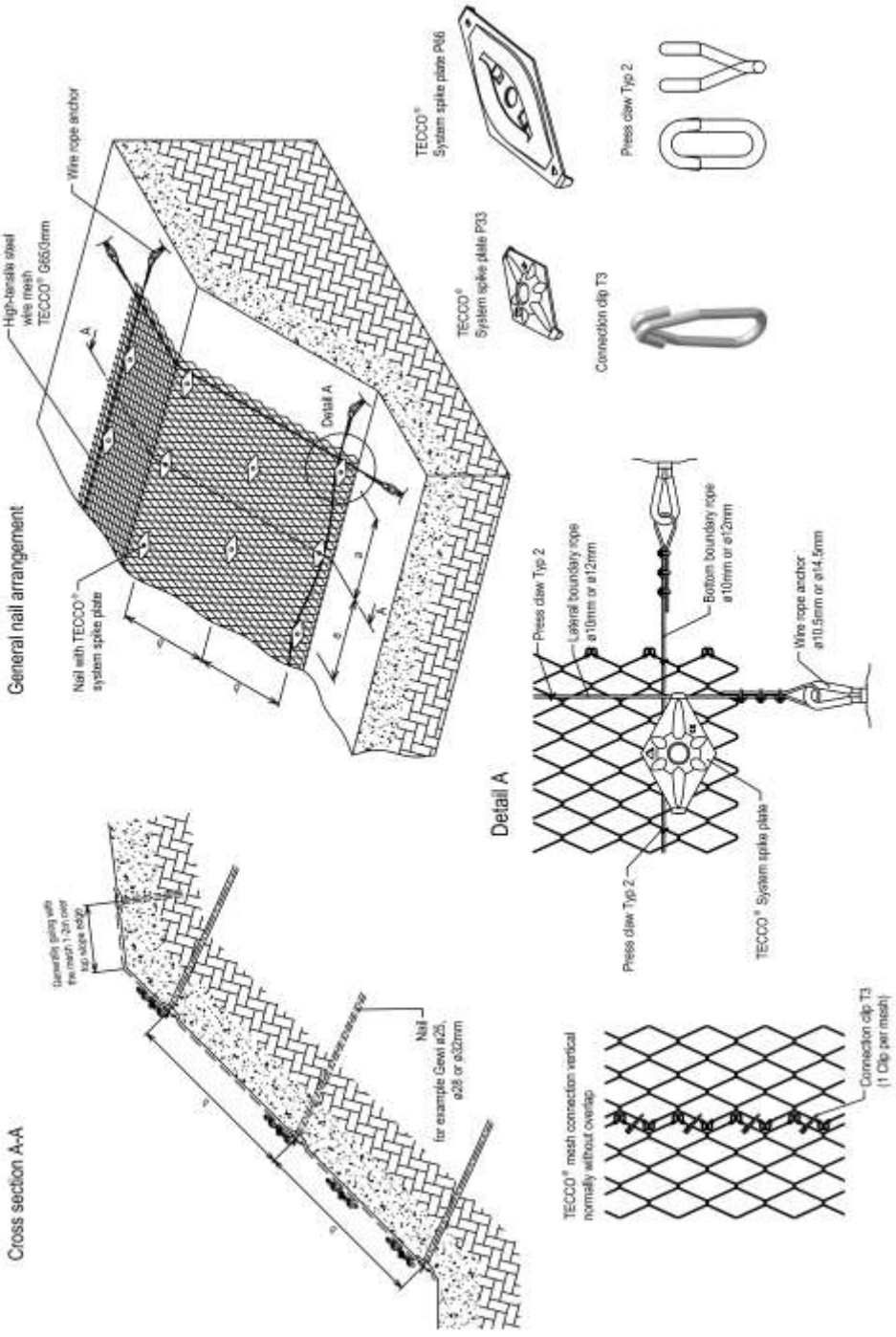

Appendix A General overview drawing of TECCO®G65/4 System (3/3)

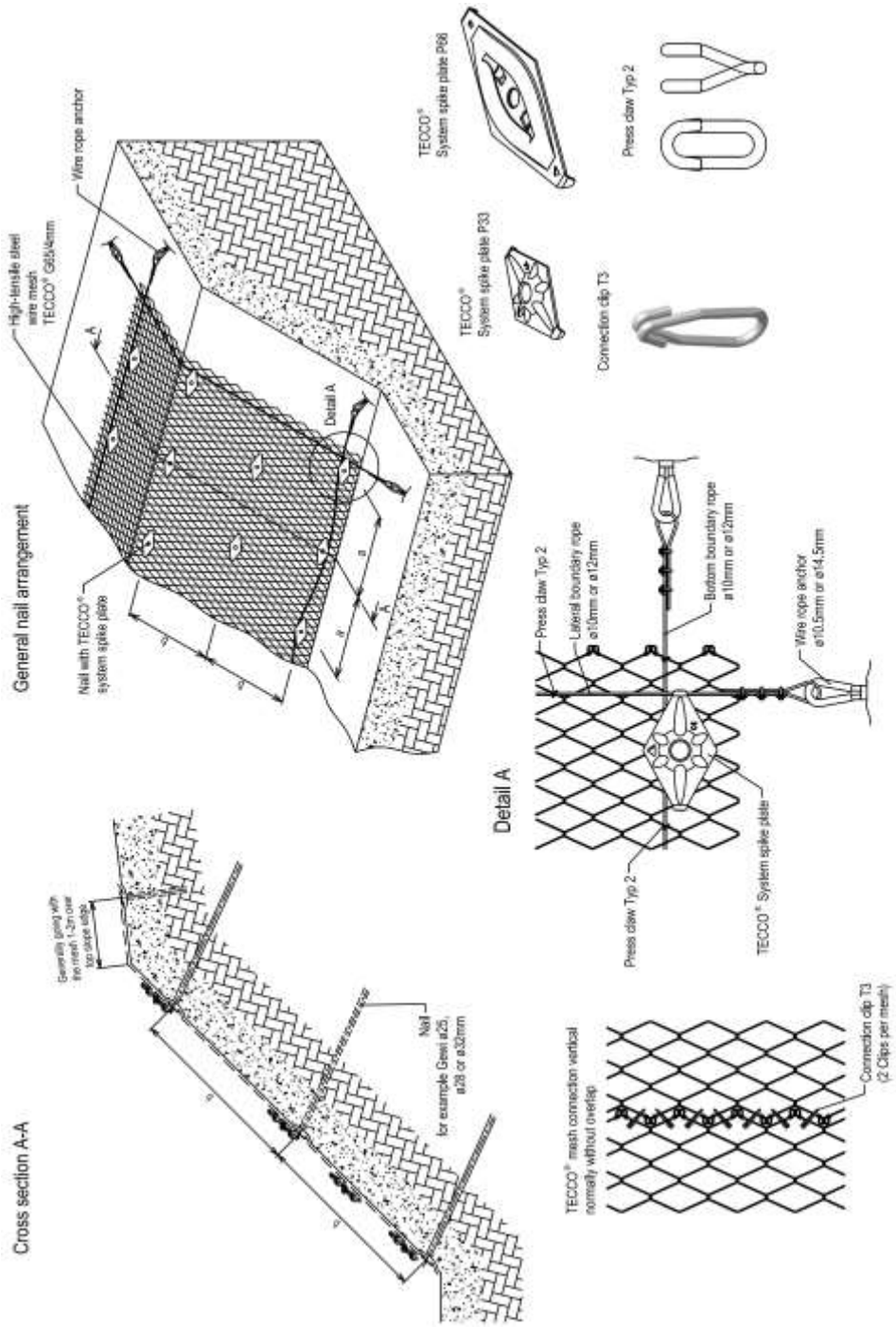

Appendix B Data sheet of high-tensile steel wire mesh (1/3)

TECHNICAL DATA SHEET

High-tensile steel wire mesh TECCO® G45/2

TECCO® high-performance steel wire mesh	
Mesh shape:	rhomboid
Diagonal:	x · y = 82 · 95 mm (+/- 3%)
Mesh width:	D_i = 48 mm (+/- 3%)
Angle of mesh:	ε = 54°
Total height of mesh:	h_{tot} = 7.0 mm (+/- 1 mm)
Clearance of mesh:	h_i = 3.0 mm (+/- 1 mm)
No. of meshes longitudinal:	n_l = 10.5 pcs/m
No. of meshes transversal:	n_q = 16.1 pcs/m

TECCO® steel wire	
Wire diameter:	d = 2.0 mm
Tensile strength:	f_i ≥ 1'770 N/mm²
Material:	high-tensile steel wire
Tensile resistance of a wire:	Z_w = 5.5 kN

TECCO® corrosion protection **)	
Corrosion protection:	GEOBRUGG SUPERCOATING®
Compound:	95% Zn / 5% Al
Coating:	min. 115 g/m²

Load capacity (standard version)	
Tensile strength of mesh:	z_k ≥ 85 kN/m'
Bearing resistance against puncturing:	D_R ≥ 80 kN / 110 kN *)
Bearing resistance against shearing-off:	P_R ≥ 40 kN / 55 kN *)
Bearing resistance against slope-parallel tensile stress:	Z_R ≥ 10 kN / 10 kN *)
Elongation in longitudinal tensile strength test:	δ < 6.0 % *)
Classification according to EAD 230025-00-0106	group 4, class A (P25 and P33)

TECCO® mesh standard roll	
Roll width:	b_{Roll} = 3.5 m
Roll length:	l_{Roll} = 30 m
Total surface per roll:	A_{Roll} = 105 m²
Weight per m²:	g = 1.15 kg/m²
Weight per mesh roll:	G_{Roll} = 121 kg
Mesh edges:	mesh ends knotted

*) As in EAD 230025-00-0106 and referring to TSUS test report 11/2016 using spike plate P25 / P33

**) Next to the standard version with Zn/Al coating, the high-tensile steel wire mesh is also available in stainless steel (INOX) in 1.4462 (AISI 318) sea water resistant quality.

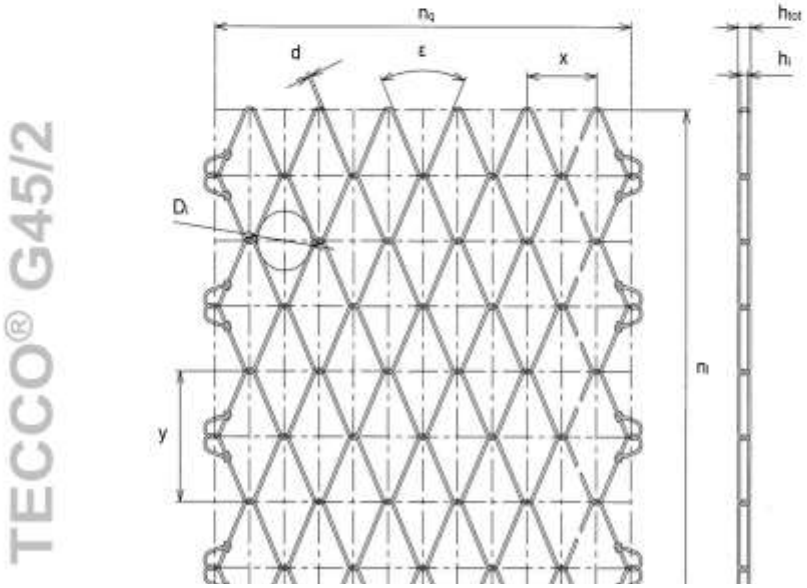

Appendix B Data sheet of high-tensile steel wire mesh (2/3)

TECHNICAL DATA SHEET

High-tensile steel wire mesh TECCO® G65/3

TECCO® high-performance steel wire mesh	
Mesh shape:	rhomboid
Diagonal:	x · y = 83 · 143 mm (+/- 3%)
Mesh width:	D_i = 65 mm (+/- 3%)
Angle of mesh:	ε = 49°
Total height of mesh:	h_{tot} = 11.0 mm (+/- 1 mm)
Clearance of mesh:	h_i = 5.0 mm (+/- 1 mm)
Number of meshes longitudinal:	n_l = 7 pcs/m
Number of meshes transversal:	n_q = 12 pcs/m

TECCO® steel wire	
Wire diameter:	d = 3.0 mm
Tensile strength:	$f_t \geq 1770$ N/mm²
Material:	high-tensile steel wire
Tensile resistance of a wire:	Z_w = 12.5 kN

TECCO® corrosion protection **)	
Corrosion protection:	GEOBRUGG SUPERCOATING®
Compound:	95% Zn / 5% Al
Coating:	min. 150 g/m²

Load capacity (standard version)	
Tensile strength of mesh:	$z_k \geq 150$ kN/m' *)
Bearing resistance against puncturing:	$D_R \geq 160$ kN / 240 kN *)
Bearing resistance against shearing-off:	$P_R \geq 90$ kN / 120 kN *)
Bearing resistance against slope-parallel tensile stress:	$Z_R \geq 30$ kN / 45 kN *)
Elongation in longitudinal tensile strength test:	$\delta < 6.0$ % *)
Classification according to EAD 230025-00-0106	group 2, class A (P33 and P66)

TECCO® mesh roll	
Roll width:	b_{Roll} = 3.9 m
Roll length:	l_{Roll} = 30 m
Total surface per roll:	A_{Roll} = 117 m²
Weight per m²:	g = 1.65 kg/m²
Weight per mesh roll:	G_{Roll} = 193 kg
Mesh edges:	mesh ends knotted

*) As in EAD 230025-00-0106 and referring to TÜV Rheinland LGA test report 01/2014 using spike plate P33 / P66

**) Next to the standard version with Zn/Al coating, the high-tensile steel wire mesh is also available in stainless steel (INOX) in 1.4462 (AISI 318) sea water resistant quality.

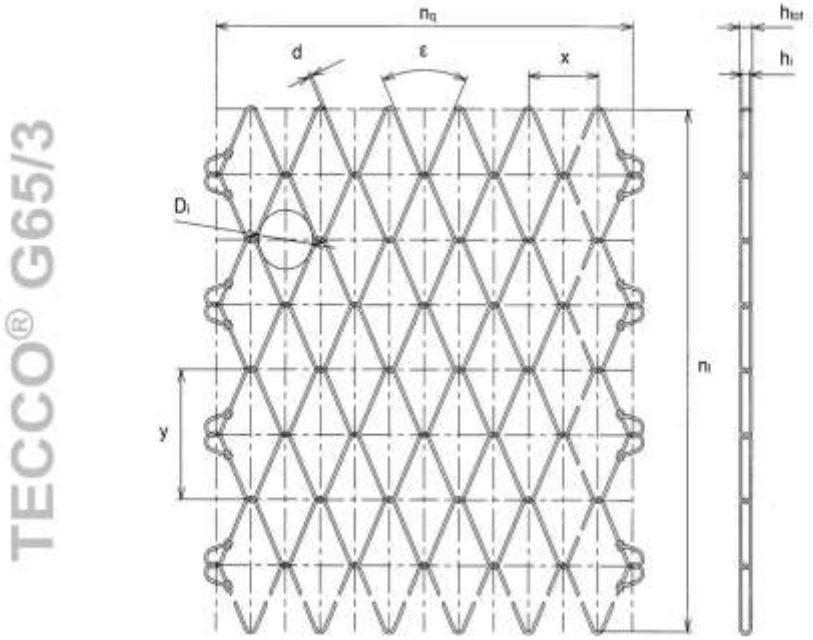

Appendix B Data sheet of high-tensile steel wire mesh (3/3)

TECHNICAL DATA SHEET

High-tensile steel wire mesh TECCO® G65/4

TECCO® high-performance steel wire mesh	
Mesh shape:	rhomboid
Diagonal:	x · y = 83 · 138 mm (+/-3%)
Mesh width:	D_i = 63 mm (+/-3%)
Angle of mesh:	ε = 49°
Total height of mesh:	h_{tot} = 15 mm (+/-1 mm)
Clearance of mesh:	h_i = 7 mm (+/-1 mm)
No. of meshes longitudinal:	n_l = 7.2 pcs/m
No. of meshes transversal:	n_q = 12.0 pcs/m

TECCO® steel wire	
Wire diameter:	d = 4.0 mm
Tensile strength:	f_t ≥ 1770 N/mm²
Material:	high-tensile steel wire
Tensile resistance of a wire:	Z_w = 22 kN

TECCO® corrosion protection	
Corrosion protection:	GEOBRUGG SUPERCOATING®
Compound:	95% Zn / 5% Al
Coating:	min. 150 g/m²

Load capacity	
Tensile strength of mesh:	z_k ≥ 260 kN/m' *)
Bearing resistance against puncturing:	D_N ≥ 280 kN / 370 kN *)
Bearing resistance against shearing-off:	P_K ≥ 140 kN / 185 kN *)
Bearing resistance against slope-parallel tensile stress:	Z_R ≥ 50 kN / 75 kN *)
Elongation in longitudinal tensile strength test:	δ < 6.0 % *)
Classification according to EAD 230025-00-0106	group 1, class A (P33 and P66)

TECCO® mesh-standard roll	
Roll width:	b_{Roll} = 3.5 m
Roll length:	l_{Roll} = 20 m
Total surface per roll:	A_{Roll} = 70 m²
Weight per m²:	g = 3.3 kg/m²
Weight per mesh roll:	G_{Roll} = 231 kg
Mesh edges:	mesh ends knotted

*) As in EAD 230025-00-0106 and referring to TÜV Rheinland LGA test report 01/2014 using spike plate P33 / P66

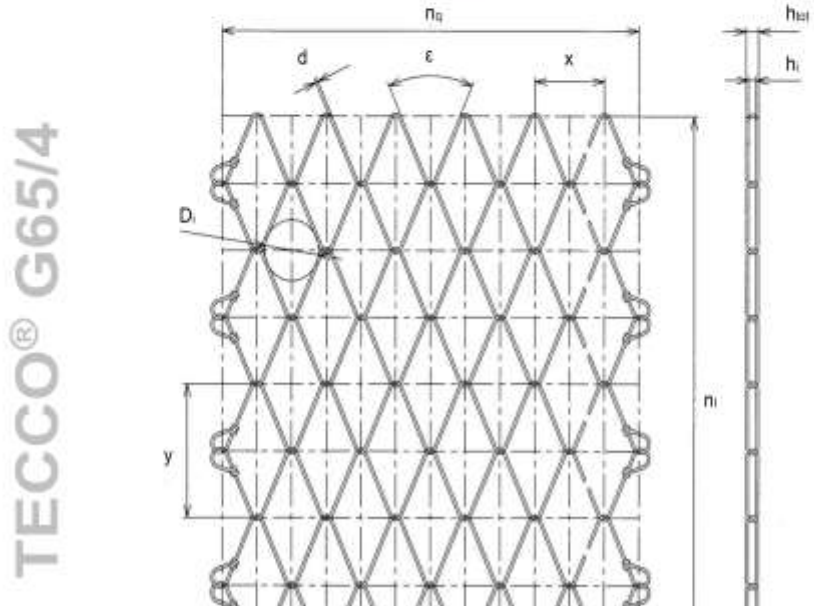

Appendix C Principle drawing of TECCO® spikeplate P25 (1/3)

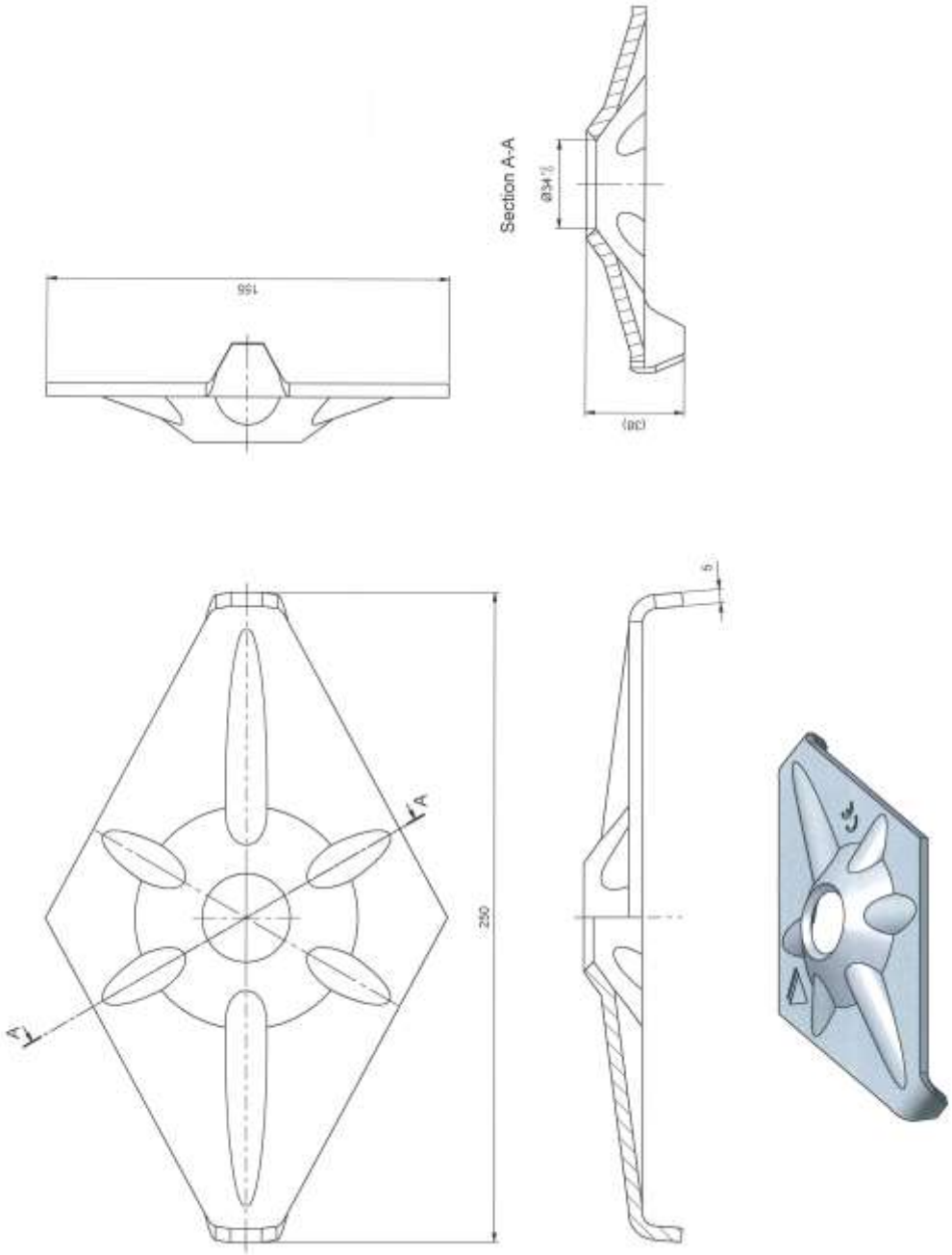

Appendix C Principle drawing of TECCO® spike plate P33 (2/3)

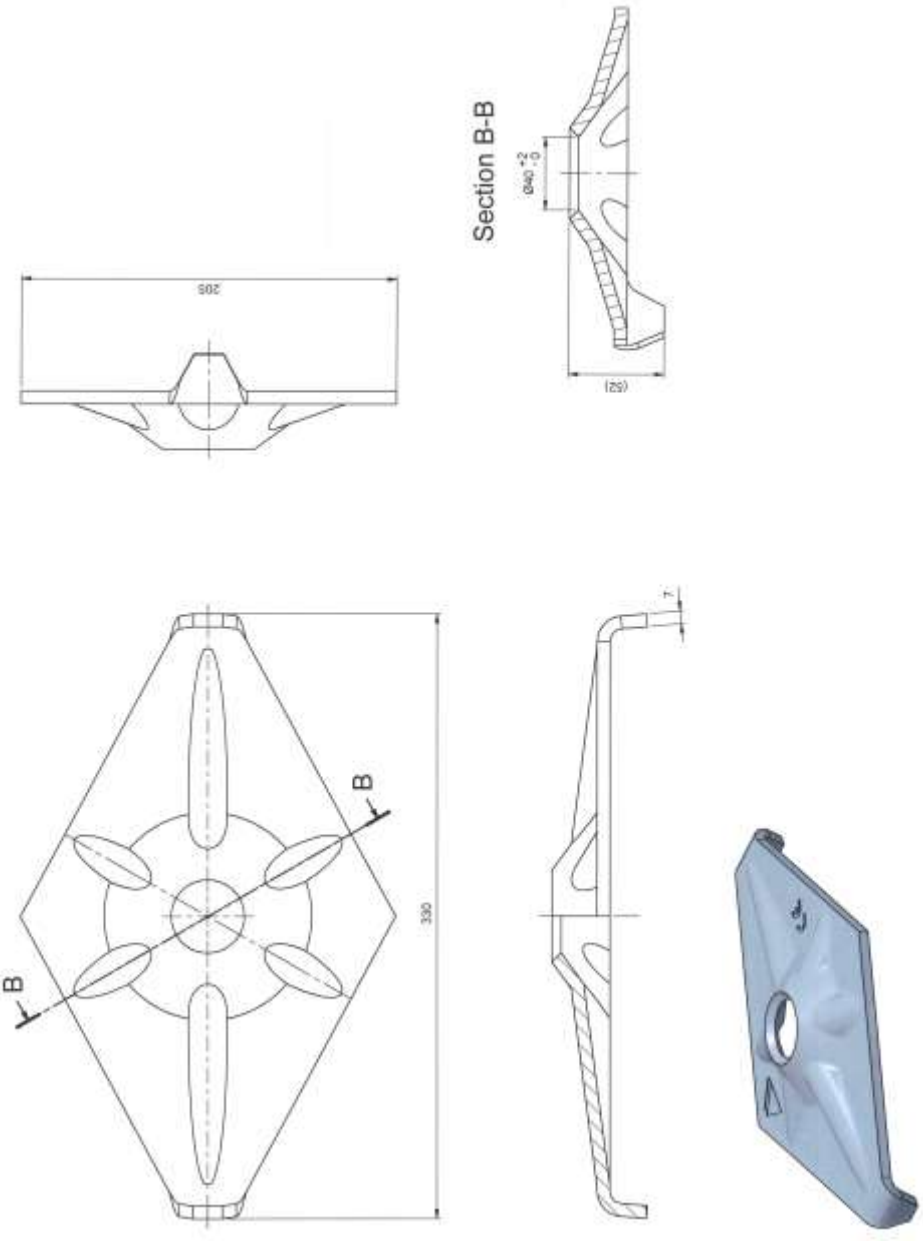

Appendix C Principle drawing of TECCO® spikeplate P66 (3/3)

Appendix D Principle drawing of connection clip

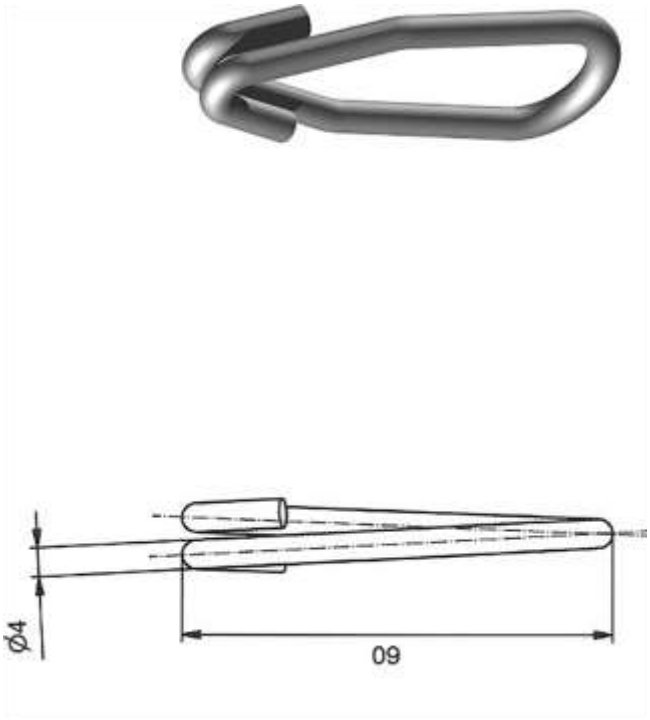

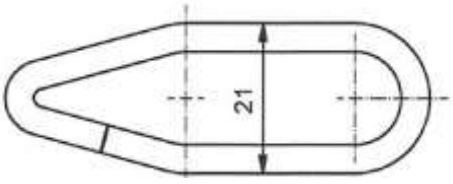

Appendix E Example for high-tensile steel wire test series

Since the beginning of production of high-tensile steel wire meshes, raw material control of steel wire was and still is always of great importance. All production companies are carrying out random tests to check their provided technical information.

For example, BAREMO GmbH (Romanshorn, Switzerland) is one of the independent companies for material testing. This company is testing the wire samples in accordance to standard DIN 51210 to verify the technical information provided by the steel wire supplier. Thereby, the following tests are being carried out:

- Tensile tests at an individual steel wire (determination of the breaking load)
- Bending tests
- Torsion tests
- Determination of the corrosion protection coating thickness

To analyse the probabilistic distribution of the tensile strength of the high-tensile steel wire, the provided data by the steel suppliers is evaluated and summarized. In order to give an overview of this procedure, a sample of a French supplier of wires is illustrated as follows:

- Number of considered coils: $n = 139$
- Average value of the yield strength (under tensile load) $f_y = 1860.6$ N/mm^2
- Minimum value of the yield strength (under tensile load) $f_{y,\min} = 1783.0$ N/mm^2
- Maximum value of the yield strength (under tensile load) $f_{y,\max} = 1920.0$ N/mm^2
- Standard deviation $s = 25.33$ N/mm^2

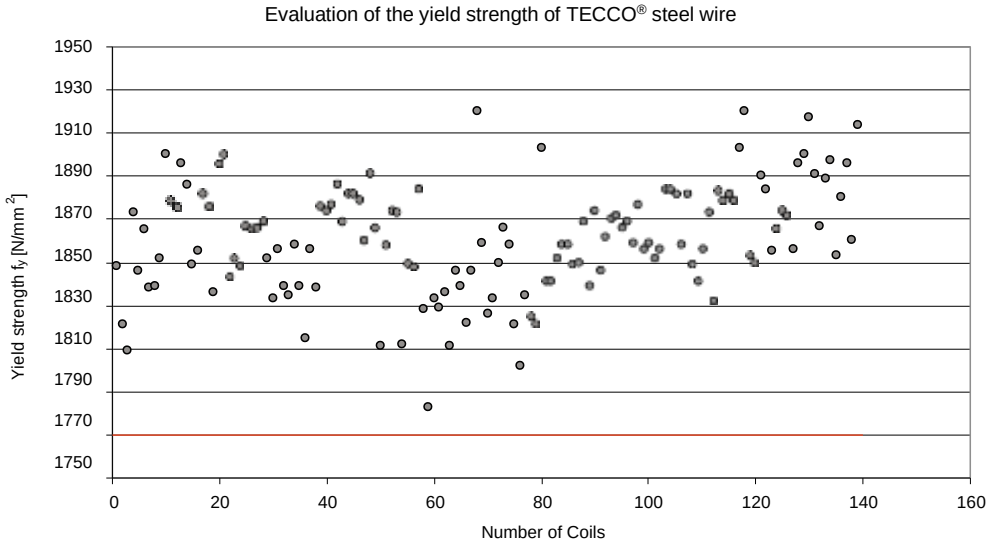

Figure E.1 Probabilistic evaluation of the tensile strength of supplied coils of high-tensile steel wire (used for TECCO® mesh)

Appendix F Model tests regarding bearing resistances

Based on the RUVOLUM® method, flexible slope stabilization system such as the TECCO® system, can be dimensioned against superficial instabilities. Next to slope-parallel failure mechanisms, local instabilities between the single nails are investigated.

Based on practical experiences as well as experiences during model tests (figure F.1), it is generally assumed that if a certain mass would slide down, tensile forces in the mesh occur as a result of friction or interaction, respectively, between the subsoil and the mesh. Above of the considered sliding mechanism, the wire mesh is fixed at the nail head with a TECCO® system spike plate. A certain amount of this tensile forces is transferred from the wire mesh via the spike plate onto the nail and finally into the stable subsoil. This additional stabilizing effect can be taken into account in the consideration of equilibrium in the context of superficial instabilities.

To determine the maximum possible tensile force to be transmitted from the steel wire mesh via the TECCO® system spike plate onto the nail, corresponding tests as presented in picture F.1 were carried out. It is important to differentiate between the capacity of the wire mesh to this kind of local force transmission and the tensile strength of the steel wire mesh in longitudinal as well as transversal direction. During the tensile tests, the stress transmission is more or less uniform over the width of the test sample. In contrast to this, in the tests as shown in picture F.1, the load distribution is concentrated very much around the nail head.

The bearing resistances of the steel wire mesh to tensile stress in longitudinal as well as transversal direction mainly serve to characterize the product. But this information cannot be used directly for the dimensioning of the stabilization system against superficial instabilities because the effective kind of stresses occur in different ways.

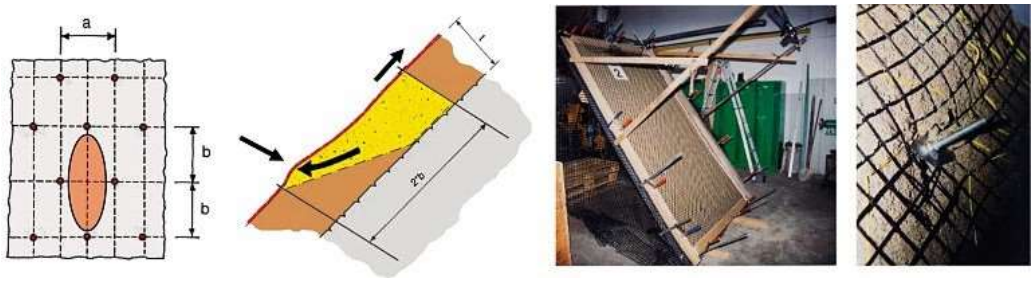

Figure F.1 Left side: model for the investigation of local instabilities between the single nails based on the RUVOLUM® method.
Right side: model tests with a scale of 1: 5 with an inclined plane. The photographs on the very right side shows the deformation behaviour of the system around the nail head area in a near vertical state. Just below the thread bar, a hole was created due to moving down of the sandy material. The geogrid is tensioned and pulls at the nail head. At the same time on the upper side of the steel plate, the geogrid would like to be sheared off. The sliding mass is pushing out the flexible system. In this test, the resistance of the system against shearing-off is sufficient. But of course, a geogrid should not be used for stabilizing real slopes due to its low resistance. In this model test, it was not possible to use a scaled TECCO® mesh.

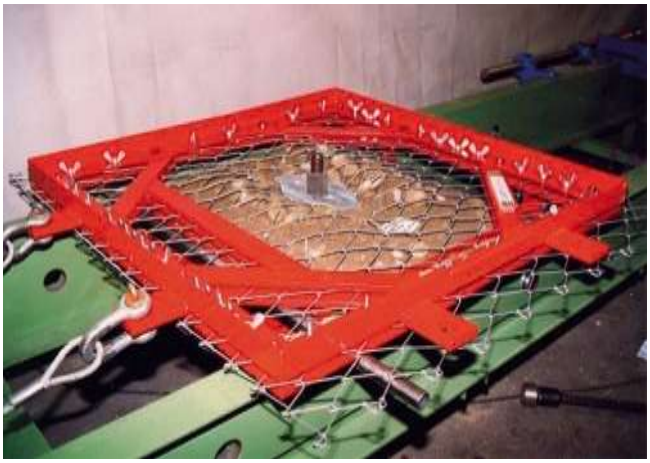

Picture F.1 Test setup to determine the bearing resistance of the high-tensile steel wire mesh system against selective, slope-parallel tensile stress. In this test series, the tensile forces have to be transmitted from the pulling machine, via wire ropes and shackles, the steel frame and the steel wire mesh onto the spike plate as well as the nail into the subsoil. The box filled up with sandy gravel and the central arranged nail with the spike plate are fix. The red frame and the attached steel wire mesh TECCO® can move freely on the green steel profiles

Appendix G Material descriptions and calculation of carbon footprint analysis and comparison

TECCO®– System		**Material**	**Weight** (kg)
Pinning (WT 32 gross)			
	Nail = 4.0 m	steel	1817.3
	Nail = 6.0 m	steel	4088.9
	Injection for nails	cement, w/c= 0.4	23400.0
Wire mesh			
	TECCO® mesh	high-strength wire	1963.6
	Corrosion protection: galvanization	zinc	169.6
	Corrosion protection: galvanization	aluminium	8.9
	Gripping plate	sheet steel	495.0
	Corrosion protection for gripping plate	zinc coating	
	Press claws	steel	123.8
	Corrosion protection	zinc coating	
	Stranded rope (as side guys, top/bottom)	high-strength wire	100.0
	Corrosion protection for stranded rope	zinc coating	0.5
	Spiral rope anchor = 4.0 m (top/bottom)	high-strength wire	42.4
	Corrosion protection for spiral rope anchor	zinc coating	0.2
	Injection for spiral rope anchors	cement	896.0
Planting			
	TECMAT erosion protection mat	polypropylene	714.0

Table G.1: Materials used for a slope stabilisation structure constructed using flexible TECCO® wire netting for a slope 100 m long

Shotcrete placement		**Material**	**Weight** (kg)
Pinning (WT 28 gross)			
	Nails = 4.0m	steel	1081.9
	Nails = 5.0m	steel	6713.7
	injection for nails	cement, w/c = 0.4	40350.0
Shotcrete			
	Total shotcrete (spraying loss ~25%)		564360.0
	Clips	Steel	6324.8
	Top plate	Steel	589.2
	Corrosion protection for top plate	Zinc coating	
Drainage			
	Drainage pipes	PVC	64.0

Table G.2 Materials used for a slope stabilisation structure constructed using shotcrete placement for a slope 100 m long

Consideration of the CO_2 equivalent level of pollution (in kg CO_2 equivalent)

TECCO®-System

Process	**Total**	**Pinning**	**Mesh**	**Planting**
Total for all processes	35586.6	28041.0	6037.6	1508.0
Portland cement, strength class Z 42.5, at plant/CH S	20245.2	19498.6	746.6	0.0
Reinforcing steel, at plant/RERS	8134.6	7363.1	771.4	0.0
Steel, converter, low-alloyed, at plant/RERS	3571.8	0.0	3571.8	0.0
Transport, lorry 28t/CH S	1644.0	1179.3	385.1	79.5
Polypropylene, granulate, at plant/RERS	1428.5	0.0	0.0	1428.5
Zinc for coating, at regional storage/RER S	437.1	0.0	437.1	0.0
Aluminium, primary, at plant/RERS	106.4	0.0	106.4	0.0
Transport, transoceanic freight ship/OCE S	19.2	0.0	19.2	0.0

Table G.3 Detailed consideration of the emissions which might affect climate change during the service life of a comparable structure produced using different processes

Shotcrete placement

Process	Total	Shotcrete	Pinning	Drainage
Total for all processes	147479.6	102231.2	45108.6	139.8
Concrete, exacting, at plant/CH S	80772.4	80772.4	0.0	0.0
Portland cement, strength class Z 42.5, at plant/CH S	33622.5	0.0	33622.5	0.0
Reinforcing steel, at plant/RER S	18338.2	8619.6	9718.6	0.0
Transport, lorry 28t/CH S	14578.7	12809.8	1767.5	1.4
Polyvinylchloride, at regional storage/RER S	138.4	0.0	0.0	138.4
Zinc for coating, at regional storage/RER S	29.5	29.5	0.0	0.0

Consideration of the CO_2 pollution from fossil fuels (in kg CO_2)

TECCO®-System

Process	Total	Pinning	Mesh	Planting
Total for all processes	25053.4	22040.0	2949.8	63.6
Transport, lorry 28t/CH S	1282.6	920.0	300.5	62.1
Transport, transoceanic freight ship/OCE S	0.2	0.0	0.2	0.0
Portland cement, strength class Z 42.5, at plant/CHS	18586.0	17900.0	686.0	0.0
Reinforcing steel, at plant/RER S	3557.4	3220.0	337.4	0.0
Steel, converter, low-alloyed, at plant/RER S	1522.7	0.0	1522.7	0.0
Polypropylene, granulate, at plant/RER S	1.5	0.0	0.0	1.5
Zinc for coating, at regional storage/RER S	85.9	0.0	85.9	0.0
Aluminium, primary, at plant/RER S	17.0	0.0	17.0	0.0

Shotcrete placement

Process	Total	Shotcrete	Pinning	Drainage
Total for all processes	122480.4	85960.0	36518.0	2.5
Transport, lorry 28t/CH S	11372.3	9993.2	1378.0	1.1
Concrete, exacting, at plant/CHS	72200.0	72200.0	0.0	0.0
Portland cement, strength class Z 42.5, at plant/CHS	30900.0	0.0	30900.0	0.0
Reinforcing steel, at plant/RER S	8001.0	3761.0	4240.0	0.0
Polyvinylchloride, at regional storage/RER S	1.4	0.0	0.0	1.4
Zinc for coating, at regional storage/RER S	5.8	5.8	0.0	0.0

Table G.3 Continued

Process	CO_2 emissions (%)	SO_x emissions (%)	NO_x emissions (%)	Soot and Dusts emissions (%)
Material	84.9	63.2	40.6	27.9
Construction	4.9	9.5	16.0	19.2
Dismantlement	5.3	14.9	28.7	31.4
Abandonment and recycling	1.2	1.9	1.6	2.1
Transportation	3.6	10.5	13.1	19.4

Table G.4 Process rate of concrete life cycle

Industrial method	Material	Emission basic unit	
		Value	Unit
High-tensile steel wire mesh system (TECCO® system)	Grout	937.6	kg-CO_2/m^3
	Wire	1.3	kg-CO_2/kg
	Steel bar	1.2	kg-CO_2/kg
Concrete/shotcrete system	Grout	937.6	kg-CO_2/m^3
	Shotcrete (mortar)	320.7	kg-CO_2/m^3
	Wire	1.3	kg-CO_2/kg
	Steel bar	1.2	kg-CO_2/kg

Table G.5 CO_2 emissions source unit of each material

Method of construction	Material	Use quantity		CO_2 emissions standard physical unit		CO_2 emissions
		Quantity	Unit	Value	Unit	(kg-CO_2)
TECCO® system	Grout	0.9	m^3	937.6	kg-CO_2/m^3	844
	Wire	2,124.0	kg	1.3	kg-CO_2/kg	2,761
	Steel bar	2,775.0	kg	1.2	kg-CO_2/kg	3,330
	Total					6,935
Concrete frame	Grout	1.4	m^3	937.6	kg-CO_2/m^3	1,313
	Shotcrete/ concrete (mortar)	141.0	m^3	320.7	kg-CO_2/m^3	45,219
	Wire	4,463.0	kg	1.3	kg-CO_2/kg	5,802
	Steel bar	11,167.0	kg	1.2	kg-CO_2/kg	13,400
	Total					65,734

Table G.6 Calculation results of CO_2 emissions per 1'000 m^2 slope surface

TECCO® system CO_2 emissions (A)	Shotcrete CO_2 emissions (B)	$\frac{A}{B}$	Reduction rate $\frac{(B-A)}{B} \times 100\ (\%)$
6,935 kg-CO_2	65,734 kg-CO_2	6.935/65.734 = 1/9.5	(65.734 – 6.935)/65.734 × 100 = 89.4%

Table G.7 Environmental impact by high-tensile steel wire mesh system (TECCO® system)

Appendix H Example for output data of RUVOLUM® Dimensioning Software (1/6)

RUVOLUM® ONLINE TOOL

RUVOLUM® - The Program to dimension the slope stabilization system TECCO®/SPIDER®

Project No.:
Project Name: Example from chapter 9.4
Date, Author: 2019, Armin Roduner

Input quantities			
Slope inclination	α=	60.0	degrees
Layer thickness	t=	1.00	m
Friction angle ground (characteristic value)	Φ_k=	35.0	degrees
Volume weight ground (characteristic value)	γ_k=	22.0	kN/m³
Nail inclination	β=	25.0	degrees
Nail distance horizontal	a=	2.65	m
Nail distance in line of slope	b=	2.65	m

Load cases			
Streaming pressure		No	
Earthquake		No	
Coefficient of horizontal acceleration due to earthquake	a_h=	0.000	[-]
Coefficient of vertical acceleration due to earthquake	a_v=	0.000	[-]

Partials and Safety Factors			
Cohesion ground (characteristic value)	c_k=	0.0	kN/m²
Radius of pressure cone, top	r_0=	0.15	m
Inclination of pressure cone to horizontal	δ=	45.0	degrees
Slope parallel force	E_d=	15.0	kN
Preserving force of the system	W=	30.0	kN
Partial safety correction value for friction angle	γ_Φ	1.25	[-]
Partial safety correction value for cohesion	γ_c	1.25	[-]
Partial safety correction value for volume weight	γ_γ	1.00	[-]
Model uncertainty correction value	γ_{Rm}	1.10	[-]

Dimensioning quantities			
	Φ_d=	29.5	degrees
	c_d=	0.0	kN/m²
	γ_d=	22.0	kN/m³

Appendix H Example for output data of RUVOLUM® Dimensioning Software (2/6)

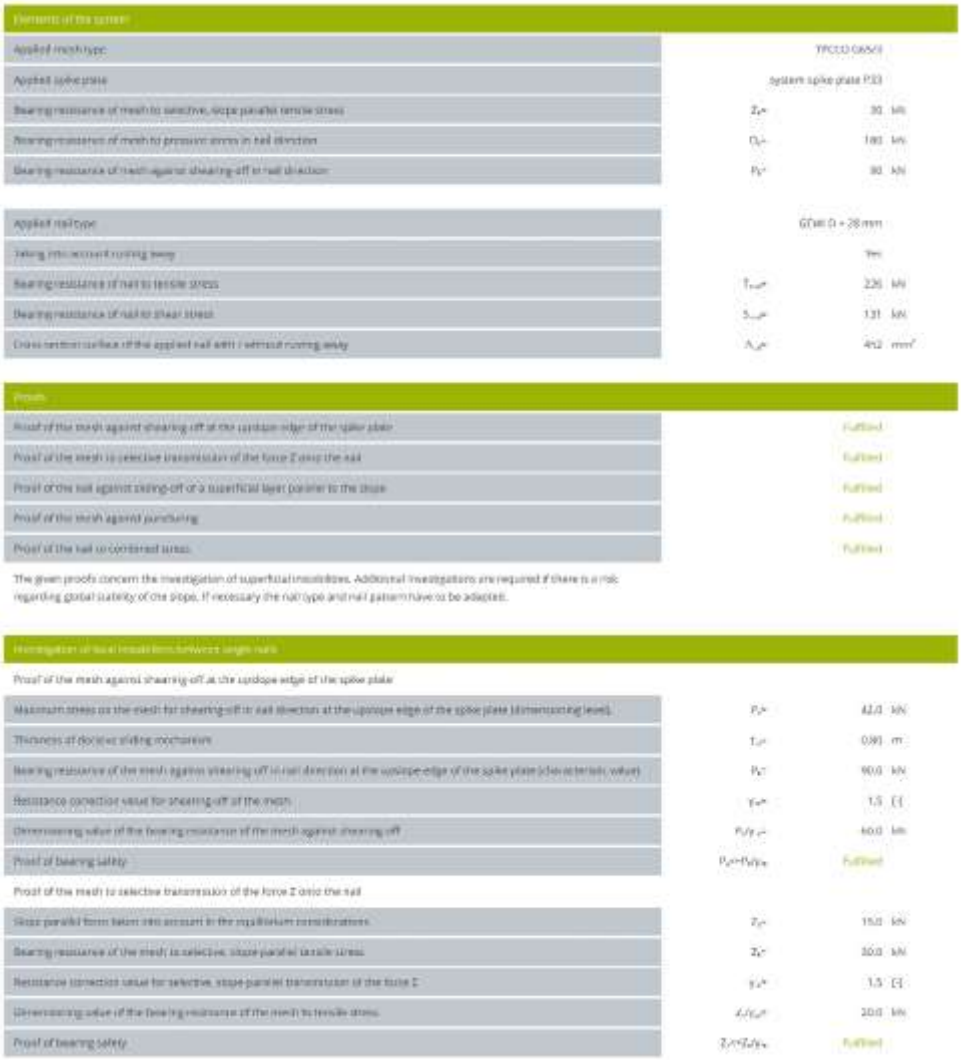

Applied mesh type:		TPC3.0 GA5/3
Applied spike plate:		system spike plate P33
Bearing resistance of mesh to selective, slope parallel tensile stress	$Z_{R,\parallel}$	30 kN
Bearing resistance of mesh to pressure stress in nail direction	$D_{R,\perp}$	180 kN
Bearing resistance of mesh against shearing off in nail direction	P_R	80 kN

Applied nail type:		GEWI D = 28 mm
Taking into account rusting away:		Yes
Bearing resistance of nail to tensile stress	$T_{R,\perp}$	226 kN
Bearing resistance of nail to shear stress	$S_{R,\perp}$	131 kN
Cross section surface of the applied nail with / without rusting away	$A_{s,\perp}$	452 mm²

Proof of the mesh against shearing off at the upslope edge of the spike plate	Fulfilled
Proof of the mesh to selective transmission of the force Z onto the nail	Fulfilled
Proof of the nail against sliding-off of a superficial layer parallel to the slope	Fulfilled
Proof of the mesh against puncturing	Fulfilled
Proof of the nail to combined stress	Fulfilled

The given proofs concern the investigation of superficial instabilities. Additional investigations are required if there is a risk regarding global stability of the slope. If necessary the nail type and nail pattern have to be adapted.

Proof of the mesh against shearing off at the upslope edge of the spike plate

Maximum stress on the mesh for shearing off in nail direction at the upslope edge of the spike plate (dimensioning level)	P_d	42.0 kN
Thickness of decisive sliding mechanism	t_{cr}	0.91 m
Bearing resistance of the mesh against shearing off in nail direction at the upslope edge of the spike plate (characteristic value)	P_R	90.0 kN
Resistance correction value for shearing off of the mesh	γ_M	1.5 [-]
Dimensioning value of the bearing resistance of the mesh against shearing off	P_R/γ_M	60.0 kN
Proof of bearing safety	$P_d \leq P_R/\gamma_M$	Fulfilled

Proof of the mesh to selective transmission of the force Z onto the nail

Slope parallel force taken into account in the equilibrium considerations	Z_d	15.0 kN
Bearing resistance of the mesh to selective, slope parallel tensile stress	Z_R	30.0 kN
Resistance correction value for selective, slope parallel transmission of the force Z	γ_M	1.5 [-]
Dimensioning value of the bearing resistance of the mesh to tensile stress	Z_R/γ_M	20.0 kN
Proof of bearing safety	$Z_d \leq Z_R/\gamma_M$	Fulfilled

Appendix H Example for output data of RUVOLUM® Dimensioning Software (3/6)

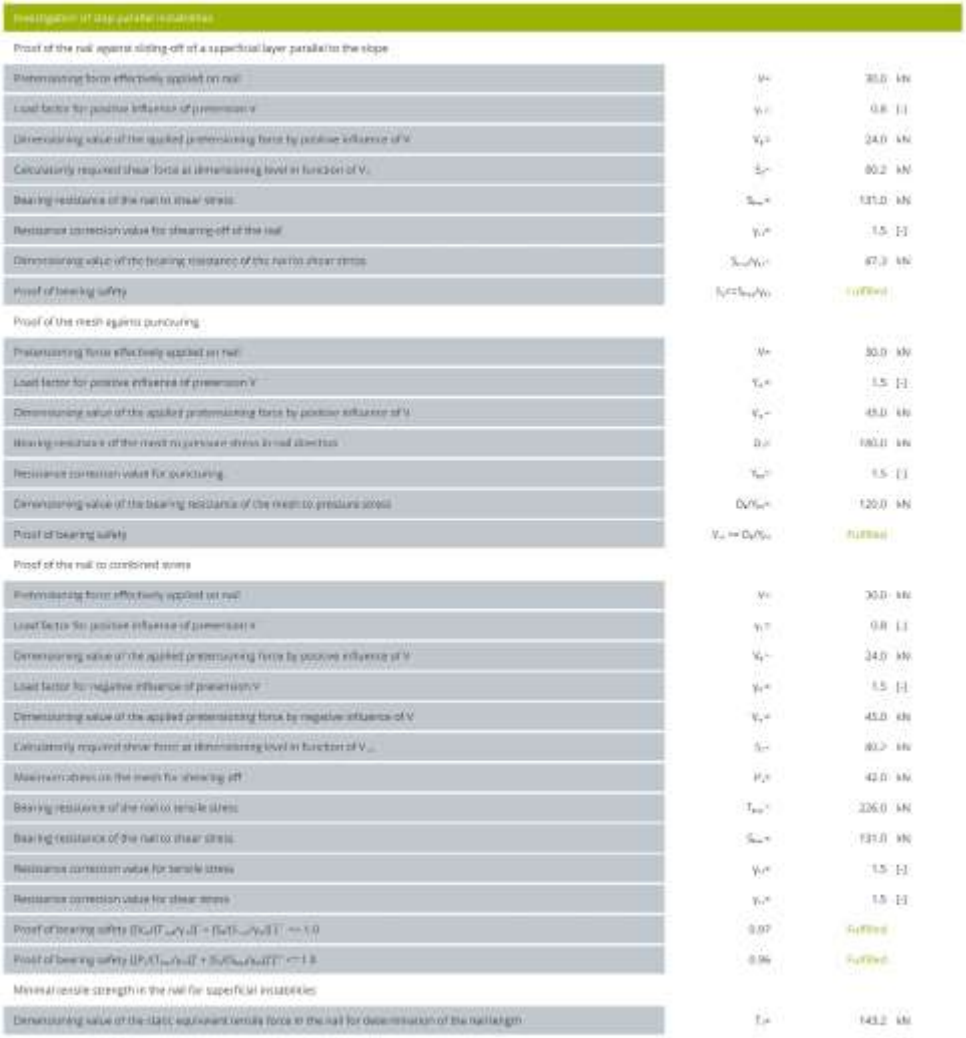

Investigation of slip parallel instabilities		
Proof of the nail against sliding-off of a superficial layer parallel to the slope		
Prestressing force effectively applied on nail	V_{m}	30.0 kN
Load factor for positive influence of prestressing	$\gamma_{G,+}$	0.8 [-]
Dimensioning value of the applied prestressing force by positive influence of V	$V_{d,+}$	24.0 kN
Calculatorily required shear force at dimensioning level in function of $V_{d,+}$	$S_{d,+}$	80.2 kN
Bearing resistance of the nail to shear stress	$S_{res,+}$	131.0 kN
Resistance correction value for shearing-off of the nail	$\gamma_{R,+}$	1.5 [-]
Dimensioning value of the bearing resistance of the nail to shear stress	$S_{res,+}/\gamma_{R,+}$	87.3 kN
Proof of bearing safety	$S_{d,+} \leq S_{res,+}/\gamma_{R,+}$	fulfilled
Proof of the mesh against puncuring		
Prestressing force effectively applied on nail	V_{m}	30.0 kN
Load factor for positive influence of prestressing V	$\gamma_{G,+}$	1.5 [-]
Dimensioning value of the applied prestressing force by positive influence of V	$V_{d,+}$	45.0 kN
Bearing resistance of the mesh to puncuture stress in nail direction	$D_{,+}$	180.0 kN
Resistance correction value for puncturing	$\gamma_{R,+}$	1.5 [-]
Dimensioning value of the bearing resistance of the mesh to pressure stress	$D_{,+}/\gamma_{R,+}$	120.0 kN
Proof of bearing safety	$V_{d,+} \leq D_{,+}/\gamma_{R,+}$	fulfilled
Proof of the nail to combined stress		
Prestressing force effectively applied on nail	V_{m}	30.0 kN
Load factor for positive influence of prestressing	$\gamma_{G,+}$	0.8 [-]
Dimensioning value of the applied prestressing force by positive influence of V	$V_{d,+}$	24.0 kN
Load factor for negative influence of prestressing V	$\gamma_{G,+}$	1.5 [-]
Dimensioning value of the applied prestressing force by negative influence of V	$V_{d,+}$	45.0 kN
Calculatorily required shear force at dimensioning level in function of $V_{d,+}$	$S_{d,+}$	80.2 kN
Maximum stress on the mesh for shearing off	$P_{,+}$	42.0 kN
Bearing resistance of the nail to tensile stress	$T_{res,+}$	226.0 kN
Bearing resistance of the nail to shear stress	$S_{res,+}$	131.0 kN
Resistance correction value for tensile stress	$\gamma_{R,+}$	1.5 [-]
Resistance correction value for shear stress	$\gamma_{R,+}$	1.5 [-]
Proof of bearing safety $(S_{d,+}/(T_{res,+}/\gamma_{R,+}))^2 + (S_{d,+}/(S_{res,+}/\gamma_{R,+}))^2 \leq 1.0$	0.97	fulfilled
Proof of bearing safety $(P_{,+}/(T_{res,+}/\gamma_{R,+}))^2 + (S_{d,+}/(S_{res,+}/\gamma_{R,+}))^2 \leq 1.0$	0.96	fulfilled
Minimal tensile strength in the nail for superficial instabilities		
Dimensioning value of the static equivalent tensile force in the nail for determination of the nail length	$T_{,+}$	143.2 kN

Appendix H Example for output data of RUVOLUM® Dimensioning Software (4/6)

RUVOLUM® ONLINE TOOL

RUVOLUM® - The Program to dimension the slope stabilization system TECCO®/SPIDER®

Project No.: -
Project Name: Example from chapter 9.4
Date, Author: 2019, Armin Rickauer

Input quantities		
Slope inclination	$\beta =$	60.0 degrees
Layer thickness	$t =$	0.50 m
Friction angle ground (characteristic value)	$\varphi_k =$	35.0 degrees
Volume weight ground (characteristic value)	$\gamma_k =$	22.0 kN/m³
Nail inclination	$\psi =$	25.0 degrees
Nail distance horizontal	$a_h =$	3.00 m
Nail distance in line of slope	$a_s =$	3.00 m

Load cases		
Steaming pressure		No
Earthquake		No
Coefficient of horizontal acceleration due to earthquake	$\kappa_h =$	0.000 [-]
Coefficient of vertical acceleration due to earthquake	$\kappa_v =$	0.000 [-]

Defaults and Safety Factors		
Cohesion ground (characteristic value)	$c_k =$	0.0 kN/m²
Radius of pressure cone, top	$r_P =$	0.15 m
Inclination of pressure cone to horizontal	$\Delta =$	45.0 degrees
Slope parallel force	$Z_k =$	15.0 kN
Prestressing force of the system	$vr =$	30.0 kN
Partial safety correction value for friction angle	γ_φ	1.25 [-]
Partial safety correction value for cohesion	γ_c	1.25 [-]
Partial safety correction value for volume weight	γ_γ	1.00 [-]
Model uncertainty correction value	γ_{Rm}	1.10 [-]

Dimensioning quantities		
	$\varphi_d =$	29.3 degrees
	$c_d =$	0.0 kN/m²
	$\gamma_d =$	22.0 kN/m³

Appendix H Example for output data of RUVOLUM® Dimensioning Software (5/6)

Elements of the system		
Applied mesh type		TECCO G65/3
Applied spike plate		system spike plate P33
Bearing resistance of mesh to selective, slope parallel tensile stress	Z_R =	30 kN
Bearing resistance of mesh to pressure stress in nail direction	D_R =	180 kN
Bearing resistance of mesh against shearing off in nail direction	F_R =	90 kN

Applied nail type		GEWI-D = 28 mm
Taking into account rusting away		Yes
Bearing resistance of nail to tensile stress	$T_{n,R}$ =	226 kN
Bearing resistance of nail to shear stress	$S_{n,R}$ =	131 kN
Cross section surface of the applied nail with / without rusting away	$A_{n,R}$ =	452 mm²

Proofs	
Proof of the mesh against shearing-off at the upslope edge of the spike plate	Fulfilled
Proof of the mesh to selective transmission of the force Z onto the nail	Fulfilled
Proof of the nail against sliding-off of a superficial layer parallel to the slope	Fulfilled
Proof of the mesh against puncturing	Fulfilled
Proof of the nail to combined stress	Fulfilled

The given proofs concern the investigation of superficial instabilities. Additional investigations are required if there is a risk regarding global stability of the slope. If necessary the nail type and nail pattern have to be adapted.

Investigation of local instabilities between single nails		
Proof of the mesh against shearing-off at the upslope edge of the spike plate		
Maximum screw on the mesh for shearing off in nail direction at the upslope edge of the spike plate (dimensioning level)	F_d =	58.8 kN
Thickness of decisive sliding mechanism	t_{cr} =	0.50 m
Bearing resistance of the mesh against shearing off in nail direction at the upslope edge of the spike plate (characteristic value)	F_R =	90.0 kN
Resistance correction value for shearing off of the mesh	γ_M =	1.5 [-]
Dimensioning value of the bearing resistance of the mesh against shearing off	F_R/γ_M =	60.0 kN
Proof of bearing safety	$F_d \leq F_R/\gamma_M$	Fulfilled
Proof of the mesh to selective transmission of the force Z onto the nail		
Slope parallel force taken into account in the equilibrium considerations	Z_d =	10.0 kN
Bearing resistance of the mesh to selective, slope parallel tensile stress	Z_R =	30.0 kN
Resistance correction value for selective, slope parallel transmission of the force Z	γ_M =	1.5 [-]
Dimensioning value of the bearing resistance of the mesh to tensile stress	Z_R/γ_M =	20.0 kN
Proof of bearing safety	$Z_d \leq Z_R/\gamma_M$	Fulfilled

Appendix H Example for output data of RUVOLUM® Dimensioning Software (6/6)

Investigation of slope parallel instabilities		
Proof of the nail against sliding off of a superficial layer parallel to the slope		
Prestressing force effectively applied on nail	V_{vorh}	30.0 kN
Load factor for positive influence of prestressing V	$\gamma_{G,V}$	0.8 [-]
Dimensioning value of the applied prestressing force by positive influence of V	$V_{d,V}$	24.0 kN
Calculatorily required shear force at dimensioning level in function of $V_{d,V}$	S_{erf}	46.3 kN
Bearing resistance of the nail to shear stress	S_{vorh}	131.0 kN
Resistance correction value for shearing off of the nail	$\gamma_{M,V}$	1.5 [-]
Dimensioning value of the bearing resistance of the nail to shear stress	$S_{vorh}/\gamma_{M,V}$	87.3 kN
Proof of bearing safety	$S_{erf} \leq S_{vorh}/\gamma_{M,V}$	Fulfilled
Proof of the mesh against puncturing		
Prestressing force effectively applied on nail	V_{vorh}	30.0 kN
Load factor for positive influence of prestressing V	$\gamma_{G,V}$	1.5 [-]
Dimensioning value of the applied prestressing force by positive influence of V	$V_{d,V}$	45.0 kN
Bearing resistance of the mesh to pressure stress in nail direction	D_{vorh}	180.0 kN
Resistance correction value for puncturing	$\gamma_{M,V}$	1.5 [-]
Dimensioning value of the bearing resistance of the mesh to pressure stress	$D_{vorh}/\gamma_{M,V}$	120.0 kN
Proof of bearing safety	$V_{d,V} \leq D_{vorh}/\gamma_{M,V}$	Fulfilled
Proof of the nail to combined stress		
Prestressing force effectively applied on nail	V_{vorh}	30.0 kN
Load factor for positive influence of prestressing V	$\gamma_{G,V}$	0.8 [-]
Dimensioning value of the applied prestressing force by positive influence of V	$V_{d,V}$	24.0 kN
Load factor for negative influence of prestressing V	$\gamma_{Q,V}$	1.5 [-]
Dimensioning value of the applied prestressing force by negative influence of V	$V_{d,V}$	45.0 kN
Calculatorily required shear force at dimensioning level in function of $V_{d,V}$	S_{erf}	46.3 kN
Maximum stress on the mesh for shearing off	P_{d}	58.8 kN
Bearing resistance of the nail to tensile stress	$T_{vorh,z}$	216.0 kN
Bearing resistance of the nail to shear stress	S_{vorh}	131.0 kN
Resistance correction value for tensile stress	$\gamma_{M,T}$	1.5 [-]
Resistance correction value for shear stress	$\gamma_{M,V}$	1.5 [-]
Proof of bearing safety $(V_{d,V}/T_{vorh,z}/\gamma_{M,T})^2 + [S_{d}/(S_{vorh}/\gamma_{M,V})]^2 <= 1.0$	0.61	Fulfilled
Proof of bearing safety $(P_{d}/T_{vorh,z}/\gamma_{M,T})^2 + [S_{d}/(S_{vorh}/\gamma_{M,V})]^2 <= 1.0$	0.88	Fulfilled
Minimal tensile strength in the nail for superficial instabilities		
Dimensioning value of the static equivalent tensile force in the nail for determination of the nail length	T_{d}	82.0 kN

List of References

[1] Abramson, L. W.; Thomas, S. L.; Sharma, S.; Boyce, G. M.: Slope stability and stabilization methods. John Willey & Sons Inc., New York, USA, 1996.

[2] Apel, G.; Nünninghoff, R.; Sczepanski, K.: Galfan – ein neuer Korrosionsschutz für Seile, Draht 39 (1988) Nr. 4 + 5, Germany, 1988.

[3] American Society for Testing and Materials, ASTM B117: Saltspray Accelerated Weathering Test, USA, 2003.

[4] American Society for Testing and Materials, ASTM A-975: Hexagonal Steel Wire Meshes, USA, 2003.

[5] Bachmann, H.: Stahlbeton, Vorlesungen Abteilung Bauingenieurwesen der ETH Zürich, IBK, Institut für Baustatik und Konstruktion, Swiss Federal Institute of Technology, Switzerland, 1991.

[6] Balcerek, B.: Wybrane problemy ochrony środowiska w drogownictwie – Selected environmental problems in road industry, Pages 60–67, Polskie Drogi – Polish Roads No. 12 (148), Poland, 2007.

[7] Balcerek, B.: Umacnianie skarp drogowych a sprawność systemu odwodnienia i podczyszczania wód – Strengthening of the road slopes, drainage system and the efficiency of water pre-treatment, Pages 86 – 90, Polskie Drogi – Polish Roads No. 5 (172), Poland, 2010.

[8] Baraniak, P.; Mrozik, M.: Konstrukcje chroniące przed spływami gruzowymi oraz spadającymi odłamkami skalnymi – testowanie, wymiarowanie, instalacja, użytkowanie – Protection systems against debris flow and rockfalls – testing, dimensioning, installation, exploitation, Konstrukcje stalowe w geotechnice – Steel structures in geotechnics, pages 79–88; Poland, 2010.

[9] Bergische Universität Wuppertal, Germany; Prof. Dr.-Ing. Rolf Nünninghoff: Test Report No. 9811, GALFAN-coated steel wire mesh in alkaline environment, Longterm field study report 3/2004, Germany, 2004.

[10] Bergische Universität Wuppertal, Germany; Prof. Dr.-Ing. Rolf Nünninghoff: Test Report No. 9811, Comparison between different different corrosion laboratory tests Zn-coated and Zn–Al-coated steel wires, Germany, 2006.

[11] Böhni, H.: Werkstoffe I, Vorlesung Abteilung Bauingenieurwesen der ETH Zürich, IBWK, Institut für Baustoffe, Werkstoffchemie und Korrosion, Swiss Federal Institute of Technology, Switzerland, 1994.

[12] Böhni, H.: Werkstoffe IV, Vorlesung Abteilung Bauingenieurwesen der ETH Zürich, IBWK, Institut für Baustoffe, Werkstoffchemie und Korrosion, Swiss Federal Institute of Technology, Switzerland, 1995.

[13] Brändlein, P.: Monitoring and supervision of laboratory testing of TECCO® mesh and system components. LGA Nuremberg, Germany, Test report BGT 0230101, Germany, 2003.

[14] Brisbé York, A. M.; Flum, D.; Roth, A.; Roduner, A.: RUVOLUM® Dimensioning Software 7.0, Spain and Switzerland, 2006.

[15] Bromhead E. N., Landslide slip surfaces: their origins, behavior and geometry, Landslides: Evaluation and Stabilisation (edited by Lacerda, Erlich, Fontura & Sayao), Taylor & Francis Group, London, pp. 3–21, Rio de Janeiro, 2004.

[16] Bundesamt für Umwelt, Wald und Landschaft BUWAL und Eidgenössische Forschungsanstalt WSL: Typenliste Ankermörtel; Ankermörtel, die für den Lawinenverbau und Steinschlagverbau zugelassen sind, Switzerland, 2004.

[17] Bundesamt für Umwelt, Wald und Landschaft BUWAL und Eidgenössische Forschungsanstalt WSL: Lawinenverbau im Anbruchgebiet – Technische Richtlinie als Vollzugshilfe, Switzerland, 2007.

[18] Cała, M.; Flisiak, J.: Slope stability analysis with FLAC and limit equilibrium methods, Proceedings of the 2nd Geomechanical International Symposium, Lyon, France, 2001.

[19] Cała, M.; Flisiak, J.; Tajduś, A.: Slope stability analysis with modified shear strength reduction technique. Landslides: evaluation and stabilization. Proceedings of the ninth international symposium on Landslides, 2004, eds. Willy A. Lacerda [et al.]. Taylor & Francis Group, London, pp. 1085–1089, Rio de Janeiro, 2004.

[20] Cała, M.; Roth A.: Możliwości zastosowania siatek stalowych w warunkach zagrożeń dynamicznych. Górnictwoi Geoinżynieria, Vol 31, z. 3, pp. 125–134. Poland, 2007.

[21] Cała, M.; Flisiak, J.; Tajduś, A.: Slope stability with FLAC in 2D and 3D. Proc of 4th Int. FLAC Symposium. FLAC and Numerical Modeling in Geomechanics. Itasca Consulting Group. Madrid., Spain, 2006.

[22] Cała, M.: Convex and concave slope stability analysis with numerical methods. Archives of Mining Sciences. Vol. 52, Issue 1. pp. 75–89. Wydawnictwo Instytutu Mechaniki Górotworu PAN. Kraków, Poland, 2007.

[23] Cała, M.: Numeryczne metody analizy stateczności zboczy. Wydawnictwa AGH, seria rozprawy i monografie nr 171. Kraków, Poland, 2007.

[24] Cała, M.; Kowalski M.: Reinforced slope stability analysis with FLAC, Continuum and distinct element numerical modeling in geo-engineering, Proceedings of the 1st inter-national FLAC/DEM Symposium, USA, 2008.

[25] Cała, M.; Kowalski M.: Reinforced slope stability analysis with FLAC, Geobrugg Annual Conference 2008, Switzerland, 2008.

[26] Caprez, M.; Dietrich, K.: Geotechnik und Strassenbau, Institut für Verkehrsplanung, Transporttechnik, Strassen- und Eisenbahnbau, IVT, Eidgenössische Technische Hochschule, Polytechnical University of Zurich, Switzerland, 1996.

[27] Chen F. H., Soil Engineering, Testing, Design and Remediation, CRC Press, Boca Raton FL, 2000.

[28] Cheng Y. M.; Lansivaara T.; Wei W. B.: Two-dimensional slope stability analysis by limit equilibrium and strength reduction methods, "Computers and Geotechnics", Vol. 34, pp. 137–150, 2007.

[29] Center of Environmental Information Science: Table of CO_2 emissions standard physical unit (version 2007), Japan, 2007.

[30] Dawson E. M.; Roth W. H.: Slope stability analysis with FLAC, 1999, FLAC and numerical modeling in geomechanics (edited by Detournay & Hart). A. A. Balkema, Rotterdam, pp. 3–9, Netherlands, 1999

[31] Drzymała, I.: Problemy z osuwiskami – Problems with landslides, Autostrady – Highways Magazin, 7/2009, Poland, 2009.

[32] Duncan J. M.; Wright S. G.: Soil strength and slope stability, John Wiley & Sons Inc., Hoboken, New Jersey, USA, 2005.

[33] DIN 1055-100: Einwirkung auf Tragwerke – Grundlagen der Tragwerksplanung – Sicherheitskonzept und Bemessungsregeln, 2001.

[34] DIN 1055-9: Einwirkung auf Tragwerke – Außergewöhnliche Einwirklungen, 2003.

[35] DIN 18127: Baugrund – Untersuchung von Bodenproben – Proctorversuch, 1997.

[36] DIN 18196: Erd- und Grundbau – Bodenklassifizierung für bautechnische Zwecke, 2006.

[37] DIN 1055-9: Einwirkung auf Tragwerke – Aussergewöhnliche Einwirklungen, 2003.

[38] DIN 18800-1: Bemessung und Konstruktion, 1990.

[39] DIN 4022-1: Benennung und Beschreibung von Boden und Fels, 1987.

[40] DIN EN 10002: Tensile tests of steel wire.

[41] DIN EN 13411-5 (2003): Rope loops with wire rope clips.

[42] DIN 50018: Kesternich Accelerated Weathering Test (SO_2 Spraytest).

[43] DIN 50021: Saltspray Accelerated Weathering Test.

[44] EN 10244-2 (2001): Non-ferrous metallic coatings on steel wire.

[45] EN 10264-2 (2002): Steel wire and wire products – Steel wire for ropes – Part 2: Cold drawn non alloy steel wire for ropes for general applications.

[46] ETAG-027: Guideline for European Technical Approval of Falling Rock Protection Kits, EOTA, Brussels, EU, 2008.

[47] EUROCODE 7: Geotechnical design – Part 1: General rules, 2004.

[48] European Commitee for Standardization: Steel wire and wire products – Steel wire for ropes, Part 2: Cold drawn non alloy steel wire for ropes for general applications, 2002.

[49] European Commitee for Standardization: EN 13411 – 5: Terminations for steel wire ropes. Safety. U-Bolt wire rope grips, 2003.

[50] FHWA, Soil Nailing, Filed Inspector's Manual, USA, 1996.

[51] Flum, D.; Guasti, G.; Rüegger, R.: Dimensionamento di sistemi di consolidamento flessibili superfi ciali costituiti da reti in acciaio ad alta resistenza in combinazione a elementi di ancoraggio in barra. GEAM – Associazione Georisorse e Ambiente Torino, Bonifi ca di versanti rocciosi per la protezione del territorio, Trento, Italy, 2004.

[52] Flum, D.; Rüegger, R.: Dimensioning of flexible surface stabilization systems made from high-tensile steel wire meshes in combination with nailing and anchoring in soil and rock. IX International Symposium on Landslides, Rio de Janeiro, Brazil, 2004.

[53] Flum, D.; Rüegger, R.: Dimensioning of flexible surface stabilization systems made from high-tensile steel wire meshes in combination with nailing and anchoring in soil and rock. XIII. Danube-European Conference on Geotechnical Engineering, Ljubljana, Slovenia, 2006.

[54] Flum, D.; Rüegger, R.; Weingart, K.: Pressklaue F4 zur Verbindung der Geflechtsbahnen des Böschungsstabilisierungssystems TECCO®, Report über die Zugversuche in der Periode April – Juli 2008, Test report Rüegger Systeme AG, Switzerland, 2008.

[55] Fredlund D.; Scoular R.: Using limit equilibrium concepts in finite element slope stability analysis, 1999. Slope Stability Engineering (edited by Yagi, Yamagami & Jiang), A. A. Balkema, Rotterdam, pp. 31–47, Netherlands, 1999.

[56] Fritz, P.; Kovari, K.: Böschungsstabilität mit ebenen, keilförmigen und polygonalen Gleitflächen. Rock Mechanics, Suppl. 8, 291–316 (1979). Springer-Verlag, Germany, 1979.

[57] Geiger, B.; Fleischer, T.: Stoffliche und energetische Lebenszyklusanalysen von Wohngebäuden, Gesamtheitliche Betrachtung von Energiesystemen. VDI-1328, Düsseldorf, Germany, 1997.

[58] Gerber, W.; Baumann, R.; Wartmann, S.; Buri, H.; Honegger, R.; Kaufmann, R.; Testi, R.; Haller, B.; Toniolo, M.: Guideline for the approval of rockfall protection kits, Swiss Agency for the Environment Forests and Landscape (SAEFEL), Switzerland, 2000.

[59] Grassl, H. G.: Experimentelle und numberische Modellierung des dynamischen Trag- und Verformungsverhaltens von hochflexiblen Schutzsystemen gegen Steinschlag. Doktorarbeit, Eidgenössische Technische Hochschule Zürich, Switzerland, 2002.

[60] Griffiths, D. V.; Lane, P. A.: Slope stability analysis by finite elements, "Geotechnique", Vol. 49 (3), pp. 387–403, 1999.

[61] Gudehus, G.: Soil Mechanics (Bodenmechanik), Ferdinand Enke Verlag, Stuttgart, Germany, 1981.

[62] Hungr, O.: An extension of Bishop's simplified method of slope stability analysis to three dimensions, "Geotechnique", Vol. 37 (3), pp. 113–117, 1987.

[63] Institut für Korrosionsschutz Dresden, Vorlesungen über Korrosion und Korrosionsschutz von Werkstoffen I, II, III; Germany, 1996.

[64] Institute of Civil and Environmental Engineering, HSR Hochschule für Technik Rapperswil, IBU Institut für Bau und Umwelt; Kytzia, S.; Hardegger, P.; Schnellmann, R.; Scherrer, B.: CO_2 footprint of slope stabilization methods: The TECCO® system (mesh) compared to shotcrete, Switzerland, 2008.

[65] Japan Society of Civil Engineers: Environmental impact evaluation of concrete (2), concrete technical series 62, Japan, 2007.

[66] Kantonale Gebäudeversicherung: Objektschutz gegen gravitative Naturgefahren, Switzerland, 2005.

[67] Kasser, U: Gebäude gesamtenergetisch beurteilt. Sonderdruck aus: Schweizer Architekt, Nr. 13.; Switzerland, 1998.

[68] Kim, J.; Salado, R.; Lee, J.: Stability analysis of complex soil slopes using limit analysis, "Journal of Geotechnical and Geoenvironmental Engineering", Vol. 128 (7), pp. 546–557, 2002.

[69] Korzeniowski, W.: Piechota St. Rozkład siły osiowej wzdłuż kotwi na podstawie badań. Przegląd Górniczy; 2000 T. 56, nr. 12, pp. 22–28, Poland, 2000.

[70] Kowalski, B.: Jak walczyć z niszczącą siłą osuwisk? – How to fight the destructive power of landslides?, Polskie Drogi – Polish Roads, 9 (165), pp. 58–62, Poland, 2009.

[71] Krahn, J.: The 2001 R. M. Hardy Lecture: The limits of limit equilibrium analyses, "Canadian Geotechnical Journal", Vol. 40, pp. 643–660, Canada, 2003.

[72] Kuchling, H.: Taschenbuch der Physik, VEB Fachbuchverlag Leipzig, Germany, 1989.

[73] Kühne, M.; Einstein, H. H.; Krauter, E.; Klapperich, H.; Pöttler, R.: International Conference on Landslides, Causes, Impacts and Countermeasures. Davos, Switzerland, 2001.

[74] Landslides, Investigation and Mitigation, Special Report 247. Transportation Research Board, National Research Council. National Academy Press, Washington, D. C., USA, 1996.

[75] Lang, H.-J.; Huder, J.: Bodenmechanik und Grundbau, Switzerland, 1994.

[76] Leite Rodrigues, B.; Lapolli, M.: O Túnel do Moro Agudo, Florianópolis, Pandion editora, Brasil, 2010.

[77] Leser, H.: Geomorphologie; Westermann Schulbuchverlag GmbH, Germany, 2003.

[78] LGA Nuremberg, Brändlein, P.: Monitoring and supervision of laboratory testing of the TECCO® slope stabilization system, Test report BPI 0400046/1, Germany, 2004.

[79] LGA Nuremberg, Brändlein, P.; Deppisch, J.: Tensile tests on high-tensile steel wire mesh TECCO® G65/3 mm in comparison to a hexagonal mesh 80 × 100/3 mm with wire rope 8 mm, Monitoring and supervision of laboratory testing, Test report BBW4 0548034/02, Germany, 2005.

[80] LGA Nuremberg, Brändlein, P.; Deppisch, J.: Tensile tests on high-tensile steel wire mesh TECCO® G65/3 mm in comparison to a chain-link mesh 50 × 50 mm/4.6 mm, Monitoring and supervision of laboratory testing, Test report BBW4 0548034/01, Germany, 2005.

[81] LGA Nuremberg, Brändlein, P.; Deppisch, J.: Zugversuche am hochfesten Stahldrahtgeflecht TECCO® G65/3 mm, Leitung und Überwachung von Laborversuchen, Test report BBW40648022/02, Germany, 2006.

[82] Loipersberger, A.; Sadgorski, C.; Rimböck, A.; Hübl, J.; Pichler, A.; Strobl, Th.: Schwemmholz in Wildbächen, Naturversuch Seilsperren zum Schwemmholzrückhalt in Wildbächen, Lehrstuhl und Versuchsanstalt für Wasserbau und Wasserwirtschaft, Technische Universität München, Germany, 2002.

[83] Luis Fonseca, R.: Desarrollo de neuvos sistemas de protección de taludes y laderas rocosas, pantallas dinámicas, Tesis doctoral Universidad de Cantabria, Santander, Spain, 1995.

[84] Majcherczyk, T.; Niedbalski, Z.; Małkowski, P.: Analiza warunków geo-technicznych w otoczeniu tunelu drogowego. Górnictwo i Geoinżynieria. 2009 R. 33 z. 3/1 pp. 239–255, Poland, 2009.

[85] Mrozik, M.; Sierant, J.: Zagwoździowane skarpy przy modernizowanych drogach S1, S7 i DK 69 – Nailed slopes at the upgraded roads S1, S7 i DK 69, Nowoczesne Budownictwo Inżynieryjne - Modern Construction Engineering, 5 (26), Poland, 2009.

[86] Mrozik, M.; Flum, D.; Zueger, M.: Stabilization of a 30m deep cutting along the highway A63 Kaiserslautern – Mainz, Germany, with a flexible slope stabilization system consisting of high-tensile steel wire mesh in combination with nailing. Autostrada Polska, Kielce, Poland, 2006.

[87] Mrozik, M.: Obecność firmy Geobrugg AG w Polsce – Geobrugg AG in Poland, Geoinży-nieria – drogi mosty tunele Geoingineering - roads bridges tunnels, 01/2008 (16), pp. 24–26, Poland.

[88] Muhunthan, B.: Tensile Capacity Testing of Twisted Wire Mesh and Cable Net Mesh for Use as Rock Fall Protection, University of Washington State, Department of Civil and Environmental Engineering, Wood and Engineering Laboratory, Report No. WMEL 03-043, USA, 2004.

[89] Muraishi, H.; Sano, S.: Full Scale Rockfall test of ringnet barrier and components, PWRI, Japan, 1997.

[90] Norman; Norrish; Duncan: Landslides, investigation and mitigation, special report 247. Rock slope stability analysis (chapter 15). National Academy Press Washington D.C., USA, 1996.

[91] Nünninghoff, R.; Sczepanski, K.: Galfan – an improved corrosion protection for steel wire, Part 1: Improvement of metallic corrosion protection for steel wire, Wire 37, Germany, 1987.

[92] Nünninghoff, R.; Sczepanski, K.: Galfan – an improved corrosion protection for steel wire, Part 2: Applications of aluminium-zinc coated steel wires and tests with coated products, Wire 37, Germany, 1987.

[93] Nünninghoff, R.; Sczepanski, K.: Galfan – ein neuartiger, verbesserter Korrosionsschutz für Stahldraht, Draht 38 (1987) Nr. 1+ 2, Germany, 1987.

[94] Nünninghoff, R.; Sczepanski, K.; Valtinat, G.: Schutzmantel – Galfanierung von Draht und hochfesten Schrauben, Drahtwelt 1 + 2 (1992).

[95] Nünninghoff, R.; Hagebölling, V.: Metallkundliche Untersuchung der Diffusionsvorgänge in einer Zn/Al-5 Gew.-%-Legierung, Draht 46 (1995) Nr. 3, Germany, 1995.

[96] Nünninghoff, R.; Hagebölling, V.: Metallkundliche Untersuchung des Korrosionsmechanismus einer Zn/Al-5 Gew.-%-Legierung, Draht 46 (1995) Nr. 4, Germany, 1995.

[97] Nünninghoff, R.: Langzeiterfahrungen mit Galfan, Draht 2/2003 April, Germany, 2003.

[98] Nünninghoff, R.: Long-term experience with Galfan, Wire 3/2003 June, Germany, 2003.

[99] Oztekin B.; Topal T.; Kolat C.: Assesment of degradation and stability of a cut slope in limestone, Ankara-Turkey, "Engineering Geology", Vol. 84, pp. 12–30, Turkey, 2006.

[100] Palkowski, S.: Statik der Seilkonstruktionen, Springer Verlag, Germany, 1990.

[101] Passaclacqua, R.; Baretto, A.; Dalerci, G.: A slice method for embankment and excavation stability analyses, XII European Congress of Soil Mechanics and Geotechnical Engineering (edited by Vanicek et al.), CGtS, Praga, Czech Republic, 2003.

[102] Potts, D. M.: Numerical analysis: a virtual dream or practical reality? "Geotechnique", Vol. 53, nr. 6, pp. 535–573, France, 2003.

[103] Rickenmann, D.: Estimation of debris flow impact on flexible barriers, Birmensdorf, interner Bericht, Switzerland, 2001.

[104] Rimböck, A., Strobl, Th.: Schwemmholzrückhalt in Wildbächen, Grundlagen zu Planung und Berechnung von Seilnetzsperren, Lehrstuhl und Versuchsanstalt für Wasserbau und Wasserwirtschaft, Technische Universität München, Germany, 2003.

[105] Rimböck, A.: Schwemmholzrückhalt in Wildbächen, Doktorarbeit, Technische Universität München, Germany, 2003.

[106] Rorem, E.; Flum, D.: TECCO® high-tensile Wire Mesh & Revegetation, System for Slope Stabilization. International Erosion Control Association, IECA's 35th annual conference. Philadelphia, USA, 2003.

[107] Rüegger, R.; Wartmann S.; Haller B.: Dimensioning of flexible slope stabilization system made from high-tensile steel wire mesh, First International Geobrugg Asia Conference, Hong Kong, 2000.

[108] Rüegger, R.; Flum, D.; Wartmann S.; Haller B.: TECCO® Slope Stabilization System, Internal Geotechnical Geobrugg Conference Egnach, Switzerland, 2000.

[109] Rüegger, R.; Flum, D.; Haller, B.: Hochfeste Geflechte aus Stahldraht für die Oberflächensicherung in Kombination mit Vernagelungen und Verankerungen. Technische Akademie Esslingen, Beitrag für 2. Kolloquium "Bauen in Boden und Fels", Germany, 2000.

[110] Rüegger, R.; Flum, D.: Slope Stabilization with High-performance Steel Wire Meshes in Combination with Nails and Anchors. Int. Symposium, Earth Reinforcement, IS Kyushu, Fukuoka, Japan, 2001.

[111] Rüegger, R.; Flum, D.; Haller, B.: Hochfeste Geflechte aus Stahldraht für die Oberflächensicherung in Kombination mit Vernagelungen und Verankerungen (Ausführliche Bemessungshinweise). Technische Akademie Esslingen, Beitrag für 3. Kolloquium "Bauen in Boden und Fels", Germany, 2002.

[112] Rüegger, R.; Flum, D.: Anforderungen an flexible Böschungsstabilisierungssysteme bei der Anwendung in Boden und Fels. Technische Akademie Esslingen, Beitrag für 4. Kolloquium "Bauen in Boden und Fels", Germany, 2006.

[113] Sarma, S. K., Tan D. Determination of critical slip surface in slope analysis, "Geotechnique", Vol. 56, pp. 539–550, 2006.

[114] Sayir, M. B.: Mechanik I, II, III, Vorlesungen, Institut für Mechnik, ETH Zürich, Swiss Federal Institute of Technology, Switzerland, 1994.

[115] Schindler, C.; Nievergelt, P.: Geologie und Petrographie, Geologisches Institut der Eidgenössischen Hochschule Zürich ETH, Ingenieurgeologie, Polytechnical University of Zurich, Switzerland, 1990.

[116] Schröter, W.; Lautenschläger K. H.; Bibrack, H.: Taschenbuch der Chemie, VEB Fachbuchverlag Leipzig, Germany, 1986.

[117] Shimojo, K.; Umezawa, H.: Environmental impact by TECCO® stabilization system – Comparison of CO_2 emission between free frame and TECCO® net system, TOA GROUT Kogyo Co., LTD. Yotsuya, Tokyo, Japan, 2008.

[118] SIA 260 (Swiss Standardization): Grundlagen der Projektierung von Tragwerken, Switzerland, 2003.

[119] SIA 261 (Swiss Standardization): Einwirkungen auf Tragwerke, Switzerland, 2003.

[120] SIA 261 (Swiss Standardization): Einwirkungen auf Tragwerke – Ergänzende Festlegungen, Switzerland, 2003.

[121] SIA 263 (Swiss Standardization): Stahlbau, Switzerland, 2003.

[122] SIA 267 (Swiss Standardization): Ankernorm, Switzerland, 2003.

[123] Sierant, J.: Projekt i realizacja konstrukcji ściany gwoździowanej – Design and realization of construction of the nailed wall, Inżynieria i Budownictwo – Engineering and Construction, pp. 79–88, 10/2010, Poland, 2010.

[124] Spang, R.; Bollinger, R.: Vom Holzzaun zum Hochenergienetz – Die Entwicklung des Steinschlagschutzes von den Anfängen bis zur Gegenwart, Fatzer AG, Geobrugg Schutzsysteme, Switzerland, 2001.

[125] TÜV Rheinland, LGA Bautechnik GmbH, Kompetenzzentrum Metall; Stradtner, G.; Steidl, F.: Tensile tests on high-tensile steel wire mesh TECCO® G65/3 mm with connection clips TECCO® T3, Test report 69608285-01 en, Germany, 2009.

[126] TÜV Rheinland, LGA Bautechnik GmbH, Kompetenzzentrum Metall; Stradtner, G.; Steidl, F.: Zugversuche an hochfestem Stahldraht TECCO® G65/3 mm im Vergleich mit einem Quadratmaschengeflecht 50 × 50/4.6 mm, Test report 69613683/01 de, Germany, 2009.

[127] TÜV Rheinland, LGA Bautechnik GmbH, Kompetenzzentrum Metall; Stradtner, G.; Steidl, F.: Slope stabilization system TECCO® G65/3, Monitoring and supervision of laboratory testing, Test report 69616481/02, Germany, 2010.

[128] University of Cantabria, School of Civil Engineering, General Report TECCO® Mesh G65 – Mechanical Mesh Properties and Simulations Models, Sandander, Spain: Puncture Test of TECCO® Mesh G-65 3 mm, Spain, 2001.

[129] University of Cantabria, E.T.S.I. CAMINOS, CANALES Y PUERTOS, Laboratory of Structures, Sandander, Spain: Puncture Test of TECCO® Mesh G-653 mm, Spain, 2001.

[130] University of Cantabria, E.T.S.I. CAMINOS, CANALES Y PUERTOS, Laboratory of Structures, Sandander, Spain: Evaluation of high-tensile strength steel wire mesh with a wire cut, Unravelling Test Report, Spain, 2002.

[131] University of Cantabria, E.T.S.I. CAMINOS, CANALES Y PUERTOS, Laboratory of Structures, Sandander, Spain: TEST OF THE MECHANICAL PROPERTIES TECCO® Mesh G-65 3 mm Flat, Spain, 2003.

[132] Vischer, D.; Huber, A.: Wasserbau, Hydrologische Grundlagen, Elemente des Wasserbaus, Nutz- und Schutzbauten an Binnengewässern, Institut für Wasserbau ETH, Swiss Federal Institute of Technology, Switzerland, 1993.

[133] Volkwein, A.: Numerische Simulation von flexiblen Steinschlagschutzsystemen, Doktorarbeit ETH Zürich, Switzerland, 2004.

[134] Wartmann, S.; Gerber, W.: Field Testing of Rockfall Protection Barriers; Comparison between the "Two Most Important Test Methods", Swiss Federal Research Institute WSL, Birmensdorf, Switzerland, 2001.

[135] Wartmann, S.; Salzmann, H.: Debris Flow and Floating Tree Impacts on Flexible Barriers, IMM Conference, Hong Kong, 2002.

[136] Wartmann, S.; Salzmann, H.; Roth, A.: Debris Flow Protection by using Flexible Barriers – Mechanics, Prediciton and Assessment, Third International Conference on Debris-Flow Hazard Mitigation, Davos Switzerland, Federal Office for Environment, Forest and Landscape/Federal Office for Water and Geology/Swiss Federal Research Institute WSL, Switzerland, 2003.

[137] Wartmann, S.; Salzmann, H.; Roth, A.: Debris Flow Protection by using Flexible Barriers, Österreichische Wasser- und Abfallwirtschaft, Heft 3–4, Austria, 2004.

[138] Wartmann, S.; Roth, A.: Experimental and Numerical Modelling of Highly Flexible Rockfall Protection Systems, International Symposium Society for Rock Mechanics and Engineering (CSRME), China, 2005.

[139] Wartmann, S.; Wendeler, C.; Volkwein, A.; Roth, A.; Denk, M.: Field measurements used for numerical modelling of flexible barriers, Proceedings of the 4th International Conference on Debris Flow Hazard Mitigation, pp. 681–690, China, 2007.

[140] Wartmann, S.; Flum, D.; Rüegger, R.: New generation of spiral rope nets for rockfall protection, tests, design and application, Highway Geological Symposium (HGS), USA, 2008.

[141] Wartmann, S.; Roduner, A.; Flum, D.: Product Manual TECCO® Slope Stabilization System, Geobrugg AG, Switzerland, 2010.

[142] Wartmann, S.: The Method of Designing of Flexible Slope Stabilization Systems with High-Tensile Steel Wire Meshes, Doctoral Thesis, AGH University of Science and Technology, April 2011.

[143] Wendeler, C.: Murgangrückhalt in Wildbächen – Grundlagen zu Planung und Berechnung von flexiblen Barrieren, Diss. ETH Nr. 17916; Switzerland, 2008.

[144] Weingart, K.; Rüegger, R.; Bickel, M.: Flexible Oberflächenstabilisierungssysteme aus hochfesten Drahtgeflechten in Kombination mit Boden- und Felsnägeln, 3 Fallbeispiele. Technische Akademie Esslingen, Beitrag für 4. Kolloquium "Bauen in Boden und Fels", Germany, 2004.

[145] Wichter, L.: RUVOLUM® Dimensioning Concept for Flexible Slope Protection Systems with Nails and Wire Meshes, Comments on the geotechnical and safety-theoretical aspects of an application in Germany, University of Cottbus, Faculty for Rock and Soil Mechanics, Germany, 2001.

[146] Wittke, W.; Erichsen, C.: Standsicherheitsuntersuchungen auf der Grundlage der Mechanik starrer Körper. Grundbau-Taschenbuch, Teil 1: Geotechnische Grundlagen, 6. Auflage, Germany, 2001.

[147] Wittmann, F. H.: Werkstoffe V, Vorlesung Abteilung Bauingenieurwesen der ETH Zürich, IBWK, Institut für Baustoffe, Werkstoffchemie und Korrosion, Swiss Federal Institute of Technology, Switzerland, 1997.

[148] Zettler, A. H.; Poisel, R.; Roth, W.; Preh, A.: Slope stability analysis based on the shear reduction technique in 3D. FLAC and numerical modeling in geomechanics (edited by Detournay & Hart), A. A. Balkema, Rotterdam, pp. 11–16, Netherland, 1999.

[149] Zhu, D. Y.; Lee, C. F.; Jiang, H. D.: Generalised framework of limit equilibrium methods for slope stability analysis, "Geotechnique", Vol. 53(4), pp. 377–395, 2003.

Minutes

Minutes

Minutes

Minutes

Flexible slope stabilization systems made from conventional wire meshes in combination with nails or nailing are widely used in practice to stabilize soil and rock slopes. They are traditional solutions and provide an alternative to measures based on rigid concrete liner walls, shotcrete applications or massive supporting structures.

Slope protection by means of common wire mesh and wire rope nets is known accordingly, but the transfer of forces by mesh as pure surface protection devices is limited on account of their tensile strength and above all also by the possible force transmission to the anchoring points (nails, anchors).

Strong wire rope nets offer certain possibilities for slope stabilizations with greater distances between nails and anchors. However, they are comparatively expensive in relation to the protected surface and the size of the individual nets is relatively small, resulting in higher installation cost and less flexibility to local terrain conditions.

Today, apart from solutions using conventional steel wire, new meshes from high-tensile steel wire are now also available on the market. The latter can absorb substantially higher forces and transfer them onto the nailing.

A new special method has been developed for the designing of flexible slope stabilization systems with high-tensile steel wire meshes for the use on steep slopes in more or less homogeneous soil or heavily weathered loosened rock.

The interaction of mesh and fastening to nails has been investigated in comprehensive laboratory tests. This enabled also to find a suitable fastening spike plate which allows an optimal utilization of the strength of the mesh in tangential (slope-parallel) as well as in vertical direction (perpendicular to the slope).

The trials also confirmed that the high-tensile wire meshes, in combination with suitable plates, enable substantial pretensioning of the system. Such pretensioning increases the efficiency of the protection system. This restricts deformations in the surface section of critical slopes which might otherwise cause slides and movements as a result of dilatation. Suitable dimensioning models permit to correctly dimension such systems.

Various implemented stabilizations in soil and rock, with and without vegetated face, confirm that these measures are suitable for practical application and provide useful information for the optimized handling and installation process.

Geotechnical, civil and mining engineers, geologists, professors and students, designers, public authorities as well as any decision takers will receive a detailed insight into the subject of slope stabilization with the new high-tensile steel wire mesh and the new dimensioning method for flexible slope stabilization systems which allow simple and safe concepts including cost saving installation processes. This provides new interesting solutions for traditional geotechnical problems which, in the meantime, are executed and applied globally on all continents.